



HAL
open science

On the performance of oxidation catalysts and SCR catalysts in the presence of alkali compounds representative of biofuel contaminants: from the commercial catalysts to the active phase

Yiquan Xie

► **To cite this version:**

Yiquan Xie. On the performance of oxidation catalysts and SCR catalysts in the presence of alkali compounds representative of biofuel contaminants: from the commercial catalysts to the active phase. Chemical engineering. Université Pierre et Marie Curie - Paris VI, 2017. English. NNT : 2017PA066494 . tel-01942792

HAL Id: tel-01942792

<https://theses.hal.science/tel-01942792>

Submitted on 3 Dec 2018

HAL is a multi-disciplinary open access archive for the deposit and dissemination of scientific research documents, whether they are published or not. The documents may come from teaching and research institutions in France or abroad, or from public or private research centers.

L'archive ouverte pluridisciplinaire **HAL**, est destinée au dépôt et à la diffusion de documents scientifiques de niveau recherche, publiés ou non, émanant des établissements d'enseignement et de recherche français ou étrangers, des laboratoires publics ou privés.

Université Pierre et Marie Curie

Ecole doctorale 391

Institut Jean Le Rond d'Alembert / Fluides Réactifs et Turbulence

On the Performance of Oxidation Catalysts and SCR Catalysts in the Presence of Alkali Compounds Representative of Biofuel Contaminants: from the Commercial Catalysts to the Active Phase

Par M. Yiquan XIE

Thèse de doctorat de Génie Chimique

Dirigée par M. Patrick DA COSTA et Mme. Maria Elena GALVEZ-PARRUCA

Présentée et soutenue publiquement le 25/10/2017

Devant un jury composé de :

M. DUJARDIN Christophe, Professeur des Universités, École Nationale Supérieure de Chimie de Lille (Rapporteur)

M. GARIN Francois, Professeur, Université de Strasbourg (Rapporteur)

M. CAVADIAS Siméon, Professeur, Université Pierre et Marie Curie (Examineur)

M. DA COSTA Patrick, Professeur, Institut Jean le Rond d'Alembert, Université Pierre et Marie Curie (Directeur de Thèse)

Mme. GALVEZ-PARRUCA Maria Elena, Maître de Conférences (Habilitation), Institut Jean le Rond d'Alembert, Université Pierre et Marie Curie (Co-Directeur de Thèse)

M. TATOULIAN Michael, Professeur, Chimie ParisTech, CNRS Institut de Recherche de Chimie Paris (Examineur)



Except where otherwise noted, this work is licensed under
<http://creativecommons.org/licenses/by-nc-nd/3.0/>

Université Pierre et Marie Curie

Ecole doctorale 391

Institut Jean Le Rond d'Alembert / Fluides Réactifs et Turbulence

On the Performance of Oxidation Catalysts and SCR Catalysts in the Presence of Alkali Compounds Representative of Biofuel Contaminants: from the Commercial Catalysts to the Active Phase

Par M. Yiquan XIE

Thèse de doctorat de Génie Chimique

Dirigée par M. Patrick DA COSTA et Mme. Maria Elena GALVEZ-PARRUCA

Présentée et soutenue publiquement le 25/10/2017

Devant un jury composé de :

M. DUJARDIN Christophe, Professeur des Universités, École Nationale Supérieure de Chimie de Lille (Rapporteur)

M. GARIN Francois, Professeur, Université de Strasbourg (Rapporteur)

M. CAVADIAS Siméon, Professeur, Université Pierre et Marie Curie (Examineur)

M. DA COSTA Patrick, Professeur, Institut Jean le Rond d'Alembert, Université Pierre et Marie Curie (Directeur de Thèse)

Mme. GALVEZ-PARRUCA Maria Elena, Maître de Conférences (Habilitation), Institut Jean le Rond d'Alembert, Université Pierre et Marie Curie (Co-Directeur de Thèse)

M. TATOULIAN Michael, Professeur, Chimie ParisTech, CNRS Institut de Recherche de Chimie Paris (Examineur)



Except where otherwise noted, this work is licensed under
<http://creativecommons.org/licenses/by-nc-nd/3.0/>

Acknowledgments

This doctoral thesis, though published by one author, could not have been possible without the aid of dozens of other people in a way or other over the course of my three-year study at UPMC. It has been an unforgettable, rewarding, interesting, and sometimes even challenging experience pursuing this Ph.D., and it is difficult to show my gratitude to everyone appropriately for their contributions to my persistence and success along this very journey.

First of all, I would like to express my genuine appreciation to Professor Patrick DA COSTA, Dr. Hab. Marie Elena GALVEZ and Dr. Alexis MATYNIA for being my thesis supervisors. Without their scientific guidance, advice and patience, this dissertation can by no means come to public notice. A special thank is due to Prof. Patrick DA COSTA for encouraging me to do a PhD thesis, and for accepting me to his laboratory. As a member of the Fluides Réactifs et Turbulence (FRT) group of Prof. DA COSTA, I appreciate deeply his spiritual support, his pronounced organization of the research topic, his permanent readiness for discussion, his great interest in the success of this work and his high motivation for all his group members.

I was also quite fortunate that my PhD thesis can be examined by two reviewers, Prof. Christophe DUJARDIN (Ecole Nationale Supérieure de Chimie de Lille) and Prof. François GARIN (Université de Strasbourg). Special thanks belong to them for making my thesis better. Furthermore, I would like to express my gratitude to other members of my Jury, Prof. Siméon CAVADIAS (UPMC) and Prof. Michael TATOULIAN (Chimie ParisTech). I thank all the members of my Jury for bringing this thesis to a close.

I thank Dr. Acácio Mendes, for getting me familiar with the experimental facilities and for his team building effort, in particular, during the first year of my thesis. I also wish to acknowledge other members of the FRT group, Hongrui LIU, Sandrine DUONG, Armando IZQUIERDO, Radosław DEBEK, Johnny ABOUD and Laureanne PARIZOT. I thank all of you for all the aid you provided, all the moments we shared and all the conversation we had.

Acknowledgments

Meanwhile, I want to convey my gratitude to all other professors, researchers, administrators, engineers and technicians from the laboratory where I carried out my research activities and to whom I can turn for help, namely, Prof. Stéphane ZALESKI, Prof. Philippe GUIBERT, Prof. Guillaume LEGROS, Maya DAOU, Evelyne MIGNON, Anne MARCHAL, Renaud JALAIN, Jean-Marie CITERNE, Jérôme BONNETY, Hugo DUTILLEUL, Christian OLLIVON, Dominique BUSQUET, Jérôme PÉQUIN, and Frédéric SEGRETAIN.

I was quite privileged to work with 2 master students over the past 3 years: Elza RODRIGUES and Achraf HAMSİ. Elza worked with me on the aging study of monolith diesel oxidation catalysts, and this led to the publication of my first article during this thesis. Achraf came to the FRT group when I was at the final year of my thesis, and he aided me in the poisoning study of monolith selective catalytic reduction catalysts. Their help in conducting some of the catalytic tests and catalysts characterizations as part of my thesis was indispensable to its completion. I am sincerely grateful to both of them.

Prior to my arrival at UPMC, I was inspired by many devoted teachers, friends and classmates. Particularly, I would like to use this opportunity to show my gratitude to Prof. Haochun ZHANG for acting as my guarantor without hesitation when I asked. Undoubtedly, I am indebted to all the teachers, friends and classmates who witnessed my personal growth and even contributed to it.

ZNN has, for over two years, chosen to enhance the cohesion of our coterie, sharing with me her life and her knowledge, for which I am exceptionally grateful. She has been a supportive person throughout my late 20s, ensuring that the stress was never overwhelming and walking with me through up and down. In addition, she has patiently dealt with my awful interaction in communication, even occasionally having to bear it. I look forward to journeying with you as a member of a "big" group.

I would be incredibly remiss if I did not acknowledge the immense love and support from my family. I feel blessed to have you as a strong backing for my pursuing greater success and impenitent life. I dedicate this thesis to you.

Acknowledgments

Institutional acknowledgements belong to the two providers for catalysts, *Continental AG* for the commercial diesel oxidation catalysts, *Umicore* for the commercial selective catalytic reduction catalysts, and to *China Scholarship Council (CSC)* for the financial support of my three-year PhD thesis program.

Abstract

Due to global lean exhaust gas and new emission regulations, exhaust after-treatment systems of diesel engines are getting more and more sophisticated and comprise a series of catalytic units. In the present work, two of these catalytic systems were studied, Diesel Oxidation Catalysts (DOC) and Selective Catalytic Reduction (SCR) catalysts. Particular attention is paid to their performance in the presence of alkali compounds when bio-diesel is utilized as the alternative fuel.

Firstly, this thesis focuses on the catalytic behavior of the Diesel Oxidation Catalyst using different aging characteristics of road mileage in order to improve the efficiency of an ammonia SCR system on an after-treatment line composed by a DOC + DPF + SCR. The studied catalyst is a commercial diesel oxidation catalyst (Pt/Pd/Al₂O₃) provided by Continental. Hydrothermal aging under different conditions on carrots of monolith were performed. The results of aging study on DOC reveal that thermal aging significantly affects the overall oxidation activities of the catalysts. It turns out that mild thermal aging actually activates the catalyst. Mild thermal aging on the catalyst improves the oxidation performance of C₃H₆ as well as CO to a large extent while severe aging contributes a little bit. NO oxidation over severely aged catalyst, however, gets better.

Also studied in the monolith form over the commercial DOC, the influence of the addition of different alkali metal species (K and Na) on the commercial DOC through catalytic tests performed on this structured catalyst under multicomponent (C₃H₆ / CO / NO / NO₂) co-feeding conditions was explored. The results of doping of alkali metals on a commercial DOC illustrate that the introduction of dopants leads to either negative or positive impacts on the catalytic oxidation. The K addition leads to a promotion of oxidation reactions while the Na addition inhibits the same reactions. There is no impact of exhaust gas composition on the ranking of catalysts. However, it was shown that the presence of NO₂ promotes the oxidation reaction whereas in the presence of NO, the competition in terms of oxidation in the same catalytic sites leads to a shift of light off temperature for CO and C₃H₆ to higher temperatures.

Aiming at investigating the effects of the presence of different alkali metal species on the DOC at the level of active phase, homemade bimetallic DOC is prepared and then different alkali metal species incorporated. The catalytic activities test results of doping of alkali metals on a model DOC demonstrate that the addition of alkali compound (K or/and Na) leads to a promotion of the C₃H₆ oxidation reactions while incurs an inhibition on the NO conversion. From the analysis of changing the pollutants in the feed, it's concluded that C₃H₆ and NO are mutually inhibitor to each other when it comes to their oxidation.

Finally, encouraged by the evident influence of alkali compounds on DOCs, their impacts on the downstream SCR catalysts are also studied in this thesis. The studied SCR catalyst is a commercial V₂O₅-based catalyst provided by UMICORE company. The results of doping of alkali metals on a commercial SCR catalyst indicate that the introduction of dopants leads to either negative impacts on the catalytic performance of the used catalysts. In terms of poisoning effect, it seems that Na exhibits stronger inhibition than K on the same mass basis. Furthermore, it's found that their combination usually leads to the complete loss of activities whether it's with respects to Standard SCR or Fast SCR.

Keywords: Exhaust after-treatment systems; DOC; SCR; Bio-diesel; Alkali compounds; Hydrothermal aging; Performance; Multicomponent co-feeding; Promotion; Inhibition

Résumé

En raison des de l'augmentation de la pollution à l'échelle mondial du notamment aux gaz d'échappement des automobiles, de nouvelles réglementations d'émissions ont été mises en place depuis les années 1990. Ces réglementations ont conduit à une évolution des carburants traditionnels vers les biocarburants et à des systèmes de post-traitement des gaz d'échappement, notamment pour les moteurs diesel, de plus en plus sophistiqués. Ils comprennent à ce jour une série d'unités catalytiques, contenant un filtre à particules, un catalyseur d'oxydation pour traiter le monoxyde de carbone et les hydrocarbures et enfin un catalyseur pour réduire les oxydes d'azote.

Dans ce travail de thèse, deux de ces systèmes catalytiques industriels ont été étudiés, les catalyseurs à l'oxydation diesel (DOC) et les catalyseurs de réduction catalytique sélective (SCR). Une attention particulière est accordée à leur performance en présence de composés métaux alcalins. En effet, les alcalins sont présent dans les biocarburants et lorsque le biodiesel est utilisé comme carburant de remplacement, ils vont donc être présents dans les gaz d'échappement et à priori dans les systèmes de post-traitement.

Tout d'abord, cette thèse se concentre sur le comportement catalytique du Catalyseur d'Oxydation Diesel en utilisant différentes caractéristiques de vieillissement simulant le kilométrage routier. Le catalyseur étudié est un catalyseur commercial d'oxydation diesel (Pt / Pd / Al₂O₃) fourni par Continental AG. Le vieillissement hydrothermal dans des différentes conditions sur les carottes de monolithe a également été effectué. Les résultats de l'étude du vieillissement sur le DOC révèlent que le vieillissement affecte de manière significative les activités globales d'oxydation des catalyseurs. Il s'avère que le vieillissement à basse température (750°C) active le catalyseur. Le vieillissement hydrothermal léger sur le catalyseur améliore les performances d'oxydation de C₃H₆ ainsi que le CO dans une large mesure, tandis que le vieillissement sévère contribue un peu. L'oxydation des catalyseurs sévèrement vieillis, cependant, s'améliore.

Résumé

Nous avons également étudié sur le DOC commercial sous forme de carotte de monolithe, l'influence de l'addition de différentes espèces de métaux alcalins (K et Na) par des essais catalytiques réalisés avec des mélange complets ($C_3H_6 / CO / NO / NO_2$). Les conditions d'opérateurs ont été également étudiées. Les résultats du dopage des métaux alcalins sur un DOC commercial montrent que l'introduction de dopants entraîne des impacts négatifs ou positifs sur l'oxydation catalytique selon la réaction étudiée ou l'alcalin utilisé. L'addition K conduit à une promotion des réactions d'oxydation tandis que l'addition de Na inhibe les mêmes réactions. Il n'y a aucun impact de la composition des gaz d'échappement sur le classement des catalyseurs. Cependant, il a été démontré que la présence de NO_2 favorise la réaction d'oxydation alors qu'en présence de NO, la concurrence en termes d'oxydation dans les mêmes sites catalytiques conduit à un décalage de la température de la lumière pour CO et C_3H_6 à des températures plus élevées.

Dans le but d'étudier les effets de la présence de métaux alcalins sur le DOC au niveau de la phase active, un DOC bimétallique a été préparé sous forme de poudre, puis différentes espèces de métaux alcalins sont incorporées. Les résultats des tests d'activité catalytique du dopage des métaux alcalins sur un modèle DOC démontrent que l'addition de composé alcalin (K ou / et Na) conduit à une promotion des réactions d'oxydation de C_3H_6 tout en entraînant une inhibition de la conversion du NO. À partir de l'analyse de la modification des polluants dans l'alimentation, on conclut que C_3H_6 et NO sont mutuellement inhibiteurs l'un de l'autre en ce qui concerne leur oxydation.

Enfin, encouragés par l'influence évidente des composés alcalins sur les DOC, leurs impacts sur les catalyseurs SCR en aval sont également étudiés dans cette thèse. Un catalyseur SCR commercial à base de V_2O_5 fourni par Umicore a également été étudié. Les résultats du dopage de métaux alcalins sur un catalyseur SCR commercial indiquent que l'introduction de dopants conduit à des impacts négatifs sur la performance catalytique des catalyseurs usés. En termes d'effet d'empoisonnement, il semble que Na présente une inhibition plus forte que K sur la même base de masse. En outre, il est constaté que leur combinaison entraîne généralement la perte complète d'activités, que ce soit en respectant SCR standard ou Fast SCR.

Résumé

Mots clés: Systèmes de post-traitement des échappements; DOC; SCR; Bio-diesel; Composés alcalins; Vieillissement hydrothermal

Table of Contents

Table of Contents

Acknowledgments.....	I
Abstract.....	IV
Résumé.....	VII
Table of Contents.....	XI
1. Introduction.....	1
1.1 Overview.....	1
1.2 Objectives of the current work.....	7
2. Literature Review.....	9
2.1 Catalytic converters for pollutant abatement.....	9
2.1.1 Types of catalytic converters for automotive exhaust emission.....	11
2.1.1.1 The Two-way catalyst.....	12
2.1.1.2 The Three-way catalyst.....	13
2.1.1.3 Diesel oxidation catalyst (DOC).....	13
2.1.1.4 Selective catalytic reduction (SCR).....	14
2.1.2 Focus on Diesel Oxidation Catalysts (DOC).....	16
2.1.2.1 CO oxidation.....	18
2.1.2.2 Hydrocarbon oxidation.....	22
2.1.2.3 NO oxidation.....	24
2.1.3 Selective catalytic reduction of NO _x with ammonia (NH ₃ -SCR).....	28
2.1.3.1 Catalysts.....	29
2.1.3.2 Reaction mechanism of NH ₃ -SCR over V-based catalysts.....	30
2.2 Catalyst deactivation.....	34

Table of Contents

2.2.1 Mechanical deactivation (Fouling)	35
2.2.2 Chemical deactivation (Poisoning)	35
2.2.3 Thermal deactivation (Sintering / Aging)	36
2.2.3.1 Support sintering	36
2.2.3.2 Active phase sintering	38
2.3 Effects of biodiesel on engine-out emissions and on catalytic after-treatment systems	40
2.3.1 Effects of biodiesel on engine-out regulated emissions	42
2.3.2 Effects of biodiesel on the DOC	43
2.3.3 Effects of biodiesel on the SCR	44
3. Experimental	47
3.1 Description of lab-scale devices	47
3.1.1 Experimental device for monolithic catalysts	47
3.1.1.1 Experimental device for monolithic DOC	47
3.1.1.2 Experimental device for monolithic SCR catalysts	50
3.1.2 Experimental device for DOC study in powder form	51
3.2 Characterization techniques	53
3.2.1 XRD	54
3.2.2 Transmission electron microscope (TEM)	55
3.2.3 Nitrogen adsorption measurements at 77 K	56
3.2.4 Temperature programmed reduction (TPR)	57
4. On the performance of oxidation catalysts using different aging characteristics or/and in the presence of alkali compounds representative of biofuel contaminants ..	59

Table of Contents

4.1 Influence of different aging characteristics on the performance of a commercial Pt-Pd/Al ₂ O ₃ diesel oxidation catalysts.....	59
4.1.1 Experimental.....	60
4.1.1.1 Catalysts samples.....	60
4.1.1.2 Characterization of catalysts.....	60
4.1.1.3 Catalytic activity studies.....	61
4.1.2 Effects of different aging characteristics on the performance of oxidation catalysts.....	62
4.1.2.1 Effect of different aging characteristics on a DOC under mixtures representative of diesel exhaust.....	62
4.1.2.2 Effect of the gas composition.....	66
4.1.3 Concluding remarks.....	71
4.2 Influence of the presence of alkali compounds on the performance of a commercial Pt-Pd/Al ₂ O ₃ diesel oxidation catalyst.....	72
4.2.1 Experimental.....	73
4.2.1.1 Catalysts samples.....	73
4.2.1.2 Characterization of catalysts.....	74
4.2.1.3 Catalytic activity studies.....	74
4.2.2 Effects of the presence of alkali compounds on the performance of a commercial oxidation catalyst.....	75
4.2.2.1 Effect of the gas compositions.....	75
4.2.2.2 Effect of alkali metals on a DOC under mixtures representative of diesel exhaust.....	81
4.2.3 Concluding remarks.....	90
4.3 Influence of the dual aging (hydrothermal and chemical) on the performance of a commercial Pt-Pd/Al ₂ O ₃ diesel oxidation catalysts.....	90

Table of Contents

4.3.1 Experimental	90
4.3.1.1 Catalysts samples	90
4.3.1.2 Characterization of catalysts	91
4.3.1.3 Catalytic activity studies	91
4.3.2 Effects of the dual deactivation (hydrothermal and chemical) on the performance of a commercial oxidation catalyst	92
4.3.2.1 Effect of the dual deactivation on a DOC under mixtures representative of diesel exhaust	92
4.3.2.2 Effect of the gas compositions	99
4.3.3 Concluding remarks	101
4.4 Influence of the presence of alkali compounds on the performance of a lab-made Pt-Pd/Al ₂ O ₃ diesel oxidation catalyst in the powder form	102
4.4.1 Experimental	102
4.4.1.1 Catalysts preparation	102
4.4.1.2 Characterization of catalysts	103
4.4.1.3 Catalytic activity studies	103
4.4.2 Effects of presence of alkali compounds on the performance of oxidation catalysts	103
4.4.2.1 Effect of alkali metals on a DOC under gaseous mixtures representative of diesel exhaust	103
4.4.2.2 Effect of the gas composition	109
4.4.3 Concluding remarks	111
4.5 Comparison of lab-based research work on monolith DOC to model DOC in the presence of alkali compounds	111
4.5.1 Experimental	111
4.5.2 Results and discussion	112

Table of Contents

4.5.3 Concluding remarks	120
5. On the performance of SCR catalysts in the presence of alkali compounds representative of biofuel contaminants	121
5.1 Influence of the presence of alkali compounds on the performance of a commercial V ₂ O ₅ -based SCR catalyst in the monolith form.....	123
5.1.1 Experimental.....	123
5.1.1.1 Catalysts samples	123
5.1.1.2 Catalytic activity studies	124
5.1.2 Focus on the Fresh commercial V ₂ O ₅ -based SCR catalyst in monolith form	125
5.1.2.1 NH ₃ oxidation capability of the Fresh commercial V ₂ O ₅ -based SCR catalyst in the monolith form	125
5.1.2.2 NO oxidation capability of the Fresh commercial V ₂ O ₅ -based SCR catalyst in monolith form.....	126
5.1.2.3 Performance of the Fresh commercial V ₂ O ₅ -based SCR catalyst in monolith form under NH ₃ +NO atmosphere.....	126
5.1.3 Effects of the presence of alkali compounds on the performance of a commercial V ₂ O ₅ -based SCR catalyst in monolith form.....	128
5.1.4 Concluding remarks	133
6. Conclusions and perspectives	135
References.....	137
List of Figures	151
List of Tables	155
Annexes.....	156
Annex A. Abbreviations and symbols	156
Annex B. Results of Mix 6_TPD tests for home-made DOC.....	158

CHAPTER 1: INTRODUCTION

1. Introduction

1.1 Overview

In its latest report on world energy, petroleum industry company BP projected the world's population would reach 8.8 billion by 2035. Meanwhile, global Gross Domestic Product (GDP) is expected to almost double over the next 20 years ^[1]. As known to all of us, the global economy is powered by energy. Growth in the world economy requires more energy consumption. As expected, the global energy consumption is always increasing.

Along with ever increasing energy consumption, its pressure on natural resources and the damage to the environment is causing growing concern. Growth in the global energy consumption means tons of pollutants. Pollutants mainly come from the energy consumption process among which transportation plays a major part. It takes up around one quarter of total energy consumption (Fig. 1.1) ^[2].

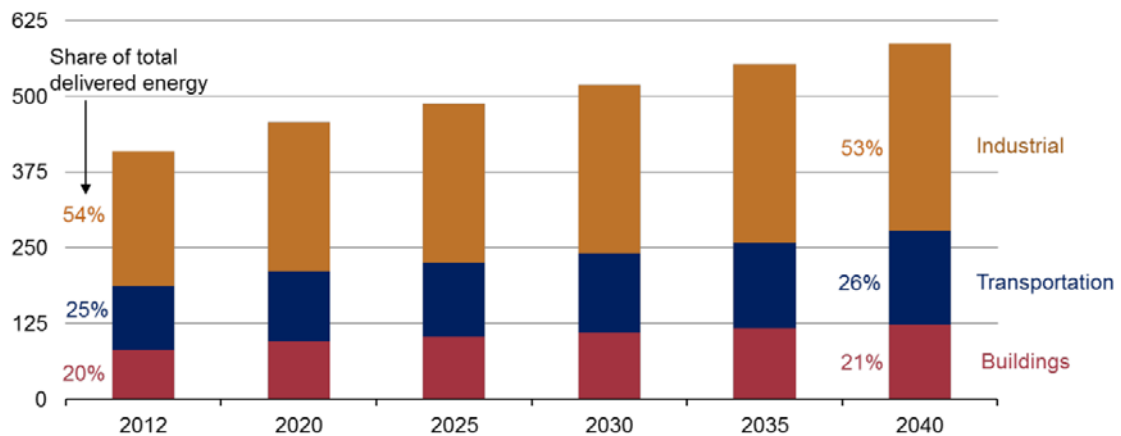


Fig. 1.1 World delivered energy consumption by end-use sector (quadrillion Btu), 2012-2040^[2].

In 1886, Karl Benz invented a machine the likes of which the world had never seen before: the automobile ^[3]. The invention of the modern car became the departure point into the future of mobility.

The automotive industry begun in the 1890s brought far-reaching implications for the nature of societies. For decades, the U.S. took the lead in total automobile production. The output of global automobile production, which has been increasing rapidly, stood at 90.8 million units in 2015. With 24.5 million units manufactured in 2015, China doubled the U.S. production

(12.1 million units), while the EU-27 member countries in the second place with a fleet of 18.2 million [4].

Total global registrations or sales of new vehicles were around 89.7 million in 2015 [5], making the number of vehicles in use worldwide surpass the 1.2 billion-unit mark, but Navigant Research suggests that annual sales could jump to 127 million by 2035, bringing the world vehicle population to more than 2 billion [6].

Most automobiles in operation today are powered by an internal combustion engine, with gasoline or diesel as the fuel. The use of fossil fuels for internal combustion engines inherently gives out emissions that have environmental and health implications [7]. Their removal from exhaust gases is desired, if not mandated [8].

Europe is heavily dependent on diesel, unlike the US, China and Japan (Fig. 1.2) [9]. Europe's vehicle fleets have been persistently transformed from being petrol-powered to diesel-powered over the last 26 years (Fig. 1.3) [10, 11]. In Western Europe, diesel vehicles are a popular choice for consumers, with almost half now opting for this type of powertrain [11]. Overall in 2016, 49.5% of all new passenger car registrations in Western Europe were powered by diesel and 45.8% by petrol [12].

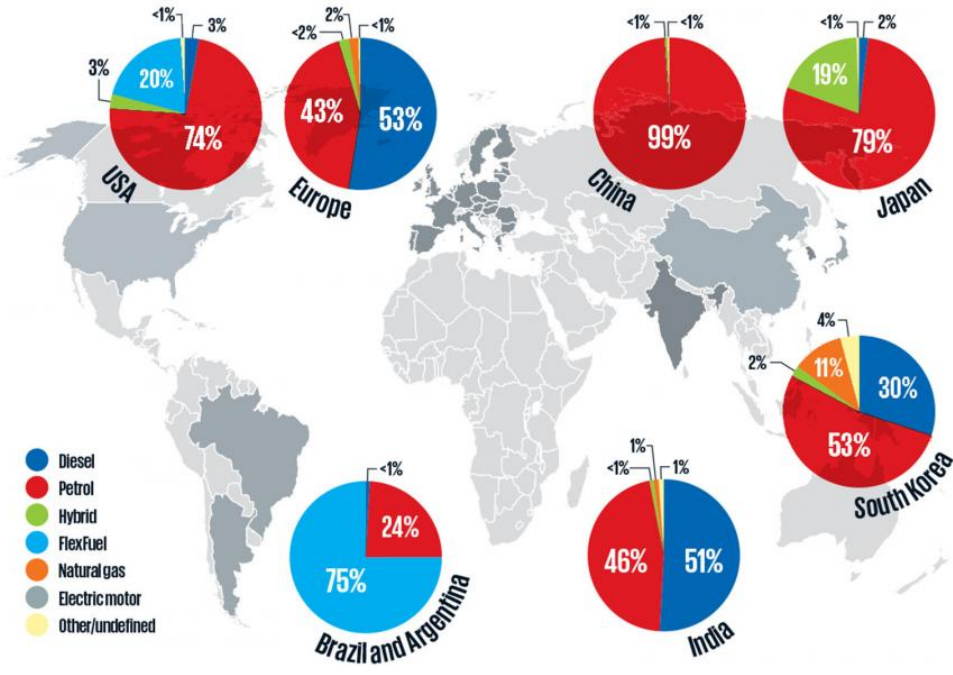


Fig. 1.2 Powertrain map of major markets [9].

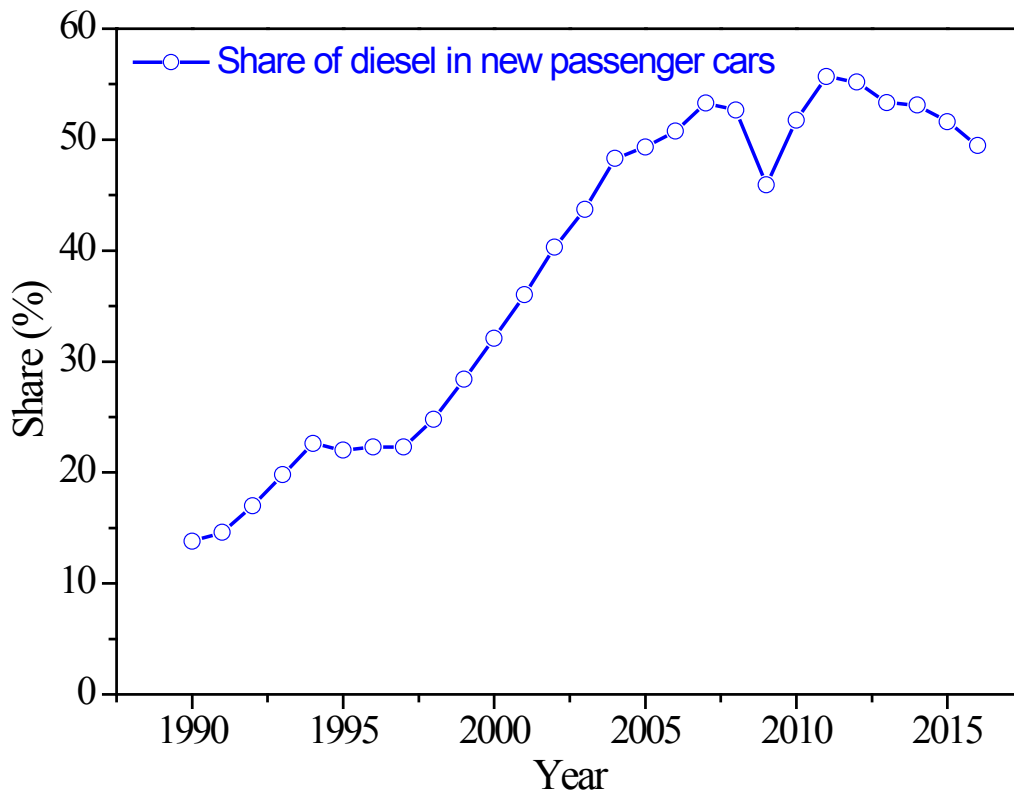


Fig. 1.3 Share of diesel in new passenger car registrations in Western Europe, 1990-2016 ^[11].

Emissions are formed in numerous ways. Incomplete combustion of fossil fuels generates carbon monoxide (CO), unburned hydrocarbons (HCs), and soot as well. Other hydrocarbon reactions can form polynuclear aromatic components and other volatile organic compounds (VOCs), which can themselves be emissions or further react with nitrogen oxides (NO_x) in sunlight. NO_x forms from the N₂ in air during combustion, and to a much lesser extent from fuel-bound nitrogen ^[13]. While NO_x emissions are primary pollutants, they also undergo photochemical reactions to generate ozone (O₃), a strong oxidizer, irritant, and smog component ^[14].

Long-term compliance with automotive exhaust gas emission regulations is one of the challenges confronting the automotive industry. The EU emissions standards Euro 5 took effect on September 1st 2009. At the same time, the automotive industry has already been informed of the proposed limits of the Euro 6 standard by the EU (effective from 2014) ^[15].

Increasingly stringent emission standards (Table 1.1) and concern on the depletion of the fossil fuels propel work on seeking improvements in automotive emission control systems

including new engine designs, novel fuel concepts, and in the design of exhaust catalysis [8, 16].

Table 1.1 EU emissions standards for diesel passenger cars, g/km

Tier	Date	CO	NO _x	HC+NO _x	PM	PN (#/km)
Euro 1	1992.07	2.72	-	0.97	0.14	-
Euro 2	1996.01	1.0	-	0.7	0.08	-
Euro 3	2000.01	0.64	0.50	0.56	0.05	-
Euro 4	2005.01	0.50	0.25	0.30	0.025	-
Euro 5a	2009.09	0.50	0.180	0.230	0.005	-
Euro 5b	2011.09	0.50	0.180	0.230	0.005	6×10 ¹¹
Euro 6	2014.09	0.50	0.080	0.170	0.005	6×10 ¹¹

Positioned in the exhaust pipe, catalytic converters are emission control devices through a combination of catalysts. The catalytic converters employed in gasoline vehicles include oxidation (two-way) catalysts and oxidation-reduction (three-way) catalysts. Emission control catalysts were first introduced on gasoline-fueled vehicles in the mid-1970s [17]. Three-way catalyst (TWC) technology was introduced in the 1980s and later became an integral part of the stoichiometric gasoline-fueled vehicles [18].

The TWC is capable of oxidizing hydrocarbons (HCs) and CO, and simultaneously reducing NO_x on the principle of non-selective catalytic reduction by CO and HC if the engine is operated at a nearly stoichiometric air-to-fuel (A/F) ratio [19]. The latest systems can simultaneously reduce all three pollutants by more than 99% after the catalyst has reached normal operating temperature if the air-fuel ratio is controlled pretty precisely at stoichiometry [8].

Lean-burn (fuel-lean, oxygen-rich) gasoline and diesel vehicles are arousing more and more interest, especially in Europe, because of their better fuel economy than stoichiometric gasoline counterparts. Lean-burn engines, particularly diesels, have higher thermal efficiency and can help reduce carbon dioxide emissions [20]. Higher thermal efficiency contributes to reducing the environmental impact of road transport and to helping the transition towards a low-carbon economy. Other benefits brought by lean-burn technique include, for diesel engines particularly, higher power production and superior durability [21, 22]. These characteristics have promoted the widespread use of diesel engine in the passenger vehicle market [23].

Diesel exhaust is lean because the engine injects only the required amount of fuel into compressed hot air to generate the desired power [13]. Partly due to the excess air input, diesel exhaust is also typically lower in temperature than gasoline counterparts. The abatement of both NO_x and particulate matter (PM) emissions is more difficult result from the low temperature of diesel exhaust, generally between 200-300 °C (light-duty engine) or 300-450 °C (heavy-duty engine) [14].

Due to the lean combustion of diesel engines, the TWC used for stoichiometric-burn gasoline engines fails to efficiently operate in diesel exhaust. The presence of excess oxygen in the exhaust makes it much less effective in reducing NO_x to N₂ [24]. To achieve the same emissions targets, diesel exhaust after-treatment systems require multiple strategies and system integration, encompassing a series of catalytic units [25]. Typically, the first component following the engine is the diesel oxidation catalyst (DOC). As the name suggests, oxidation reactions of CO, hydrocarbon and NO readily occur over the DOC, although total NO_x emissions are not necessarily altered.

NO_x and PM emission control from diesel vehicles is far more complicated and requires the implementation of relatively innovative technologies (Fig. 1.4) [26]. NO_x emission levels complemented in emission standards Euro 6 are reduced by 56% from Euro 5, requiring NO_x abatement devices [8, 27]. Meeting this target is estimated to increase health benefits by 60-90 percent over Euro 5 [28]. The NO_x abatement systems for diesel emission control, such as the lean NO_x trap (LNT) or NO_x storage and reduction (NSR) [29 - 32] and selective catalytic reduction (SCR) catalysts [33], are placed downstream of the DOC [21]. In order to comply with particle number standards in Euro 6, diesel vehicles will need diesel particulate filter (DPF) technology [28].

Advanced catalyst-based technologies will play a central role in the emission control system of the future [34]. The diesel exhaust after-treatment line is now composed by a DOC, a DPF and a NO_x abatement system [8]. A typical diesel exhaust after-treatment line is illustrated in Fig. 1.5.

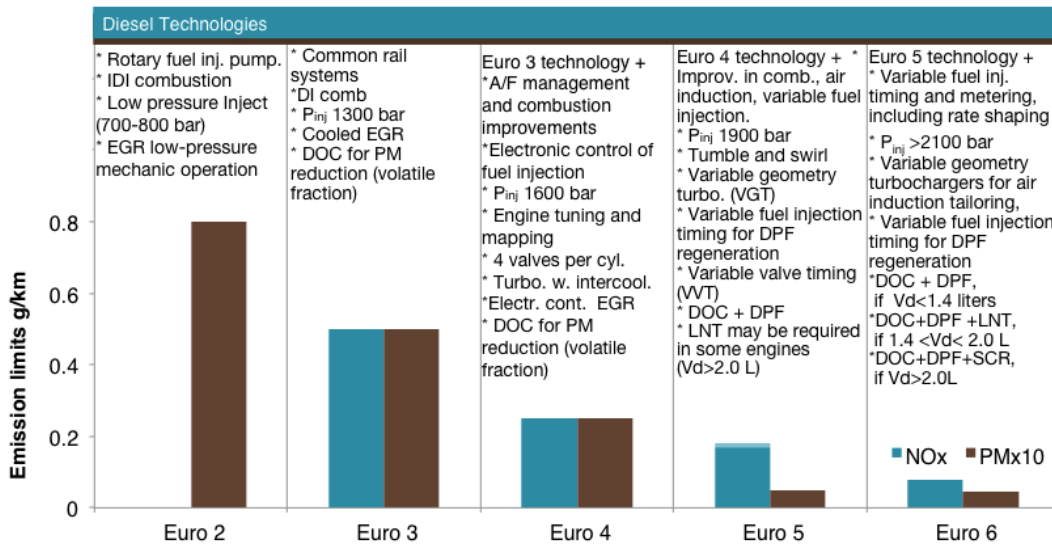
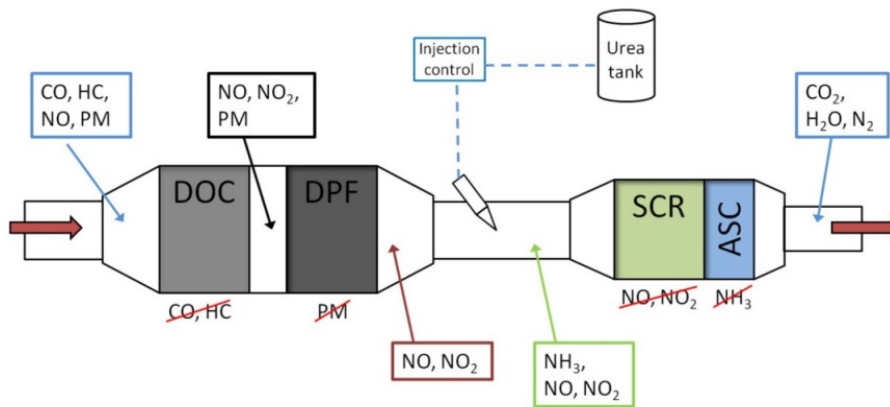


Fig. 1.4 Technologies required for compliance: Diesel [26].



ASC: ammonia slip catalyst

Fig. 1.5 Combination of catalysts to control diesel exhaust emissions [25].

In the present work, two of these catalytic systems were studied. Oxidation catalysts in charge of the oxidation of CO, hydrocarbons and NO were examined in monolith and flow reactor experiments. A V_2O_5 -based SCR catalyst, devoted to the catalytic NO_x reduction by ammonia was also investigated. Particular attention was paid to the influence of the introduction of alkali compounds resulting from the use of biofuel on the performance of the exhaust after-treatment systems.

1.2 Objectives of the current work

With the oil resources depletion and the always-increasing oil demand, the choice of future engines should not rely only on oil-based fuels; rather several feasible fuels should be considered and at least regionally offered in the market place. As such, the EU has suggested a substitution of approximately 20% of oil-based fuel for road vehicles by natural gas, hydrogen or biofuel [35].

The use of renewable biofuels in transport vehicles has been considered in the last decades as a way of stabilizing CO₂ anthropogenic emissions, inherent to fossil-fuel utilization [36, 37]. Among them, biodiesel is one of the main options considered. However, its real impact on emissions (NO_x, soot, unburnt hydrocarbons, CO) and engine performance are not yet quite well known [38, 39]. Moreover, the presence of alkali compounds coming out of the engine together with soot, soluble organic fraction (SOF: unburned fuel and lubricating oil) or directly in the gas stream, will have an impact on the efficiency of the after-treatment technologies used for exhaust cleaning.

The objective of the present study is to investigate the influence of the presence of different alkali metal species (K and Na) on catalytic after-treatment systems: Oxidation and SCR catalysts. In general, it can be divided into two main parts. The first part is on the DOCs in both the monolith and powder form. Monolithic DOCs are from the commercial source while powder DOCs self-made. The second part is concerned with commercial V₂O₅-based SCR catalyst in the monolith form. The method of interest is involved with catalytic tests of the target catalysts employing synthetic gas bench (SGB) plants.

After a literature review, the first part of this thesis deals with the study of the performance of oxidation catalysts in the presence of alkali compounds representative of biofuel contaminants. Systematic methods were employed to get insights into the influence of the presence of different alkali metal species (K and Na): from the commercial catalysts to the active phase, from the activity tests to building the structure-activity relationship.

The second part of this thesis focuses on the NH₃-SCR after-treatment system. Particularly, the performances of automotive SCR catalysts in the presence of alkali compounds representative of biofuel contaminants were investigated utilizing the same systematic methods as in the first part.

CHAPTER 2: LITERATURE REVIEW

2. Literature Review

In this chapter, the widely-used catalytic converters for pollutant abatement will be first mentioned and reviewed. This section is followed by a review on the deactivation of the catalysts. Finally, the effects of biodiesel on engine-out emissions and on catalytic after-treatment systems were addressed.

2.1 Catalytic converters for pollutant abatement

The environmental disaster of the industrialized Meuse Valley, Belgium^[40], proved for the first time that air contamination in an industrial community can actually cause acute disabling diseases. The link between health and air pollution during the episode was evident since a soaring air pollution levels was immediately followed by sharp increases in morbidity and mortality.

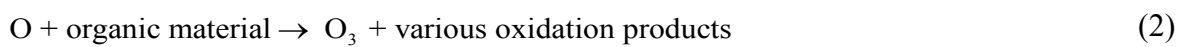
No major incident has since occurred in the Meuse Valley, but the warnings did not prevent similar events from taking place around the globe, toxic and lethal smog in Donora claiming 20 lives while the Great Smog of London causing as many as 12,000 deaths^[41 - 43].

In 1954, Los Angeles experienced a series of severe photochemical smog episodes, leading to the closure of schools and industry for almost a month^[44]. It prompted concerns about possible serious health implications, particularly in light of the recent Donora and London disasters^[45].

Unlike the sulfurous smog that claimed lives in Donora and London, the smog in Los Angeles had a "bleach-like" odor, destroying rubber tires and damaging crops. It would take years for scientific community to solve the puzzle of the Los Angeles smog and decades to implement policies to improve the air quality^[44].

It was Arie Jan Haagen-Smit who made the discovery of the chemical nature and source of smog and linked smog to automobile^[46]. Moreover, he convinced politicians, regulators and industry that automobiles were the principal smog culprit in Los Angeles and had to be regulated. The three main exhaust gas pollutants are hydrocarbons (including partially oxidized organic compounds), carbon monoxide and nitrogen oxides^[20].

By the 1960s, automobiles had been in large-scale mass production for decades. Increased use of automobiles had resulted in serious concerns about urban air quality caused by engine exhaust gas emissions themselves, and by the more harmful species derived from them via photochemical reactions ^[20]. The photochemical reactions is initiated by the dissociation of NO₂ into NO and atomic oxygen under the influence of sunlight ^[47]. This reactive oxygen attacks organic material, i.e., hydrocarbons, resulting in the formation of ozone and various oxidation products presented in the following steps.



Because of their environmental and health implications engine exhaust emissions have to be strictly controlled. With the passage of the Clean Air Act of 1970, engine modifications alone were not sufficient enough to get the automobile out of the local air pollution problem. That's where the add-in type catalytic converter comes in.

The catalytic converter was invented by Eugene Houdry, a French American engineer who moved to the US in 1930 ^[48, 49]. Houdry first developed catalytic converters for smoke stacks and for indoor forklifts using low grade non-leaded gasoline.

About 1950, when the results of early studies of smog in Los Angeles were published, Houdry became concerned about the role of automobile exhaust in air pollution and founded a company, *Oxy-Catalyst*, to develop oxidizing catalysts to clean up exhaust gases from gasoline engines ^[50]. His generic catalytic converter, which makes a drastic reduction in CO emissions and unburned HCs in automobile exhausts, was awarded U.S. Patent in 1956 ^[51].

Catalytic converters were further developed by a series of engineers including Carl Keith and John Mooney at the Engelhard Corporation (now BASF), Rodney Bagley and Irwin Lachman at Corning Glass Works, creating the first production of catalytic converter in 1973 ^[48, 52]. It was widely introduced in automobiles in the US market in 1975 to comply with EPA regulations on automobile exhaust emissions. Today, this invention comes standard on every automobile in production for controlling emission. The automobile equipped with catalytic

converters will cease to be a significant part of the air pollution problem in most areas of the world.

Widespread adoption of the lead-intolerant catalytic converters, however, didn't occur until tightening emission regulations forced the elimination of the extremely effective anti-knock agent tetra-ethyl lead (lead was introduced in the 1920s to raise octane levels) from most gasoline, because the Pb poisons the catalyst by forming a coating on the catalyst's surface and would makes the converter function poorly, if at all ^[53].

As the best effective way to control automobile exhaust emission among all the types of technologies developed so far, catalytic converters with different kind of catalysts at the core that converts NO_x, CO and unburned HCs into benign gases have undergone several stages of development over the years ^[48].

2.1.1 Types of catalytic converters for automotive exhaust emission

Catalytic oxidation was initially associated with the early development of catalysis and it subsequently became a part of many chemical processes, so it is not surprising it was exploited to oxidize hydrocarbons and carbon monoxide in the post-engine exhaust when it became necessary to control these emissions from automobiles in 1975 ^[54].

The oxidizing catalytic converter is one of the pronounced environmental success stories of the last century. It evolved in two directions due to the differences of the exhaust environment between gasoline and diesel: (a) from two-way converters to three-way converters for gasoline applications; (b) from oxidizing converters to diesel oxidation converters, with other pollution-control devices downstream responsible for the abatement of regulated emissions for diesel counterparts.

The earliest converters dating back to 1970s were "oxidizing" or "two-way" converters because only the oxidations of HCs and CO in the exhaust happened over the catalyst. These older converters did nothing to control NO_x in the exhaust. NO_x emissions standards were left out of the requirements by the U.S. EPA at that time so researchers could focus on HCs and CO. But when they took effect in 1981, the same catalytic system would have to convert NO_x to N₂ ^[55]. That's how three-way catalyst converters came into the scenario (Fig. 2.1).

Oxidizing converters were first used on gasoline vehicles to cut tailpipe emissions. Diesel vehicles did not need such technology at that moment thanks to their already low HC and CO emissions [25]. However with increasingly tightening emission standards, the utilization of oxidation catalyst was extended to diesel vehicles, with the title diesel oxidation catalysts (DOC) [56]. Over DOC, oxidation of hydrocarbons and carbon monoxide is plainly evident, except that it has the additional task to convert NO into NO₂, which participates in particulate filter regeneration and improves the downstream NO_x abatement process.

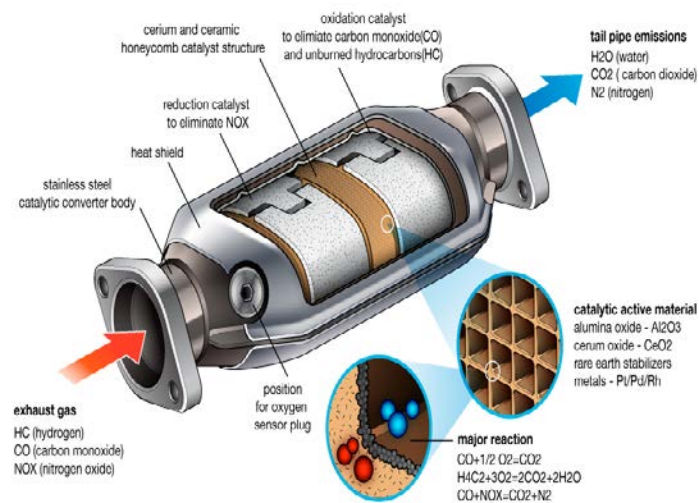


Fig. 2.1 Schematic diagram of a three-way catalyst converter (Image courtesy of ClearMechanic.com)

2.1.1.1 The Two-way catalyst

Catalytic emissions control was first introduced in the form of platinum-based oxidation catalysts that resulted in drastic reduction in hydrocarbons and CO emissions [20]. The first catalysts used a simple formulation of platinum (Pt) deposited on aluminium oxide which in turn was coated onto a support material so that it could be placed in the exhaust clean-up line of the vehicle [57].

These designs were essentially two-way oxidation catalysts since they aided in both reactions of the hydrocarbons and CO with the remaining oxygen in the exhaust. It has two simultaneous tasks: a. oxidation of CO to CO₂; b. oxidation of unburned hydrocarbons to CO₂ and H₂O.



Two-way catalytic oxidizing converters are widely used on gasoline vehicles in US through 1981 when they were superseded by three-way catalysts due to their inability to control nitrogen oxides ^[18].

2.1.1.2 The Three-way catalyst

When NO_x emissions standards required by the EPA took effect in 1981, the same catalyst system that added oxygen to hydrocarbons and CO would have to remove oxygen from NO_x, to give out nitrogen (N₂).

Reduction of NO_x to N₂ was initially achieved over a platinum/rhodium catalyst in fuel-rich exhaust gas before air was added to permit oxidation of HC and CO over an oxidation catalyst ^[20]. Two catalytic converters were used in series, one for reducing, the other oxidizing. Some of the older three-way converters have an air pipe connected to an air pump or aspirator valve to supply air between the oxidation and reduction catalysts. This approach, however, was not technical and economical satisfactory. It would add significantly to the bulk and cost of the device.

It was observed a platinum/rhodium catalyst could, under appropriate air-fuel conditions, simultaneously convert CO and HC and reduce NO_x with high efficiency. This catalyst concept became known as a three-way catalyst (TWC) ^[20]. Simultaneous conversion of all three pollutants over a single TWC to harmless products became possible when the composition of the exhaust gas could be maintained close to the stoichiometric point. Such three-way catalysts are still being used and improved on. Today, modern gasoline vehicles with three-way catalysts can achieve almost complete removal of all three exhaust pollutants over the lifetimes of the vehicles ^[20].

2.1.1.3 Diesel oxidation catalyst (DOC)

The diesel oxidation catalyst (DOC) has been part of diesel exhaust systems since regulations were introduced to limit the amount of harmful emissions released to the environment from diesel engines ^[14]. The first commercial DOC application on a new vehicle was unveiled by automaker Volkswagen in 1989 when it added platinum-based diesel oxidation catalysts, similar to the first conventional two-way gasoline catalysts, to its diesel-powered Golf "Umwelt" model ^[58]. This application was, however, voluntary. The DOC didn't spread out on a large scale until the introduction of the Euro 2 standard in 1996. It was stricter Euro 3 standard (2000) which made them standard devices on all diesel-powered passenger vehicles ^[59].

With excess oxygen in the diesel exhaust, the operating requirements for DOC are different from those for TWC. The temperature of diesel exhaust is typically lower than that of gasoline counterparts partly due to the excess air input. Operated under lower temperature conditions, DOCs have 2~3 times the amount of catalytic material as a TWC for the same quantity of exhaust clean-up ^[14, 23].

Enclosed by a highly oxidizing environment, the primary functions of DOC are oxidation of CO, unburned hydrocarbons and NO. Undesirable oxidation of SO₂ also occurs over DOC. The oxidation of hydrocarbons over DOC can be used to generate exotherms required for downstream pollution-control devices. Moreover, converted NO₂ can be exploited to improve the performance of some particulate filters and NO_x abatement systems downstream DOC ^[14].

2.1.1.4 Selective catalytic reduction (SCR)

NO_x is effectively controlled from gasoline exhaust by a TWC under stoichiometric conditions ^[60]. However, it fails to remove NO_x in the case of lean-burn gasoline and diesel engines ^[61]. For lean diesel conditions, selective catalytic reduction (SCR) is currently the leading technique of remediation ^[60].

The SCR reaction requires reductant for the control of nitrogen oxides. The reductant, such as ammonia (NH₃), which needs to be introduced to the exhaust, selectively reduces the NO_x with the aid of specific catalysts, rather than being oxidized by the excess oxygen ^[60].

While compressed or liquefied ammonia is appropriate for the stationary SCR applications, the odorous ammonia gas had to be replaced in mobile applications by an ammonia precursor such as urea which can be safely stored and reliably release ammonia [60]. Other reducing agents were also proposed to avoid handling NH₃.

Based on the utilized reductants, major SCR techniques can be categorized into three groups [62]: a), HC-SCR [63], b), H₂-SCR [64 - 66], and c), NH₃-SCR [67]. Among them, NH₃-SCR is considered as the top choice.

The novel idea employing urea to reduce NO_x sources for diesel engines dated back to 1988 [68, 69]. Not surprisingly, urea was already exploited as an NH₃ precursor for stationary SCR applications at 1985 [70]. Down to the core, urea-SCR is NH₃-SCR. First results on mobile urea-SCR were publically presented in 1990, showing remarkable NO_x conversions [68]. In addition, urea is neither toxic nor corrosive, and can easily be handled as aqueous solutions, such as a urea-water-solutions (UWS) with a concentration of 32.5 wt.%, bearing the trade name AdBlue® [60].

Since the introduction of AdBlue® in 2004, it has been widely adopted for heavy-duty diesel applications [60, 71, 72]. In some countries, the solution became known as Diesel Exhaust Fluid (DEF) or as Aqueous Urea Solution (AUS) [60].

In practice, urea solution is stored onboard in an additional tank (Fig. 2.2) and this solution is atomized into the main exhaust pipe where it decomposes due to the hot exhaust gas stream and on the SCR catalyst to yield the actual reducing agent NH₃ [60, 73 - 75].

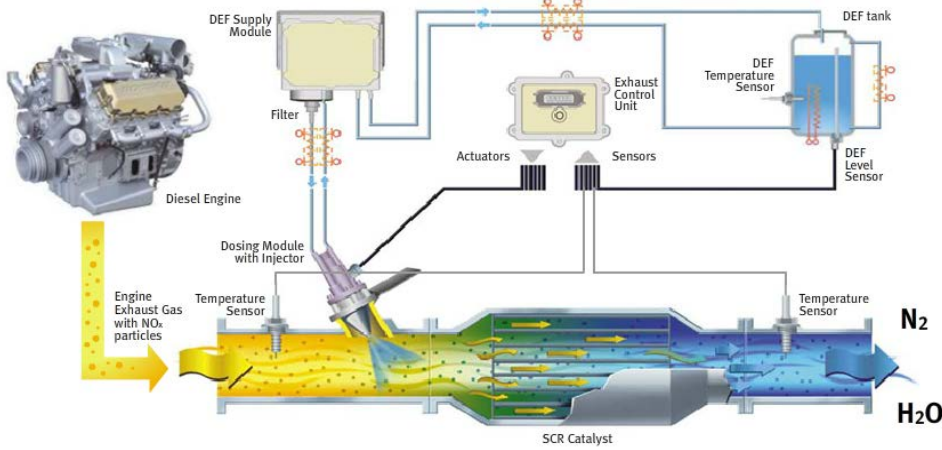


Fig. 2.2 Schematic diagram of a urea-SCR system [73].

2.1.2 Focus on Diesel Oxidation Catalysts (DOC)

DOCs are precious metal based catalysts. Platinum group metals (PGMs), such as platinum (Pt) and palladium (Pd), showed high oxidation performance as well as pronounced thermal durability, proving their cost-effectiveness^[54]. By contrast, base metals such as copper and nickel were too sensitive to fuel impurities and lacked sufficient thermal durability, making them improper candidates though able to perform the job at low cost^[76]. Pt and Pd, as catalytic species, are typically dispersed on high surface area carriers like alumina which are generally called washcoat. The most common practice for dispersing the catalytic components within the carrier is by impregnating an aqueous solution containing a salt of the catalytic element(s). Following impregnating, drying and calcination of the catalyzed carrier are needed to obtain the finished catalyst in the powder form. Monolithic catalysts, however, are usually prepared in this way: the catalyzed carrier is made into an acidified aqueous slurry; the honeycomb monolith is dipped into the slurry which contains the washcoat; the excess mixture is air blown to clear the channels and dried at about 110°C; the final step is calcination, performed in air at temperatures between 300 and 500°C. Commercial catalysts often contain additives as stabilizers or promoters that improve their thermal stability and durability or provide a promoting function such as oxygen storage capacity^[25].

The catalytically active metal(s) is usually deposited on a support or carrier. The role of the support is to provide a matrix that stabilizes the catalytically active component in small particles, hence, increasing the availability of the catalytically active surfaces to the reactants. It also increases the thermal stability of the active component. The properties of the support material used, is of great importance in determining the performance of the final catalyst. These properties include the support surface area, pore volume, surface acidity and reactivity, thermal conductivity, and thermal expansion^[77].

Great efforts have been devoted to most effectively employing the precious metal components in automotive depollution since their inception in 1970s in recognition of their remarkable thermal stability, their lower tendency (compared to the base metals) to react with support materials and less sensitivity to fuel contaminants^[78, 79]. Distilled to its core, the story of diesel exhaust cleaning revolves around three precious metals—platinum (Pt), palladium (Pd), and rhodium (Rh)^[7, 54, 80]. Pt and Pd have been considered as clear choices for the commercial oxidation catalysts, especially since Rh is relatively scarce compared to Pt and Pd, and shows lower activity for olefin conversion under oxidizing conditions^[78, 81].

Platinum has historically been favored for use in diesel aftertreatment because the diesel exhaust stream is highly oxidizing and, under these conditions, palladium is readily converted to its metal oxides form which is less catalytically-active, whereas platinum remains in its metallic form ^[57, 82]. Palladium is not an equally effective catalyst for each of the oxidation reactions it is required to perform. It is not particularly effective at converting some of the hydrocarbons as well as NO present in diesel exhaust gas while platinum is a better catalyst for these reactions. NO oxidation to NO₂ was found to always depend directly on the content of platinum ^[83, 84].

However, palladium is effective for the CO oxidation, particularly at high concentrations of this gas ^[57, 85]. Skoglundh et al. found that for the oxidation of CO, the light-off temperature over monometallic palladium catalyst was much lower than that of platinum ^[86]. The addition of a small amount of Pt (Pd:Pt = 80:20), however, slightly decreased the light-off temperature ^[14, 86]. In this sense, Platinum acts a promotor for palladium concerning the CO oxidation though not to a large degree.

For control of sulfates, palladium is preferred over platinum since Pd catalysts are less likely to form sulfates by direct oxidation ^[87, 88]. Meanwhile, the scarcity and high cost of Pt makes it desirable to attempt to use palladium alongside platinum in diesel oxidation catalysts. Moreover, the presence of palladium can provide much-needed thermal stability in a catalyst followed by a DPF ^[84]. The use of platinum, however, remains important in providing high catalytic activity ^[57, 86]. Palladium does not promote the oxidation of some hydrocarbons and NO over platinum ^[86].

The high temperatures experienced by the catalyst during the regeneration events resulting from the regeneration process of the DPF mean that the thermal stability of the catalyst becomes more desirable where a filter is fitted, making the use of platinum/palladium technology more attractive ^[57].

The first public announcement of the fabrication of such a bimetallic platinum/palladium catalyst was made in 2004 and the very first commercial catalysts were fitted to vehicles one year later ^[57]. With a wider range of possible roles for the DOC, no single catalyst formulation can be universally applied ^[57].

A typical DOC formulation currently in use might have a Pt/Pd ratio of 2:1 on the basis of mass (or approximately 1.1:1 on the basis of atom). Raising the share of palladium among the certain total amount of metals without sacrificing the catalytic performance is highly desirable from the economic point of view. The performance and properties of bimetallic catalysts depend on the total amount of metals, composition, method of catalyst preparation, thermal history, etc ^[86].

The performance of DOC is generally evaluated in terms of the oxidation reactions that occur over it. The oxygen-rich environment of diesel exhaust makes it remarkably important the interaction of oxygen with the catalyst and other reactants.

Gland et al. found that during the interaction of oxygen with the Pt(111) surface (low index plane) over the temperature range between 100 and 1400 K, three states of oxygen have been characterized: molecular adsorption predominates below 120 K; adsorbed atomic oxygen predominates in the 150 to 500 K temperature range; subsurface "oxide" formation may occur in the 1000 to 1200 K temperature range ^[89]. Imbihl et al. investigated the oxygen adsorption on a Pd(111) surface in the temperature range from 30 K to 300 K, concluding that the dissociation process was completed around 200 K and the dissociative chemisorption of oxygen on Pd(111) does not proceed in a single step but through a sequence of several well defined molecular precursor states ^[90].

The chemisorption of oxygen over Pt metals as well as Pd metals is dissociative: O₂ adsorbs onto the metal surface and quickly dissociates well below practical temperatures ^[91, 92]. It is only possible at special surface sites which are capable of breaking the bond of the O₂ molecule. These sites are believed to be linked with some type of structure defects such as atomic step. It follows that the minimum energy pathway leading to thermal dissociation of adsorbed O₂ lies below the energetic barrier for thermal desorption ^[92]. The associative desorption of adsorbed O atoms as O₂ occurs at high temperatures (above 445°C) ^[92 - 94], such that for the typical DOC operating range, oxygen adsorption is irreversible.

2.1.2.1 CO oxidation

Due to its strong toxicity, CO must be strictly controlled in the automotive exhaust. One of the primary functions of the DOC is to oxidize carbon monoxide into carbon dioxide.

Mechanism

The whole process of CO oxidation over DOC is complicated though it seems that it's just simple catalytic reaction that readily occurs.

The catalytic reaction of CO oxidation relies on the interaction between the active sites and the reactants, manifesting as a series of chemisorption-desorption and surface reaction steps^[93]. Both reactants adsorb on the catalyst surface prior to reacting to form CO₂.

The kinetics of this catalytic oxidation reaction has been the subject of intensive studies^[95, 96]. It is currently widely accepted that the dominant mechanism for this reaction over a wide range of conditions is the Langmuir-Hinshelwood dual-site mechanism^[95, 97 - 99]. It is well established and proceeds via the following schematic steps:



Where \otimes denotes a free adsorption site on the catalyst surface, $\otimes - \otimes$ two adjacent free sites. Eq. (6) corresponds to molecular adsorption/desorption of reactant CO, Eq. (7) the dissociative adsorption of O₂, while Eq. (8) the surface reaction by the diffusion of a CO towards an adsorbed atomic oxygen due to its higher mobility on the surface, forming CO₂, which immediately leaves the surface.

It is well known that the coadsorption characteristics of CO and O₂ are quite different, relying on the sequence of the adsorption. The inhibition of adsorption of CO and O₂ is asymmetric as preadsorbed CO blocks oxygen adsorption due to the lack of available pairs of neighbor sites while at all oxygen coverages there is still enough place to accommodate CO molecules, a phenomenon named *asymmetric inhibition*^[100].

Bonzel et al. explored the kinetics of the carbon monoxide oxidation on a clean Pt(110) crystal in an UHV (ultra-high vacuum) system by utilizing Auger electron spectroscopy (AES), low-energy electron diffraction (LEED) and residual gas analysis^[101]. They concluded that two different catalytic reaction mechanisms were found to prevail for the

experimental conditions chosen: Langmuir-Hinshelwood (L.H.) mechanism and Eley-Rideal (E.R.) mechanism. The oxidation of preadsorbed CO characterized by an induction period because of temperature corresponded to L.H. mechanism while the reaction of CO with preadsorbed oxygen atoms exhibited the characteristics of an E.R. mechanism. Moreover, they concluded that the saturation coverage for CO and oxygen on Pt(110) was approximately the same.

Barteau et al. first examined the adsorption/desorption characteristics of CO, O₂, and H₂ on the Pt(100)-(5×20) surface using flash desorption spectroscopy, pointing out the phenomenon of reconstruction^[102]. Then they studied the kinetics of the CO oxidation reaction on the Pt(100)-(5×20) surface under UHV conditions, confirming the applicability of Langmuir-Hinshelwood kinetics for both the reaction of CO with preadsorbed oxygen atoms and the oxidation of preadsorbed CO^[99]. The reaction kinetics in both cases changed dramatically below 300 K due to phase separation at low temperature. What's more, they found that oxygen atoms were adsorbed in islands on the metal surface. Strong attractive interactions within the oxygen islands were at least partially responsible for this difference, the activation energy calculated for the reaction of CO with preadsorbed oxygen being 30 kcal/mol greater than the activation energy measured for the reaction of O₂ with preadsorbed CO.

Goodman et al. found that at near atmospheric pressures, the reaction kinetics fall into three regimes: i, a CO-inhibited regime at low temperatures where CO desorption is the rate-determining step; ii, a mass transfer limited regime at high temperatures; iii, a transient, high-rate regime which lies in between the other two regimes^[103]. With the aid of surface-sensitive techniques amenable to high pressure environments (e.g. PM-IRAS), they also focused on producing a definitive picture of the CO oxidation reaction on PGMs (Rh, Pd, Pt, and Ru) across the 'pressure gap'. Their studies of both low and high pressures demonstrated that: (a) Langmuir-Hinshelwood kinetics adequately described CO oxidation kinetics on PGMs (Pt, Pd and Rh) (i.e. there is no pressure gap) and (b) the most active surface was one containing minimal coverage of CO plus a chemisorbed atomic oxygen^[96].

Carlsson et al. experimentally investigated the oxidation of CO over supported Pt/Al₂O₃ catalysts operating in oxygen excess at atmospheric pressure, stressing that the conventional three-step L.H. scheme used to interpret CO oxidation on Pt surfaces must be complemented by a Pt oxidation and reduction mechanism during transient conditions^[104]. Sales et al. developed a simple physical model to explain the oscillatory oxidation of CO over PGMs-

based (Pt, Pd and Ir) catalysts, assigning the oscillations to a cycle of slow oxidation and reduction of the metal surface layer inducing transitions between two branches of a L.H. scheme ^[105].

Salomons et al. presented experiments and model predictions for the oxidation of CO over a monolithic platinum catalyst ^[93]. A hysteresis effect demonstrating the presence of multiple steady states was observed from the light-off curves. The two branches corresponded to the two states of predominantly CO covered or oxygen covered. The model assuming dissociative chemisorption of oxygen on two surface sites based on adsorption and surface reaction using the L.H. approach best reproduced the light-off behavior.

Enhancement factors

As far as the simple two involving reactants are concerned, it is widely accepted that O₂ promotes while CO inhibits the reaction in the temperature range 225-425°C. A state with high O coverage exhibits high rate of CO₂ production ^[100]. Rise in temperatures leads to the drop of the strong self-inhibition by CO since CO desorption increases significantly which leads to more empty sites allowing a higher reaction rate ^[100].

Studies on the effect of different Pt particles sizes illustrated that the specific reaction rate was higher for the large particles ^[106]. It is possibly because the larger Pt particles result in weaker bonds between the metal surface and the oxygen ^[14, 106, 107] or due to the easier desorption of CO from the surface ^[108].

Inhibition factors

When it comes to the factors inhibiting the CO oxidation, the mention of strong self-inhibition by CO is inevitable. The chemisorption of CO blocks oxygen adsorption to the surface sites and thus inhibits the reaction, exhibiting low rate of CO₂ production ^[93, 104].

Goodman et al. classified the reaction limitations according to the parameters pressure and temperature: CO inhibition dominated the low temperature region irrespective of pressure and it's dictated by CO desorption; oxygen inhibition prevailed under the condition of high

temperature but low pressure; both oxygen inhibition (oxidation at sufficiently high O₂/CO ratios) and mass transfer limitations must be considered under the condition of high temperature plus high pressure^[95, 103, 109].

2.1.2.2 Hydrocarbon oxidation

Due to its environmental and health implications, hydrocarbons must be strictly reduced to its minimum in the automotive exhaust. One of the primary functions of the DOC is to oxidize hydrocarbons into carbon dioxide and water.

In diesel exhaust there exist different kinds of HCs, including saturated and unsaturated components. They represent a large group of chemical compounds exhibiting different stability. Saturated HCs (alkanes or paraffins) with short carbon chain, such as methane, are usually stable because its C-H bonds are difficult to break up. As the carbon chain length increases, the adsorption of the alkanes gets harder because more adjacent sites are required, resulting in their slow reaction rates^[109]. Unsaturated HCs (alkenes or olefins), such as propene (also known as propylene, C₃H₆), are characterized by a C=C double bond that offers them a higher reactivity than their saturated counterparts, namely alkanes.

In general, propane and propene were used to represent saturated HCs and unsaturated HCs, respectively, to test HCs oxidation over catalysts^[110].

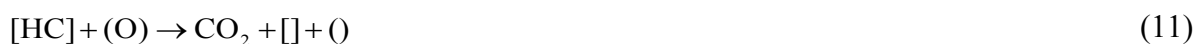
Yao et al. observed a strong chemisorption of propene but no propane chemisorption after exposure of Pt/Al₂O₃ to propane (C₃H₈) and propene (C₃H₆), illustrating that the high electron density of propene favors the interaction and adsorption on a catalytic surface^[25, 111]. They also showed that over the same Pt/Al₂O₃ catalysts the light-off temperature of propene was lower than that of propane.

In this thesis, propene was exploited as a representative hydrocarbon in the diesel exhaust.

Mechanism of propene oxidation

As with CO, the Langmuir-Hinshelwood dual-site mechanism is the currently preferred mechanism to describe the complete oxidation of propene^[14].

The total oxidation of propene tends to proceed via the following schematic steps^[112]:



Where [] and () denote free adsorption sites on the catalyst surface. Eq. (9) corresponds to molecular adsorption/desorption of reactant HC, Eq. (10) the dissociative adsorption of O₂, while Eq. (11) the surface reaction, currently accepted as the rate-determining step^[14]. At temperatures below light-off, HC adsorption is stronger than that of oxygen, thus inhibiting the process indicated as Eq. (10)^[113].

Benard et al. conducted the kinetic study of propene total oxidation on a Pt/Al₂O₃ catalyst in excess of oxygen, concluding propene was adsorbed more easily and strongly than oxygen on the Pt surface^[113]. Also, their TPD results of propene and oxygen revealed that propene was associatively adsorbed on the Pt surface.

In terms of activation energies, they varied in the literature: 16-29 kJ/mol^[114], 20-50 kJ/mol^[115], 41.9 kJ/mol^[116] and 85.8 kJ/mol^[113].

Enhancement factors

When examining the influence of Pt crystallite size on the catalytic oxidation of propylene, Carballo and Wolf found that larger crystallites effectively favored the oxidation of propylene^[116].

Among the parameters investigated by Denton et al., they concluded only the Pt dispersion was a major factor affecting the intrinsic activity^[117]. The intrinsic activity increased with decreasing dispersion. Other factors such as the nature of the support and the nature of the platinum precursor were not easily discernable and less important.

By contrast, regarding the Pt dispersion, Haneda et al. observed the enhancement of C₃H₆ oxidation with the increasing dispersion [118]. They found that the TOF values for C₃H₆ oxidation over Pt/Al₂O₃ catalysts rose with the increasing Pt dispersion. In other words, the C₃H₆ oxidation was promoted over high-dispersion catalysts.

Inhibition factors

As with CO, propene is self-inhibiting at high concentration by covering the platinum sites and blocking oxygen adsorption to the surface sites and thus inhibits the reaction. In their work, Carballo and Wolf concluded that at low C₃H₆ concentration, the oxidation reaction rate increased with the C₃H₆ concentration until it reached a maximum. A further increase in the concentration after that led to a decrease in reaction rate, demonstrating negative-order behavior [116].

In the presence of other gases such as NO, the catalytic oxidation of C₃H₆ is strongly influenced by surface interaction among O₂, C₃H₆ and other gases. The presence of NO would result in the increase of the light-off temperature and it's attributed to the occupation of active sites by NO [119].

2.1.2.3 NO oxidation

The oxidation of NO is an exothermic reaction, with the standard enthalpy being -57.19 kJ/mol [25]. The equation of the global reaction is:



The forward reaction of the NO oxidation is favored at low temperature since the oxidation of NO is exothermic, as shown in Fig. 2.3, with NO₂ predominating at lower temperatures. In other words, the oxidation of NO is thermodynamically limited at higher temperatures [14]. It therefore requires the DOC to work pronouncedly at relatively low temperature. On the other hand, it's noteworthy that NO oxidation is kinetically limited at low temperatures. Thus, these two constraints narrow the temperature range which is appropriate for DOC.

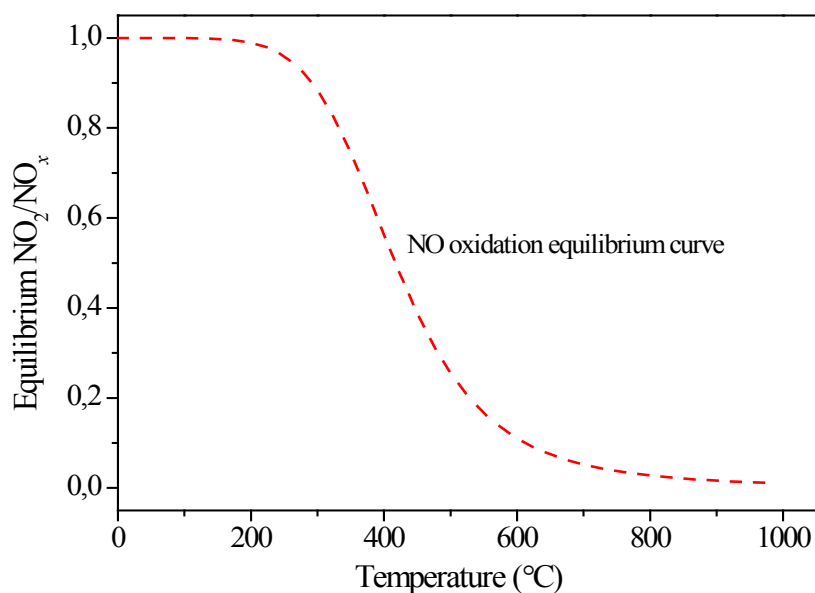


Fig. 2.3 NO oxidation thermodynamic equilibrium curve for a stream initially of 300 ppm NO and 10% O₂.

Mechanism

The vital schematic steps of NO oxidation are listed as follows ^[14, 120]:



Where * denotes the Pt surface site. Eq. (13) corresponds to molecular (associative) adsorption of O₂. Eq. (14) corresponds to the dissociation of adsorbed O₂ via reaction with a vicinal site to form chemisorbed atomic oxygen. Eq. (15) corresponds to the reaction of adsorbed O₂ with chemisorbed NO to form adsorbed NO₂ and O*. Eq. (16) corresponds to the

adsorption of NO. Eq. (17) corresponds to the surface reaction. Eq. (18) does not actually represent an elementary reaction as written, reflecting instead a sequence of quasi-equilibrated steps ^[120]. In the quasi-equilibrated steps of NO reacting with O*, NO₂ as well as vacancies is formed.

It's generally found that the forward rate of NO oxidation reaction was nearly first order in both NO and O₂ and nearly negative first order in NO₂ ^[24, 121 - 124].

When investigating the inhibition effect of NO₂ on the NO oxidation reaction, Mulla et al. proposed the associative adsorption of O₂ as the rate-determining step (RDS, the rate-limiting step is assumed to be the step/steps that consumes the most free energy.), adsorbed atomic oxygen as the most abundant surface intermediate ^[122, 125]. These were later verified by Bhatia et al. in their microkinetic analysis of the NO oxidation reaction ^[24]. Moreover, adsorbed NO was the other of the two predominant surface species ^[24].

Based on their calculations of the Gibbs free energy, Olsson et al. asserted the rate-determining step was the oxidation of NO, $\text{NO} + \text{O}^* \leftrightarrow \text{NO}_2^*$, since this step got the largest value of $|\Delta G|$ ^[126]. These authors also found that either mechanism (Langmuir-Hinshelwood, Eley-Rideal, or their combination) is most appropriate for NO oxidation as all of them seem to describe the experiments equally satisfactorily ^[122, 127]. However, to describe NO oxidation as well as NO₂ decomposition to NO and O resulting in a surface mostly covered by oxygen, the Langmuir-Hinshelwood model was suggested.

Meanwhile, the capacity of the Langmuir-Hinshelwood model to predict the NO conversion dependence on NO concentration at low NO concentrations which was experimentally observed by Despres et al. showed its applicability ^[14, 124]. At high NO concentrations, Despres et al. found that the NO conversion was low. By contrast, the Eley-Rideal mechanism failed to explain the observed effects so that it was rejected by Olsson et al. though it was used by Crocoll et al. for NO oxidation due to a low NO adsorption above 200°C ^[25, 127, 128].

Enhancement factors

In a whole scenario, the parameters involving the materials and operation can impact the performance of NO oxidation.

It was suggested that larger particles have a higher intrinsic activity, supported by a higher turn-over rate (rate of moles of NO converted per Pt site) ^[25]. The reason behind this is the greater resistance towards oxidation of the larger particles.

In their investigation, Denton et al. concluded only the Pt dispersion (particle size) was a major factor affecting the intrinsic activity ^[117]. The intrinsic activity increased with decreasing dispersion. Other factors such as the nature of the support and the nature of the platinum precursor were not easily discernable and less important. There existed a lower limit on Pt dispersion to improve the NO oxidation activity which is discussed by Clayton et al ^[129].

Matam et al. suggested that particle morphology played an even more important role than particle size in the NO oxidation activity ^[130]. They found that the one with higher dispersion presented the higher normalized rate constant, owing to more active particle morphology. They concluded that cuboctahedral morphology was the best configuration compared to truncated cubic and spherical Pt particles ^[25].

Among the three types of platinum catalysts over different supports examined by Xue et al. for the oxidation of NO to NO₂, the activity was found to be in the order Pt/SiO₂>Pt/γ-Al₂O₃>Pt/ZrO₂ ^[131].

Inhibition factors

As kinetic studies showed, the forward rate of NO oxidation reaction was nearly negative first order for NO₂, indicating inhibition by NO₂ ^[24, 121 - 124]. In their study, Mulla et al. found that the apparent activation energy of NO oxidation in the presence of NO₂ was twice as that of without NO₂. The increase of the apparent activation energy clearly demonstrated the negative effect of NO₂.

The formation of an inverse hysteresis when the catalysts were successively heated up and cooled down under NO oxidation conditions were found by multiple investigators: The NO conversion was higher during catalyst heat-up than cool-down ^[14, 25, 132 - 134]. It's said to be

caused by the reversible formation of platinum oxide ^[132]. As a strong oxidant, NO₂ played a major role in reducing the catalyst activity ^[24].

At highly lean conditions, as Hauff et al. discovered, the oxidizing effect of NO₂ was drastically reduced ^[133]. Oxygen, instead, was responsible for the formation of platinum oxide and complete oxidation of the particle surface led to catalyst deactivation ^[25, 121, 123].

2.1.3 Selective catalytic reduction of NO_x with ammonia (NH₃-SCR)

Since the first commercial installations in Japan around 1975, SCR system has evolved in response to increasingly strict regulations and changing application conditions ^[135, 136]. Currently, the most commonly used NO_x abatement technique is NH₃-SCR providing high NO_x removal efficiency ^[61].

The catalytic reduction of NO_x in exhaust gases from stationary sources and mobile sources can be carried out selectively using ammonia or ammonia precursor such as urea ^[137]. In typical exhaust gases, NO_x is composed mainly of NO (>90%) ^[138], which reacts with NH₃ according to the Standard SCR reaction ^[139, 140]:



Under the usual operating conditions of diesel exhaust, the standard SCR reaction has a high potential of NO_x reduction at temperatures above 300°C ^[139]. On the other hand, the DOC upstream of the SCR catalyst can produce great amount of NO₂. When both NO and NO₂ are present in the exhaust, the two following reactions can occur:



The Eq. (20) is referred to as "Fast SCR" because it proceeds faster than the Standard SCR reaction and shows a maximum rate with an equimolar mixture of NO and NO₂ ^[141 - 144]. The Eq. (21) describes the reaction between NO₂ and NH₃, denoted as "NO₂ SCR". However, its reaction rate is much slower than the Fast SCR ^[143]. Compared with Standard SCR, its

relative rate depends on the catalyst and the conditions under which it is used. The NO₂ SCR can be faster over a Fe-zeolite catalyst^[145] while slower over a vanadia-based catalyst^[146].

In an NH₃-SCR system, vaporized ammonia is injected into the flue-gas at about 300-400°C, which is then passed over a catalyst. The catalyst promotes reactions between NO_x and NH₃ to form molecular nitrogen and water vapor.

2.1.3.1 Catalysts

Though there exists many types of catalysts used in SCR process and many new ones are being developed, they can be grouped into three main categories^[61]:

- i. Noble metal-based catalysts^[137, 147, 148], e.g. Pt/Al₂O₃
- ii. Metal oxide-based catalysts^[144, 146], e.g. V₂O₅-WO₃/TiO₂
- iii. Zeolites-based catalysts^[149 - 154], e.g. Fe-ZSM5.

Among the extensively investigated catalysts for NH₃-SCR, it's concluded the use of Pt-based catalysts has been rather limited due to its narrow optimal temperature range and that the most effective ones are metal oxides-based^[137, 155].

Metal oxides-based catalysts such as V₂O₅-WO₃/TiO₂ have been extensively studied due to their excellent activity, selectivity and stability^[137, 144, 146]. Their major drawbacks are high activity for the undesired oxidation of SO₂, the high toxicity of vanadia and a lack of efficiency at low and high temperatures^[25, 154, 156]. Nonetheless, their strengths give them an edge for commercialization. The most widely used catalyst for the SCR process is V₂O₅ dispersed over the TiO₂ anatase support promoted by WO₃ (and/or MoO₃). In general, the overall surface area of the catalysts is 50-100 m²/g, with V₂O₅ virtual contents of 0.5-3% (w/w) and MoO₃ or WO₃ contents of 5-10% (w/w). Infrared and Raman studies show that vanadyl, wolframyl and molybdenyl species are present on the dry surfaces of these catalysts^[157]. Due to its unrivalled price/performance ratio, it will continue to be a major catalyst in the SCR industry^[158].

Recently, zeolites-based catalysts are attracting more and more attention, especially metal ion exchanged zeolites-based catalysts such as Fe-ZSM-5 and Cu-ZSM-5^[141, 159]. The reason

behind this is that ion-exchanged zeolite catalysts feature in high activity in a wide temperature window of operation and high durability [61, 150, 160].

The ideal catalyst for an automotive application should cover a wide range of temperature since it is low during the cold start of the engine and high during the exothermic regeneration of the particulate filter upstream of SCR system [25, 61].

2.1.3.2 Reaction mechanism of NH₃-SCR over V-based catalysts

To improve the performance of the commercially available catalysts used today and design more effective catalysts for the future, it is vital to understand the underlying mechanism governing the SCR chemistry. Actually, this endeavor has been underway since the 1970s, with a number of reaction mechanism proposed [33, 144, 161 - 167].

Inomata et al. proposed that ammonia is first adsorbed as NH₄⁺ at a Brønsted acid site (V-OH) adjacent to a V(5+)=O site and then reacts with gas-phase NO according to an Eley-Rideal mechanism to form N₂ and H₂O, along with the formation of V(4+)-OH. Later, V(4+)-OH species are re-oxidized to V(5+)=O by gaseous oxygen [162].

The mechanism was confirmed and slightly modified by Janssen et al. who proposed that V=O Lewis acid sites are the active centers for ammonia adsorption and demonstrated that one N atom of the N₂ product comes from NH₃ and the other from NO [163].

Based primarily on FT-IR studies, Ramis et al. proposed the "amide-nitrosamide" mechanism, as shown in Fig. 2.4 [164]. This mechanism consists of the following steps: NH₃ is adsorbed over a Lewis acid site where it is activated to form an amide NH₂ species; this amide species then reacts with gas-phase NO via a radical coupling, giving rise to a nitrosamide intermediate, which then decomposes into N₂ and H₂O; the catalytic cycle is closed by re-oxidation of the reduced catalyst by gaseous oxygen [164, 168 - 170]. This mechanism has been successfully realized by computer modelling by Jug et al. [171].

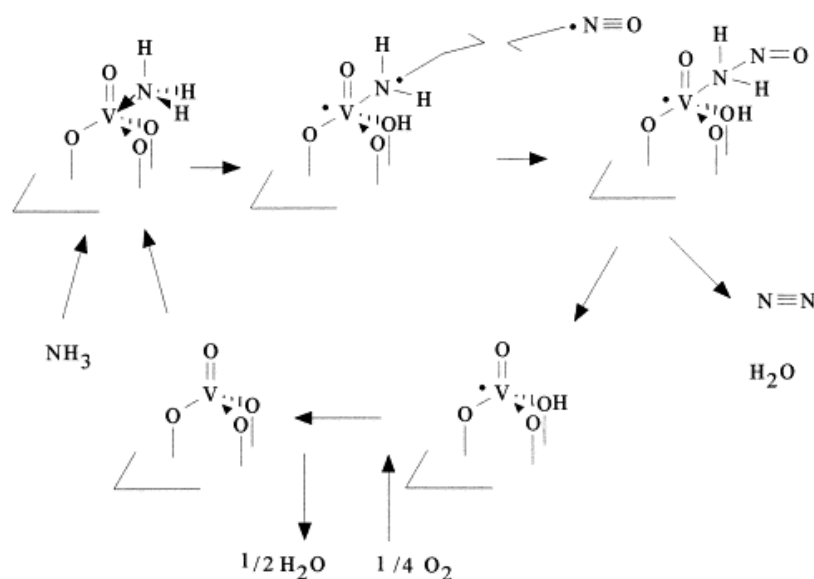


Fig. 2.4 Mechanism of the NO–NH₃ reaction over vanadia-based catalysts proposed by Ramis et al. in the presence of oxygen ^[164].

On the basis of in situ FTIR studies under steady-state conditions, Topsøe et al. came up with the mechanistic scheme shown in Fig. 2.5 ^[165]. The proposed catalytic cycle consists of both acid–base and redox functions. In this mechanism, the catalytic activity is found to be related to the ammonia adsorbed on the Brønsted acid sites (V–OH). Also, V(5+)=O groups are involved in the reaction, specifically in the activation of adsorbed ammonia. Ammonia is adsorbed over a V(5+)–OH Brønsted acid site and is activated by an adjacent V(5+)=O group. This activation process involves the transfer or partial transfer of a hydrogen from the NH₃ molecule and accordingly leaves behind a reduced V(4+)–OH site. Once ammonia has been activated, NO reacts from the gas-phase with the activated ammonia complex leading to the formation of an intermediate which finally decomposes to N₂ and H₂O. The catalytic cycle is closed by the re-oxidation of V(4+)–OH to V(5+)=O by gaseous oxygen. This mechanism can be regarded as a modification of the mechanism by Ramis et al., with the Brønsted acid sites instead of the Lewis acid sites serving as the ammonia adsorption sites ^[164, 165, 172]. It is worth noting Topsøe et al. failed to follow the behavior of coordinated NH₃ because the spectral region below 1300 cm⁻¹ was cut in their spectra ^[33, 165].

The NH₃ adsorption mode on the active site has been a topic of intensive debate: whether it is found to be coordinated on a Lewis acid site or protonated to NH₄⁺ on a Brønsted acid site (V–OH). Whoever play(s) the role in adsorbing and activating ammonia, the role of nitrosamide-like intermediates which decomposes selectively to N₂ and H₂O is widely recognized ^[157, 169].

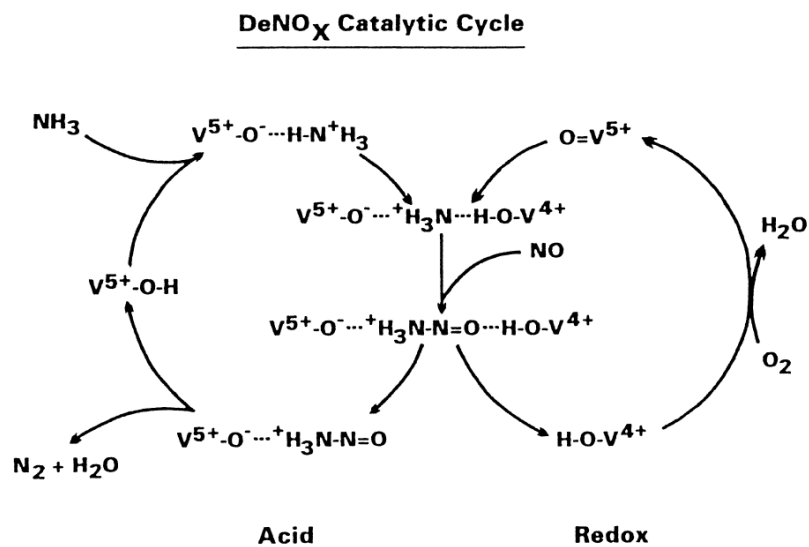


Fig. 2.5 Scheme illustrating the catalytic cycle of the SCR reaction over vanadia/titania catalyst in the presence of oxygen proposed by Topsoe et al ^[165].

Also, it is worth mentioning, particularly for commercial catalysts (low V loading, high W or Mo and Ti coverage), that other catalyst components (W or Mo, and Ti surface sites) can adsorb ammonia and participate in the reaction as "reservoir" of adsorbed ammonia species ^[169, 173]. Accordingly, a distinction should be made between the "adsorption" sites and the "reaction" sites of ammonia ^[169].

In spite of the ongoing disagreement on whether coordinated or protonated ammonia play(s) the role of reactive intermediate species, new relevant contribution appeared in the open literature, in particular concerning the reaction mechanism and the role of preoxidation of NO to NO₂ ^[144, 157, 166, 174].

With the aid of IR spectra data, Busca et al. found that the coordinated ammonia disappears upon reaction with NO and water is formed. On the contrary, protonated ammonia grows more than disappear, particularly at the first stages of reaction. They also proposed that NO is the actual reactant but the presence of NO₂ enhances the reaction rate, possibly because of its role in reoxidizing the catalyst ^[157].

Janssens et al., for the first time, constructed a consistent NH₃-SCR reaction mechanism combining the standard and fast SCR in a complete catalytic cycle capable of producing the correct stoichiometry while allowing adsorption and desorption of stable molecules only ^[175]. A consequence of the reaction scheme is that all intermediates in fast SCR are also part of the

standard SCR cycle. They also pointed out that the oxidation of an NO molecule by O₂ to a bidentate nitrate ligand is the rate-determining step for standard SCR by the use of density functional theory (DFT) calculations. It worth mentioning, however, the new reaction scheme presented was based on a Cu-CHA catalyst.

Following the same guidelines, Arnarson et al. presented a complete catalytic mechanism describing both the Standard and the Fast SCR reactions in their correct stoichiometric form on a monomeric VO₃H/TiO₂(001) catalytic model^[167]. As they previously reported, for the particular monomeric site that the most stable structure of adsorbed NH₃ was at the Brønsted acid site, protonated as NH₄⁺^[158]. The complete mechanism is presented in Fig. 2.6. It can be regarded as the simplest possible reaction path for the SCR reaction. It consists of two cycles, a NO-activation cycle (outer) and a Fast SCR cycle (inner) that share the same reduction part but use NO + O₂ and NO₂ respectively for the reoxidation. The reaction steps in the Fast SCR cycle are all inherently part of the Standard SCR reaction since NO₂ is formed in the NO-activation cycle and is consumed in the Fast SCR cycle. In excess of NO₂, the Fast SCR cycle can run independently, which is the Fast SCR reaction. The Standard SCR reaction is the sum of the black and the blue cycle.

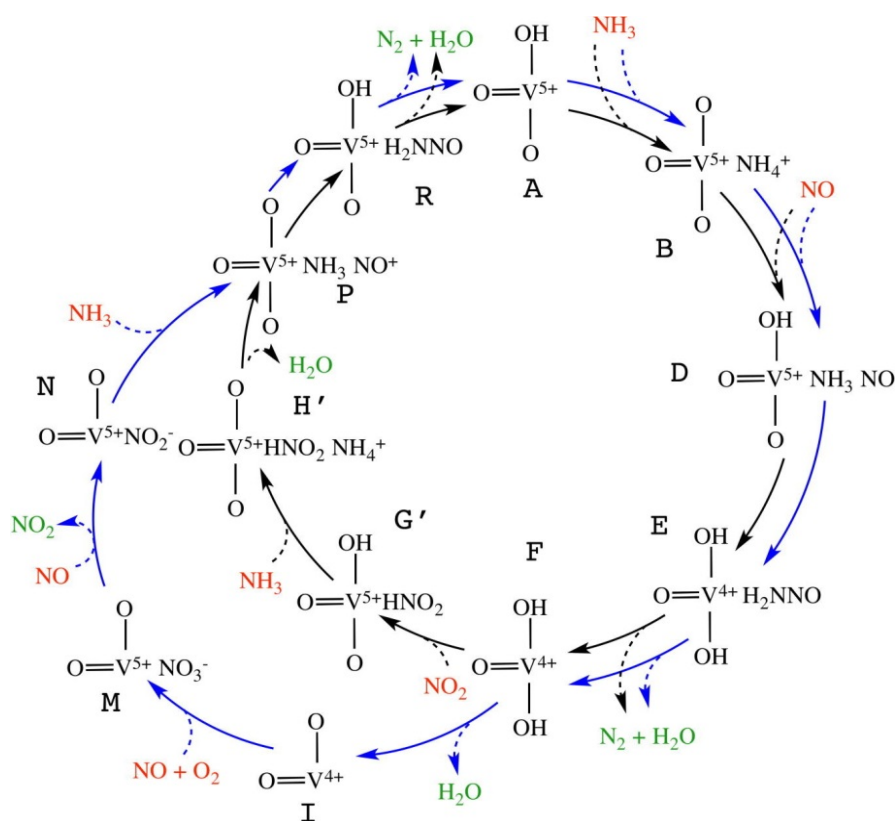


Fig. 2.6 A reaction mechanism for the SCR process proposed by Arnarson et al^[167].

Moreover, they found at low temperatures the H₂O formation and desorption is the RDS for the Standard SCR reaction. For Fast SCR, NO₂ reacts directly with the reduced site resulting in higher rate. The rate for the two reactions is the same at higher temperatures as the RDS is in the reduction part which is common to both reactions ^[167].

Now it's quite established that the SCR reaction vanadium-based catalysts is a redox process that occurs with a redox or Mars-van Krevelen-type mechanism ^[62]. Irrespective of the nature of the catalyst and the local environment of the active sites, the NH₃-SCR reaction can be divided into two parts: a reduction part where NO and NH₃ cooperate, and an oxidation part ^[62, 166, 167, 175].

2.2 Catalyst deactivation

It is inevitable that all catalysts will deactivate with time ^[176]. Catalyst deactivation, a drop of catalyst activity, can occur with its origin in the nature of physical and chemical aspects ^[177]. Three particular causes of deactivation are briefly defined in Table 2.1 and reviewed in some detail in the following subsections with an emphasis on the last one.

Catalytic converters with the catalysts at the center to reduce automotive exhaust emissions may be fouled or poisoned by fuel or lubricant additives and/or engine corrosion products. If the reaction occurred at high temperatures, thermal degradation may occur in the form of active phase crystallite growth, collapse of the support pore structure, and/or solid-state reactions of the active phase with the support ^[178].

Table 2.1 Mechanisms of catalyst deactivation ^[176]

Mechanism	Type	Brief Description / Definition
Fouling(Coking)	Physical	Deposition of species from fluid phase onto the catalytic surface and blocking of surface
Poisoning	Chemical	Strong chemisorption of species on catalytic sites, thereby blocking sites for catalytic reaction
Sintering(Aging)	Thermal	Thermally induced loss of catalytic surface area, support area and active phase-support reactions

2.2.1 Mechanical deactivation (Fouling)

Fouling is the physical (mechanical) deposition of species from the fluid phase onto the catalyst surface, which results in activity loss due to blockage of sites and/or pores^[178].

This mechanism of deactivation is common to reactions involving hydrocarbons. It results from a carbonaceous (coke) material being deposited on the surface of a porous catalyst although carbon- and coke-forming processes also involve chemisorption of different kinds of carbons or condensed hydrocarbons that may act as catalyst poisons^[178]. The schematic of deactivation by coke forming is depicted in Fig. 2.7.

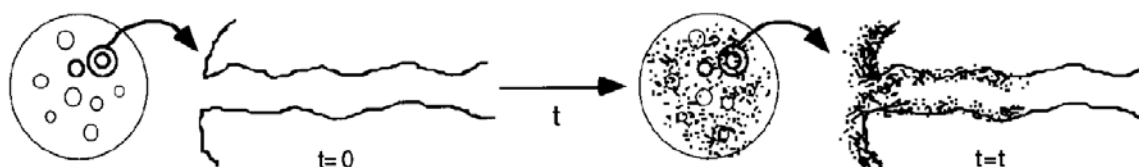


Fig. 2.7 Schematic of deactivation by coke forming.

2.2.2 Chemical deactivation (Poisoning)

Poisoning is the loss of activity due to the strong chemisorption of reactants, products, or impurities on sites otherwise available for catalysis^[178]. Thus, poisoning has operational meaning: whether a species acts as a poison depends upon its adsorption strength relative to the other species competing for catalytic sites^[178].

In addition to acting simply by physically blocking adsorption sites, adsorbed poisons may Moreover, a poison may. Poisons can also.

Adsorbed poisons can bring following effects:

- i. Inducing changes in the electronic or geometric structure of the surface^[178];
- ii. Altering the adsorptivity of other species essentially by an electronic effect^[177];

- iii. Modifying the chemical nature of the active sites or result in the formation of new compounds (reconstruction) so that the catalyst performance is undoubtedly changed [177].

It's noteworthy to make a distinction between poisons and inhibitors: the interaction of poisons with the active sites is usually strong and irreversible, whereas the adsorption of inhibitors onto the catalyst surface is generally weak and reversible [177].

Actually, poisoning itself may be reversible or irreversible [178]. In the first case, the poison is not too strongly adsorbed and accordingly reactivation of the catalyst is usually achieved by simply removing the poison from the feed. This is the case, for instance, of oxygen-containing compounds (e.g. H_2O and CO_x) impacting the catalysts for ammonia synthesis. These compounds can hinder nitrogen adsorption, thus diminishing the catalyst activity, but elimination of these compounds from the feed and reduction with hydrogen to remove the adsorbed oxygen can restore the iron surface [177]. Thus, these gaseous catalyst poisons are called temporary poisons which lower the activity only while present in the synthesis gas [179]. However, gross oxidation with oxygen results in bulk changes which cannot be readily reversed, causing an irreversible loss of catalyst activity. In other cases, poisons such as sulfur accumulate upon the catalyst surface, resulting in irreversible poisoning and may be detected by chemical and spectroscopic analysis. They are permanent poisons.

The poisoning reaction should be viewed like any other chemical reaction between a gas phase reactant and the solid surface, where the poisoned sites are distributed throughout the catalyst pore structure as a function of poison diffusion into the catalyst and the rate of the poisoning reaction [180].

2.2.3 Thermal deactivation (Sintering / Aging)

Thermal deactivation usually refers to a physical process where the active surface area of the catalyst shrinks via structural changes [14]. This process is often designated as sintering, and is physical in nature [177]. It occurs, unequally, to both the catalyst support and active phase, based on exhaust gas conditions [14, 178].

2.2.3.1 Support sintering

Heterogeneous catalysis is an interface phenomenon and it is advantageous to prepare catalysts with the highest possible surface area with the aid of support [181]. Thermodynamically, this is an unfavourable state since minimal surface free energy is associated with material coalesced into a sphere. Thus, there is always a tendency for catalysts to sinter and the driving force for sintering is to lower the surface energy [77, 181].

When sintering occurs over supported metal catalysts, the loss of support area due to support collapse can happen [176]. The transport of material leads to coalescence of particles, particle growth and closure of the pores [77]. When it occurs, surface area shrinks, porosity alters and the activity of catalysts drops [77].

Temperature, particle size and the atmosphere are three main parameters determining the sintering of a given support [77]. Among them, studies showed that temperature and the atmosphere were two factors mostly affecting sintering rates of supported metal catalysts [177].

It is useful to consider the behavior of alumina as a particular example when examining the support materials sintering since this support is one of the most common materials as support for in oxidizing atmospheres and exhibits many of the sintering characteristics.

In the case of alumina, temperature plays a major part in its sintering which is accompanied by phase transformation (Fig. 2.8) [77, 178, 182]. Obviously, sintering becomes much more significant at higher temperatures.

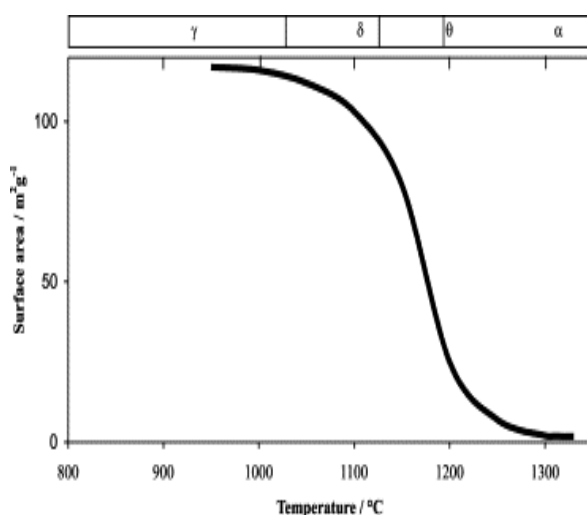


Fig. 2.8 Phase transformation and specific surface area of alumina.

The reaction atmosphere also affects the sintering: water vapor accelerates support sintering by forming mobile surface hydroxyl groups that are subsequently removed at higher temperatures (Fig. 2.9) ^[77, 178, 181].

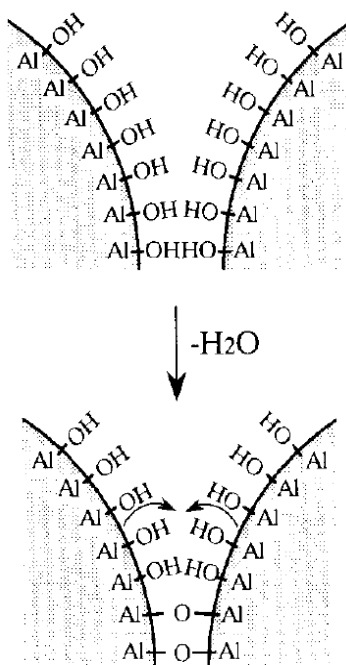


Fig. 2.9 Schematic of surface dehydroxylation from contact area of two adjacent particles.

2.2.3.2 Active phase sintering

Sintering occurs both in supported metal catalysts and unsupported catalysts ^[177]. Most of the previous sintering studies concentrate on supported metals: the active metals are usually deposited on a carrier in a form of small particles (crystallites) ^[77, 178].

Active phase sintering generally occurs via agglomeration and coalescence of small metallic particles into larger ones ^[77]. This leads to a drop of the surface-to-volume ratio and a decrease in precious metal dispersion ^[14]. As a result, there is less surface exposed to the reactants for catalysis.

Two sintering models have been proposed for supported metal catalysts: a), atomic migration, and b), crystallite migration ^[77, 177]. Atomic migration involves detachment of metal atoms or molecular metal clusters from crystallites, migration of these atoms over the support surface,

and ultimately, capture by larger crystallites because the larger crystallites require a low concentration of migrating metal atoms to reach equilibrium ^[14, 178, 183]. Crystallite migration model suggests that the metal crystallites themselves travel along the surface, followed by collision and coalescence ^[14, 178]. Wanke et al. suggested that crystallite migration may be feasible in the early stages of sintering, but it is unlikely to be the prevailing mechanism throughout the entire process ^[14, 184]. The processes of atomic and crystallite migration are vividly illustrated in Fig. 2.10 ^[178].

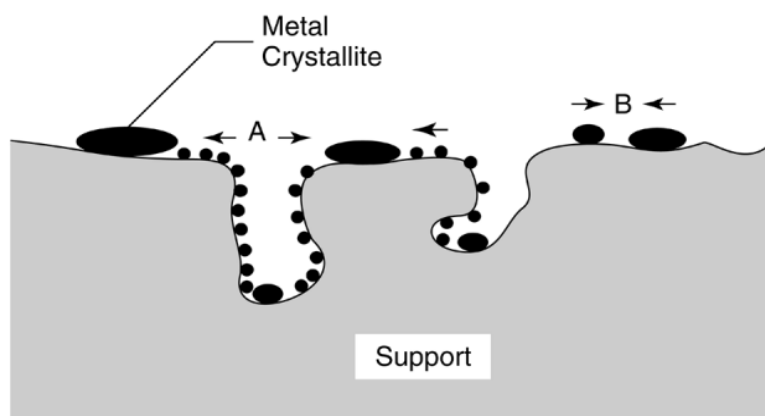


Fig. 2.10 Two principal mechanisms of metal crystallite growth due to sintering: (A), atomic migration, and (B), crystallite migration ^[178].

The nature of metal and the carrier would definitely affect the metal sintering. Also, the temperature and to a less degree the reaction atmosphere controls the metal sintering ^[77].

Experimental observations proved that temperature had remarkable effect on the extent of sintering: the higher the temperature, the higher the sintering; and the longer the high temperature exposure, the higher the sintering ^[14, 178, 185].

When investigating the sintering-induced redispersion of supported platinum in oxygen, Fiedorow et al. found that at higher temperatures, rapid, time-dependent decreases in dispersion occurred ^[186]. At high temperatures, Pt activity decreases due to thermal degradation. In the same way, Pd-based catalysts are also deactivated by high temperature exposure, which can cause sintering and decomposition of the active PdO to Pd, thereby decreasing catalyst activity ^[77]. The sintering of Pt and other precious metals generally occurs at high temperatures (more than 600 °C) ^[14].

In terms of atmosphere, oxidizing environment tends to cause more rapid sintering compared to sub-stoichiometric conditions, especially at high temperatures ^[14, 183, 187, 188]. For example, the sintering of platinum is reported to be higher in oxidizing environment compared to neutral or reducing environments ^[183].

Water vapor also increases the sintering rate of supported metals, likely through chemical-assisted sintering effects ^[178].

2.3 Effects of biodiesel on engine-out emissions and on catalytic after-treatment systems

Biodiesel is a renewable, alternative diesel fuel of domestic origin derived from a variety of fats and oils by a transesterification reaction ^[189]. It is defined by the American Society for Testing and Materials (ASTM) as "a fuel comprised of mono-alkyl esters of long-chain fatty acids derived from vegetable oils or animal fats, designated B100" ^[190].

Pure biodiesel contains approximately 10% oxygen on the basis of mass. Nevertheless, many of these fuels were not as pure as was originally intended because of high levels of impurities in the feedstocks ^[191]. These fuels covered a very wide range of feedstocks as well as systematically varying chemical properties such as fatty acid chain length and number of double bonds in the fatty acid chain ^[191].

Besides being renewable and of domestic origin, advantages of biodiesel include biodegradability, reduction of most regulated exhaust emissions, miscibility in all ratios with conventional diesel, and compatibility with the existing fuel distribution infrastructure ^[192].

In practical use, it is typically blended with petroleum diesel at levels up to 20% (B20), bearing the potential to replace some of the conventional diesel market ^[193]. The high presence of oxygen in the fuel leads to a reduction in emissions of hydrocarbons (HC) and toxic compounds, CO, and PM when biodiesel blends are burned in diesel engines ^[189, 193]. These reductions are robust and have been observed in numerous engine and vehicle testing studies ^[193].

Technical problems with biodiesel include oxidative stability, cold flow, and increased NO_x exhaust emissions [192, 194]. Engine dynamometer studies reviewed in a 2002 report from EPA show a 2% increase in oxides of nitrogen (NO_x) emissions for B20 [193].

Another problem associated with biodiesel is the possible introduction of metallic contaminants from the production process [195]. The biodiesel processing flow diagram was illustrated in Fig. 2.11 [196]. The transesterification process occurs in the presence of a catalyst, typically sodium hydroxide or potassium hydroxide. Following transesterification and separation of the glycerin, the biodiesel must go through the purification process to get rid of the impurities. In this process, residual amounts of sodium (Na) or potassium (K) from the catalyst can remain, though [197]. Meanwhile, small amounts of calcium (Ca) or magnesium (Mg) can be added to the fuel during the purification process [197]. These metallic fuel contaminants can be converted in the combustion process and form an inorganic ash that can be deposited onto the diesel exhaust emission control devices, causing negative impact [197].

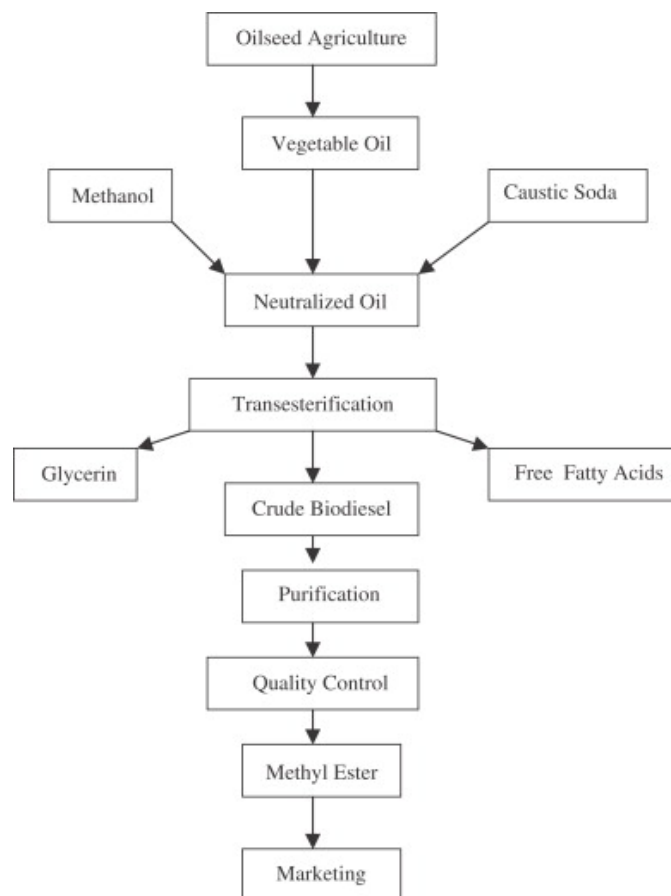


Fig. 2.11 Biodiesel processing flow diagram [196].

2.3.1 Effects of biodiesel on engine-out regulated emissions

The emission impacts of biodiesel in different kinds of diesel engine have been investigated by a number of studies [198 - 204].

A major review was conducted by the U.S. Environmental Protection Agency (EPA) and the average emission changes for B20 from statistical analysis were shown in Table 2.2 [193, 205]. Fig. 2.12, taken from the same EPA report, shows the overall trends as a function of biodiesel content for all four regulated pollutants [193, 205]. Compared to conventional diesel, use of biodiesel is generally found to result in reduction of emissions of HC, CO and PM, with the exception of increased NO_x emissions [193].

Table 2.2 Average emissions change for B20 from published engine dynamometer data in the EPA review [205]

Pollutant	Percent Change
HC	-21.1
CO	-11.0
NO _x	+2.0
PM	-10.1

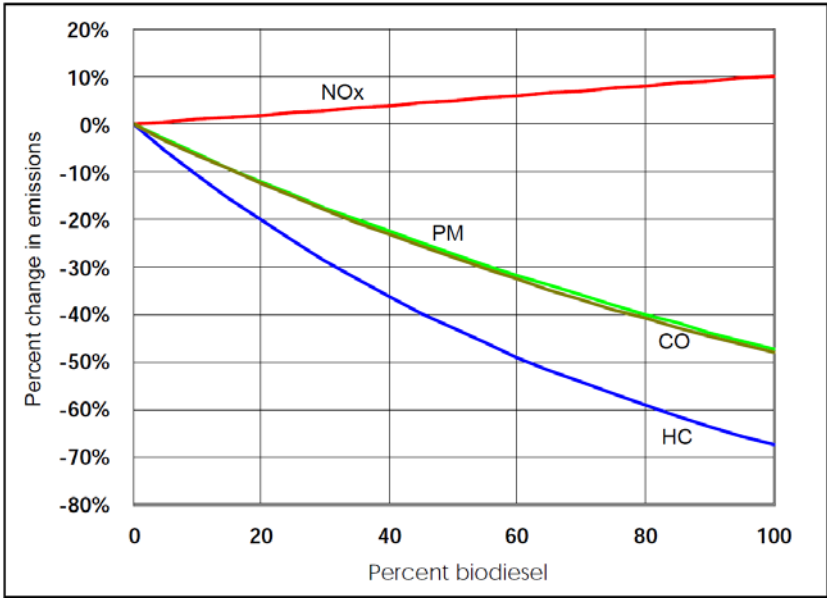


Fig. 2.12 Average emission impacts of biodiesel content as estimated from published engine dynamometer data in the EPA study [205].

In their study, McCormick et al. reviewed and summarized relevant literature concerning biodiesel NO_x effect, and pertinent theories to explain this effect [190]. In modern diesel

engines, several factors related to fuel composition and engine control strategies are important, though no single theory provides an adequate explanation of the biodiesel NO_x effect under all conditions^[190].

2.3.2 Effects of biodiesel on the DOC

When it comes to the effects of biodiesel on the DOC, it is mainly about the impacts brought by the contaminants from biodiesel. The main contaminants are K, Na, Mg, Ca, P and S.

Alkali metals are well known poisons for catalysts and have been shown to negatively impact the mechanical properties of ceramic substrates^[206].

Cavataio et al. exploited a laboratory flow reactor study to determine the durability impact of alkali metal (K and Na) exposure on three Pt/Pd-based DOCs. By evaluating for changes in CO and HC light-off to acquire the activity impact on the contaminated DOCs, they found that contamination levels of 3.0 wt% Na had a higher negative impact on Pt-based DOC for T-50 CO and HC light-off^[207].

Williams et al. conducted a study to determine if a fuel containing metals (K, Na, Ca and Mg) at the ASTM limits could cause adverse impacts on the performance and durability of diesel emission control systems. Their results demonstrated that a decrease in DOC activity was seen after exposure to 150,000 mile equivalent aging, resulting in higher HC slip and a reduction in NO₂ formation^[197].

In another study, Williams et al. investigated the metal exposure of alkali and alkaline earth metal impurities (K, Na and Ca) on diesel exhaust catalysts^[208]. The studied exhaust systems included a diesel oxidation catalyst (DOC), selective catalytic reduction (SCR) catalyst, and diesel particulate filter (DPF). The electron probe microanalysis (EPMA) imaging of aged catalyst parts found that both the K and Na penetrated into the washcoat of the DOC, while Ca remained on the surface of the washcoat.

Lance et al. aimed to elucidate the potential of alkali and alkaline earth metal impurities (K, Na, Ca and Mg) to degrade diesel emissions control systems^[209]. Na, in particular, was found to have minimal impact on DOC activity.

The sulfur originated from the fuel and lubricants is oxidized in the engine, predominantly forming SO₂. When the flue gases are passing over an oxidizing catalyst, a significant part of SO₂ is oxidized to SO₃. Once it is formed it is stable until T>700 °C [77]. It can act as a catalyst poison or interact with water vapor to form sulfuric acid and contribute to additional problems/emissions [77]. The presence of sulfur on the DOC results in the deterioration of its CO oxidation performance, and more significantly affects the oxidation of HC [14, 22].

2.3.3 Effects of biodiesel on the SCR

Commercial V/Ti-based SCR catalysts generally have to be cleaned or substituted due to the accumulated deactivation by alkaline metals that exist in exhaust gases [210]. This deteriorates when it comes to the utilization of biomass (straw, wood) because the biomass-fired flue gas becomes highly poisonous due to increased contents of potassium and sodium (almost up to 2 wt.%) [211 - 213]. Thus, in the case of biodiesel, its impact on SCR system, particularly the effects from the metal impurities, should be examined.

The study conducted by Lisi et al. offered us some general idea on the effect of deposition of alkali metals on SCR catalysts, though the catalyst was targeted for the stationary applications [214]. The negative impact of alkali metals (K and Na) on vanadia-based SCR catalysts was illustrated. The explanation for this was thought to be a significant loss of surface acidity which itself is result from the alkali metals deposited on the catalysts surface. It occurs in the way that acid sites were neutralized by alkali metals. In terms of neutralizing effect, potassium seems stronger than sodium. Specifically, the catalyst exposed to 0.18 wt.% of Na resulted in a 40% reduction in NO conversion [197].

Cavataio et al. employed a laboratory flow reactor study to determine the durability impact of alkali metal (Na and K) exposure on vanadium-based SCR catalysts [207]. They concluded that SCR catalysts showed significant irreversible deactivation in the NO_x activity and NH₃ storage capacity due to the alkali metal (Na and K) exposure. Specifically, increased amounts of K contamination led to the linear decline of BET surface area, NH₃ storage capacity, and the subsequent NO_x conversion [207].

Williams et al. conducted a study to determine if a fuel containing metals (K, Na, Ca and Mg) at the ASTM limits could cause adverse impacts on the performance and durability of diesel

emission control systems ^[215]. It turned out that the metal-zeolite SCR catalyst experienced a slight loss in activity after exposure to 435,000 mile equivalent aging.

In another study, Williams et al. investigated the metal exposure of alkali and alkaline earth metal impurities (Na, K and Ca) on SCR catalyst ^[208]. The electron probe microanalysis (EPMA) imaging of aged catalyst parts found that both the Na and K penetrated into the washcoat of the SCR catalysts, while Ca remained on the surface of the washcoat. They also showed that the first inch of the SCR catalysts exposed to Na and K had reduced NO_x conversion and NH₃ storage capacity. The SCR catalyst exposed to Ca had similar NO_x conversion and NH₃ storage performance compared to the catalyst aged with ultra-low sulfur diesel (ULSD).

CHAPTER 3: EXPERIMENTAL

3. Experimental

In this chapter, the lab-scale devices, devoted to studies on both monolith and powder catalysts for diesel exhaust cleaning-up, will be described first. Subsequently, the characterization techniques pertinent to this thesis are detailed.

3.1 Description of lab-scale devices

3.1.1 Experimental device for monolithic catalysts

3.1.1.1 Experimental device for monolithic DOC

The apparatus for the catalytic activities tests of DOC, shown schematically in Fig. 3.1, mainly comprised three parts: gas-supply system (see 1 in Fig. 3.2), catalytic reactor (see 3 in Fig. 3.2) and analytical instrumentation (Detectors, see 6 in Fig. 3.2).

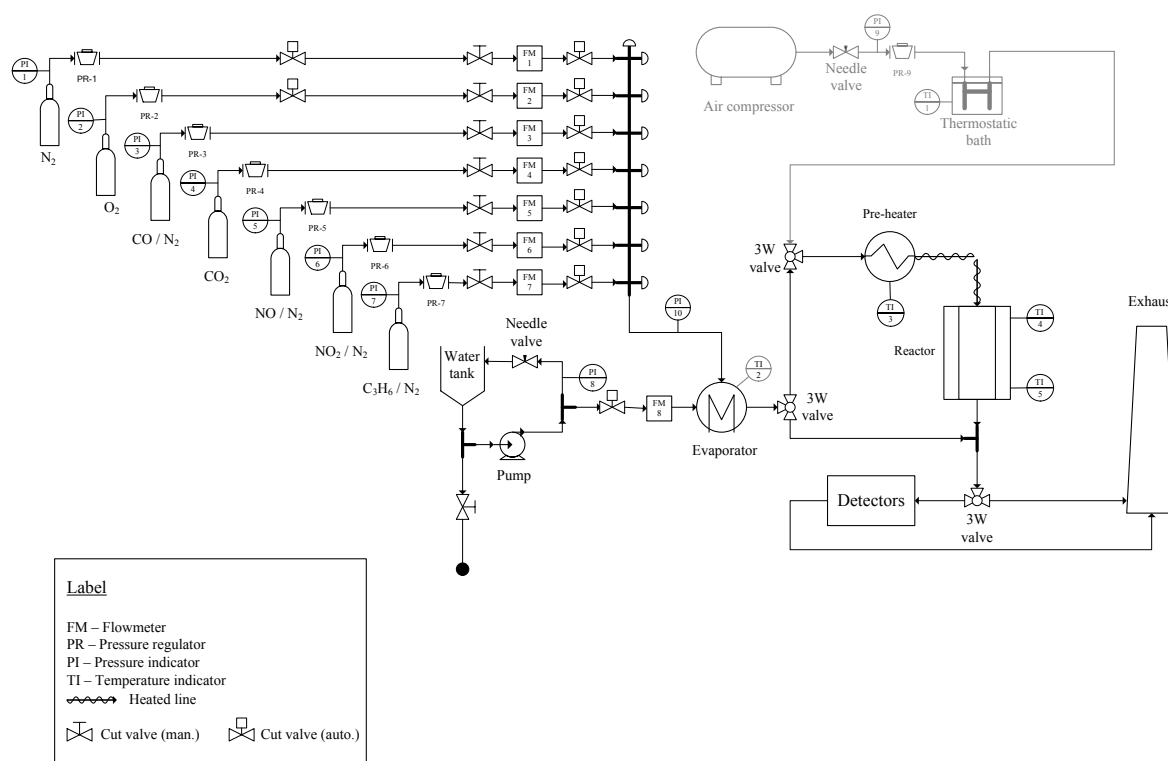


Fig. 3.1 Schematic overview of synthetic gas bench (SGB) plant for monolithic DOCs study.

As the name *synthetic gas bench (SGB)* suggests, several gases were used in order to obtain the desired reaction mixtures. All bottles of gas were supplied by Air Liquide (France). The description of supplied gas cylinders can be found in Table 3.1.

Table 3.1 Description of the gases used for monolithic DOCs study

Gas Cylinder	Composition of the gas cylinder (vol.%)
N ₂	100% N ₂
O ₂	100% O ₂
CO ₂	100% CO ₂
CO	0.5% CO + 99.5% N ₂
NO	0.8% NO + 99.2% N ₂
NO ₂	1.5% NO ₂ + 98.5 % N ₂
C ₃ H ₆	5.0% C ₃ H ₆ + 95.0% N ₂

The desired concentrations of the reactant gases were obtained by blending C₃H₆ (as a representative hydrocarbon), NO₂, NO, CO, CO₂, O₂ and N₂. The synthetic gas mixtures were controlled by mass flowmeters (*Brooks*). Water vapor (up to 5 vol.%) was added to the mixture when it passed through a water saturator.

The resulting stream was then redirected to a 3-way valve which offered two options: a), guiding the stream through the pre-heater and then through heated lines to the reactor; b), by-passing the reactor.

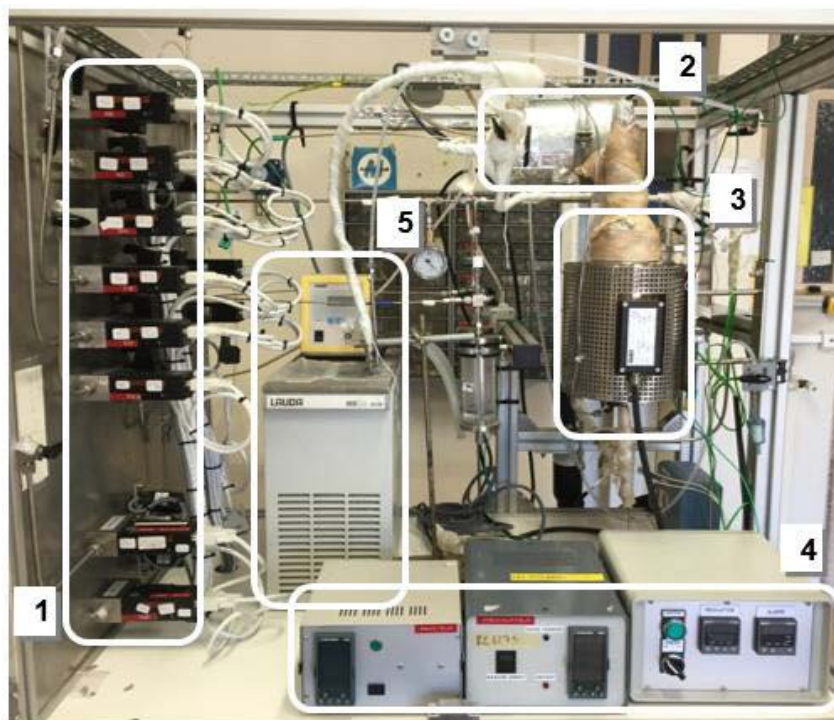
With the aid of the pre-heater as well as the heated lines, a proper heating of the stream before entering the reactor was ensured and made the gap between the temperatures upstream and downstream the monolith as small as possible. As such, the temperature field of the catalyst could be homogeneous.

The detectors exploited were listed in Table 3.2.

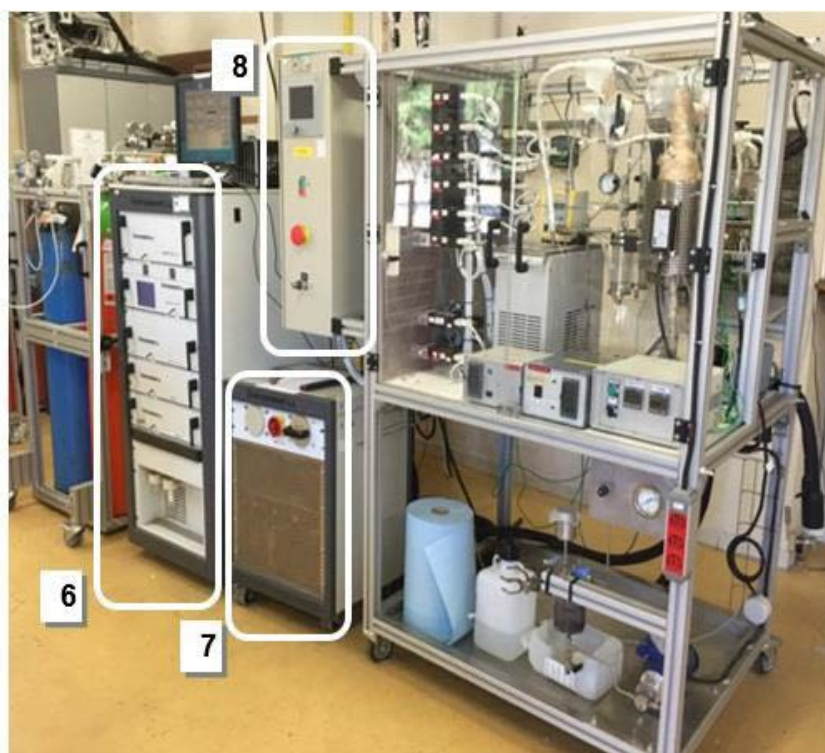
Table 3.2 Detectors of synthetic gas bench (SGB) plant for monolithic DOCs study

Detector	Component
Flame ionisation detector (<i>Environnement SA GRAPHITE 52M</i>)	HCS
Chemiluminescence analyzer (<i>Environnement SA TOPAZE 32M</i>)	NO/NO ₂
Infrared analyzer (<i>Environnement SA MIR 2M</i>)	CO/CO ₂ / O ₂ / N ₂ O

For the purpose of illustration, the pictures of the experimental setup were presented in Fig. 3.2.



1-Flowmeters; 2-Preheater; 3-Reactor; 4-Temperature Controllers; 5-Cooling System



6-Detectors; 7-Pumps; 8-Flowmeters Controller.

Fig. 3.2 Pictures of synthetic gas bench (SGB) plant for monolithic DOCs study.

3.1.1.2 Experimental device for monolithic SCR catalysts

The apparatus for the catalytic activities tests of SCR catalysts, shown schematically in Fig. 3.3, mainly included three parts: gas-supply system, catalytic reactor and analytical instrumentation (Detectors).

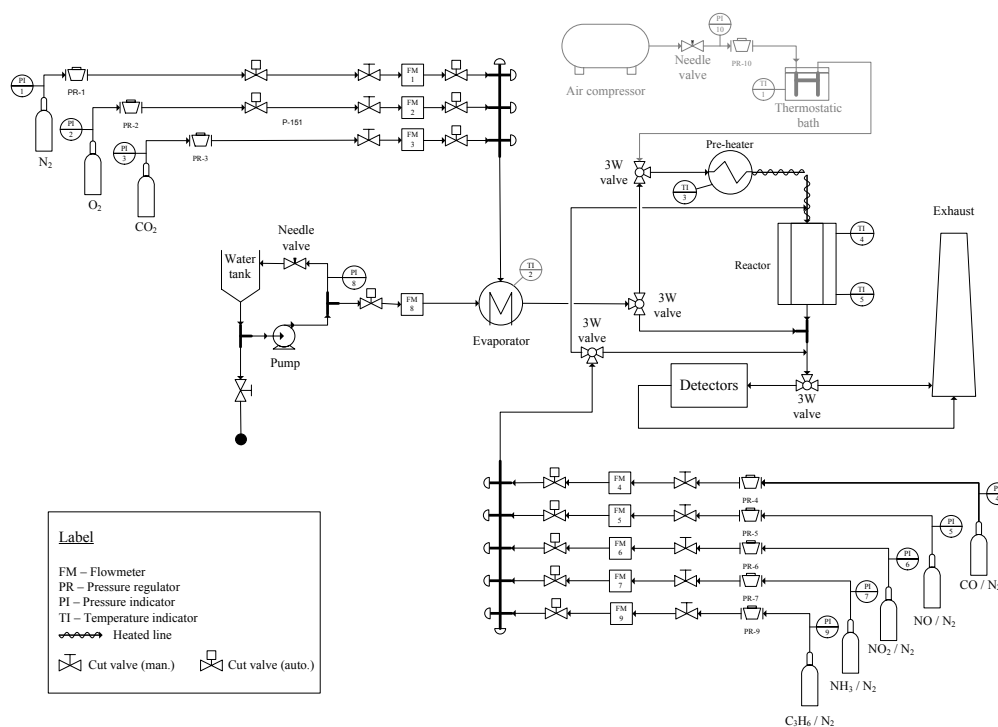


Fig. 3.3 Schematic overview of synthetic gas bench plant for monolithic SCR catalysts study.

As the name *synthetic gas bench (SGB)* suggests, several gases were used in order to obtain the desired reaction mixtures. All bottles of gases were supplied by Air Liquide (France). The description of supplied gas cylinders can be found in Table 3.3.

Table 3.3 Description of the gases used for monolithic SCR catalysts study

Gas Cylinder	Composition of the gas cylinder (vol.%)
N ₂	100% N ₂
O ₂	100% O ₂
NO	0.8% NO + 99.2% N ₂
NO ₂	1.5% NO ₂ + 98.5 % N ₂
NH ₃	1.0% NH ₃ + 99.0% N ₂

The desired concentrations of the reactant gases were obtained by blending NH_3 , NO_2 , NO , O_2 and N_2 . The synthetic gas mixtures containing N_2 and O_2 , controlled by mass flowmeters (*Brooks*), were passed through a water saturator (to provide 5 vol.% H_2O).

The detectors employed in this plant were presented in Table 3.4.

Table 3.4 Detectors of synthetic gas bench (SGB) plant for monolithic SCR catalysts study

Detector	Component
Fourier Transform UV analyzer (<i>Environnement SA UV-TF</i>)	NH_3
Chemiluminescence analyzer (<i>Environnement SA TOPAZE 32M</i>)	NO/NO_2
Infrared analyzer (<i>Environnement SA MIR 2M</i>)	$\text{CO}/\text{CO}_2/ \text{O}_2/ \text{N}_2\text{O}$

3.1.2 Experimental device for DOC study in powder form

The apparatus for the catalytic activities tests of DOC in the form of powder, was shown schematically in Fig. 3.4. It is mainly composed of three parts: gas-supply system, a U-shaped reactor and analytical instrumentation (Detectors).

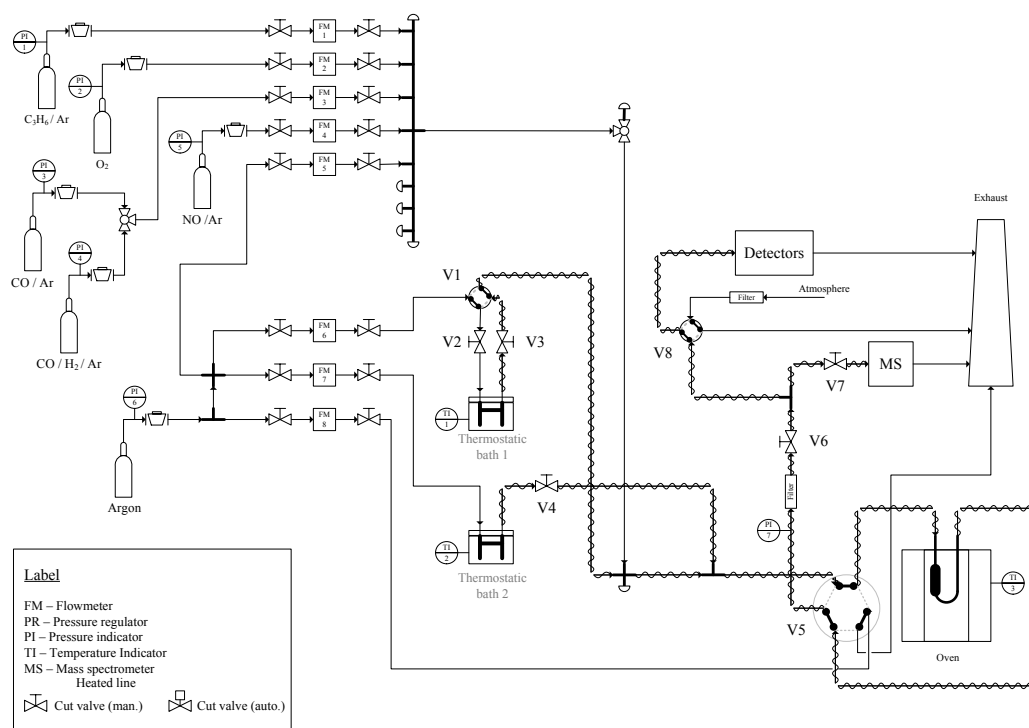


Fig. 3.4 Schematic overview of synthetic gas bench (SGB) plant for powdered DOCs study.

As the name *synthetic gas bench (SGB)* suggests, several gases were used in order to obtain the desired reaction mixtures. All bottles of gas were supplied by Air Liquide (France). The description of supplied gases can be found in Table 3.5.

Table 3.5 Description of the gases used for powdered DOCs study

Gas Cylinder	Composition of the gas cylinder (vol.%)
Ar	100% Ar
O ₂	100% O ₂
CO	0.972% CO + 99.028% Ar
NO	0.977% NO + 99.023% Ar
NO ₂	0.9% NO ₂ + 99.1 % Ar
C ₃ H ₆	0.5% C ₃ H ₆ + 99.5% Ar

The desired concentrations of the reactant gases were obtained by blending C₃H₆ (as a representative hydrocarbon), O₂, CO, NO and Ar. The streams were controlled by mass flowmeters (*Brooks Series 5850E*). Part of Ar will be fed to the water saturator inside the thermostatic bath 1 (to provide 3 vol.% H₂O in the system).

The stream containing the gases previously mixed, joined the stream coming from the water saturator. The resulting stream will be directed to a 6-way valve. The 6-way valve was fed by three inlet streams and connected to three outlet streams. It determined whether the resulting stream would go to the reactor or otherwise to the by-pass.

The reactors used in this set-up were Pyrex U-shaped tubes (L: 23 cm; ID: 2 cm). It had a reactional chamber where a porous quartz filter (porous type nr. 3) holds the catalyst.

As far as the detectors were concerned, they were detailed in Table 3.6.

Table 3.6 Detectors of synthetic gas bench (SGB) plant for powdered DOCs study

Detector	Component
Flame ionisation detector (<i>Siemens FIDAMAT 5E</i>)	HCs
Infrared analyzer (<i>Siemens Ultramat 9</i>)	CO/CO ₂
Infrared analyzer (<i>Siemens Ultramat 9</i>)	N ₂ O
Chemiluminescence analyzer (<i>Eco Physics CLD 700 AL</i>)	NO/NO ₂

For the sake of illustration, the picture of the experimental setup was shown as Fig. 3.5.

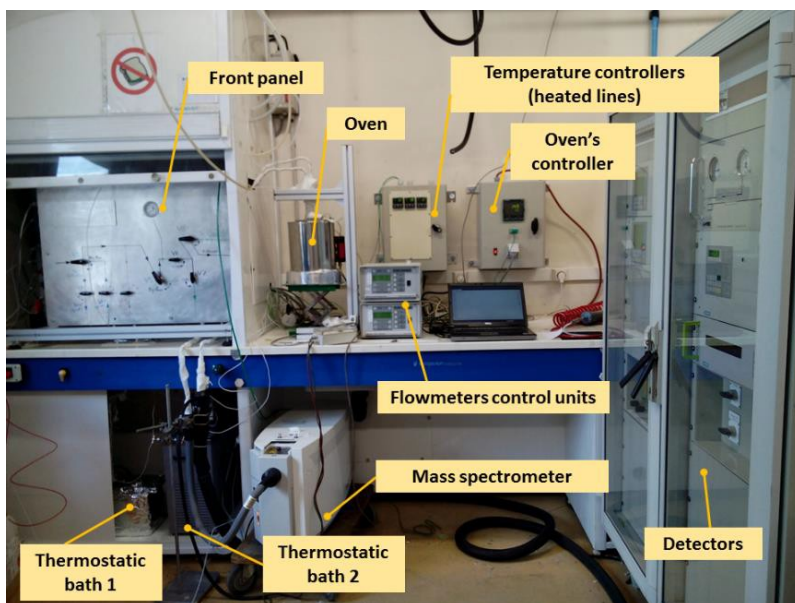


Fig. 3.5 Picture of synthetic gas bench (SGB) plant for powdered DOCs study^[75].

3.2 Characterization techniques

To get an idea of the feature of the catalyst, physiochemical characterization techniques are necessary. The techniques used in this thesis are:

- X-Ray Diffraction (XRD), in order to identify the crystalline phase of the supports and some metal species, particularly metal oxides and metallic particles in the study;
- Transmission Electron Microscopy (TEM), in order to identify palladium, platinum particles and to estimate the particle size;
- BET (Brunauer-Emmett-Teller) surface measurements, in order to follow the accessible surface for chemical reaction;
- H₂-Temperature Programmed Reduction, in order to know the oxide phases presented in the catalysts.

3.2.1 XRD

XRD can be used to get an idea of the crystallinity of the material. Also, it allows the identification of the different crystallographic phases presented in the catalyst, particularly some metal oxides and metallic particles.

The diffraction of a monochromatic beam of X-ray by a crystalline compound is the basis of this characterization technique: The monochromatic beam of X-Ray source (Cu-K α radiation, $\lambda=0.15418$ nm) is focused on the sample with different incident angles; at certain angles, if the sample is composed by one or more crystalline phases, the incident radiation is diffracted to the X-Ray detector. This phenomenon is described by Bragg's Law^[216]:

$$2d \sin \theta = n\lambda$$

Where, n is the positive integer number, λ wavelength of incident radiation, d interplanar distance (nm), θ Bragg's Angle at which the diffraction phenomenon occurs (degrees).

Diverse crystallographic phases are characterized by diffraction peaks at certain angles, with a given intensity that is up to the interplanar distance of the crystalline phase.

The diffraction patterns of PdO (ICDD 03-065-5261) and Pt (ICDD 00-004-0802) most common crystalline structures, obtained from the *PDF-2 Release 2005* database, are presented in Fig. 3.6.

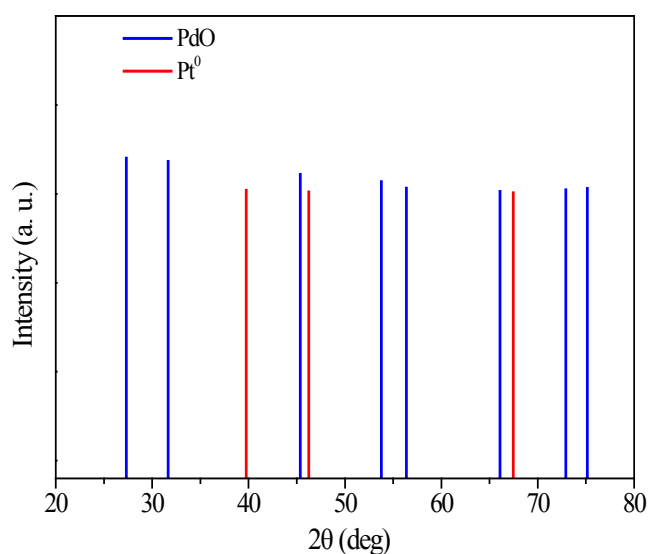


Fig. 3.6 XRD patterns obtained from the *PDF-2 Release 2005* database for PdO and Pt⁰.

In this thesis, powder XRD patterns of each catalyst were acquired on a Bruker D8 Advance diffractometer. XRD measurements were performed from 5 to 70° in an interval of 0.02° (2 θ) with a step time of 12s for each point during data acquisition. The powdered samples were put in an aluminum sample holder with a circular cavity (diameter of 25 mm, depth of 2 mm). The samples were pressed inside the cavity and their surface was flattened with a microscope slide. No pre-treatment was performed prior to data acquisition. Identification of the different crystalline phases was performed by comparison of the experimental XRD patterns with those from *PDF-2 Release 2005* database of the International Center for Diffraction Data (ICDD).

3.2.2 Transmission electron microscope (TEM)

The TEM uses a high-energy electron beam transmitted through a very thin sample to image and is capable of conducting the atomic level structural analysis. Combining different modes of observation on the same catalyst sample with the aid of high-performance detectors, precise information about the size, the morphology and the arrangement of the particles, crystal phases and composition can be obtained.

The high-energy electron beam is emitted through an electron gun and transmitted through the sample, indicating that TEM micrographs represent a plane projection of the tridimensional sample. High vacuum is required for the operation of the electron microscope, which means that TEM micrographs are obtained when the sample is under high vacuum conditions. This fact can be extremely important because some samples are vacuum-sensitive, suffering variations under these conditions.

If the electron microscope is sufficiently potent, a diffraction phenomenon occurs and the inter-reticular planes of a crystalline sample can be observed (*e.g.*, metallic particles). Thus, in addition to the morphological information that TEM provides, by measuring the distances between the inter-reticular planes of a sample and using the same database used for XRD, information on the nature of the crystalline sample can be obtained. However, it should be noted that some samples are sensitive to the electron beam. Taking into account that the higher the magnification, the higher the amount of energy of the electron beam, this limits the upper magnification range that can be attained on certain samples (*e.g.*, zeolites)^[217].

In this thesis, high resolution TEM (HRTEM) coupled with EDS was performed on a JEOL JEM-2011 transmission electron microscope (LaB6 cannon) with a spatial resolution of 0.16 nm operating at 200 kV. Prior to TEM, the sample was crushed and then dispersed with solvent ethanol on a carbon-coated copper TEM grid. Ethanol is added to the grid for the purpose of dispersing the crushed sample and improving its contact with the grid. Energy-dispersive X-ray spectroscopy (EDS) was performed with the probe PGT-Bruker.

3.2.3 Nitrogen adsorption measurements at 77 K

Surface area and porosity are two important textural characteristics of solid materials used for catalyst. They highly determine the properties and performance of the catalyst. Differences in the surface area and porosity of particles within a solid material can greatly influence its reactivity and thus can be useful in building the structure-reactivity relationship.

In general, the specific surface area and porosity of each catalyst can be determined by physical adsorption of nitrogen on the surface of the solid to obtain adsorption and desorption isotherms. The determination is usually carried out at the temperature of liquid nitrogen.

In this thesis, the adsorption and desorption isotherms of nitrogen were measured using a Micromeritics ASAP 2010 apparatus. It performs surface area analysis besides pore size and pore volume distributions. The calculations were carried out applying the BET (Brunauer-Emmett-Teller) method, to acquire the surface area, the average and total pore volume, the BJH (Barrett-Joyner-Halenda) pore size distribution and to conduct micro-pore analysis.

Before the measurements, the samples were evacuated at 200°C for 2 hours under vacuum (0.2666Pa) to remove gases and vapors that might have been physically adsorbed. This step it's fundamental, because if outgassing is not achieved, the specific surface area may be less or may be variable, since part of the surface area was already covered with molecules that were previously adsorbed.

3.2.4 Temperature programmed reduction (TPR)

TPR is highly useful in providing a quick characterization of metallic catalysts. This technique is capable of determining the reducibility of the catalysts: the reducible species (phases) present in the catalyst and the temperatures needed for the reduction of each species. It also can provide information on the eventual degree of reduction. For bimetallic catalysts, TPR patterns often show whether the two components are mixed or not^[218].

In this thesis, H₂-TPR measurements were conducted using a BELCAT-M-183 facility under 5 vol.% H₂ in a flow of Ar. The reason for the argon being chosen as a carrier gas for hydrogen is that it allows an optimization of the thermal conductivity discrepancy between the carrier gas and the reactant. 5 vol.% H₂ in a flow of Ar can provide enough instrument sensitivity while bearing a high safety factor.

The temperature program for TPR test was depicted in Fig. 3.7.

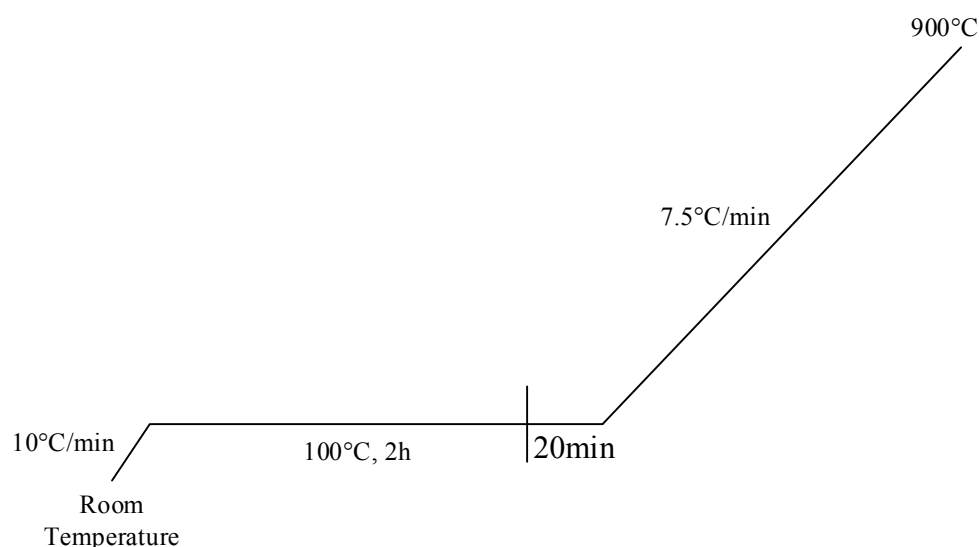


Fig. 3.7 The temperature program for TPR test.

Major steps for the H₂-TPR measurements were shown as follows:

- i. Pre-treatment: Prior to the TPR, the sample (50~60mg) undergoes a pre-treatment under flowing argon with the flow rate of 50 mL/min from room temperature (RT) to 100°C (10°C/min), kept at 100°C for 2h.

- ii. Reduction: The reduction process was carried out under a stream of 5 vol.% H₂/Ar with the flow rate of 50 mL/min, from 100°C to 900°C, at a heating rate of 7.5°C/min, while the evolution of H₂ was measured using the TCD.

**CHAPTER 4: ON THE PERFORMANCE
OF OXIDATION CATALYSTS USING
DIFFERENT AGING
CHARACTERISTICS OR/AND IN THE
PRESENCE OF ALKALI COMPOUNDS
REPRESENTATIVE OF BIOFUEL
CONTAMINANTS**

4. On the performance of oxidation catalysts using different aging characteristics or/and in the presence of alkali compounds representative of biofuel contaminants

This chapter is the first nucleus of this double-core thesis and it's mainly about the research conducted on the oxidation catalysts.

It can be divided into four main sections. In the first place, the performance of a commercial oxidation catalyst using different aging characteristics was examined. The influence of the presence of alkali compounds on the commercial honeycomb oxidation catalyst comes after it. Later, the influence of the presence of alkali compounds on a model oxidation catalyst in the form of powder was investigated. Finally, the comparison between the commercial honeycomb oxidation catalyst and the model oxidation catalyst in the form of powder was carried out.

4.1 Influence of different aging characteristics on the performance of a commercial Pt-Pd/Al₂O₃ diesel oxidation catalysts

To reduce the impact from vehicle emissions on the environment and to reach the super strict EURO VI standards, better understandings of the after-treatment systems is required. Increasingly stringed regulations on diesel engine emissions have a significant impact on the required efficiency of Diesel Oxidation Catalysts (DOC) since a complete after-treatment line is now composed by a DOC, a DPF and a NO_x abatement system (NO_x trap or NH₃-SCR) ^[14].

As the first pollution control device following the engine, lowered DOC oxidation efficiency due to thermal aging effects influences the efficiency of the exhaust cleaning-up systems downstream of the DOC and mostly on SCR systems ^[219]. It is already known that the control of the NO₂ concentration before the SCR system is pretty important, due to the so-called "FAST SCR" reactions (Eq. (20), Section 2.1.3, pg 28).

This section focuses on the catalytic behavior of the DOC using different aging characteristics of road mileage. The effect of hydrothermal aging on the reactivity and structure of a commercial DOC is investigated as a function of temperature. The goal of this study is to

understand the evolution of the active phase with the aging and to correlate these aging results with the corresponding overall catalytic activity and their impact on the reactions involved in the DOC with respect to CO, hydrocarbons and NO.

4.1.1 Experimental

4.1.1.1 Catalysts samples

The catalyst used for this study was a commercial DOC catalyst provided by Continental AG, Germany. The catalyst was composed by a bimetallic Pt/Pd (3/1 on mass basis) phase supported on alumina with a metallic loading of 80g/ft³, 400 channels per square inches (CPSI). It was cut into cylindrical "carrots" (d=2.54 cm; L=2.6 cm).

Four cylindrical "carrots" were hydrothermally aged in a laboratory box furnace (Rohde Ecotop 50, Germany) in flowing air with 10 vol.% H₂O (total flow of 19 NL.min⁻¹) under the conditions presented in Table 4.1 [220]. "F" stands for fresh, indicating no manipulation at all.

The aged catalysts are denoted as "A750", "A850_10H", "A850_24H" and "A950" respectively, because the catalysts have been aged at 750°C, 850°C and 950°C under different durations. The first two aging temperatures were chosen because they were representative of real driving cycles and the last one was selected in order to cause a severe aging of the DOC [221].

Table 4.1 Different aging methods dealing with commercial monolithic DOC

Entry	Aging conditions		
	Temp. (°C)	Duration (h)	Water (vol.%)
F	-	-	-
A750	750	4	10
A850_10H	850	10	10
A850_24H	850	24	10
A950	950	4	10

4.1.1.2 Characterization of catalysts

XRD data were recorded on a Bruker Advanced D8 using $\text{CuK}\alpha$ radiation. PXRD measurements were performed from 5 to 90° in an interval of 1° with a count time of 6s for each point. The specific surface area was obtained by using the Brunauer-Emmett-Teller (BET) method. N_2 adsorption-desorption isotherms were measured at liquid nitrogen temperature by a Micromeritics ASAP 2010. Before the measurements, the samples were evacuated at 200°C under vacuum (0.2666 Pa). High resolution TEM (HRTEM) was performed on a JEOL-JEM 2011 HR (LaB) microscope operating at 200 kV. (Presented in Section 3.2)

4.1.1.3 Catalytic activity studies

A synthetic gas bench installation was used in order to investigate the catalytic activities of these catalysts. The catalyst was put inside a stainless steel reactor, which itself was placed inside an oven reaching temperatures up to over 500°C. Two thermocouples were available to follow the reaction temperature at the inlet and the outlet of the catalyst.

A typical reactant gas mixture representative of the exhaust gases from diesel engines consists of hydrocarbon (C_3H_6 in this study), CO, NO, NO_2 , O_2 , CO_2 , H_2O and N_2 , as Mix 1 in Table 4.2. The total gas flow rate was $11.8 \text{ L}\cdot\text{min}^{-1}$ resulting in a gas hourly space velocity (GHSV) of $55,000 \text{ h}^{-1}$. Gas mixtures without NO_2 , NO, CO or NO_x were setup to investigate the influence of each gas component on the catalytic process. Table 4.2 summarized the conditions of the different experiments in terms of gas composition.

Catalysts were evaluated in terms of oxidation capacity and NO conversion for temperatures ranging from 50°C to 500°C. Exhaust gas compositions before and after the reactor were characterized by an Environnement S.A. analyzer composed of a set of modules. Among them, the TOPAZE 32M module allowed NO, NO_2 and total NO_x measurement thanks to a chemiluminescence analyzer. A MIR2M module was composed of an IR spectrogram, for the measurement of H_2O , CO and CO_2 molar fractions, and a magnetic sensor, for the O_2 molar fraction measurement. At last, a flame ionization detector (FID), present in the GRAPHITE 52M module was used for measuring total HC.

Table 4.2 Synthetic gas bench experimental conditions

	C ₃ H ₆ ppm	NO ₂ ppm	NO ppm	CO ppm	CO ₂ (%)	O ₂ (%)	H ₂ O (%)	N ₂ (%)
Mix 1	200	100	300	300	5	10	5	Balance
Mix 2	200	-	300	300	5	10	5	Balance
Mix 3	200	100	-	300	5	10	5	Balance
Mix 4	200	100	300	-	5	10	5	Balance
Mix 5	200	-	-	300	5	10	5	Balance

4.1.2 Effects of different aging characteristics on the performance of oxidation catalysts

4.1.2.1 Effect of different aging characteristics on a DOC under mixtures representative of diesel exhaust

Fig. 4.1 presents the evolution profiles of reactants of interest over studied catalysts, fresh and two aged ones, under the simulated gas condition Mix 1, which is representative of a real exhaust mixture. Compared with the fresh one, the light-off temperature of C₃H₆ over the aged ones shift to the lower temperatures, suggesting positive influence brought by the aging. In this regard, aging actually activates the catalyst and improves its performance when the aging condition is mild.

This is supported by the TEM analysis (Fig. 4.2) of the stabilized catalyst (A750): the particle distribution of the catalyst is rich and homogeneous, with the majority of particles in the range 5-25 nm. Similar results were found on Fresh catalyst (Figure not shown).

As the aging severity increases, however, sintering occurs, resulting in a drop of the specific activity of the catalyst (A950), reflected by the light-off temperature of C₃H₆ shifting to higher part. The mild hydrothermal aging of the catalyst optimizes its structure and its associated performance while further severe aging leads to the sintering of the catalyst, engendering negative influence on the conversion of C₃H₆. Similar results are obtained for CO conversion over studied catalysts, which is consistent with other study ^[220].

As for the evolution of NO_x, the stabilized catalyst (A750) stands out with more conversion of NO₂ and more formation of NO. From Fig. 4.1b and c, the conversions of NO₂ and CO can be considered as peaking simultaneously, indicating a reaction between NO₂ and CO. The NO₂ conversion after the peak is then reduced due to the increasing importance of O₂ as the

oxidizer in CO oxidation. Reactions between NO_2 and C_3H_6 are not clearly identified in these experiments. However, it is known that this reaction is possible when C_3H_6 is not burned up over the catalyst before it can selectively reduce NO_2 [222].

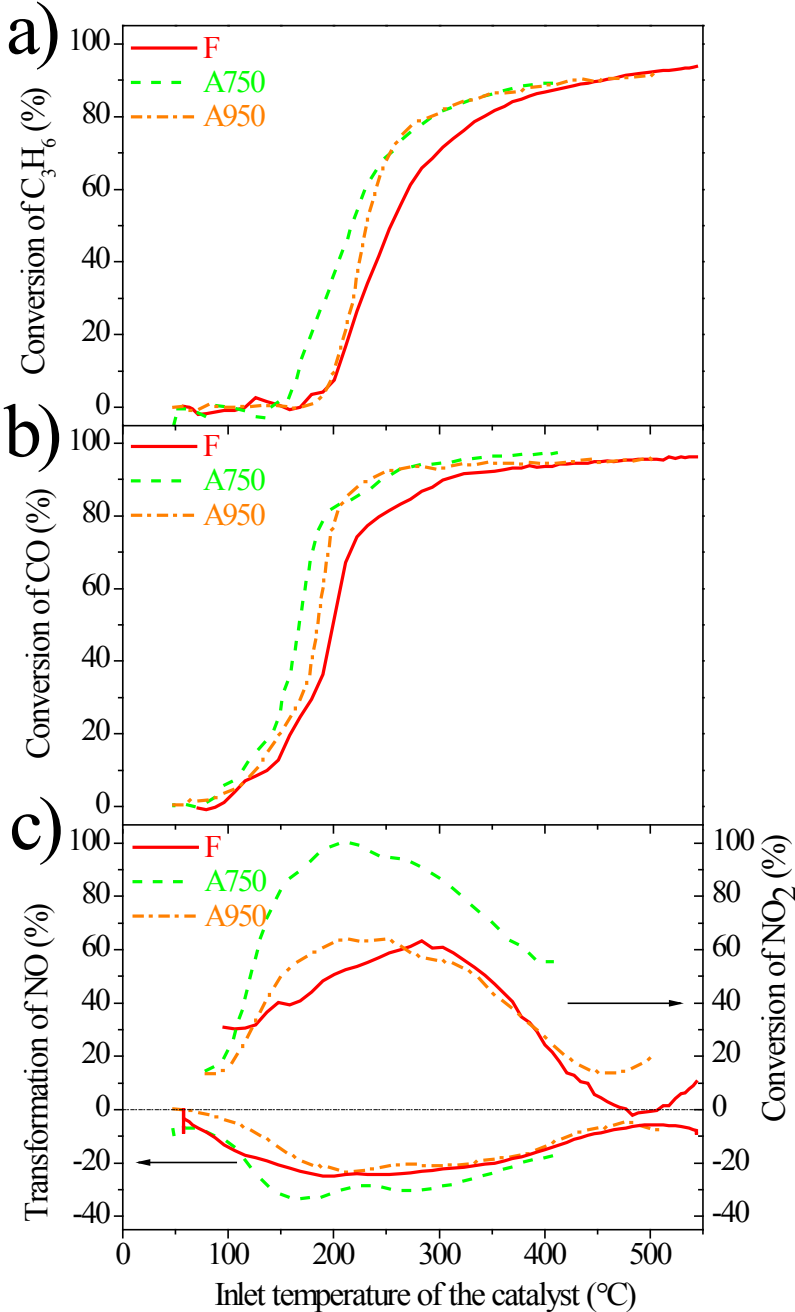


Fig. 4.1 Evolution profiles of C_3H_6 , CO and NO_x for Mix 1 versus temperature for reference and aged catalysts: (a). Conversions of C_3H_6 , (b). Conversions of CO and (c). Transformations of NO_x

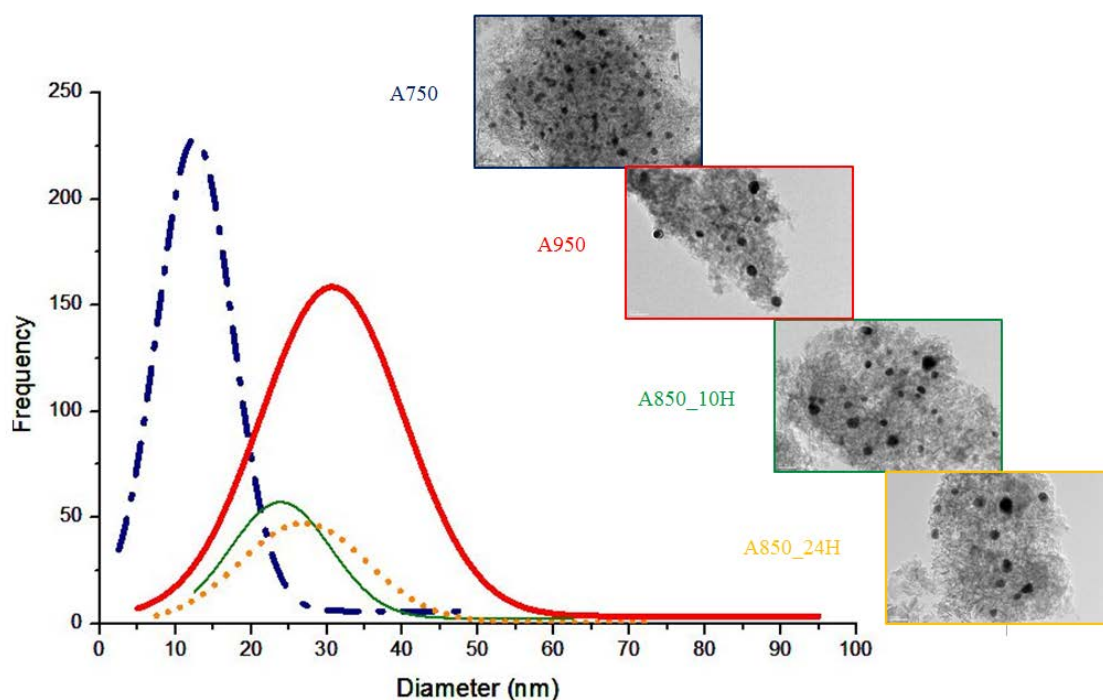


Fig. 4.2 TEM analysis of aged catalysts

Fig. 4.3 shows the evolution profiles of reactants of interest over studied catalysts, fresh and three aged ones, under the simulated gas condition Mix 2, thus in the absence of NO_2 in the feed. Compared with the fresh one, the light-off temperature of C_3H_6 over the aged ones shifts to the lower temperatures, indicating positive influence brought by the aging. This result is coherent with the results shown previously with the mixture "Mix 1", with respect to how aging affects the catalyst. As the aging severity increases, sintering occurs, resulting in a drop of the specific activity of the catalyst. As expected, the higher the aging temperature, the worse the performance of the resulted catalyst: $\text{A750} > \text{A850}_{10\text{H}} > \text{A950}$.

Similar results are obtained for CO conversion over studied catalysts. It is worth noting that the oxidation of C_3H_6 can be considered as no occurring until the complete oxidation of CO. This is attributed to the strong adsorption of CO.

As for the evolution of NO, the positive effect of aging on NO oxidation in representative mixture is quite evident: the A950 catalyst distinguishes itself from others with more conversion of NO, followed by the A850 catalyst. This might be principally due to the improved NO oxidation by O_2 , favored by bigger Pt/Pd particles. The cause of this NO oxidation activity enhancement with increased Pt particle size can be attributed to the greater resistance of larger Pt particles against forming Pt oxides, or in other words, the large Pt

particles adsorb oxygen more weakly [14, 131, 223]. Another possible reason responsible for this could be larger particles enabling stronger metal–NO bonds as reported by Benard et al. [223].

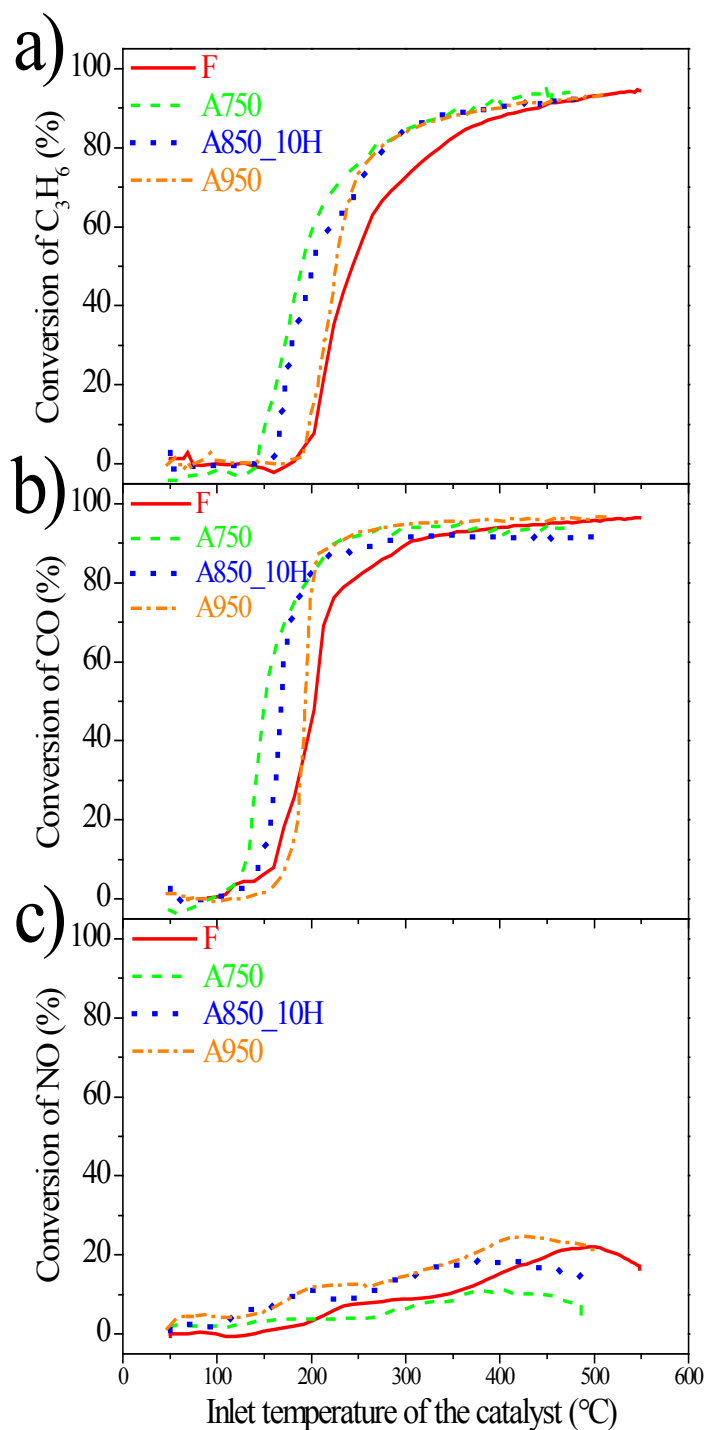


Fig. 4.3 Evolution profiles of C_3H_6 , CO and NO for Mix 2 versus temperature for reference and aged catalysts: (a). Conversions of C_3H_6 , (b). Conversions of CO and (c). Conversions of NO

Thus, it can be concluded that aging effect, which causes sintering of the particles, improves the NO conversion. It is interesting to observe that the NO conversion deteriorates with

respect to the A750 catalyst, which has the optimal activities regarding the oxidations of C_3H_6 and CO. It demonstrates that the change of the catalyst to homogeneity is not conducive to the oxidation of NO and implies different mechanisms in terms of the oxidations of these three reactants (C_3H_6 , CO and NO).

Moreover, for both fresh and aged catalysts, NO_2 is not detected at low temperature until CO is oxidized. Schmeisser et al. found that reducing agents in the lean feed such as CO and C_3H_6 hindered the formation of NO_2 [224]. Similar results have been also found in a DPNR (Diesel particulate NO_x reduction) in lean gas conditions [225].

4.1.2.2 Effect of the gas composition

In order to illustrate the effect of gas compositions on the catalytic performance of studied catalysts, different experimental conditions Mix 1 to Mix 5 were compared (Table 4.2). NO_2 is removed from the feed to form Mix 2. In Mix 3, NO is removed while CO is removed regarding Mix 4. Finally, both NO and NO_2 are removed from the feed in Mix 5.

Fig. 4.4 depicts the evolution profiles concerning C_3H_6 , CO and NO_x of fresh catalyst under different mixtures as a function of temperature. It is noteworthy that the oxidation of C_3H_6 can be considered as not occurring until the almost complete oxidation of CO, which is consistent with other studies [226]. The oxidation of CO is enhanced when NO_2 is present in the feed gas (Mix 3 and Mix 1) due to the CO/ NO_2 interaction already described elsewhere [225]. This is also supported by the simultaneously increasing conversion of NO_2 in this study (Fig. 4.4c). Moreover, the NO_2 conversion in Mix 3 is stronger than that of Mix 1, indicating the absence of NO is beneficial to the reaction between NO_2 and CO, which gives out NO. It can be ascribed to less competition for the active sites when NO is absent. Thus, the order for CO oxidation over fresh catalyst is Mix 3 > Mix 1 > Mix 2.

As expected, in terms of C_3H_6 oxidation performance, the sequence is Mix 3 > Mix 2 > Mix 1. The conversions of C_3H_6 for Mix 1 and Mix 4 can be regarded as almost the same except that the absence of CO favors the C_3H_6 conversion at temperature lower than 200°C.

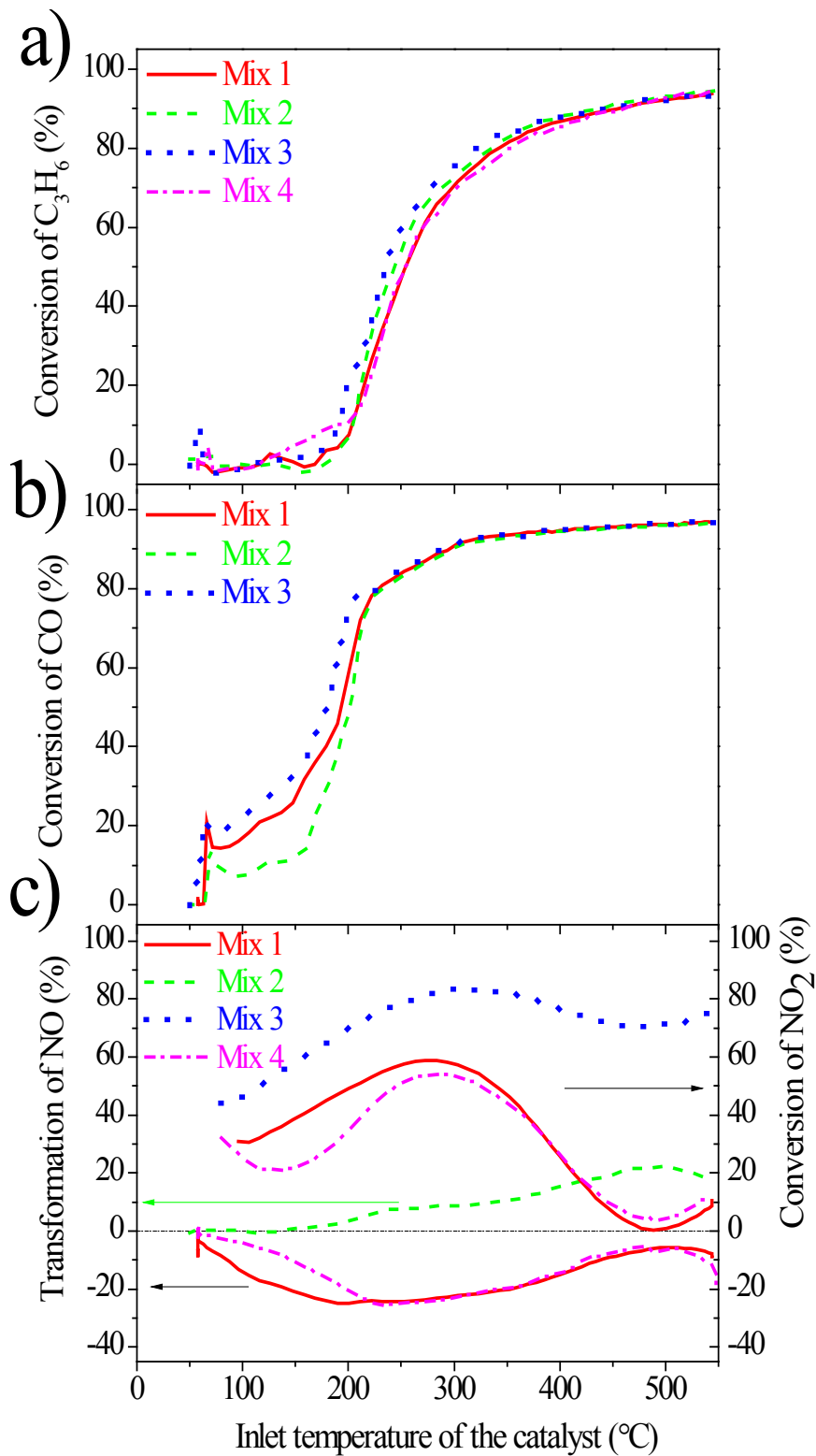


Fig. 4.4 Effect of gas compositions on the evolution profiles of fresh catalyst: (a). C₃H₆, (b). CO, and (c). NO_x

Fig. 4.5 displays the evolution profiles concerning C₃H₆, CO and NO_x of the A750 catalyst under different mixtures as a function of temperature. The reaction between NO₂ and CO at low temperature can be inferred from following observations:

- i. The comparison of the NO evolution profiles between Mix 1 and Mix 2 (mixture with and without NO₂, respectively) suggests that the presence of NO₂ contributes to the formation of NO, by reacting with CO ^[221].
- ii. The comparison of NO_x evolution profiles (NO₂ conversion and NO transformation) between Mix 1 and Mix 4 (mixtures with and without CO, respectively), supports the assertion that NO₂ reacts with CO below 150°C: When both NO₂ and CO are present as in the case of Mix 1, the conversion of NO₂ begins much earlier, enhancing the NO formation by reacting with CO at low temperature.

The reaction, however, is limited by the concentration of NO₂. Taking the Mix 1 as an example, NO₂ is approximately totally converted (refer to the formation of NO in Fig. 4.5c) when about 30% of CO has reacted (i.e., 100 ppm of reactant transformed). Actually, the comparison of the CO evolution profile between Mix 1 and Mix 2 illustrates that Mix 2 overtakes Mix 1 when about 20% of CO is reacted, suggesting the role of O₂ as the oxidizer instead of NO₂ in the oxidation of CO thereafter. At low temperature, the conversion of NO leading to NO₂ also favors the CO oxidation ^[227]. In other words, the oxidation of CO can be enhanced by the converted NO₂ serving as an intermediate. The CO oxidation enhanced by NO₂ is also embodied in the relatively high conversions of CO and NO₂ for Mix 3 and Mix 1 at low temperature (Fig. 4.5b and c).

As temperature rises, in terms of CO oxidation, with the mixture Mix 5, the conversion is higher since the absence of other reactants pays off. It is followed by Mix 2, and then Mix 3 with Mix 1 being the last, namely Mix 5 > Mix 2 > Mix 3 > Mix 1. Similar trend is applied to the conversions of C₃H₆. At temperature above 200°C where CO oxidation is almost completed, NO oxidation, however, competes for the oxidations sites against C₃H₆. It was shown that the absence of other gas leads to an increase of C₃H₆ oxidation since there is no reaction competition between NO and CO, C₃H₆ oxidation ^[227, 228]. Actually, over this stabilized catalyst, it is hard to tell the contribution to the C₃H₆ conversion from the absence of CO at low temperature though this favor is evident over the fresh catalyst as mentioned above. The conversions of C₃H₆ for Mix 1 and Mix 4 can be regarded as almost the same at the temperature of interest, especially so after the complete oxidation of CO (over 200°C).

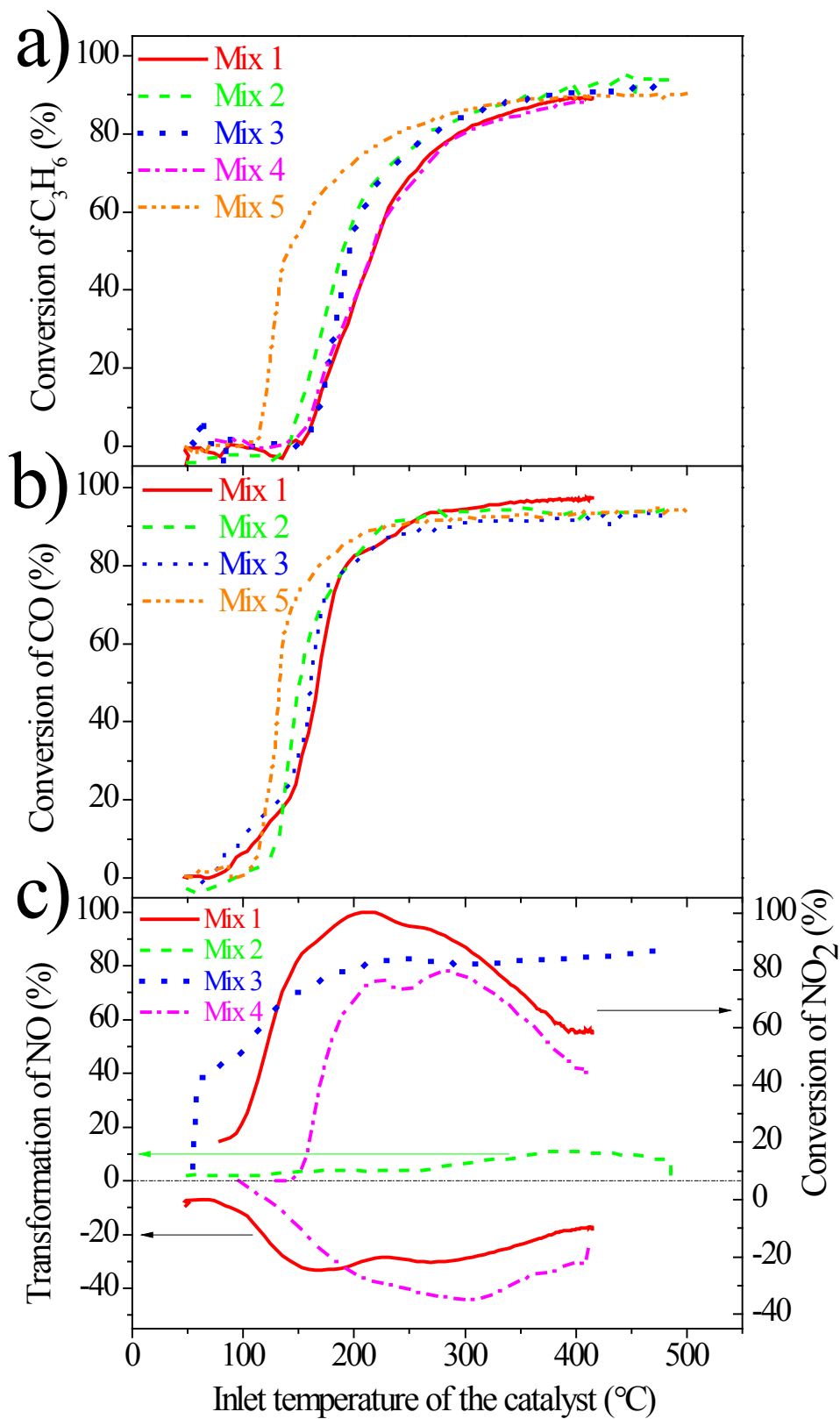


Fig. 4.5 Effect of gas compositions on the evolution profiles of A750 catalyst: (a). C₃H₆, (b). CO, and (c). NO_x

Fig. 4.6 presents the evolution profiles concerning C_3H_6 , CO and NO_x of the A950 catalyst under different mixtures as a function of temperature. It is apparent that the oxidation of C_3H_6 can be considered as not occurring until the almost complete oxidation of CO as noticed before ^[225]. What's also evident is that at low temperature, NO_2 reacts with CO to give out NO and enhance the oxidation of CO.

The comparison of evolution profiles of CO and NO_2 between Mix 1 and Mix 3 illustrates that the absence of NO is beneficial to the reaction between NO_2 and CO which gives out NO.

As temperature increases, in terms of CO oxidation, Mix 5 takes the lead since the absence of other reactants offers it an edge. Thus, there comes the order Mix 5 > Mix 1/3 > Mix 2. Mix 2 being the last can be ascribed to the lack of contribution from NO_2 (Mix 1 and Mix 2) as well as the disadvantage of NO (Mix 2 and Mix 5).

With respect to the conversions of C_3H_6 , the lead of Mix 4 at low temperature evidences that NO_2 acts as a strong oxidizer in the oxidation of C_3H_6 when there exists no CO in the feed. This narrow advantage was traded off as increasing temperature makes O_2 an important player in this field, as reflected by the Mix 5 overtaking Mix 4 in this competition. It's also said that at temperature above 200°C where CO oxidation is almost completed, NO oxidation competes for the oxidations sites against C_3H_6 . As expected, in terms of C_3H_6 oxidation performance at high temperature, the sequence is Mix 5 > Mix 4 > Mix 3 > Mix 2 > Mix 1.

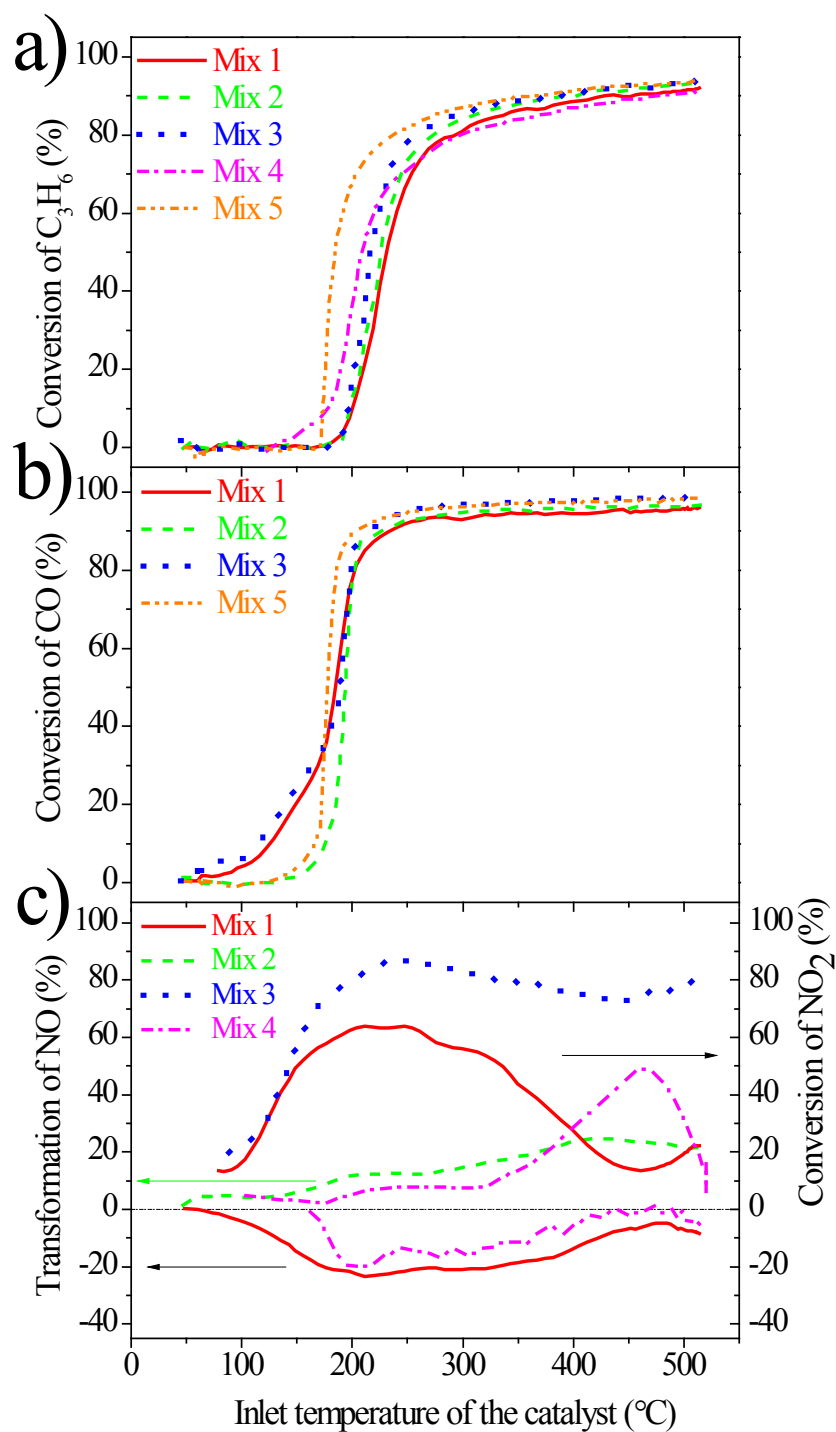


Fig. 4.6 Effect of gas compositions on the evolution profiles of A950 catalyst: (a). C₃H₆, (b). CO, and
 (c). NO_x

4.1.3 Concluding remarks

A structure-reactivity study of fresh, mildly thermal aged and severely thermal aged DOC samples in changing the pollutants in feed is presented. It is clearly showed that thermal aging significantly affects the overall oxidation activities of the catalysts. It turns out that mild

thermal aging actually activates the catalyst. Mild aging on the catalyst improves the oxidation performance of C_3H_6 as well as CO to a large extent while severe aging improves a little bit. NO oxidation over severely aged catalyst gets better.

Over these DOC samples, fresh and aged ones, the CO oxidation takes place at lower temperature than C_3H_6 oxidation. Meanwhile, the NO_2 is a strong oxidant which reacts with CO if present to give out NO, enhancing the CO oxidation and formation of NO at low temperature. Moreover, the NO competes for the oxidations sites against C_3H_6 .

In the next section, the influence of the presence of alkali compounds on the performance of a commercial Pt-Pd/ Al_2O_3 diesel oxidation catalysts will be experimentally investigated.

4.2 Influence of the presence of alkali compounds on the performance of a commercial Pt-Pd/ Al_2O_3 diesel oxidation catalyst

It is generally accepted that alkali and alkali earth compounds are able to adsorb N-species. In this way, Milt et al. reported the formation of KNO_3 species as intermediates leading to an enhancement of the performance of K/ CeO_2 traps in soot oxidation^[229]. These results were confirmed on structured catalysts for the simultaneous removal of soot and nitrogen oxides prepared by means of coating cordierite monoliths with alumina-based suspensions containing Cu, Co or V and K as the catalytically active phase. The enhancement of activity was thus ascribed to higher ability to generate NO_2 ^[230].

More recently, it was shown by Chen et al. that formaldehyde oxidation over Pt/ MnO_2 catalysts is enhanced by the presence of alkali metal salts^[231]. However, the effect of alkali metals on the DOCs has never been clearly studied, particularly the effects of the presence of alkali metals from biofuels on the performance of this commercial catalytic after-treatment system.

On the other hand, few studies were devoted to the investigation of the catalytic activity of precious-metal-based catalysts under multicomponent co-feeding conditions. Lang et al.

conducted the study on the light-off and steady-state behavior for individual oxidation and co-oxidation of CO and C₃H₆ under near-stoichiometric conditions (based on three-way catalyst) using Pd/Al₂O₃ and Pd/CeO₂-ZrO₂ monolith catalysts^[232]. The effect of C₃H₆, H₂O and their combination on NO oxidation activity over different powder catalysts (for diesel oxidation catalyst application) was also investigated by Auvray et al.^[228]. However, to the best of authors' knowledge, there is no study concerning the interaction of multi-species when they are co-fed in the simulated gas mixture over monolith bimetallic diesel oxidation catalyst.

In this sense, the objective of the present section is to investigate the influence of the addition of different alkali metal species (K and Na) on a commercial monolith Pt-Pd/Al₂O₃ DOC, through catalytic tests performed on this structured catalyst under multicomponent (C₃H₆ / CO / NO / NO₂) co-feeding conditions. Their effect was evaluated by examining the evolution profiles of C₃H₆, CO and NO_x.

4.2.1 Experimental

4.2.1.1 Catalysts samples

The catalyst used for this study was taken from the same untreated brick of the commercial DOC catalyst provided by Continental. Again, it was cut into cylindrical "carrots" (d=2.54 cm; L=2.54 cm).

Alkali metals such as potassium (K) or/and sodium (Na) were introduced to the fresh DOC monolith catalyst by impregnation from the potassium and sodium nitrate solutions with 1 wt. % loading. After drying at 110°C overnight, the samples were calcined at 550°C for 4 h. Catalysts prepared for this study were detailed in Table 4.3. It's worth noting that the prepared catalyst named K-Na contains 0.5 wt. % K and 0.5 wt. % Na, resulting in 1 wt. % loading in total.

Table 4.3 Different doping methods dealing with DOC

Entry	Catalyst condition
F	Fresh
K	1% KNO ₃
Na	1% NaNO ₃
K-Na	1% K+Na NO ₃

4.2.1.2 Characterization of catalysts

Several characterization techniques were employed to identify the physicochemical composition of the studied catalysts. XRD patterns of studied catalysts were recorded on a Bruker Advanced D8 diffractometer equipped with a graphite monochromator using Cu-K α radiation. XRD measurements were performed from 5 to 70° in an interval of 0.02° with a count time of 12s for each point. High resolution TEM (HRTEM) coupled with EDS was performed on a JEOL-JEM 2011 HR (LaB) microscope operating at 200 kV. The specific surface area was calculated by using the Brunauer-Emmett-Teller (BET) method. N₂ adsorption-desorption isotherms were acquired at liquid nitrogen temperature by a Micromeritics ASAP 2010. Before the measurements, the samples were evacuated at 200°C for 2 hours under vacuum (0.2666Pa) to remove gases and vapors that might have been physically adsorbed.

The prepared structured catalysts were also characterized by means of Scanning electron microscopy (SEM, Hitachi S-3400 N coupled with EDS analysis, Röntec XFlash).

These techniques can be referred to in Chapter 3.

4.2.1.3 Catalytic activity studies

The same synthetic gas bench installation as for the previous aging study was used to investigate the catalytic activities of these four doped catalysts.

As mentioned in the previous aging study, a typical reactant gas mixture representative of the exhaust gases from diesel engines consists of C₃H₆, CO, NO, NO₂, O₂, CO₂, H₂O and N₂, as Mix 1 in Table 4.4. For every test (Mix 1- Mix 5), the total gas flow rate was 11.8 L·min⁻¹ referenced to 293K and 1 atm, resulting in a gas hourly space velocity (GHSV) of 55,000 h⁻¹. Gas mixtures without NO₂, NO, CO or NO_x were setup to explore the influence of each gas component on the catalytic process. NO₂ is removed from the feed to form Mix 2. In Mix 3, NO is removed while CO is removed regarding Mix 4. Finally both NO and NO₂ were removed from the feed, obtaining Mix 5. Table 4.4 summarized the conditions of the different experiments in terms of gas composition.

Catalysts were evaluated in terms of oxidation capacity and NO conversion for temperatures ranging from 50°C to 500°C. Exhaust gas compositions before and after the reactor were

characterized by an Environnement S.A. analyzer composed of a set of modules. Among them, the TOPAZE 32M module allowed NO, NO₂ and total NO_x measurement thanks to a chemiluminescence analyzer. A MIR2M module was composed of an IR spectrogram, for the measurement of H₂O, CO and CO₂ molar fractions, and a magnetic sensor, for the O₂ molar fraction measurement. At last, a flame ionization detector (FID), present in the GRAPHITE 52M module was used for measuring total HC.

Table 4.4 Synthetic gas bench experimental conditions for alkali-as-dopant DOC study

	C ₃ H ₆	NO ₂	NO	CO	CO ₂	O ₂	H ₂ O	N ₂
	ppm	ppm	ppm	ppm	(%)	(%)	(%)	(%)
Mix 1	200	100	300	300	5	10	5	Balance
Mix 2	200	-	300	300	5	10	5	Balance
Mix 3	200	100	-	300	5	10	5	Balance
Mix 4	200	100	300	-	5	10	5	Balance
Mix 5	200	-	-	300	5	10	5	Balance

4.2.2 Effects of the presence of alkali compounds on the performance of a commercial oxidation catalyst

4.2.2.1 Effect of the gas compositions

In order to illustrate the effect of gas compositions on the catalytic performance of studied catalysts, different experimental conditions Mix 1 to Mix 5 were compared (Table 4.4). NO₂ is removed from the feed to form Mix 2. In Mix 3, NO is removed while CO is removed regarding Mix 4. Finally both NO and NO₂ were removed from the feed in Mix 5.

Fig. 4.7 depicts the evolution profiles of C₃H₆ for different mixtures over the studied catalysts. The evolution profile of C₃H₆ under the gas condition Mix 5 with remarkable oxidation performance is different from those obtained under other mixtures. It was shown that the absence of other gas leads to an increase of C₃H₆ oxidation since there is no reaction competition between NO and CO, C₃H₆ oxidation [227, 228]. As expected, in terms of C₃H₆ oxidation performance, the ranking is then Mix 3 > Mix 2 > Mix 1. The conversions of C₃H₆

for Mix 1 and Mix 4 can be regarded as almost the same except that the absence of CO favors the C_3H_6 conversion at temperature lower than $200^\circ C$ for the Fresh and K catalysts while lower than $250^\circ C$ for Na-associated catalysts. The absence of CO favoring the C_3H_6 conversion is due to the lack of inhibition from CO as observed by Lang et al. [232]. When CO adsorbs onto surface active sites, it can result in the decrease of C_3H_6 conversion in two ways: a), occupy the active sites which otherwise can be available for the adsorption of C_3H_6 , and b), inhibit the competitive adsorption and dissociation of oxygen. An additional point of interest is that the adsorption of CO typically requires one surface active site per molecule, while C_3H_6 requires multiple active sites for adsorption and fragmenting into smaller carbonaceous species.

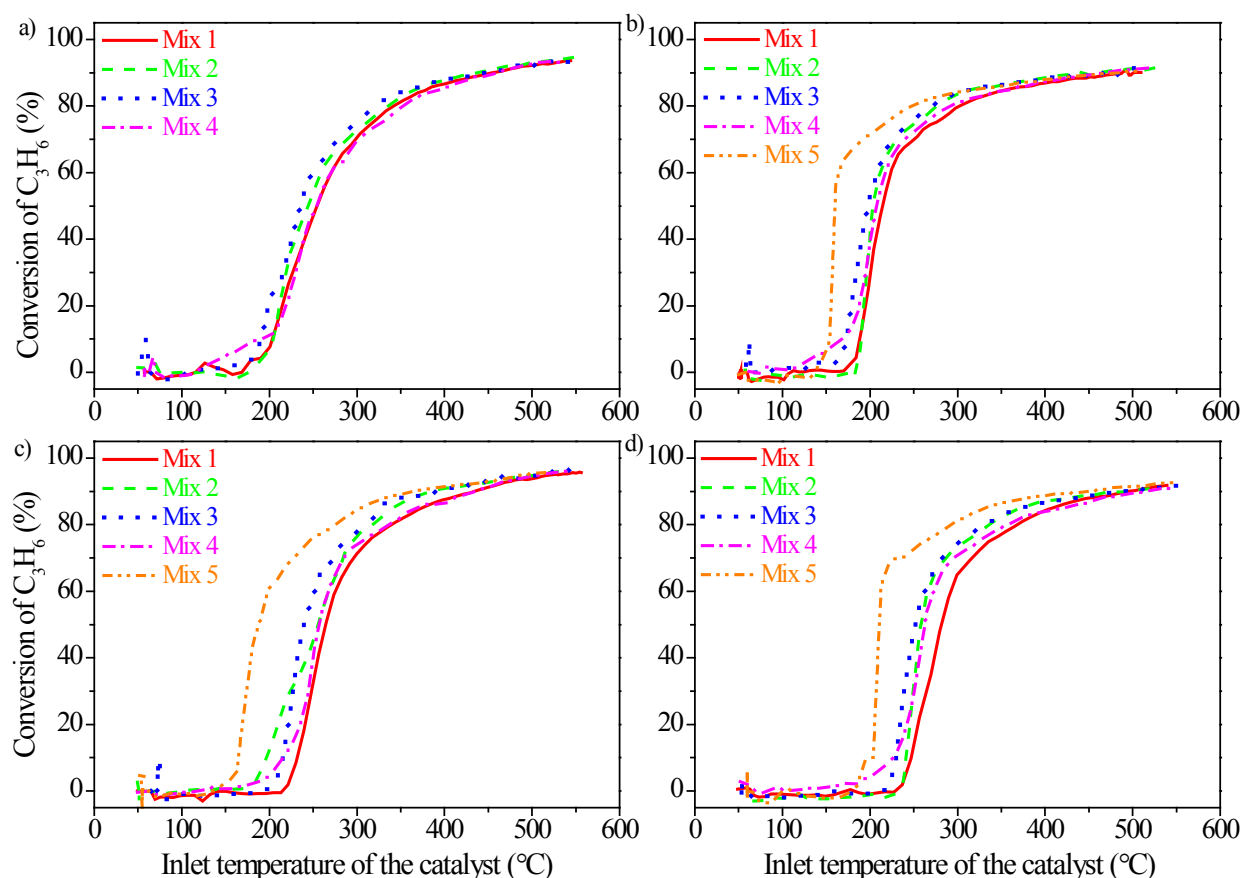


Fig. 4.7 Effect of gas compositions on the evolution profiles of C_3H_6 : (a). Fresh catalyst, (b). K-doped catalyst, (c). Na-doped catalyst and (d). K/Na-doped catalyst

Over these DOC samples, the CO oxidation (Fig. 4.8) takes place at lower temperature than C_3H_6 oxidation by comparing corresponding light-off curves. This is also consistent with the findings of Lang et al. [232]. In general, similar to that of the C_3H_6 oxidation, Mix 5 distinguishes itself from others with high CO oxidation performance.

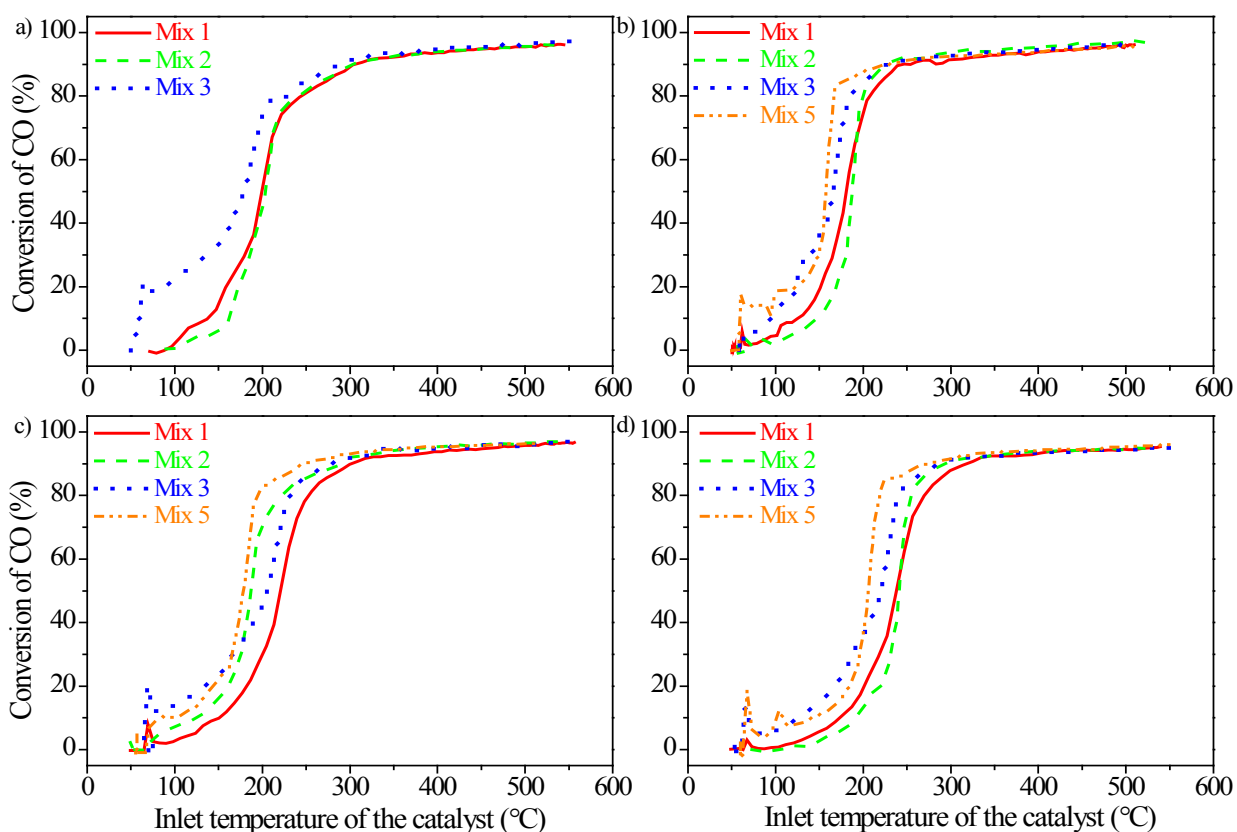


Fig. 4.8 Effect of gas compositions on the evolution profiles of CO: (a). Fresh catalyst, (b). K-doped catalyst, (c). Na-doped catalyst and (d). K/Na-doped catalyst

At low temperature, the oxidation of CO is enhanced when NO_2 (strong oxidant) is present in the feed gas (Mix 3 and Mix 5, difference in the presence of NO_2) due to the CO/ NO_2 interaction already described elsewhere ^[225]. As temperature rises, in terms of CO oxidation, Mix 5 takes the lead since the absence of other reactants pays off. The absence of NO in Mix 3 offers it an edge in terms of CO oxidation, compared with Mix 1. The presence of NO_2 in Mix 1, however, contributes to the oxidation of CO, compared to Mix 2. Thus, the order for CO oxidation in general is Mix 5 > Mix 3 > Mix 1 > Mix 2.

The NO_2 conversion in Mix 3 is stronger than that of Mix 1, supporting that the absence of NO is beneficial to the reaction between NO_2 and CO which gives out NO (Fig. 4.9). It can be ascribed to less competition for the active sites when NO is absent.

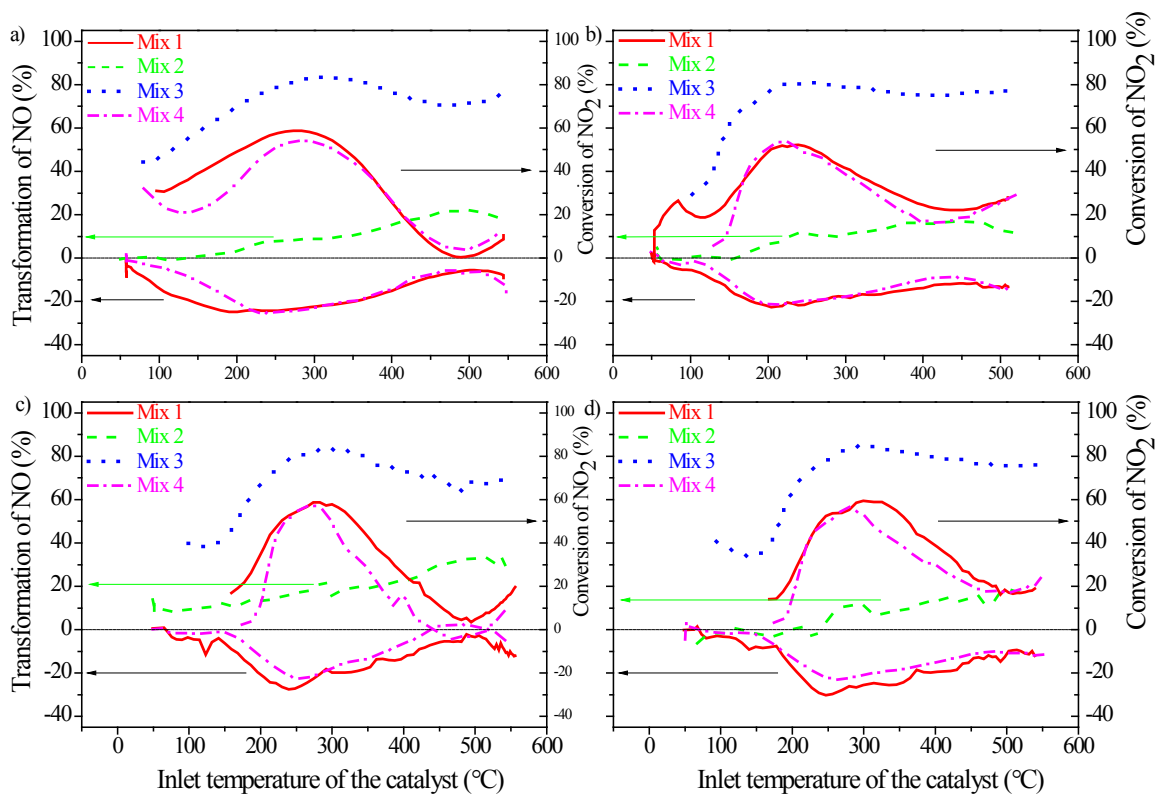


Fig. 4.9 Effect of gas compositions on the evolution profiles of NO_x : (a). Fresh catalyst, (b). K-doped catalyst, (c). Na-doped catalyst and (d). K/Na-doped catalyst

For better understanding of how multi-species interact when they are co-fed in the simulated gas mixture over studied catalysts, their behavior over the fresh catalyst was analyzed as an example. As observed from Fig. 4.10, the oxidation of C_3H_6 can be considered as no occurring until the almost complete oxidation of CO, which is consistent with other study [226]. Moreover, the oxidation of CO is enhanced when NO_2 is present in the feed gas (Mix 3 and Mix 1) due to the CO/ NO_2 interaction [225]. The reaction between NO_2 and CO at low temperature in present study is evidenced by following observations:

- i. The comparison of the NO_x evolution profiles between Mix 1 and Mix 2 (mixture with and without NO_2 , respectively) suggests that the presence of NO_2 contributes to the formation of NO, by reacting with CO.
- ii. The comparison of NO_x evolution profiles (NO_2 conversion and NO transformation) between Mix 1 and Mix 4 (mixtures with and without CO, respectively), supports this assertion that NO_2 reacts with CO below 150°C : When both NO_2 and CO are present as in the case of Mix 1, the conversion of NO_2

begins much earlier, enhancing the NO formation by reacting with CO at low temperature.

- iii. Increasing conversion of CO is accompanied by that of NO₂ in this study (Fig. 4.10c).

NO₂, however, is less reactive towards the hydrocarbon according to the study of Yentekakis et al. [233]. The comparison of conversion profiles of C₃H₆ over doped catalysts under Mix 3 and Mix 5 (mixture with and without NO₂, respectively) in present study actually demonstrates that the presence of NO₂ inhibits C₃H₆ oxidation. The NO₂ inhibition of C₃H₆ oxidation was also found by us when comparing the conversion profiles of C₃H₆ over studied catalysts when CO was further removed from the Mixes 3 and 5 (Figure not shown).

In their comparative study of the C₃H₆ + NO + O₂, C₃H₆ + O₂ and NO + O₂ reactions, Yentekakis et al. found the NO inhibition of propene combustion as well as propene acting as an inhibitor to NO + O₂ → NO₂ reaction, and they attributed the cause to the resulted change in the chemisorption of adsorbates [233].

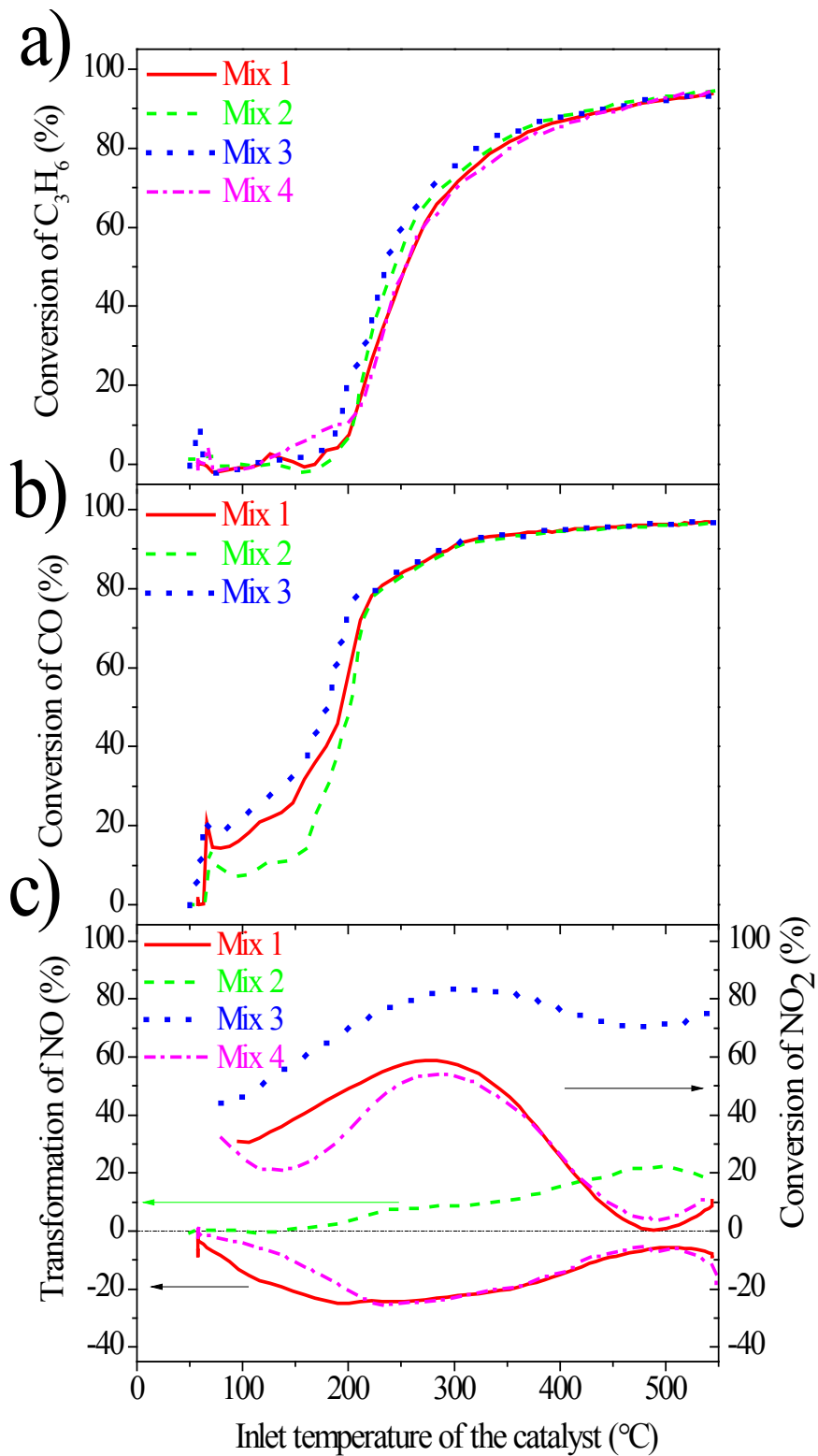


Fig. 4.10 Effect of gas compositions on the evolution profiles of Fresh catalyst: (a). C₃H₆, (b). CO, and (c). NO_x

4.2.2.2 Effect of alkali metals on a DOC under mixtures representative of diesel exhaust

Fig. 4.11 presents the evolution profiles of reactants of interest over studied catalysts, fresh and doped ones, under the simulated gas condition Mix 1, which is representative of a real exhaust mixture. Compared with the fresh one, the light-off temperature of C_3H_6 over the K-doped one shifts to the lower temperatures, suggesting positive influence brought by the introduction of K. On the contrary, the light-off temperatures of C_3H_6 over the Na-doped samples (either exclusively Na-doped or in the form of combination with K) shift to the higher temperatures, demonstrating negative influence after the doping of Na. Similar results are obtained for CO conversion over studied catalysts. Concerning the evolution of NO, the fresh catalyst stands out with more formation of NO. Obviously, the introduction of dopants hinders the formation of NO especially at low temperature, suggesting that they reduce the number of active sites.

Fig. 4.12 displays the evolution profiles of reactants of interest over studied catalysts under the simulated gas condition Mix 2, thus in the absence of NO_2 in the feed. The light-off temperature of C_3H_6 over the K-doped catalyst shifting to the lower part evidences that the addition of K improves again the catalyst performance, namely K acts as a promoter compared to the fresh one. It is not hard to observe that the light-off temperature of C_3H_6 over the Na-doped catalyst shifts to the higher part taking fresh one as the reference, suggesting the negative influence from the introduction of Na. Moreover, the combination of K and Na lead to the decrease of the activity. Similar results are obtained for the conversions of CO. As for the evolution of NO, there are more conversions of NO over K- or Na-doped ones, as already reported in other studies ^[229 - 231]. Thus, the addition of single dopant can be regarded as beneficial to the NO conversion. However, the combination of K and Na leads to a decrease of conversion.

Fig. 4.13 presents the evolution profiles of reactants of interest over studied catalysts under the simulated gas condition Mix 3, in the absence of NO in the feed. As can be seen, the presence of K improves the oxidation performance of the catalyst while Na brings the contrary effect. Also, the combination of these two stands out as the worst. Thus the absence of both NO or NO_2 does not affect the promotion of K addition or inhibition of Na addition to DO Catalysts.

Fig. 4.14 displays the evolution profiles of reactants of interest over studied catalysts under the simulated gas condition Mix 4, in absence of CO in the feed.

Again, the introduction of K obviously promotes the oxidation reaction while Na brings the opposite effect. Also, the combination of these two stands out as the worst. Thus, the absence of NO/NO₂ or CO has no effect regarding the promotion of K addition or inhibition of Na addition to the studied catalysts.

Apparently, the promotion of K addition or inhibition of Na addition to the studied catalysts is also reflected in the conversion of NO₂.

Fig. 4.15 exhibits the evolution profiles of reactants of interest over conditioned catalysts under the simulated gas condition Mix 5 in absence of both NO and NO₂ in the feed. The conversion profiles of C₃H₆ and CO in terms of performance lead to the following ranking: K>Na>K-Na. The conclusion of the effect of the alkali addition on DOC can be draw: the presence of K promotes the oxidation reaction whereas the addition of Na or K-Na inhibits the oxidation reaction.

It is commonly accepted that alkali and alkali earth compounds are able to adsorb N-species. In their study, Milt and co-workers reported the KNO₃ species formed in this way as intermediates led to the enhanced performance of K/CeO₂ traps in soot oxidation^[229]. These results were confirmed on structured catalysts for the simultaneous removal of soot and nitrogen oxides prepared by means of coating cordierite monoliths with alumina-based suspensions containing Cu, Co or V and K as the catalytically active phase^[230]. The mechanism leading to the enhancement of the activity due to the presence of alkali metals might go through the formation of adsorbed N-species (nitrites/nitrates) on the catalyst surface, favored by the presence of K or Na as proposed by Galvez et al.^[234]. The enhancement of activity was thus ascribed to higher ability to generate NO₂.

According to the reported spectroscopic study, Na exists in the form of chemical compounds such as Na₂CO₃ or NaNO₃ under C₃H₆/NO/O₂ atmosphere^[233, 235]. Both promotional and poisoning effects induced by Na in de-NO_x catalytic chemistry of platinum group metals are possible when Na is present at the catalyst surface. These effects depend on the amount of Na supplied to the catalyst surface as well as a notable dependence on reactant gas phase composition (the relative molar ratio of the electron-donating to electron-accepting adsorbates

imposed to the surface) ^[233, 235]. It's well established that Na-induced changes in the relative adsorption strengths of the various reactants are the main cause ^[233, 236 - 238].

Yentekakis et al. showed that remarkable beneficial effects on both de-NO_x efficiency and N₂ selectivity were realized with Na-doped Pt/γ-Al₂O₃ catalysts operated under lean burn conditions ^[233]. They proposed that the observed alkali promotion of activity and N₂ selectivity in de-NO_x catalysis were due to alkali-induced strengthening of the metal-NO bond (thus increasing NO coverage) and the consequent dissociation of NO molecules adsorbed on the platinum metal component of the catalyst. Later, their spectroscopic evidence for weakening of the N-O bond by means of in situ DRIFTS justified the hypothesis ^[237].

Vernoux et al. found that the addition of Na can lead to a strengthening of the Pt–electron-acceptor (O and NO) bonds and a weakening of the Pt–electron-donor (C₃H₆) bonds ^[239]. Another point of interest is that the strengthening of the Pt–O bond is much more pronounced than that of the Pt–NO bond because O is a much stronger electron-acceptor than NO ^[239]. An excessive promotion of oxygen adsorption due to the presence of Na, however, can cause severe inhibition in both C₃H₆ and NO conversions ^[233, 239]. In terms of inhibition, thick layers consisting of sodium carbonate which accounts for catalyst poisoning can be another possibility ^[235].

To sum up, the involved environment would determine whether Na acts as a promoter or an inhibitor. This is particularly reflected in Fig. 4.12 of present study: the presence of Na can enhance the conversions of CO and NO while inhibit the conversion of C₃H₆.

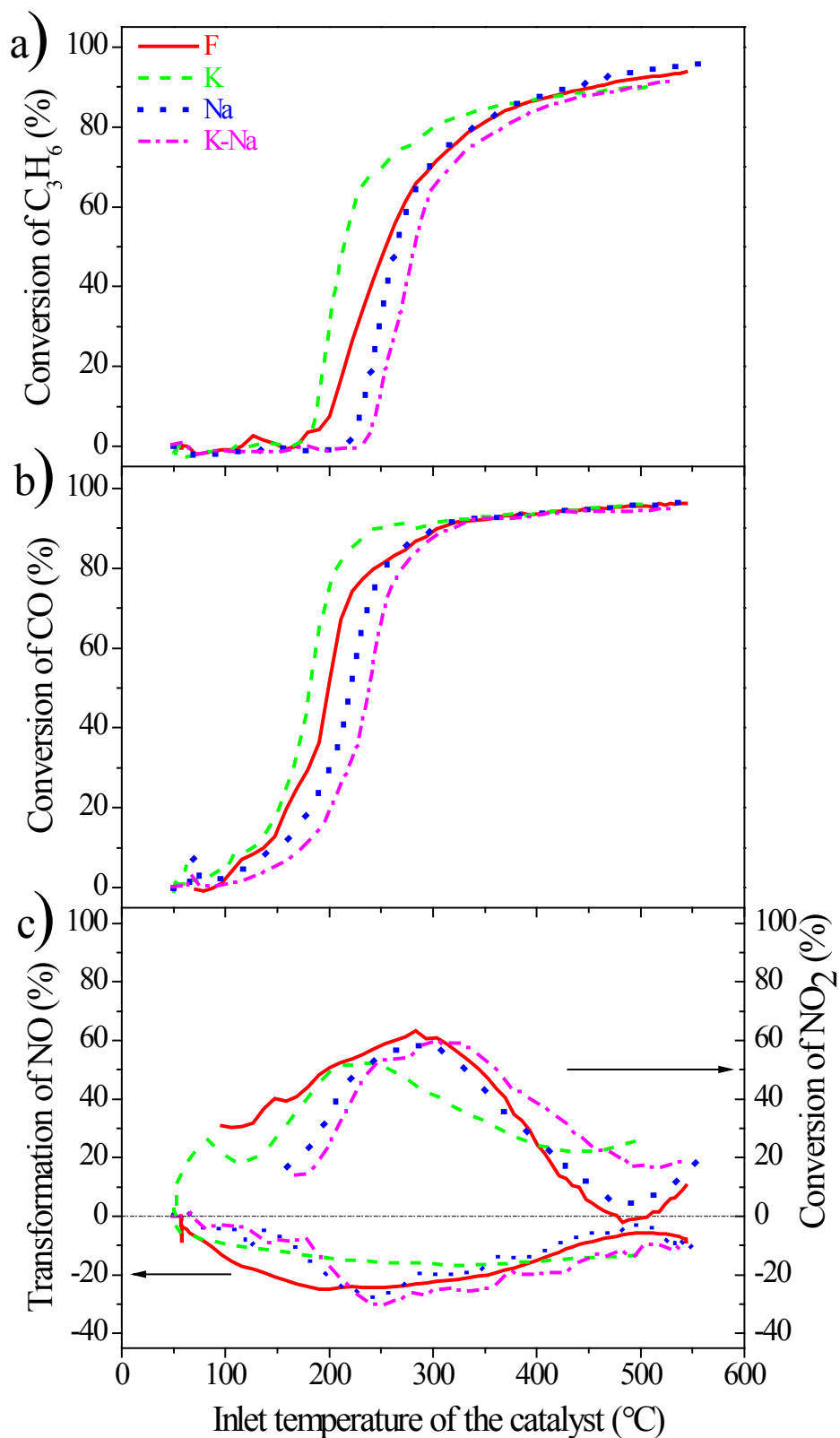


Fig. 4.11 Evolution profiles of C_3H_6 , CO and NO_x for Mix 1 versus temperature for reference and conditioned catalysts: (a). Conversions of C_3H_6 , (b). Conversions of CO and (c). Transformations of NO_x

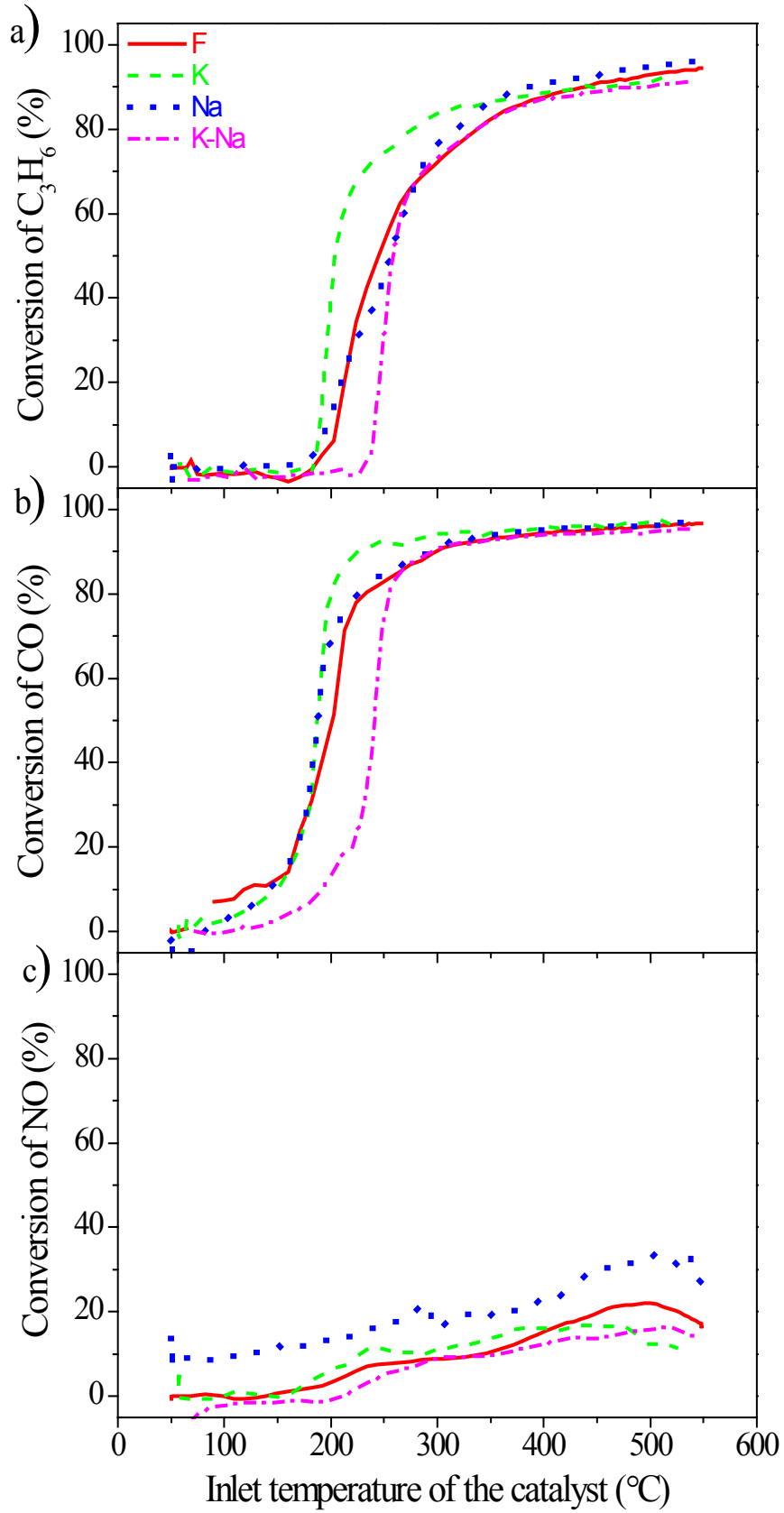


Fig. 4.12 Evolution profiles of C_3H_6 , CO and NO for Mix 2 versus temperature for reference and conditioned catalysts: (a). Conversions of C_3H_6 , (b). Conversions of CO and (c). Conversions of NO

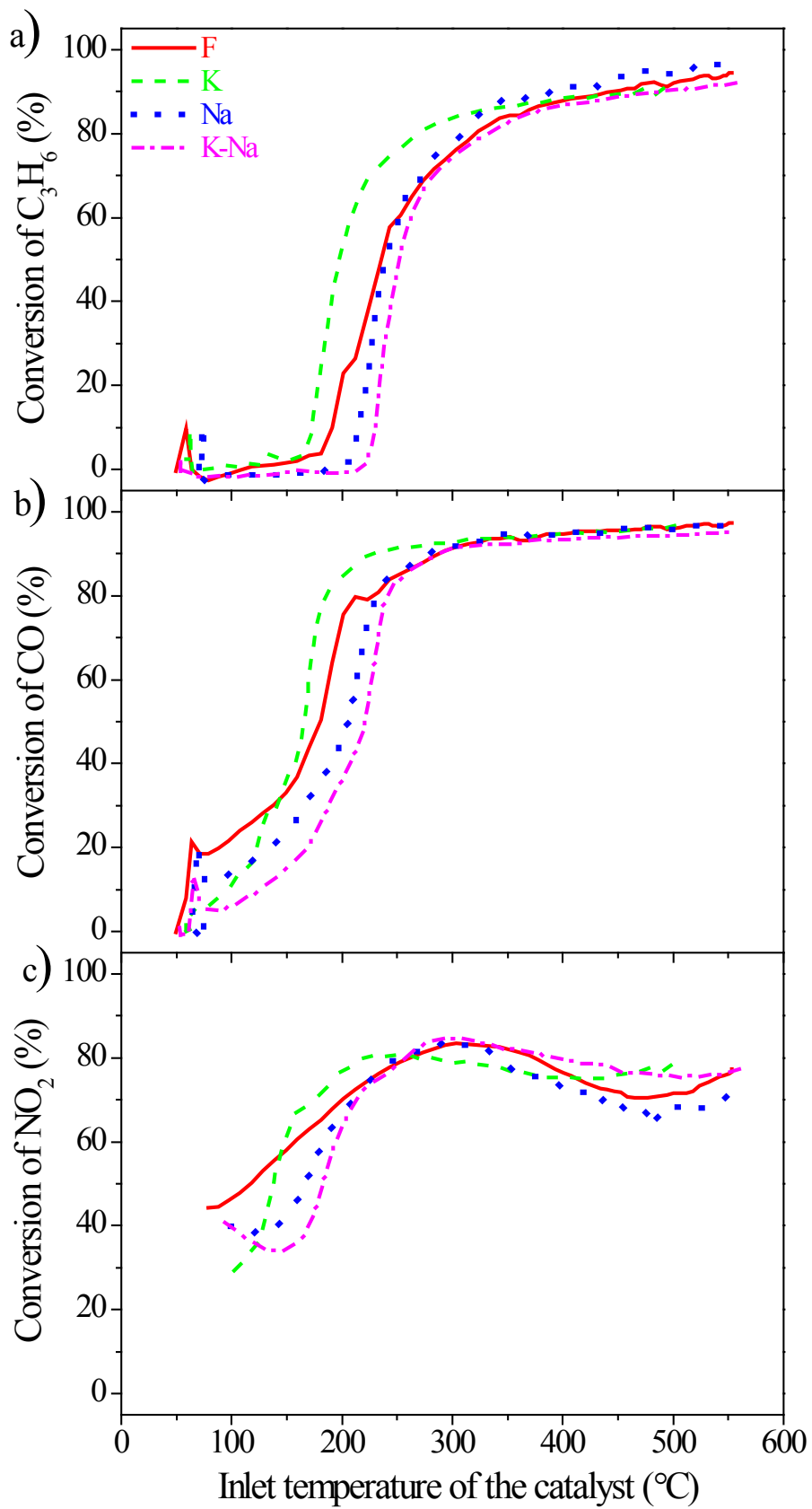


Fig. 4.13 Evolution profiles of C_3H_6 , CO and NO_2 for Mix 3 versus temperature for reference and conditioned catalysts: (a). Conversions of C_3H_6 , (b). Conversions of CO and (c). Conversions of NO_2

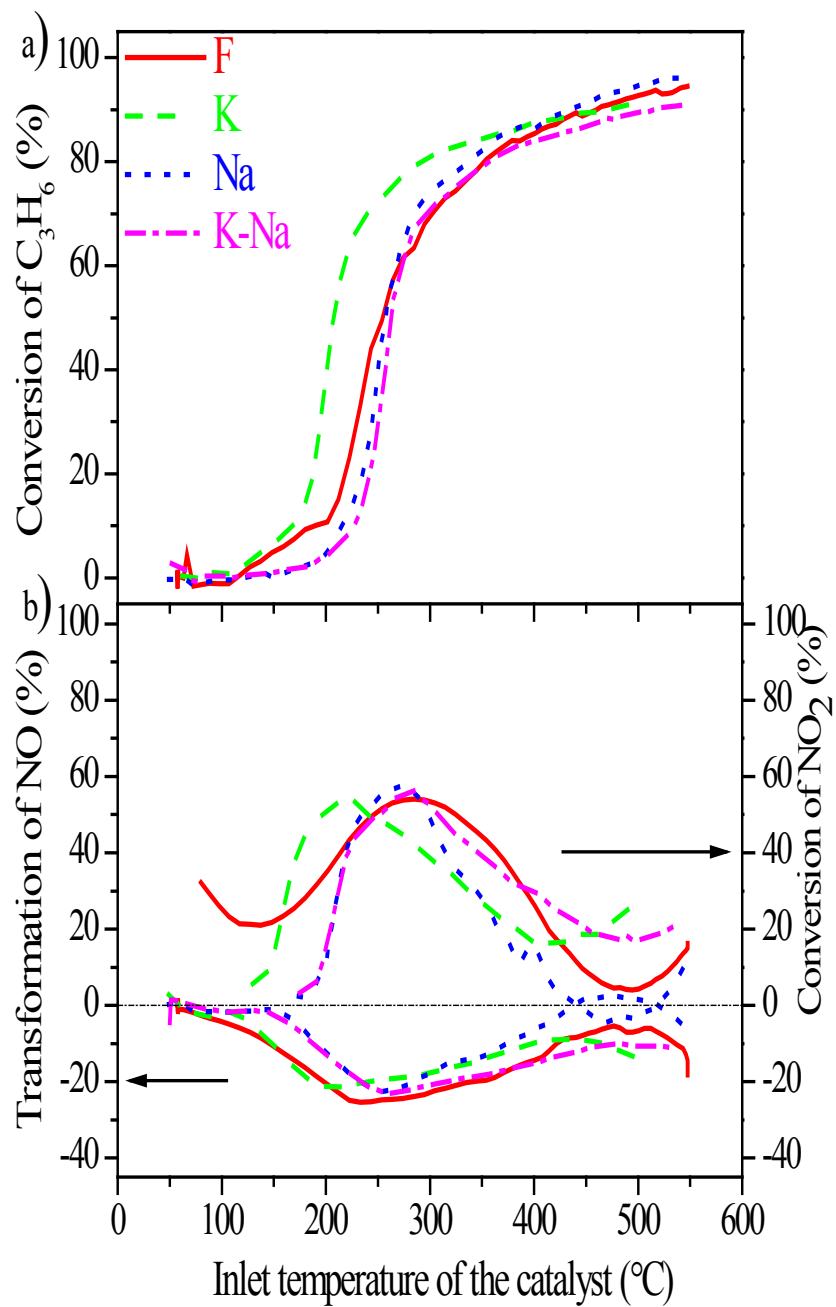


Fig. 4.14 Evolution profiles of C_3H_6 and NO_x for Mix 4 versus temperature for reference and conditioned catalysts: (a). Conversions of C_3H_6 , and (b). Transformations of NO_x

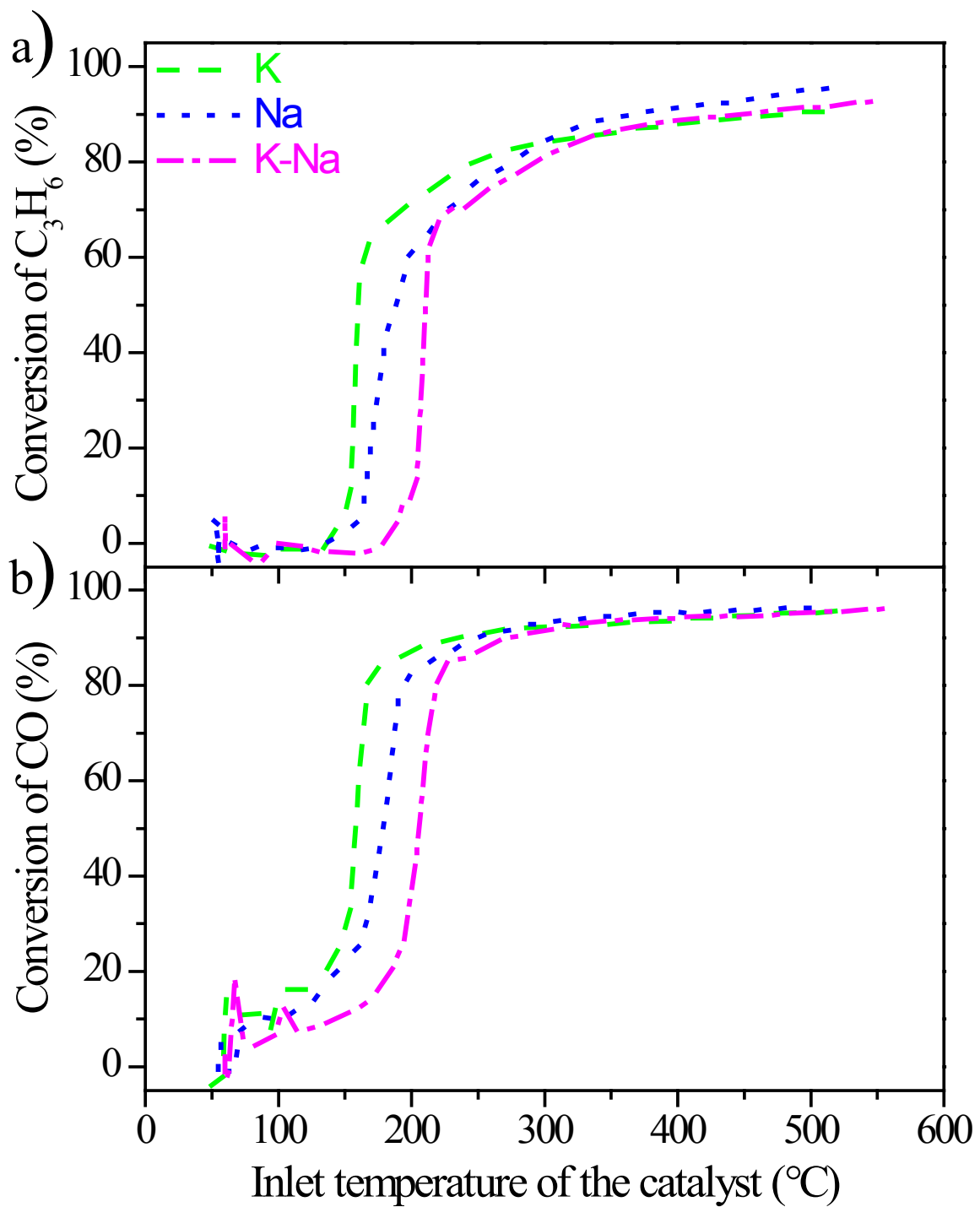


Fig. 4.15 Evolution profiles of C_3H_6 and CO for Mix 5 versus temperature for reference and conditioned catalysts: (a). Conversions of C_3H_6 , and (b). Conversions of CO

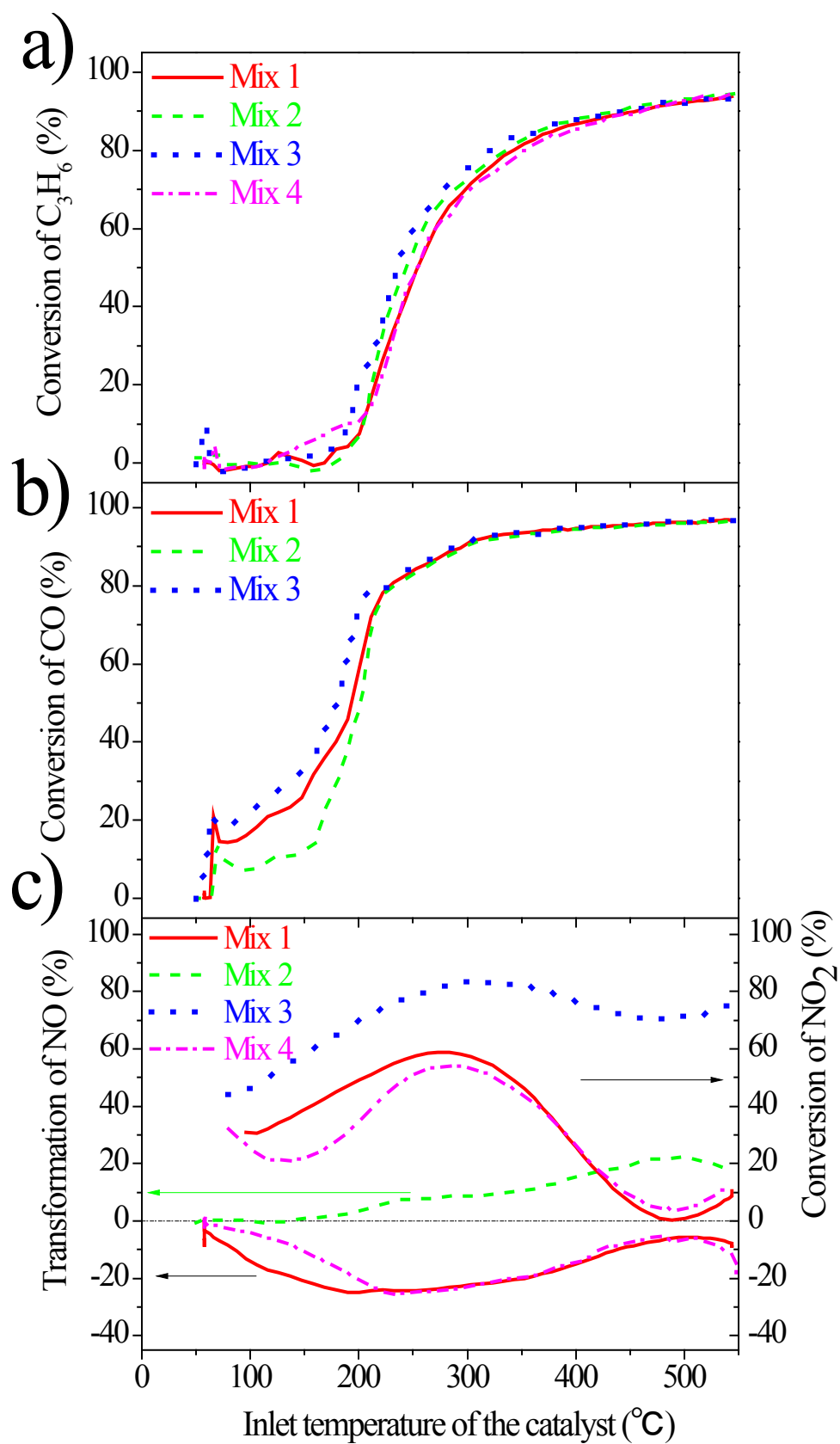


Fig. 4.16 Effect of gas compositions on the evolution profiles of Fresh catalyst: (a). C₃H₆, (b). CO, and

(c). NO_x

4.2.3 Concluding remarks

On a commercial Diesel Oxidation Catalyst, studied in the monolithic form, under representative exhaust gases mixtures, it was clearly showed that the introduction of dopants leads to either negative or positive impacts on the catalytic oxidation. The K addition leads to a promotion of oxidation reactions while the Na addition inhibits the same reactions. There is no impact of exhaust gas composition on the ranking of catalysts. However, it was shown that the presence of NO₂ promotes the oxidation reaction whereas in the presence of NO, the competition in terms of oxidation in the same catalytic sites leads to a shift of light off temperature for CO and C₃H₆ to higher temperatures.

In the next section, the influence of the dual aging (hydrothermal and chemical) on the performance of a commercial Pt-Pd/Al₂O₃ diesel oxidation catalysts will be studied.

4.3 Influence of the dual aging (hydrothermal and chemical) on the performance of a commercial Pt-Pd/Al₂O₃ diesel oxidation catalysts

4.3.1 Experimental

4.3.1.1 Catalysts samples

The catalyst used for this study was taken from the same untreated brick of the commercial DOC catalyst provided by Continental. Again, four cylindrical "carrots" (d=2.54 cm; L=2.54 cm) were cut out of it.

Two carrots were hydrothermally aged in a laboratory box furnace (Rohde Ecotop 50, Germany) in flowing air with 10 vol.% H₂O. Alkali metal (K) was introduced to one of the aged DOC monolith catalysts by impregnation from the potassium nitrate solutions with 1 wt. % loading, obtaining the dual deactivation sample.

Also, alkali metal (K) was introduced to the fresh DOC monolith catalyst using the same method of wet impregnation. After drying at 110°C overnight, the samples were calcined at 550°C for 4 h. Catalysts prepared for this study were detailed in Table 4.5.

Table 4.5 Different methods dealing with DOC for dual deactivation study

Entry	Catalyst condition
F	Fresh
A750	750_4H
K	1% KNO ₃
K-A750	750_4H + KNO ₃

4.3.1.2 Characterization of catalysts

Several characterization techniques were employed to identify the physicochemical composition of the studied catalysts. XRD patterns of studied catalysts were recorded on a Bruker Advanced D8 diffractometer equipped with a graphite monochromator using Cu-K α radiation. XRD measurements were performed from 5 to 70° in an interval of 0.02° with a count time of 12s for each point. High resolution TEM (HRTEM) coupled with EDS was performed on a JEOL-JEM 2011 HR (LaB) microscope operating at 200 kV. The specific surface area was calculated by using the Brunauer-Emmett-Teller (BET) method. N₂ adsorption-desorption isotherms were acquired at liquid nitrogen temperature by a Micromeritics ASAP 2010. Before the measurements, the samples were evacuated at 200°C for 2 hours under vacuum (0.2666Pa) to remove gases and vapors that might have been physically adsorbed.

The prepared structured catalysts were also characterized by means of Scanning electron microscopy (SEM, Hitachi S-3400 N coupled with EDS analysis, Röntec XFlash).

These techniques can be referred to in Chapter 3.

4.3.1.3 Catalytic activity studies

The same synthetic gas bench installation as for the previous aging study was used to investigate the catalytic activities of these catalysts.

As mentioned in the previous aging study, a typical reactant gas mixture representative of the exhaust gases from diesel engines consists of C₃H₆, CO, NO, NO₂, O₂, CO₂, H₂O and N₂, as

Mix 1 in Table 4.6. The total gas flow rate was $11.8 \text{ L}\cdot\text{min}^{-1}$ referenced to 293K and 1 atm, resulting in a gas hourly space velocity (GHSV) of $55,000 \text{ h}^{-1}$. Gas mixtures without NO_2 , NO , CO or NO_x were setup to explore the influence of each gas component on the catalytic process. Table 4.6 summarized the conditions of the different experiments in terms of gas composition.

Table 4.6 Synthetic gas bench experimental conditions for DOC dual deactivation study

	C_3H_6	NO_2	NO	CO	CO_2	O_2	H_2O	N_2
	ppm	ppm	ppm	ppm	(%)	(%)	(%)	(%)
Mix 1	200	100	300	300	5	10	5	Balance
Mix 2	200	-	300	300	5	10	5	Balance
Mix 3	200	100	-	300	5	10	5	Balance
Mix 4	200	100	300	-	5	10	5	Balance
Mix 5	200	-	-	300	5	10	5	Balance

4.3.2 Effects of the dual deactivation (hydrothermal and chemical) on the performance of a commercial oxidation catalyst

4.3.2.1 Effect of the dual deactivation on a DOC under mixtures representative of diesel exhaust

Fig. 4.17 presents the evolution profiles of reactants of interest over studied catalysts, fresh and conditioned ones, under the simulated gas condition Mix 1, which is representative of a real exhaust mixture. Compared with the Fresh catalyst, the light-off temperatures of C_3H_6 over both the A750 and the K-doped one shift to the lower temperatures, indicating positive influence brought by the mild aging or by the introduction of K. By contrast, the light-off temperatures of C_3H_6 over the dual deactivation sample shifts to the higher temperatures, demonstrating negative influence of this manipulation.

Evidently, compared to the Fresh catalyst, the mild aging on the catalyst can promote the oxidation activity of C_3H_6 , so can the addition of K, while other case (their combination) engenders negative influence on the conversion of C_3H_6 . Similar results are obtained for CO conversion over studied catalysts.

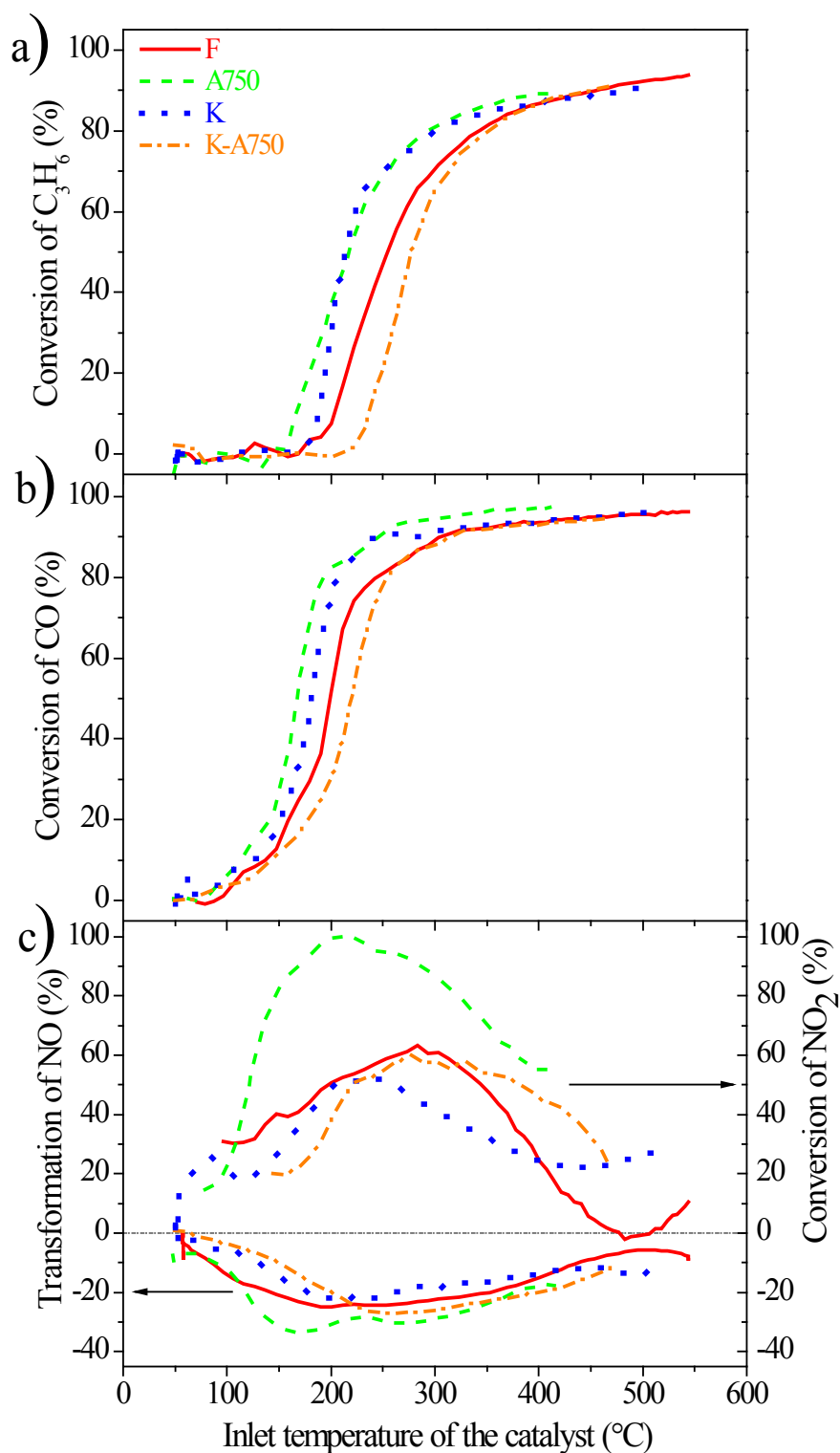


Fig. 4.17 Evolution profiles of C_3H_6 , CO and NO_x for Mix 1 versus temperature for reference and conditioned catalysts: (a). Conversions of C_3H_6 , (b). Conversions of CO and (c). Transformations of NO_x

As for the evolution of NO_x , the stabilized catalyst (A750) stands out with more conversion of NO_2 and more formation of NO. From Fig. 4.17b and c, the conversions of NO_2 and CO can be considered as peaking simultaneously, indicating the reaction between NO_2 and CO. The

NO₂ conversion after the peak is then reduced due to the increasing importance of O₂ as the oxidizer in CO oxidation. Reactions between NO₂ and C₃H₆ are not clearly identified in these experiments. Again, the performance of the K-A750 catalyst can be considered as the worst particularly from the viewpoint that the NO₂ conversion light-off occurs at much higher temperature compared to the other catalysts.

Fig. 4.18 shows the evolution profiles of reactants of interest over studied catalysts, fresh and three other manipulated ones, under the simulated gas condition Mix 2, thus in the absence of NO₂ in the feed. It's not hard to find that the absence of NO₂ does not affect the promotion by mild aging or the addition of K on both the C₃H₆ and CO oxidation activities. The inhibition influence by the manipulation of combination between the aging and doping is not affected, either. However, it's worth noting that after mild aging, the C₃H₆ oxidation activity is significantly improved. In this sense, mild aging actually activates the catalyst.

As for the evolution of NO, the effect of doping of K on NO oxidation in representative mixture is positive and strong. This promotion is even more evident when comparing the NO conversion profiles between A750 and K-A750 catalysts. The mechanism of resulted enhancement of the activity from the presence of K will most probably be linked to the formation of adsorbed N-species (nitrites/nitrates) on the catalyst surface, as proposed by Galvez et al. [234].

Moreover, for both Fresh and other manipulated catalysts, NO₂ is not detected at low temperature until CO is oxidized. Schmeisser et al. found that reducing agents in the lean feed such as CO and C₃H₆ hindered the formation of NO₂ [224]. Similar results have been also found in a DPNR (Diesel particulate NO_x reduction) in lean gas conditions [225].

Fig. 4.19 presents the evolution profiles of reactants of interest over studied catalysts under the simulated gas condition Mix 3, in the absence of NO in the feed. As can be seen, the presence of K or mild aging improves the oxidation performance of the catalyst while their combination brings the contrary effect. Thus the absence of either NO or NO₂ does not affect the promotion by mild aging or the addition of K on both the C₃H₆ and CO oxidation activities. The worst scenario incurred by the manipulation of combining the aging and doping is not affected, either.

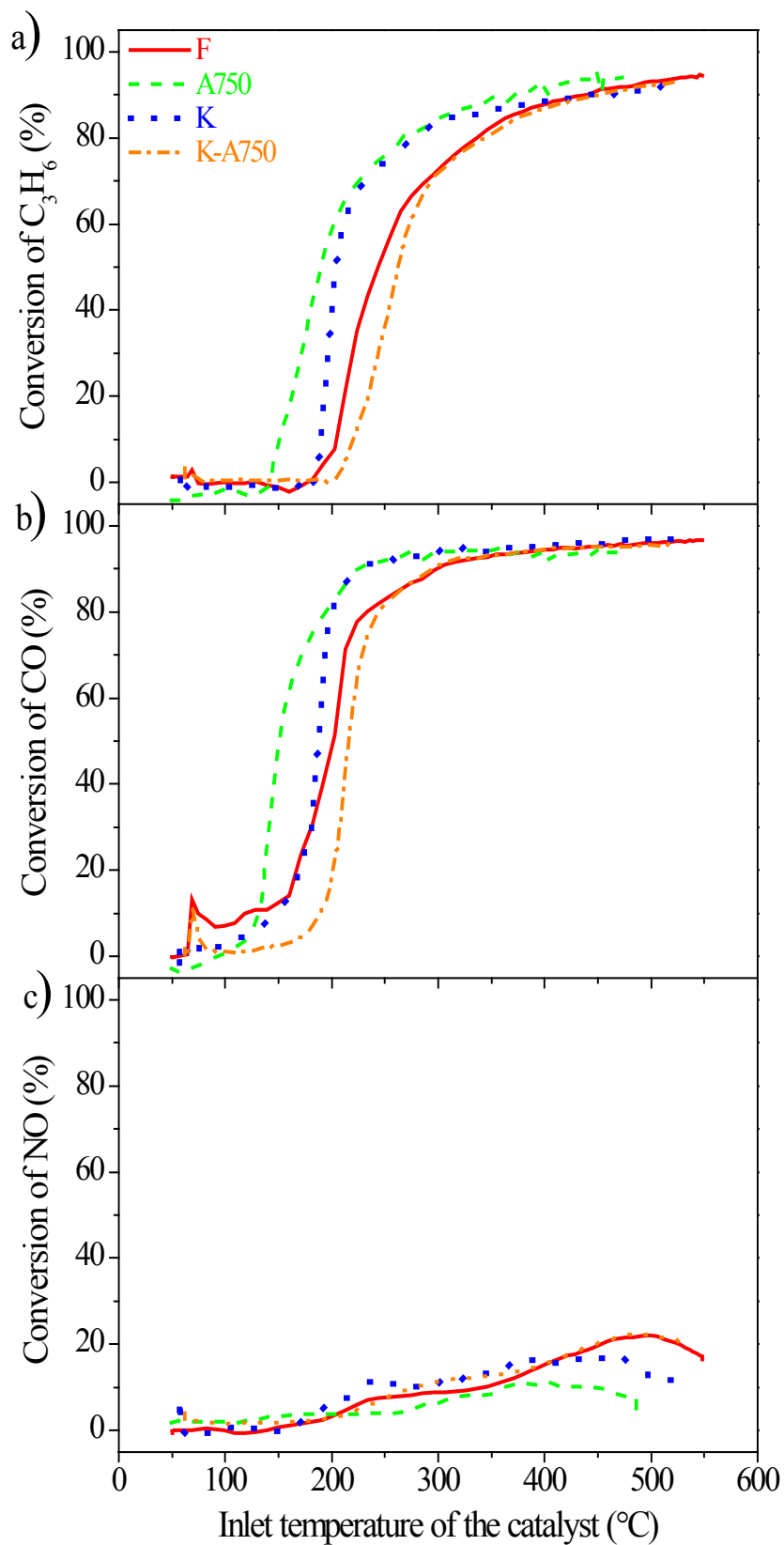


Fig. 4.18 Evolution profiles of C_3H_6 , CO and NO for Mix 2 versus temperature for reference and conditioned catalysts: (a). Conversions of C_3H_6 , (b). Conversions of CO and (c). Transformations of NO

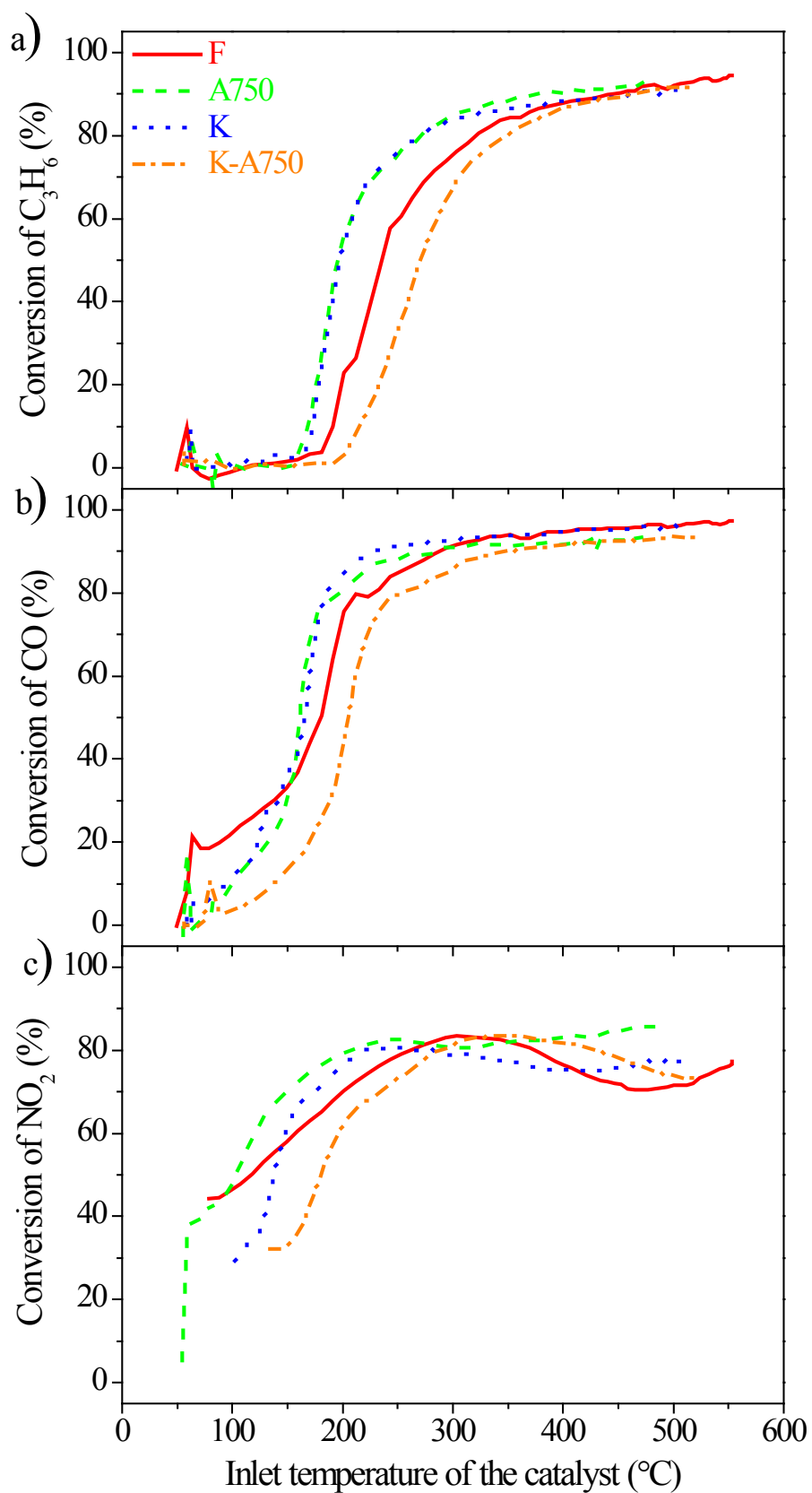


Fig. 4.19 Evolution profiles of C_3H_6 , CO and NO_2 for Mix 3 versus temperature for reference and conditioned catalysts: (a). Conversions of C_3H_6 , (b). Conversions of CO and (c). Conversions of NO_2

Fig. 4.20 displays the evolution profiles of reactants of interest over studied catalysts under the simulated gas condition Mix 4, without CO in the feed.

Again, the introduction of K or mild aging obviously promotes the oxidation reaction while their combination brings the opposite effect. Thus, the absence of NO/NO₂ or CO has no effect regarding the promotion or inhibition resulted from these manipulations to the studied catalysts.

Apparently, the promotion or inhibition resulted from these manipulations to the studied catalysts is also reflected in the conversion of NO₂ when it plays a major part as a strong oxidizer in the oxidation of C₃H₆.

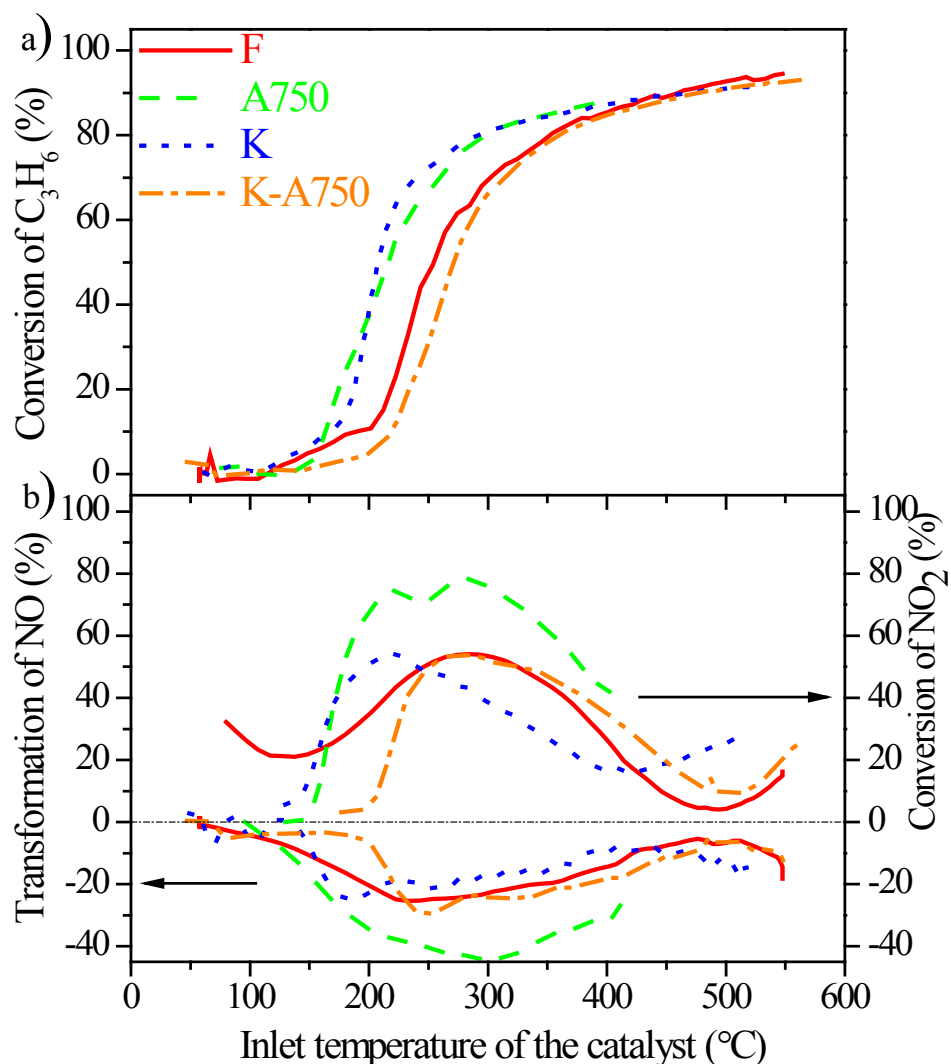


Fig. 4.20 Evolution profiles of C₃H₆ and NO_x for Mix 4 versus temperature for reference and conditioned catalysts: (a). Conversions of C₃H₆ and (b). Transformations of NO_x.

Fig. 4.21 exhibits the evolution profiles of reactants of interest over conditioned catalysts under the simulated gas condition Mix 5, in absence of both NO and NO₂ in the feed. The conversion profiles of C₃H₆ and CO in terms of performance lead to the following sequence: A750 > K > K-A750. The conclusion of the effect of the K addition to stabilized DOC can be draw: the introduction of K drastically decreases the oxidation activities of the catalyst.

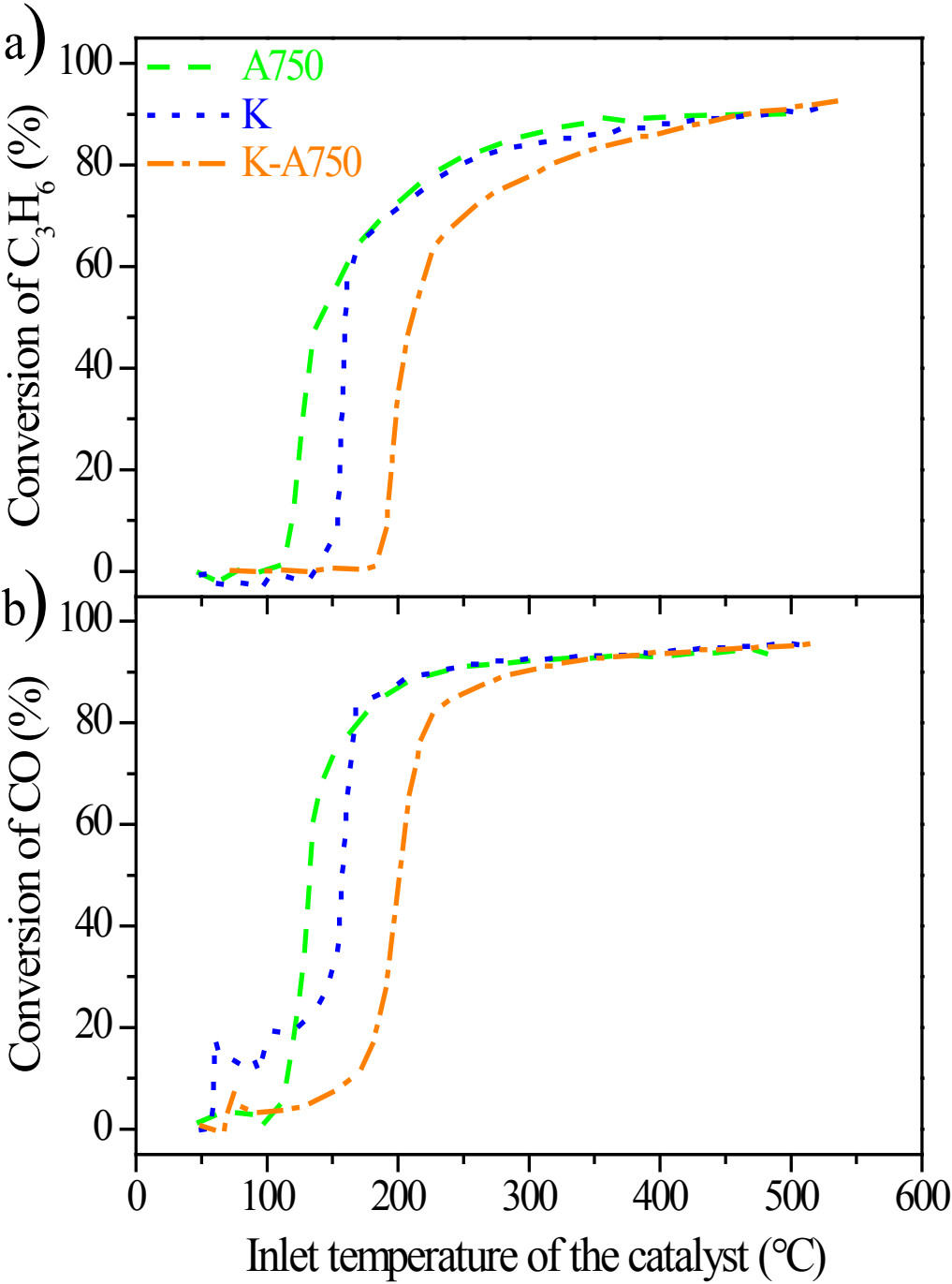


Fig. 4.21 Evolution profiles of C₃H₆ and CO for Mix 5 versus temperature for reference and conditioned catalysts: (a). Conversions of C₃H₆, and (b). Conversions of CO

4.3.2.2 Effect of the gas compositions

In order to illustrate the effect of gas compositions on the catalytic performance of studied catalysts, different experimental conditions Mix 1 to Mix 5 were compared (Table 4.6). NO_2 is removed from the feed to form Mix 2. In Mix 3, NO is removed while CO is removed regarding Mix 4. Finally both NO and NO_2 were removed from the feed in Mix 5.

Fig. 4.22 depicts the evolution profiles of C_3H_6 as a function of temperature under different mixtures over the studied catalysts. The evolution profile of C_3H_6 under the gas condition Mix 5 is not easy to neglect due to its remarkable oxidation performance. It was shown that the absence of other gas leads to an increase of C_3H_6 oxidation since there exists no reaction competition between NO and CO , C_3H_6 oxidation [227, 228]. As expected, in terms of C_3H_6 oxidation performance, the ranking for Fresh and K catalysts is then $\text{Mix 3} > \text{Mix 2} > \text{Mix 1}$ while $\text{Mix 2} > \text{Mix 3} > \text{Mix 1}$ for A750 and K-A750 catalysts. The conversions of C_3H_6 for Mix 1 and Mix 4 can be regarded as almost the same except that the absence of CO favors the C_3H_6 conversion at low temperature.

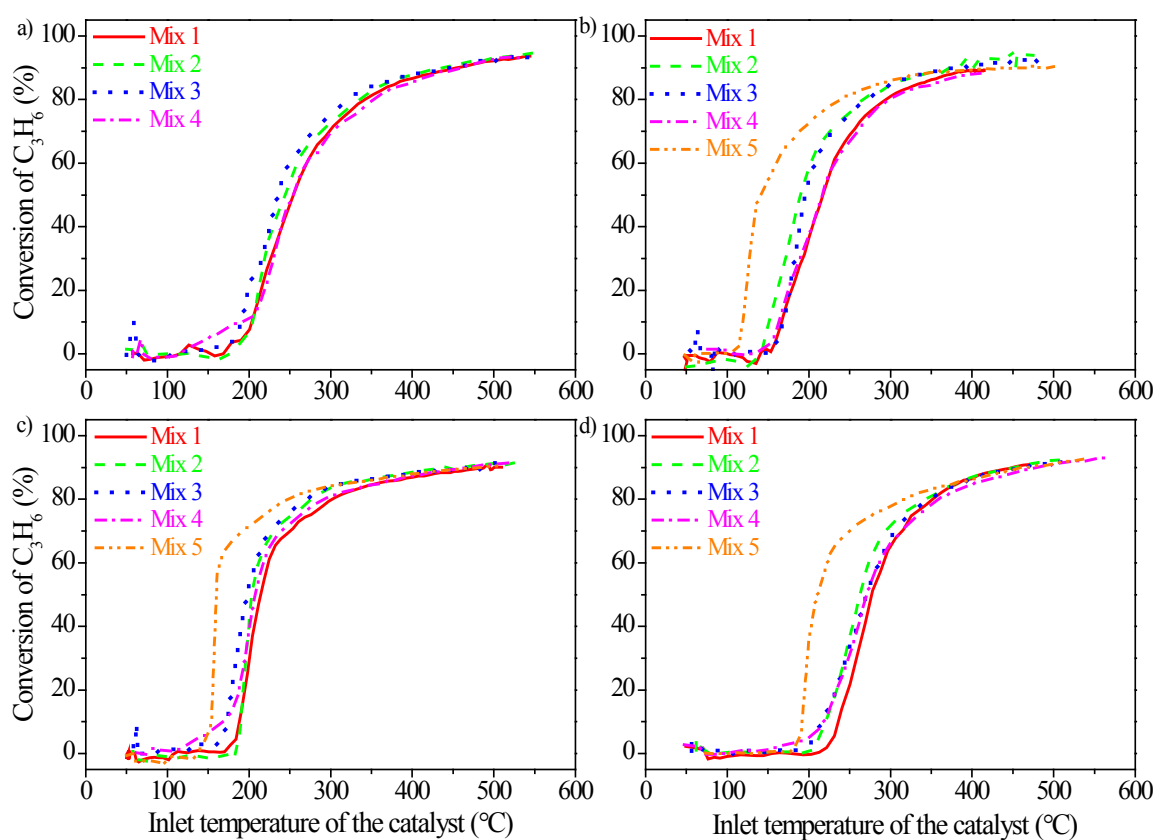


Fig. 4.22 Effect of gas compositions on the evolution profiles of C_3H_6 : (a). Fresh catalyst, (b). A750 catalyst, (c). K catalyst and (d). K-A750 catalyst

Fig. 4.23 depicts the evolution profiles of CO as a function of temperature under different mixtures over the studied catalysts.

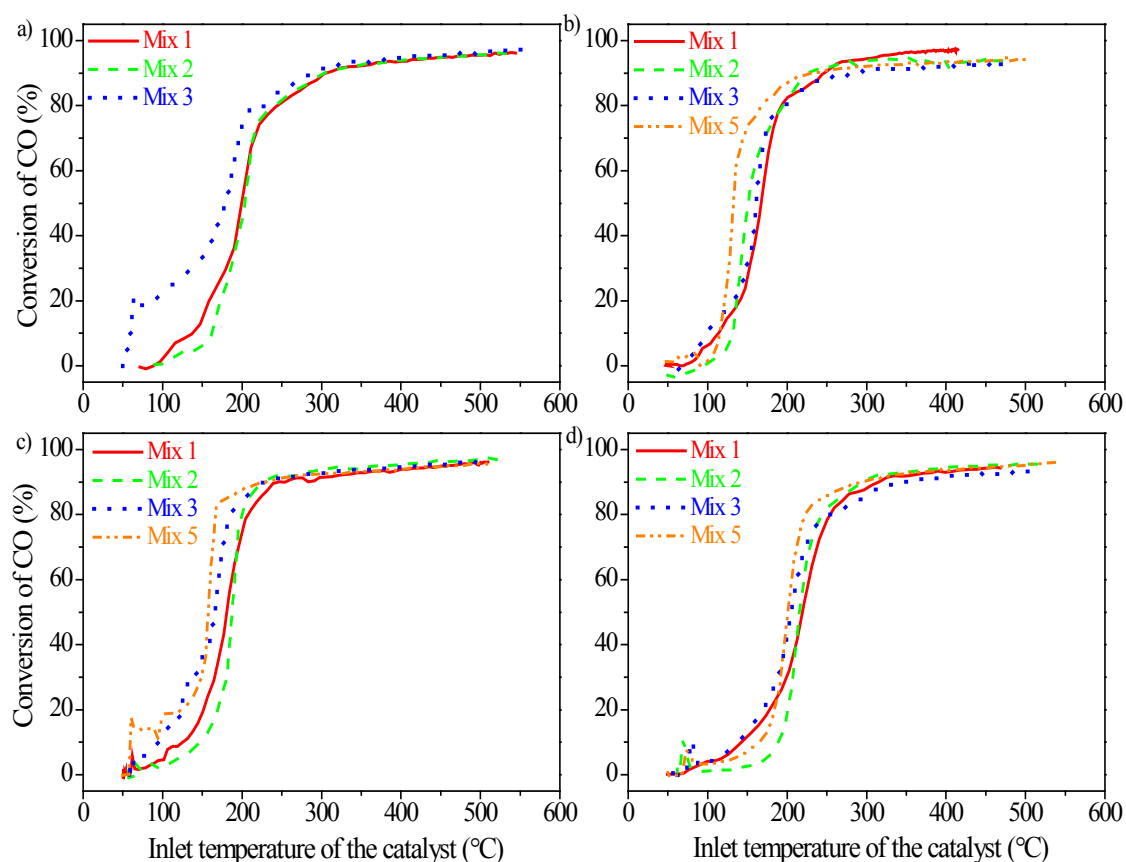


Fig. 4.23 Effect of gas compositions on the evolution profiles of CO: (a). Fresh catalyst, (b). A750 catalyst, (c). K catalyst and (d). K-A750 catalyst

Over these DOC samples, the CO oxidation takes place at lower temperature than C_3H_6 oxidation by comparing corresponding light-off curves. In general, similar to that of the C_3H_6 oxidation, Mix 5 separates itself from others with high CO oxidation performance.

At low temperature, the oxidation of CO is enhanced when NO_2 (strong oxidant) is present in the feed gas (Mix 3 and Mix 5, difference in the presence of NO_2 or not) due to the CO/ NO_2 interaction already described elsewhere ^[225]. The absence of NO in Mix 3 offers it an edge in terms of CO oxidation, compared with Mix 1. The comparison of NO_2 conversion profiles between Mix 3 and Mix 1 justifies this (Fig. 4.24). The comparison on the evolution of NO_x between Mix 1 and Mix 2 (mixture with and without NO_2 , respectively) suggests that the presence of NO_2 contributes to the formation of NO and oxidation of CO by reacting with CO ^[221]. As temperature rises, in terms of CO oxidation, Mix 5 takes the lead since the absence of other reactants pays off. The raising momentum acquired by Mix 2 with increasing

temperature is also observed, which overtakes Mix 1 finally. Thus, in general, the order for CO oxidation in general is Mix 5 > Mix 3 > Mix 2 > Mix 1.

The comparison on the evolution of NO between Mix 1 and Mix 4 (mixture with and without CO, respectively) also confirms that NO formation from reduction of NO₂ is enhanced when NO₂ reacts with CO at low temperature [221].

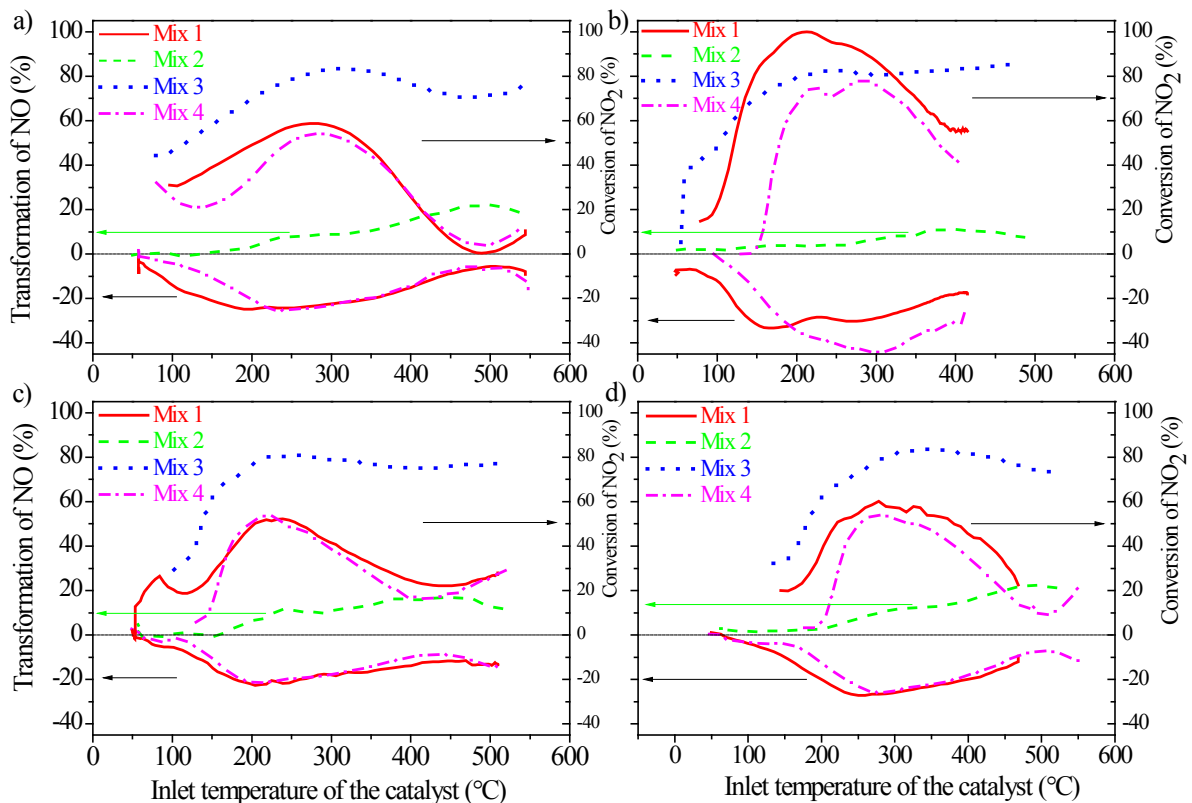


Fig. 4.24 Effect of gas compositions on the evolution profiles of NO_x: (a). Fresh catalyst, (b). A750 catalyst, (c). K catalyst and (d). K-A750 catalyst

4.3.3 Concluding remarks

On a commercial Diesel Oxidation Catalyst, studied in the monolithic form, under representative exhaust gases mixtures, it is clearly showed that the mild thermal aging leads to positive impacts on the catalytic oxidation, so does the introduction of K. Their combination, however, results in the drastic reduction of the oxidation performance.

Over these DOC samples, Fresh and manipulated ones, the CO oxidation takes place at lower temperature than C₃H₆ oxidation. Meanwhile, the NO₂ is a strong oxidant which reacts with

CO if present to give out NO, enhancing the CO oxidation and formation of NO at low temperature.

There is no impact of feed gas composition on the ranking of catalysts in terms of catalytic performance. However, it was shown that the presence of NO₂ promotes the oxidation reaction while the presence of NO competes for the same catalytic sites in terms of oxidation, leading to a shift of light-off temperature for CO and C₃H₆ to higher temperatures.

In the next section, the influence of the presence of alkali compounds on the performance of lab-made Pt-Pd/Al₂O₃ diesel oxidation catalysts in the powder form will be explored.

4.4 Influence of the presence of alkali compounds on the performance of a lab-made Pt-Pd/Al₂O₃ diesel oxidation catalyst in the powder form

4.4.1 Experimental

4.4.1.1 Catalysts preparation

Catalysts powder samples were prepared with Alumina as the support while Pt and Pd as the active phase whose ratio was 3:1 on mass basis. Alkali metals (K or/and Na, 1 wt.%) were subsequently introduced to the DOC powdered catalysts through a conventional wet impregnation method. The catalyst named K-A750 in Table 4.7 was aged for 4 hours at 750°C prior to the doping of K.

Table 4.7 Different methods dealing with powder DOC

Entry	Catalyst condition
F	Fresh
K	1% KNO ₃
Na	1% NaNO ₃
K-Na	1% K+Na NO ₃
K-A750	750_4H + KNO ₃

4.4.1.2 Characterization of catalysts

The acquired catalysts were characterized by XRD. XRD patterns of studied catalysts were acquired on a PANalytical-Empyrean diffractometer with monochromatic beam of X-Ray source (Cu-K α radiation, $\lambda=0.15406$ nm). XRD measurements were performed from 3 to 90° in an interval of 0.02° (2 θ) with a step time of 60s for each point during data acquisition.

4.4.1.3 Catalytic activity studies

A synthetic gas bench was used, the total flow rate being 250 mL·min⁻¹ (GHSV=150,000 h⁻¹). A typical reactant gas mixture (Mix 1, see Table 4.8) representative of the exhaust gases from diesel engines consists of hydrocarbon (C₃H₆ 200 ppm), CO (300 ppm), NO (300 ppm), O₂ (8%), H₂O (3%) and Ar (balance).

Table 4.8 Synthetic gas bench experimental conditions for powder DOCs

	C ₃ H ₆ ppm	NO ppm	CO ppm	O ₂ (%)	H ₂ O (%)	Ar (%)
Mix 1	200	300	300	8	3	Balance
Mix 2	-	300	300	8	3	Balance
Mix 3	200	-	300	8	3	Balance
Mix 4	200	300	-	8	3	Balance
Mix 5	200	-	-	8	3	Balance
Mix 6	-	300	-	8	3	Balance
Mix 7	-	-	300	8	3	Balance
Mix 6_TPD	-	300	-	8	3	Balance

4.4.2 Effects of presence of alkali compounds on the performance of oxidation catalysts

4.4.2.1 Effect of alkali metals on a DOC under gaseous mixtures representative of diesel exhaust

Fig. 4.25 presents the evolution profiles of reactants of interest over studied catalysts, Fresh and conditioned ones, under the simulated gas condition Mix 1, which is representative of a real exhaust mixture. As far as the conversions of C₃H₆ are concerned, the addition of dopants can be generally considered as beneficial to the catalytic performance. Among them, the

presence of Na alone exerts the most significant impact. The mechanism of resulted enhancement of the activity from the presence of Na will most probably be associated with the formation of adsorbed N-species (nitrites/nitrates) on the catalyst surface, as proposed by Galvez et al. [234].

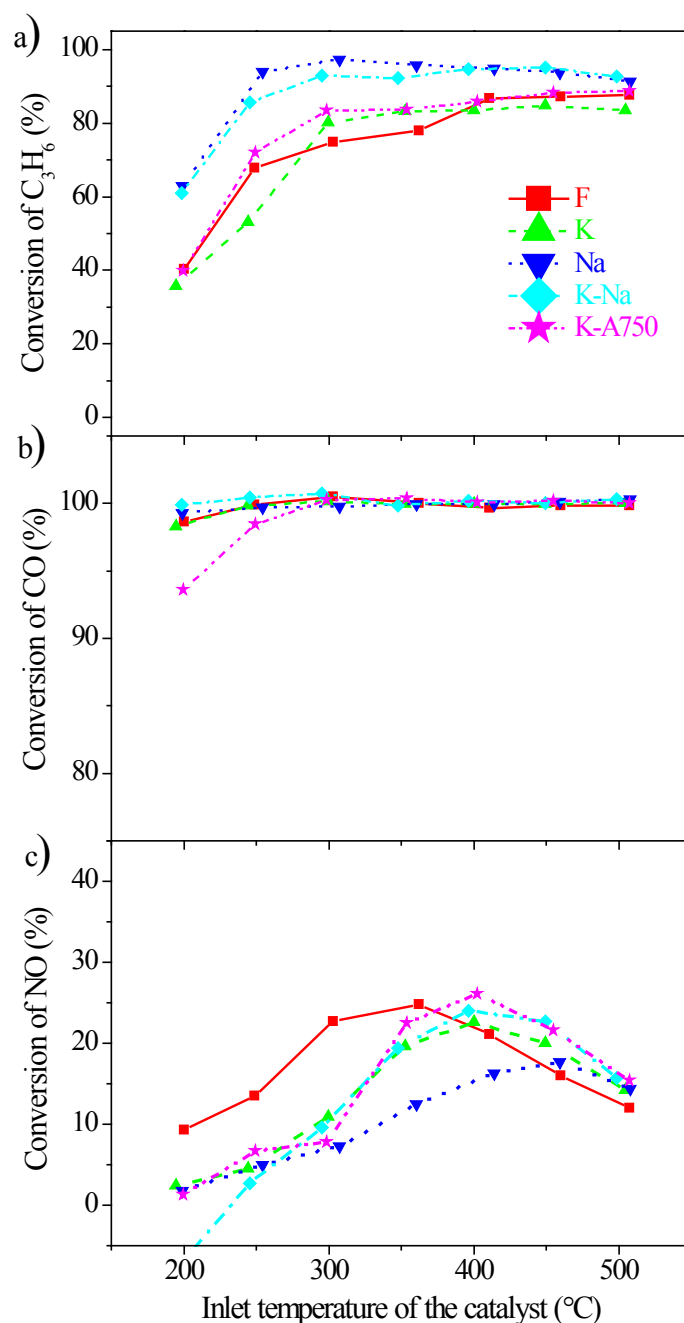


Fig. 4.25 Evolution profiles of C_3H_6 , CO and NO for Mix 1 versus temperature for reference and conditioned catalysts: (a). Conversions of C_3H_6 , (b). Conversions of CO and (c). Conversions of NO

With respect to CO conversions, there exists no remarkable difference due to the almost complete conversion above the temperature 200°C.

Particular attention should be paid to the conversions of NO. The presence of dopants, either K/Na alone or their combination, inhibits the NO conversion at temperatures below 350°C. It's obvious that the maximal conversion of NO is reached by the Fresh catalyst in the first place, followed by the ones with dopants but without Na, while the doping of Na drastically postpones it. The plausible explanation for the postponement can be attributed to the over-promotion after the addition of alkali compounds ^[233].

The comparison of the promotion on C₃H₆ oxidation reaction by the alkali compound (K or/and Na) to their respective inhibition on NO oxidation reaction sheds lights on different mechanism associated with the oxidation reactions of reactants of interest.

Fig. 4.26 displays the evolution profiles of reactants of interest over studied catalysts under the simulated gas condition Mix 2, thus in the absence of C₃H₆ in the feed.

Again, it's difficult to notice the differences among the CO conversion profiles for studied catalysts. The NO conversion profiles for studied catalysts, on the contrary, exhibits remarkable differences: in terms of the NO conversion performance, the order is Na > F > K. In other words, Na acts as a promoter compared to the Fresh catalyst while K an inhibitor. The resulted enhancement of the activity due to the presence of Na is in accord with other reported study ^[230, 231]. As for K acting as an inhibitor, it can be ascribed to the decrease of the active sites of the targeted catalyst after the introduction of K.

Fig. 4.27 presents the evolution profiles of reactants of interest over studied catalysts under the simulated gas condition Mix 3, in the absence of NO in the feed. As can be seen, the presence of alkali compound (Na or K) improves the oxidation performance of the catalyst compared to the Fresh catalyst. In terms of enhancement degree, the presence of Na engenders stronger impact than that of K.

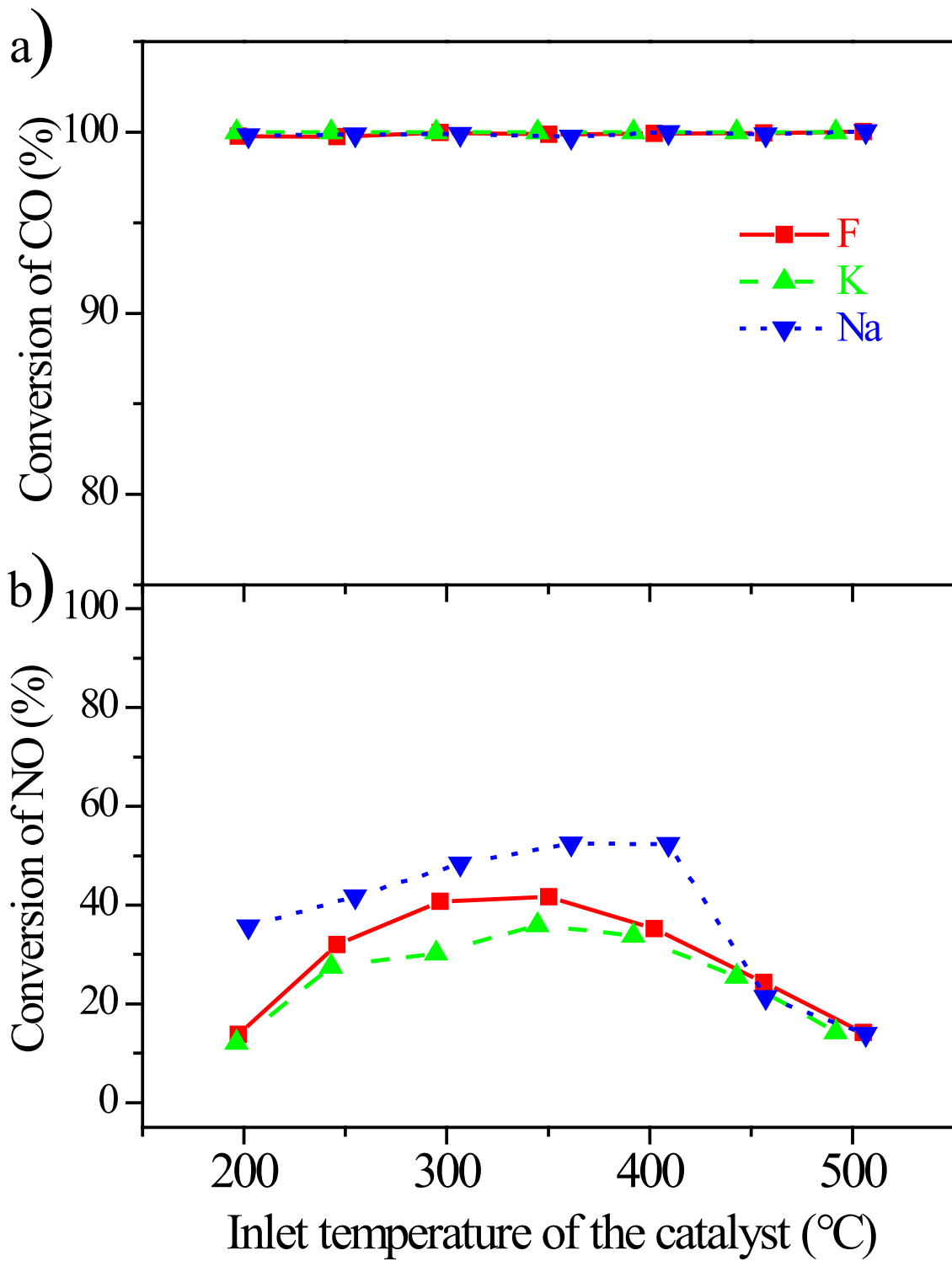


Fig. 4.26 Evolution profiles of CO and NO for Mix 2 versus temperature for reference and conditioned catalysts:
 (a). Conversions of CO and (b). Conversions of NO

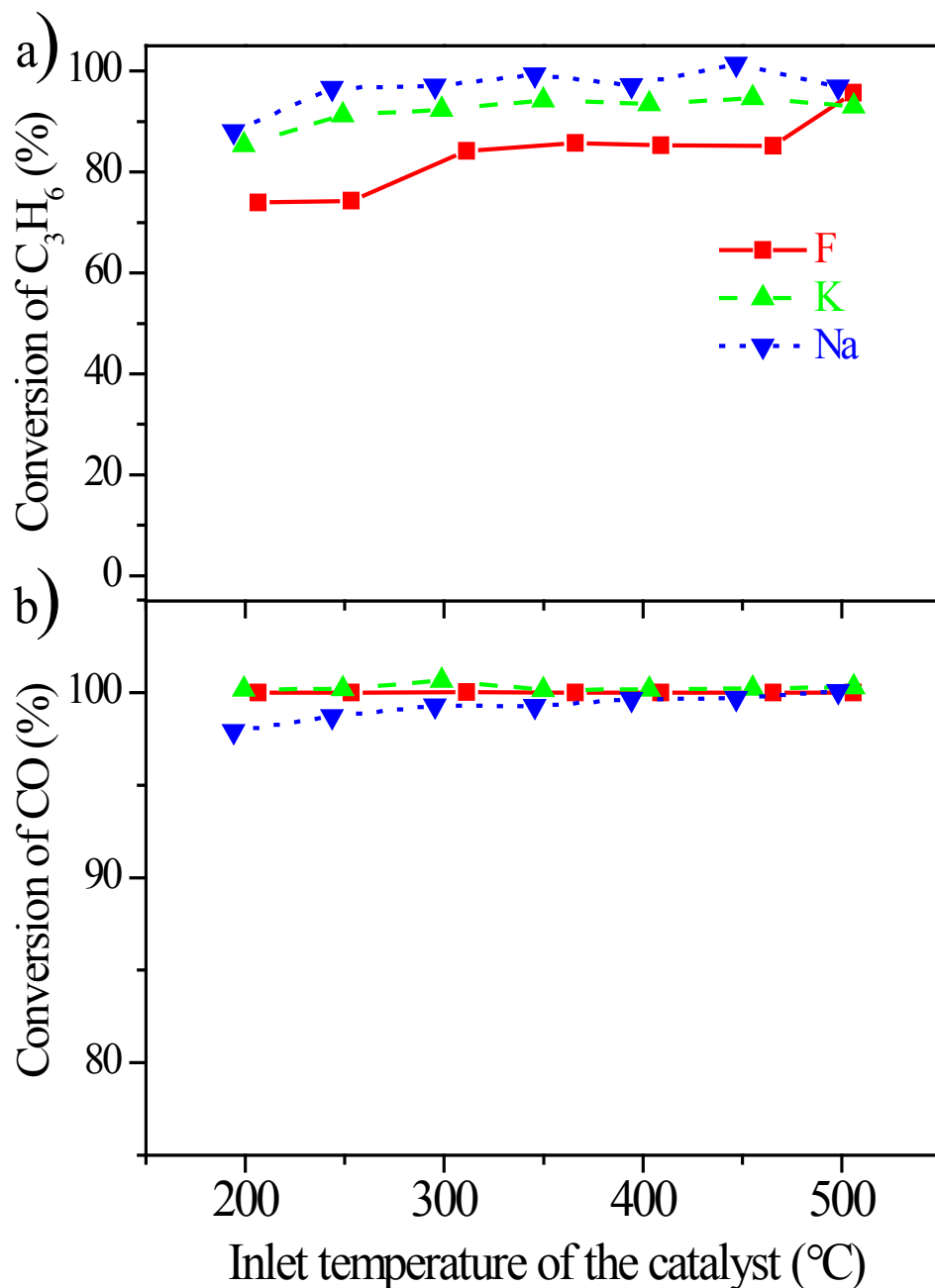


Fig. 4.27 Evolution profiles of C₃H₆ and CO for Mix 3 versus temperature for reference and conditioned catalysts: (a). Conversions of C₃H₆ and (b). Conversions of CO

Fig. 4.28 displays the evolution profiles of reactants of interest over studied catalysts under the simulated gas condition Mix 4, in absence of CO in the feed.

As can be noticed, the introduction of alkali compound (K or Na) obviously promotes the C₃H₆ oxidation reaction. Thus, the absence of NO or CO has no effect regarding the promotion on C₃H₆ oxidation of K addition or Na addition to the studied catalysts.

The introduction of alkali compound (K or Na), however, significantly inhibits the NO oxidation reaction. As pointed out before, this can be caused by the decrease of the active sites for NO oxidation reaction after the addition of K or Na.

The comparison of the promotion on C₃H₆ oxidation reaction by the alkali compound (K or Na) to their respective inhibition on NO oxidation reaction sheds lights on different mechanism associated with the oxidation reactions of reactants of interest.

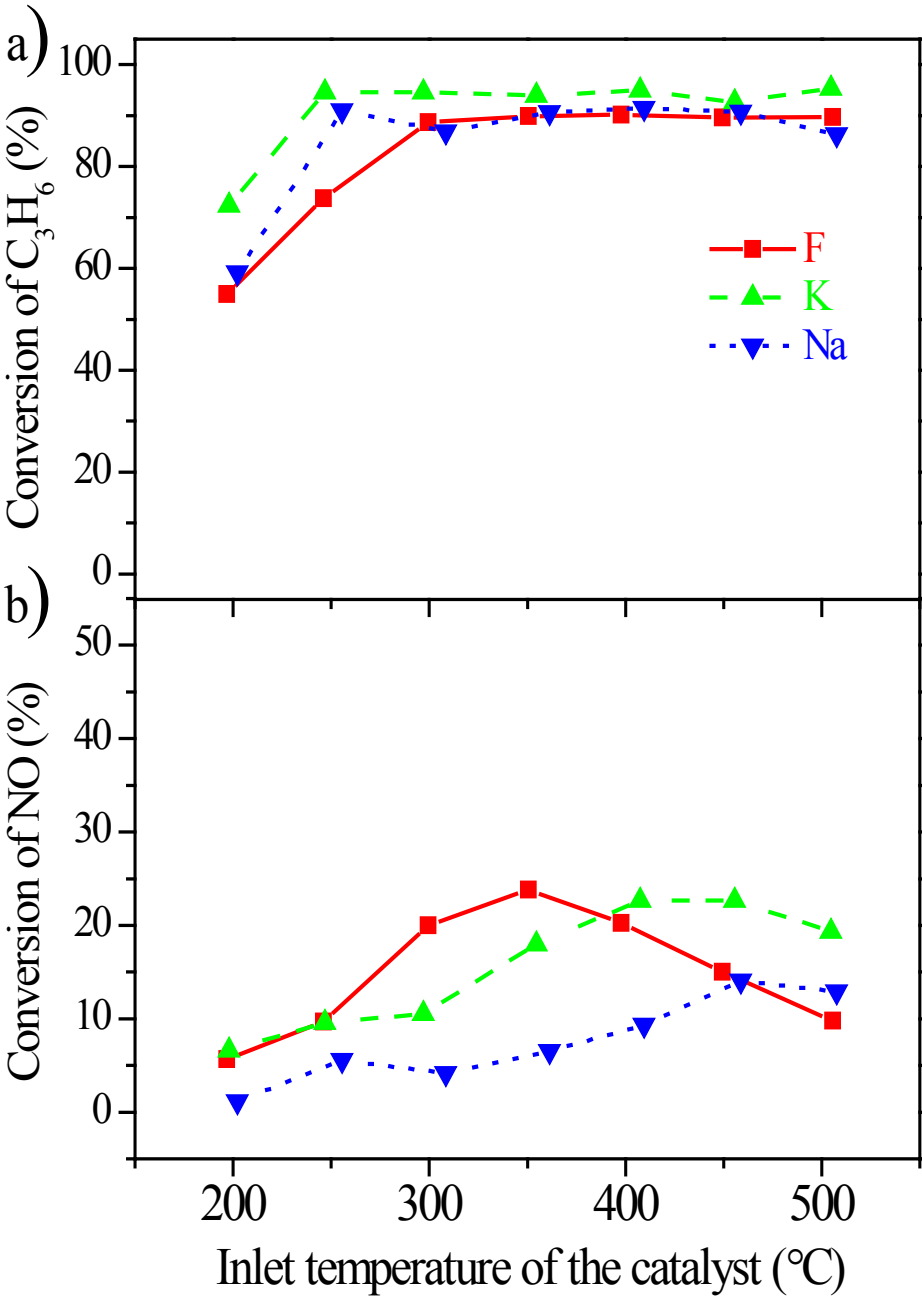


Fig. 4.28 Evolution profiles of C₃H₆ and NO for Mix 4 versus temperature for reference and conditioned catalysts: (a). Conversions of C₃H₆ and (b). Conversions of NO

4.4.2.2 Effect of the gas composition

In order to illustrate the effect of gas compositions on the catalytic performance of studied catalysts, different experimental conditions Mix 1 to Mix 4 were compared (Table 4.8). C_3H_6 is removed from the feed to form Mix 2. In Mix 3, NO is removed while CO is removed regarding Mix 4.

Fig. 4.29 depicts the evolution profiles of C_3H_6 for different mixtures over the studied catalysts.

The comparison of C_3H_6 conversion profiles between Mix 1 and Mix 4 (mixture with and without CO, respectively) evidences that the absence of CO is beneficial to the C_3H_6 oxidation. Additionally, the absence of NO has the same effect in some way from the comparison of C_3H_6 conversion profiles between Mix 1 and Mix 3 (mixture with and without NO, respectively). It was shown that the absence of other gas leads to an increase of C_3H_6 oxidation since there exists no reaction competition between NO and CO, C_3H_6 oxidation [227, 228]. As expected, in terms of C_3H_6 oxidation performance, the ranking in general is then Mix 4 > Mix 3 > Mix 1.

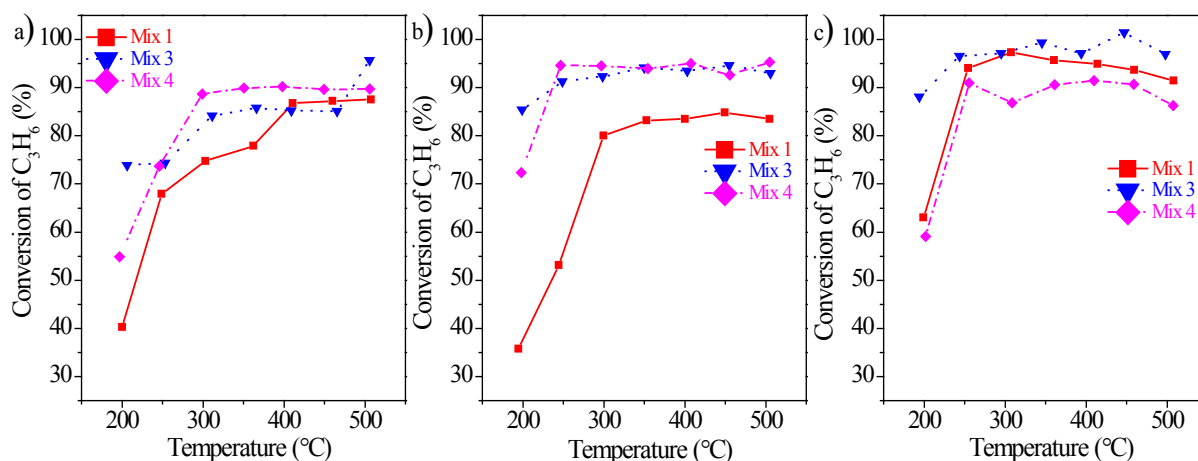


Fig. 4.29 Effect of gas compositions on the evolution profiles of C_3H_6 : (a). Fresh, (b). K and (c). Na

Fig. 4.30 depicts the evolution profiles of CO for different mixtures over the studied catalysts. No clear conclusions can be drawn from these plots since CO oxidation is almost completed above the temperature 200°C.

The NO evolution profiles under different mixtures as well as over these DOC samples vary, as presented in Fig. 4.31. Mix 2 distinguishes itself from others with impressive NO oxidation performance. Thus, it can be asserted that the presence of C₃H₆ can inhibit the NO conversion. Combining the inhibition from NO on the C₃H₆ conversion, it's safe to propose that both reactants are mutually inhibitor to each other.

Meanwhile, the comparison of NO evolution profiles between Mix 1 and Mix 4 (mixture with and without CO, respectively) demonstrates that the influence of CO on NO conversion is negligible.

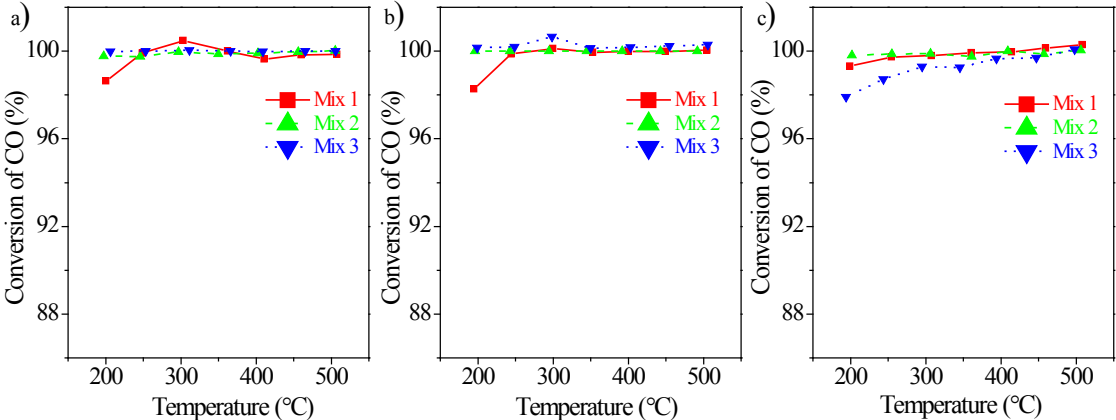


Fig. 4.30 Effect of gas compositions on the evolution profiles of CO: (a). Fresh, (b). K and (c). Na

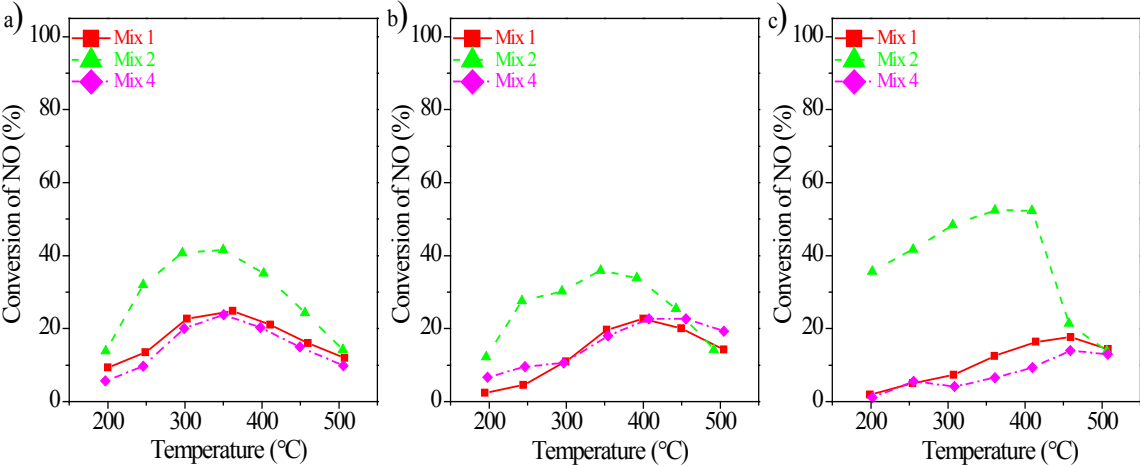


Fig. 4.31 Effect of gas compositions on the evolution profiles of NO: (a). Fresh, (b). K and (c). Na

4.4.3 Concluding remarks

On the lab-made diesel oxidation catalyst, studied in the powder form, under representative exhaust gases mixtures, it is clearly showed that the introduction of dopants leads to either negative or positive impacts on the catalytic oxidation.

In general, the addition of alkali compound (K or/and Na) leads to a promotion of the C₃H₆ oxidation reactions while incurs an inhibition on the NO conversion. From the analysis of changing the pollutants in the feed, it's concluded that C₃H₆ and NO are mutually inhibitor to each other when it comes to their oxidation. Moreover, the influence of CO on NO conversion is negligible though the presence of CO brings negative impact to the C₃H₆ oxidation. There is no impact of exhaust gas composition on the ranking of catalysts.

In the next section, the influence of the presence of alkali compounds on monolith DOC and lab-made DOC performance will be compared.

4.5 Comparison of lab-based research work on monolith DOC to model DOC in the presence of alkali compounds

As presented in previous sections, the research on the diesel oxidation catalyst varies in a broad spectra: from using different aging characteristics to the doping of alkali compounds, from employing the monolith form of catalyst to the powder form of lab-made catalyst.

In this section, the comparison of lab-based research work on monolith DOC to model DOC in the presence of alkali compounds will be performed.

4.5.1 Experimental

First, some description about the studied catalysts will be provided. The monolith DOC is a commercial catalyst, with bimetallic Pt/Pd (3/1 on mass basis) phase supported on alumina with a metallic loading of 80g/ft³, 400 channels per square inches (CPSI). It was cut into cylindrical "carrots". The used lab-made DOC also has Pt and Pd as the active phase and their mass ratio is Pt/Pd=3.

Then, related experimental conditions will be detailed, see Table 4.9 and Table 4.10.

Table 4.9 Experimental setup of monolith catalysts for the comparison study

Entry	C ₃ H ₆	NO ₂	NO	CO	CO ₂	O ₂	H ₂ O	N ₂
	ppm	ppm	ppm	ppm	(%)	(%)	(%)	(%)
Fresh monolith Mix 1	200	-	300	300	5	10	5	Balance
KNO ₃ monolith Mix 1	200	-	300	300	5	10	5	Balance
NaNO ₃ monolith Mix 1	200	-	300	300	5	10	5	Balance
K+Na NO ₃ monolith Mix 1	200	-	300	300	5	10	5	Balance
750+KNO ₃ monolith Mix 1	200	-	300	300	5	10	5	Balance

Table 4.10 Experimental setup of powder catalysts for the comparison study

Entry	C ₃ H ₆	NO ₂	NO	CO	CO ₂	O ₂	H ₂ O	Ar
	ppm	ppm	ppm	ppm	(%)	(%)	(%)	(%)
Fresh powder Mix 1	200	-	300	300	-	8	3	Balance
KNO ₃ powder Mix 1	200	-	300	300	-	8	3	Balance
NaNO ₃ powder Mix 1	200	-	300	300	-	8	3	Balance
K+Na NO ₃ powder Mix 1	200	-	300	300	-	8	3	Balance
750+KNO ₃ powder Mix 1	200	-	300	300	-	8	3	Balance

4.5.2 Results and discussion

In this section, the results of their catalytic activities tests will be presented and compared in order to shed light on the role of the catalyst form in the reaction process mainly involving C₃H₆, CO and NO.

Fig. 4.32 shows the activity profiles of C₃H₆, CO and NO as a function of temperature under Mix 1 over Fresh monolith and powder catalysts. Generally speaking, powder catalyst exhibits better performance than that of monolith DOC.

Fig. 4.33 displays the activity profiles of C₃H₆, CO and NO as a function of temperature under Mix 1 over K-doped monolith and powder catalysts. Since the CO oxidation can be considered as almost completed, attention should be focused on the conversions of C₃H₆ and NO. In terms of C₃H₆ oxidation, K-doped monolith takes the lead. Even at low temperature, it exhibits better performance than that of powder DOC. As temperature rises, it's overtaken by powder DOC as far as the NO conversion is concerned.

Fig. 4.34 presents the activity profiles of C_3H_6 , CO and NO as a function of temperature under Mix 1 over Na-doped monolith and powder catalysts. Generally speaking, powder catalyst exhibits better performance than that of monolith DOC when taking the oxidations of C_3H_6 and CO as the reference. In terms of NO conversion, however, K-doped monolith takes the lead.

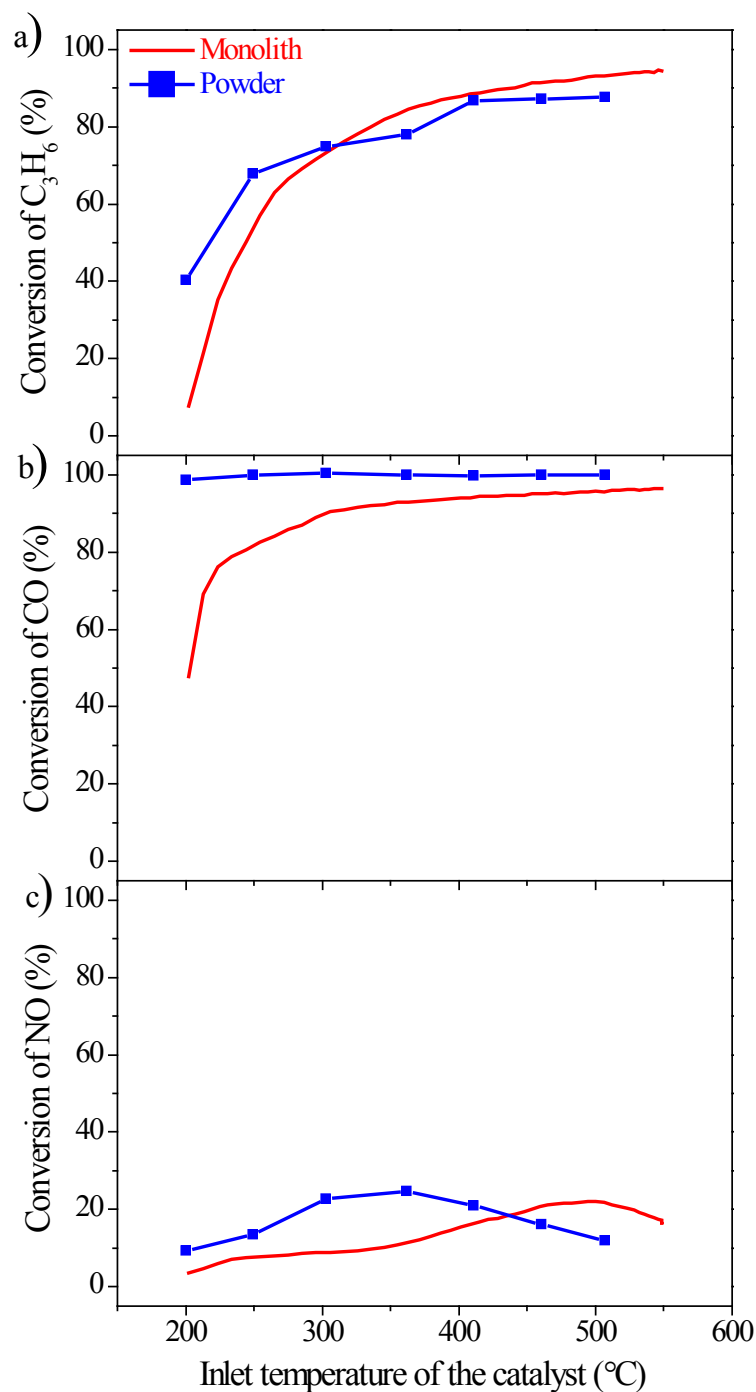


Fig. 4.32 The activity profiles of C_3H_6 , CO and NO as a function of temperature under Mix 1 over Fresh monolith and powder catalysts: (a). Conversions of C_3H_6 , (b). Conversions of CO and (c). Conversions of NO

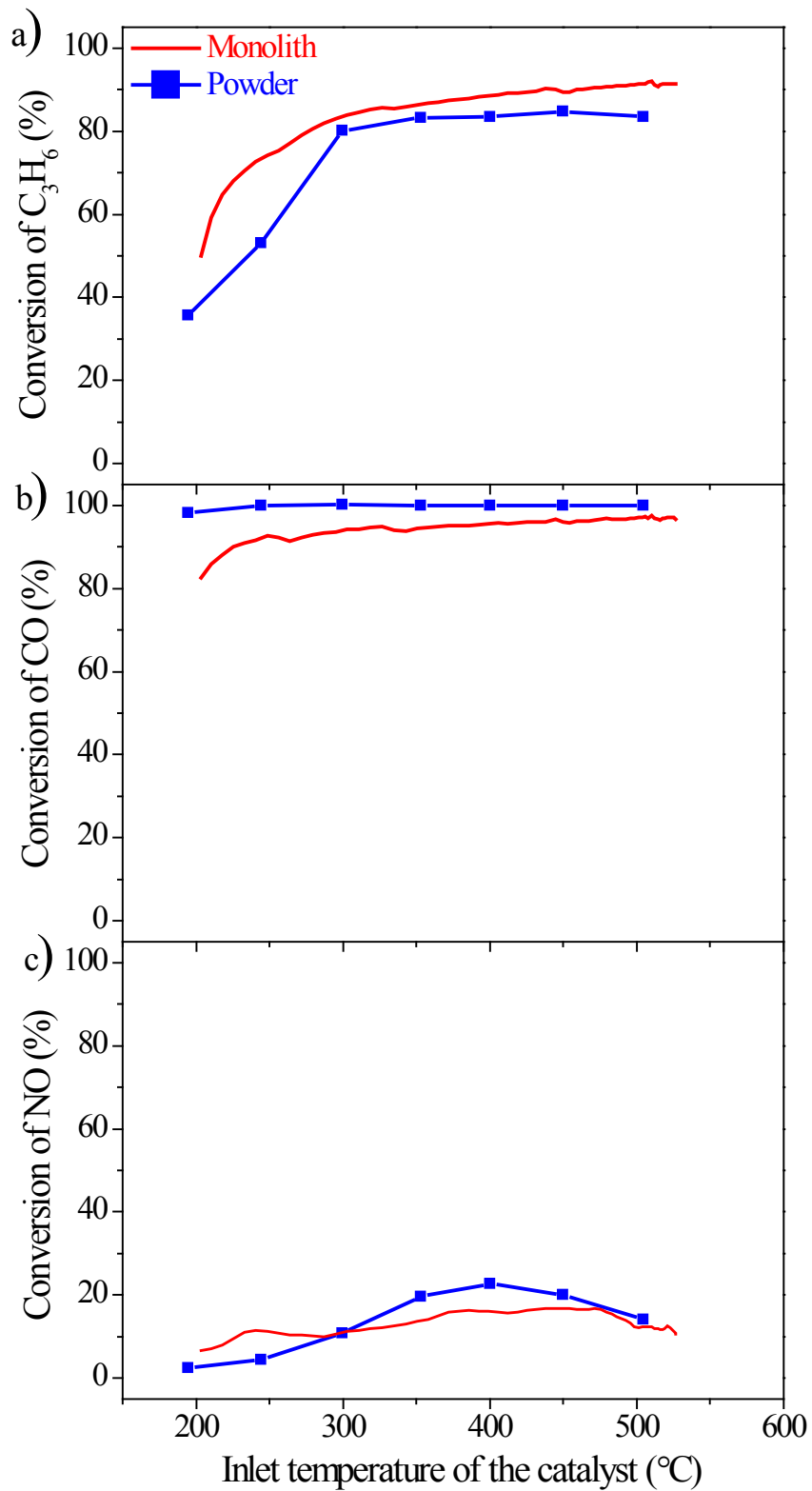


Fig. 4.33 The activity profiles of C_3H_6 , CO and NO as a function of temperature under Mix 1 over K-doped monolith and powder catalysts: (a). Conversions of C_3H_6 , (b). Conversions of CO and (c). Conversions of NO

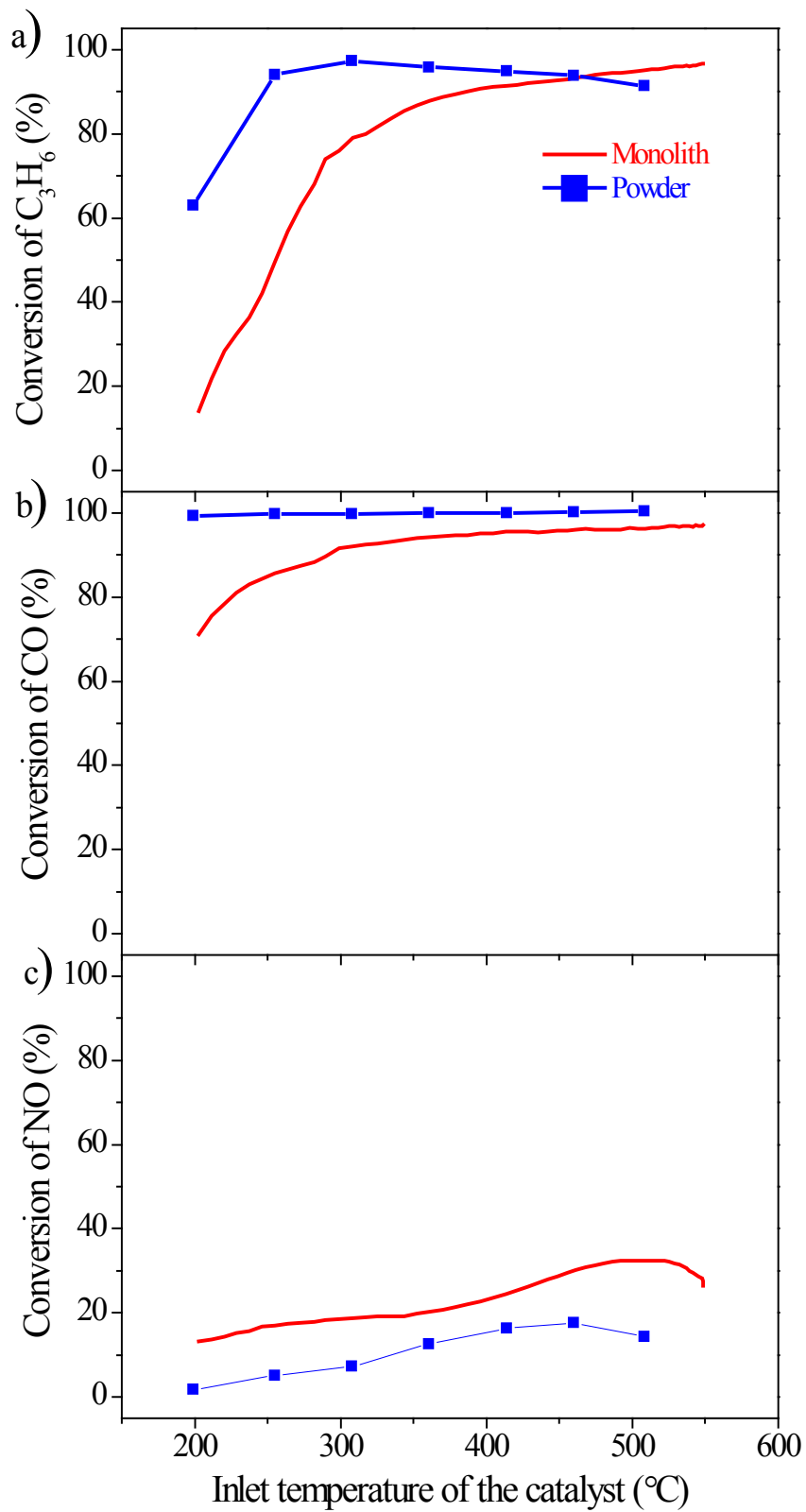


Fig. 4.34 The activity profiles of C_3H_6 , CO and NO as a function of temperature under Mix 1 over Na-doped monolith and powder catalysts: (a). Conversions of C_3H_6 , (b). Conversions of CO and (c). Conversions of NO

Fig. 4.35 describes the activity profiles of C_3H_6 , CO and NO as a function of temperature under Mix 1 over K-Na monolith and powder catalysts. Similar to what happens to the Fresh monolith and powder catalysts, powder catalyst exhibits better performance than that of monolith DOC in general.

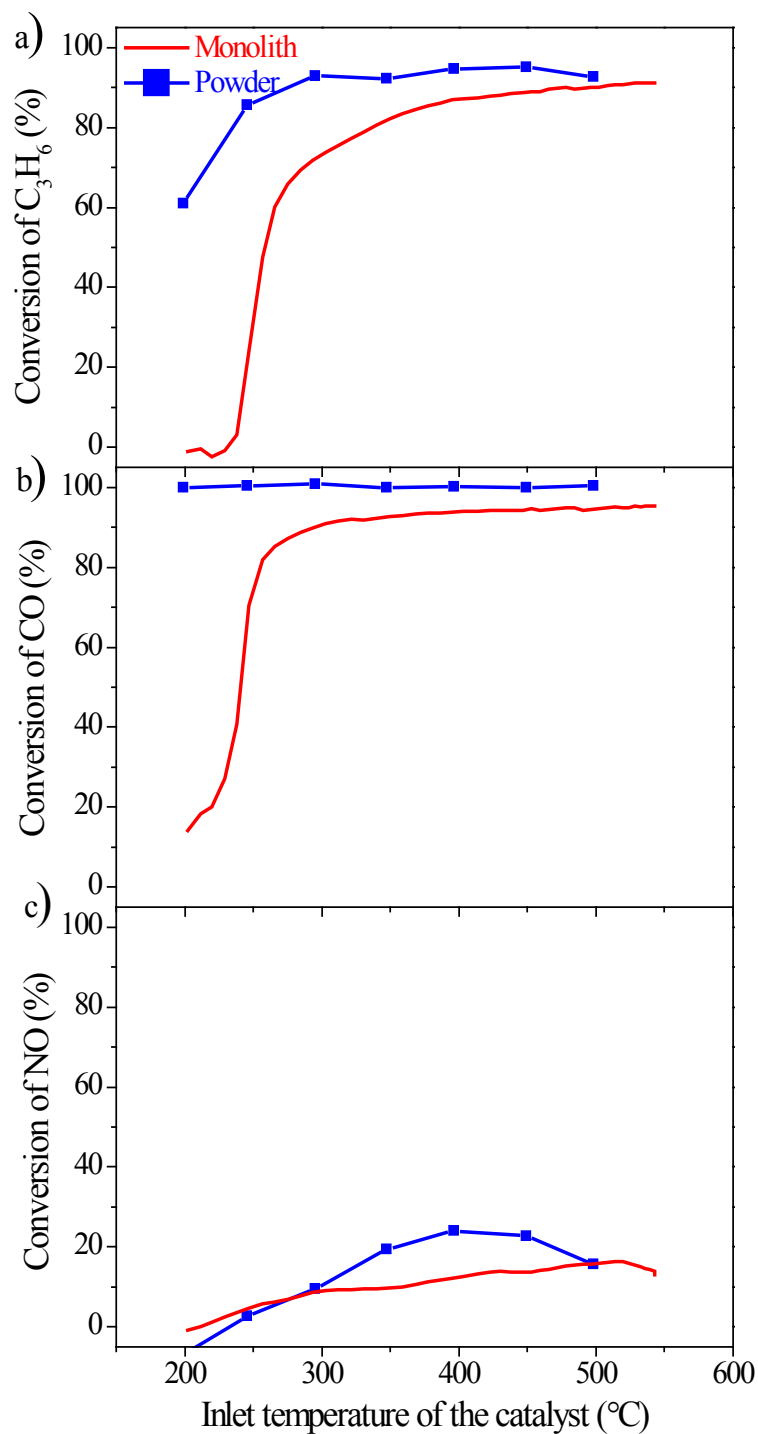


Fig. 4.35 The activity profiles of C_3H_6 , CO and NO as a function of temperature under Mix 1 over K-Na monolith and powder catalysts: (a). Conversions of C_3H_6 , (b). Conversions of CO and (c). Conversions of NO

Fig. 4.36 depicts the activity profiles of C_3H_6 , CO and NO as a function of temperature under Mix 1 over K-A750 monolith and powder catalysts. Obviously, powder catalyst exhibits better performance than that of monolith DOC. There exists a large difference regarding the conversions of C_3H_6 and CO between K-A750 powder catalyst and monolith catalyst at low temperature. At high temperature, the K-A750 powder catalyst overtakes the monolith catalyst in the NO conversion though it loses advantages in other two arenas.

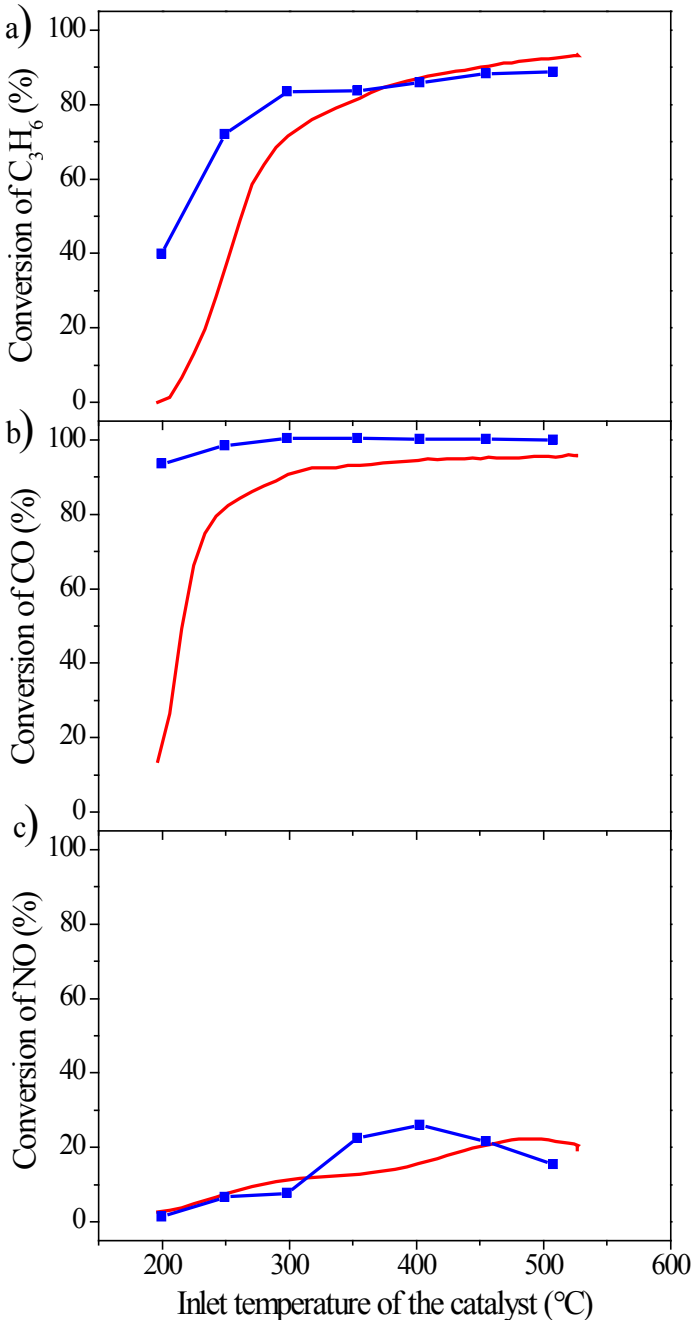


Fig. 4.36 The activity profiles of C_3H_6 , CO and NO as a function of temperature under Mix 1 over K-A750 monolith and powder catalysts: (a). Conversions of C_3H_6 , (b). Conversions of CO and (c). Conversions of NO

To better understand how the catalyst form and the dopants affect the catalyst performance, more plots are made.

Fig. 4.37 presents the conversion profiles of C_3H_6 as a function of temperature under Mix 1 over Fresh and doped monolith and powder catalysts. Overall, in terms of C_3H_6 oxidation, powder catalyst exhibits better performance than that of monolith DOC. From Fig. 4.37b, it can be asserted that the introduction of K strongly affects the catalyst activity in the monolith form, in a positive way.

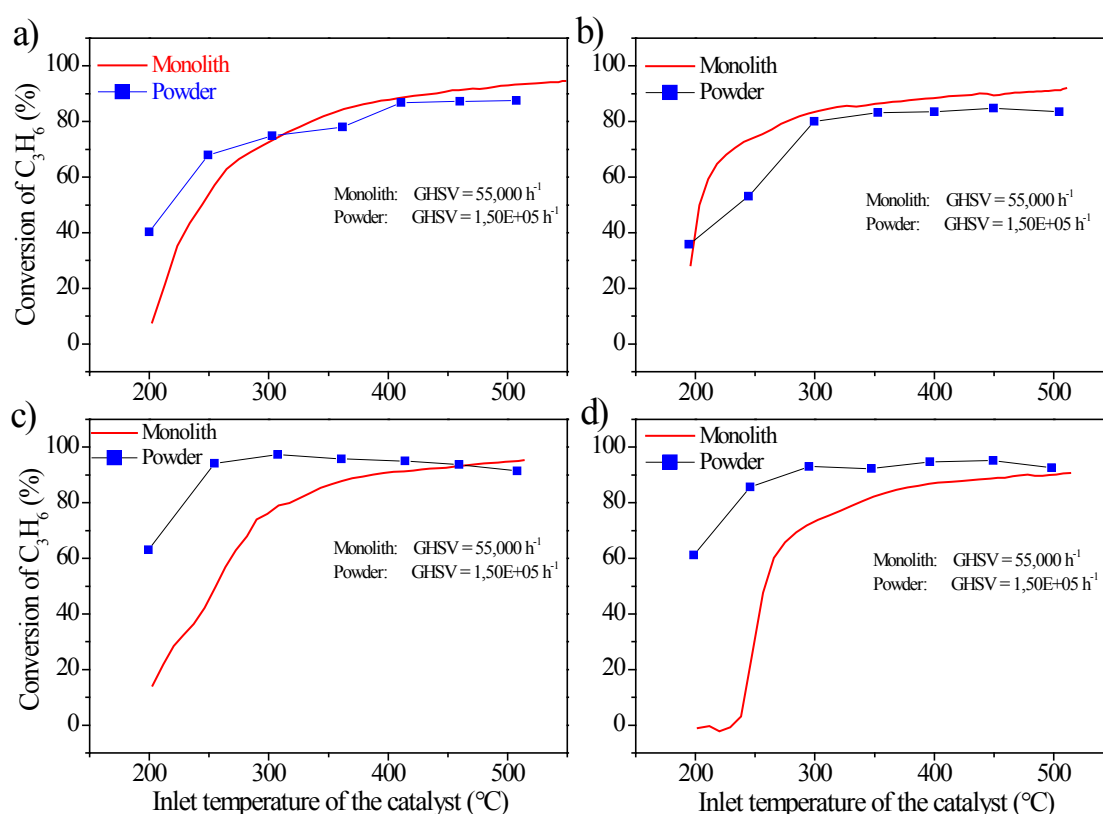


Fig. 4.37 Conversion profiles of C_3H_6 as a function of temperature under Mix 1 over Fresh and doped monolith and powder catalysts: (a). Fresh, (b). K, (c). Na, and (d) K-Na

Fig. 4.38 illustrates the conversion profiles of CO as a function of temperature under Mix 1 over Fresh and doped monolith and powder catalysts. Overall, in terms of CO oxidation, powder catalyst exhibits better performance than that of monolith DOC. From Fig. 4.38d, it can be proposed that the introduction of double dopants strongly affects the catalyst activity in the monolith form, in a negative way.

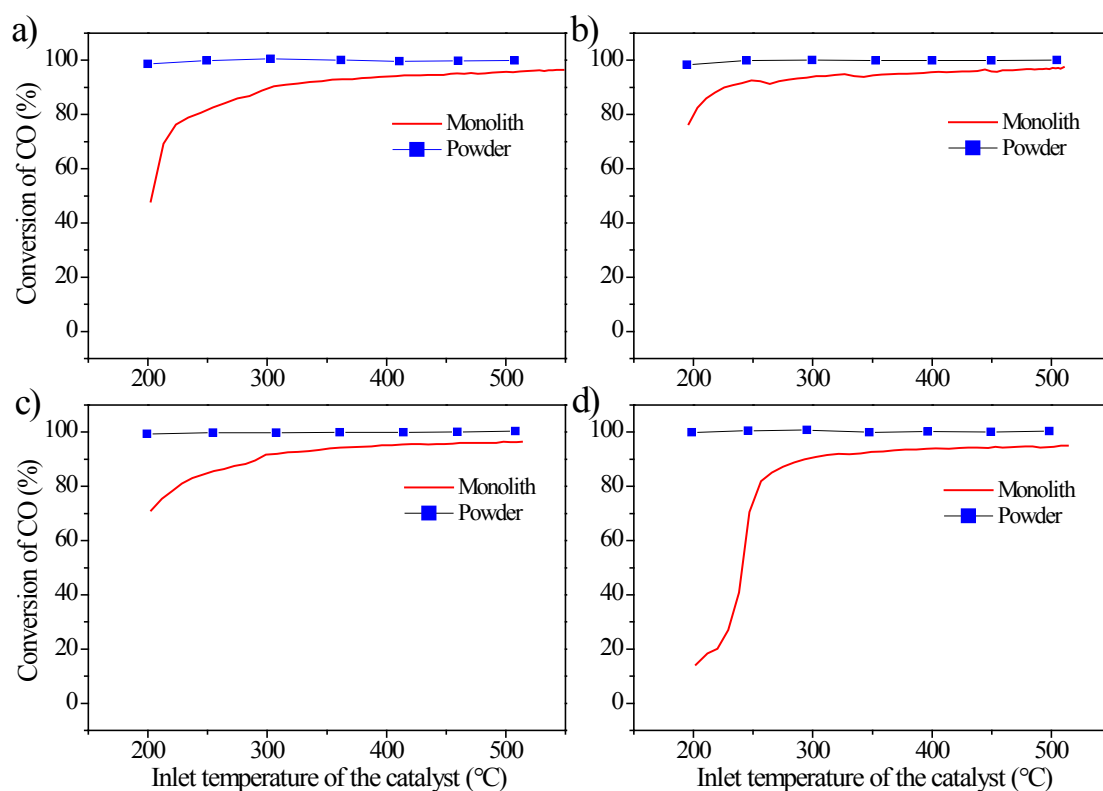


Fig. 4.38 Conversion profiles of CO as a function of temperature under Mix 1 over Fresh and doped monolith and powder catalysts: (a). Fresh, (b). K, (c). Na, and (d) K-Na

Fig. 4.39 shows the conversion profiles of NO as a function of temperature under Mix 1 over Fresh and doped monolith and powder catalysts. Overall, in terms of NO conversion, powder catalyst exhibits better performance than that of monolith DOC. From Fig. 4.39c, monolith DOC stands out with impressive NO conversion. According to previous studies, the introduction of Na strongly promotes the activity of the catalyst in the monolith form while it acts as an inhibitor when it affects the powder catalyst. Thus, there appears a large gap between these conversion profiles.

Based on the comparison of lab-based research work on monolith DOC to powder DOC in the presence of alkali compounds, it can be asserted that the homogeneity of the monolith catalyst fails to reach the high level as expected. As for the lab-made powder catalyst, it is well dispersed in terms of active metals, outperforming its monolith counterpart in general.

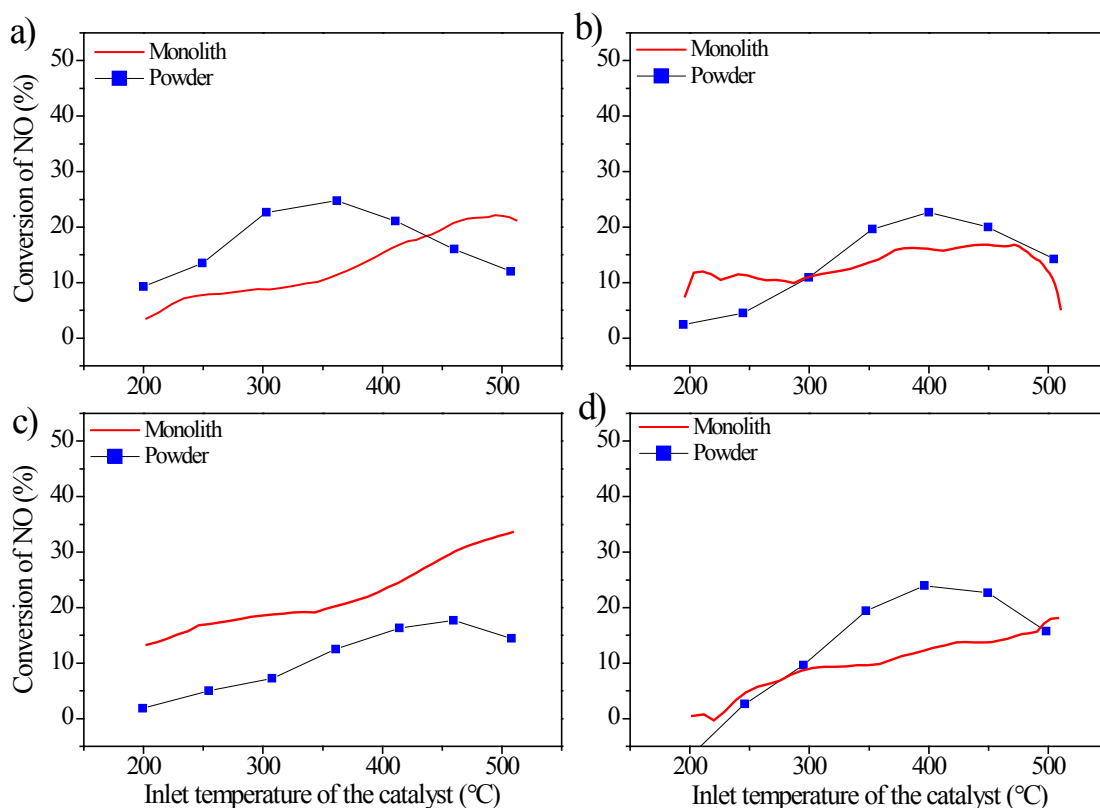


Fig. 4.39 Conversion profiles of NO as a function of temperature under Mix 1 over Fresh and doped monolith and powder catalysts: (a). Fresh, (b). K, (c). Na, and (d) K-Na

4.5.3 Concluding remarks

The comparison of lab-based research work on monolith DOC to powder DOC in the presence of alkali compounds is performed taking a typical mixture representative of diesel exhaust as an example.

It's found that the introduction of K strongly promotes the C_3H_6 oxidation reaction over the catalyst in the monolith form while the introduction of double dopants (K and Na) strongly affects the CO oxidation reaction over the catalyst in the monolith form in a negative way.

The introduction of Na strongly promotes the NO conversion over the catalyst in the monolith form while it acts as an inhibitor when it affects the powder catalyst.

**CHAPTER 5: ON THE PERFORMANCE
OF SCR CATALYSTS IN THE
PRESENCE OF ALKALI COMPOUNDS
REPRESENTATIVE OF BIOFUEL
CONTAMINANTS**

5. On the performance of SCR catalysts in the presence of alkali compounds representative of biofuel contaminants

This chapter is the second nucleus of this double-core thesis and is mainly about the research conducted on the SCR catalysts.

Emissions from the biodiesel-powered engine can contain alkali metals due to the release of the remained alkali compounds which is used in the biodiesel production^[240]. Definitely, the presence of alkali compounds coming out of the engine together with soot, soluble organic fraction such as unburned fuel and lubricating oil, or directly in the gas stream, will have an impact on the efficiency of the after-treatment technologies used for exhaust cleaning. In this sense, as a continuous effort of investigating their influence on the diesel exhaust after-treatment system such as the DOC and SCR, the impact of elements such as K and Na on the performance of SCR catalyst will be explored.

As an effective way of controlling the NO_x, SCR succeeded in establishing its existence both in the stationary and mobile applications. It has been reported that the deposition of alkali metals can decrease both the number and the strength of Brønsted acid sites vital for SCR activity, resulting in a reduced ammonia storage capacity^[214, 241 - 243]. Later, the resulted reducibility of dispersed vanadia species due to the interaction between vanadia and doped alkali metal was also demonstrated as a cause, not a major one though^[244].

Chen et al. conducted a comprehensive study of the effects of major possible poisons on the SCR process over a V₂O₅/TiO₂ catalyst for stationary application, concluding that the effect of the additive on the catalyst activity is directly related to the basicity of the additive; deactivation is caused by the weakening or destruction of Brønsted acid sites^[241]. Their Extended Hückel molecular orbital (EHMO) calculation also showed decreases in the Brønsted acidity (The extraction energy for proton from the V-OH group and the net charge of H in the V-OH group were used as indicators for Brønsted acidity) by the addition of alkali metals, and the order of the decrease follows the order of the basicity of the alkali metal^[242].

Lisi et al. evaluated the performance of two commercial SCR catalysts (with varied V loading) in the form of crushed powder, after being contacted with different amounts of Na and K and with HCl vapors, to simulate poisoning by species more specifically contained in

exhaust gases from for municipal solid waste (MSW) combustion ^[214]. They found that doping agents do not cause loss of surface area nor pore occlusion but a significant loss of surface acidity was observed upon alkali metals doping. They ascribed the significant loss of surface acidity to the decrease in the number of acid sites neutralized by alkali metals adsorbing ammonia in the temperature range typical of SCR process. Moreover, HCl promotes the formation of new acid sites, restoring to some extent surface acidity of the co-doped catalyst (alkaline metal + HCl) though showing a lower activity compared to the undoped one.

Tang et al. investigated the deactivation of lab-prepared V_2O_5/TiO_2 powder catalysts due to deposition of alkali and alkaline earth metal salts in fly ashes, finding that Na^+ ions exhibited stronger poisoning effect than Ca^{2+} ions. The surface acidity of catalyst, the reducibility of dispersed vanadia species as well, accounts for the different poisoning degree of Na^+ and Ca^{2+} ions ^[244].

Klimczak et al. studied the influence of inorganic components (K/Na from biodiesel impurities or urea solution) on the catalytic activity and selectivity of honeycomb catalysts coated with an industrial $V_2O_5-WO_3/TiO_2$ powder for NH_3 -SCR mobile application. Doping of alkaline metals results in a strong catalyst deactivation, evidenced by a reduced ammonia storage capacity. The single poisoning effect of the additives is related to the basicity of the inorganic components and decreases in the order $K > Na$. Furthermore, the influence of combinations of poisons using Design of Experiments (DOE) was determined by them. However, there was no evidence showing the experimental investigation into the co-doping effect of K and Na in their study ^[243].

More recently, the deactivation mechanisms by the alkali metals on the $V_2O_5-WO_3/TiO_2$ catalyst were extensively studied by Peng et al. with both the experimental and DFT theoretical approaches ^[245]. They asserted that alkali atom mainly influences the active site V species rather than W oxides; Alkali metals atoms can directly bonded to the active site of vanadia for the $V_2O_5-WO_3/TiO_2$ catalyst and lower the surface acidity and reducibility. The resulted decrease of reducibility by dopant atoms, however, is not the main reason responsible for the catalysts' deactivation. Instead, the lowered surface acidity, resulting in reduced amount of NH_3 adsorption, mainly accounts for the catalysts' deactivation.

So far, the combined effect of addition of potassium/sodium on vanadia-SCR for mobile applications has been less investigated, especially so on commercial V₂O₅-based SCR monolith catalyst. Partially based on this, single and combined effect of addition of 1 wt.% of potassium or sodium on the SCR activity of one commercial V₂O₅-based catalysts in monolith form has been investigated in this thesis.

5.1 Influence of the presence of alkali compounds on the performance of a commercial V₂O₅-based SCR catalyst in the monolith form

5.1.1 Experimental

5.1.1.1 Catalysts samples

The catalyst used for this study was a commercial SCR catalyst provided by Umicore, Belgium. The active material of the catalyst was mainly composed by Vanadia. In terms of its substrate, it's 400 channels per square inches (CPSI). It was cut into cylindrical "carrots" (d=2.54 cm; L=2.54 cm). One of these untreated carrots would be taken as the reference one, Fresh.

Alkali metals such as potassium (K) or/and sodium (Na) were introduced to other untreated SCR monolith catalysts by impregnation from the potassium and sodium nitrate solutions with 1 wt. % loading. After drying at 110°C overnight, the samples were calcined at 400°C for 4 h in a tubular electrical furnace under a stream of dry air. Catalysts prepared for this study were presented in Table 5.1. It is worth noting that the prepared catalyst named K-Na contains 0.5 wt. % K and 0.5 wt. % Na.

Table 5.1 Different methods dealing with monolithic SCR catalysts

Entry	Catalyst condition
F	Fresh
K	1% KNO ₃
Na	1% NaNO ₃
K-Na	1% K+Na NO ₃

5.1.1.2 Catalytic activity studies

A synthetic gas bench installation was used in order to investigate the catalytic activities of these catalysts. The carrot was put inside a stainless steel reactor, which itself was placed inside an oven reaching temperatures up to over 400°C. To ensure that the temperature field of the catalyst was homogeneous, two thermocouples were available to follow the reaction temperature at the inlet and the outlet of the catalyst.

A model lean-burn diesel exhaust together with the injected reductant NH₃ reaching the SCR system consists of NH₃, NO, NO₂, O₂, H₂O and N₂, as Mix 8 in Table 5.2. The total gas flow rate was 7.51 L·min⁻¹ resulting in a gas hourly space velocity (GHSV) of 35,000 h⁻¹. Gas mixtures without NO, NO₂, NO_x or NH₃ were setup to investigate the influence of each gas component on the catalytic process. The effects of steam on the NH₃ oxidation capability, NO oxidation capability and standard SCR reaction of studied catalysts were also investigated. Table 5.2 summarized the conditions of the different experiments in terms of gas composition.

Table 5.2 Synthetic gas bench experimental conditions for monolithic SCR catalysts

Entry	NH ₃ ppm	NO ppm	NO ₂ ppm	O ₂ (%)	H ₂ O (%)	N ₂ (%)
Mix 1	400	-	-	8	-	Balance
Mix 2	400	-	-	8	5	Balance
Mix 3	-	400	-	8	-	Balance
Mix 4	-	400	-	8	5	Balance
Mix 5	400	400	-	8	-	Balance
Mix 6	400	400	-	8	5	Balance
Mix 7	400	-	400	8	5	Balance
Mix 8	400	200	200	8	5	Balance
Mix 3-TPD	-	400	-	8	-	Balance

Catalysts were examined in terms of oxidation capacity and NO_x reduction for temperatures ranging from 50°C to 400°C. Exhaust gas compositions before and after the reactor were characterized by an Environnement S.A. analyzer composed of a set of modules. Among them, the TOPAZE 32M module allowed NO, NO₂ and total NO_x measurement thanks to a chemiluminescence analyzer. A MIR2M module was composed of an IR spectrogram, for the measurement of H₂O molar fraction, and a magnetic sensor, for the O₂ molar fraction measurement.

5.1.2 Focus on the Fresh commercial V_2O_5 -based SCR catalyst in monolith form

5.1.2.1 NH_3 oxidation capability of the Fresh commercial V_2O_5 -based SCR catalyst in the monolith form

To have an idea on the NH_3 oxidation capability of the Fresh V_2O_5 -based SCR catalyst in the monolith form, activity tests were conducted over the used catalyst under NH_3/O_2 atmosphere. Moreover, the effect of steam on the NH_3 oxidation was explored. The related results were presented in Fig. 5.1. As can be seen, the Fresh V_2O_5 -based SCR catalyst can be considered as inactive regarding NH_3 oxidation when temperature is below $300^\circ C$. With increasing temperature, the conversions of NH_3 speed up for both cases while NH_3 oxidation in the absence of steam exhibits higher activity. In their study, Li et al. found that water had a dramatic negative effect on the NH_3 conversion over the V_2O_5/TiO_2 catalyst since water is an excellent Lewis base, typically acting as an inhibitor for a catalytic reaction over metals and oxides^[246]. In parallel, water inhibition was observed by Lietti et al. when they explored the reactivity of two commercial TiO_2 -supported $V_2O_5 - MoO_3$ and $V_2O_5 - WO_3$ based catalysts in the NH_3 oxidation reaction under dry and wet conditions^[247].

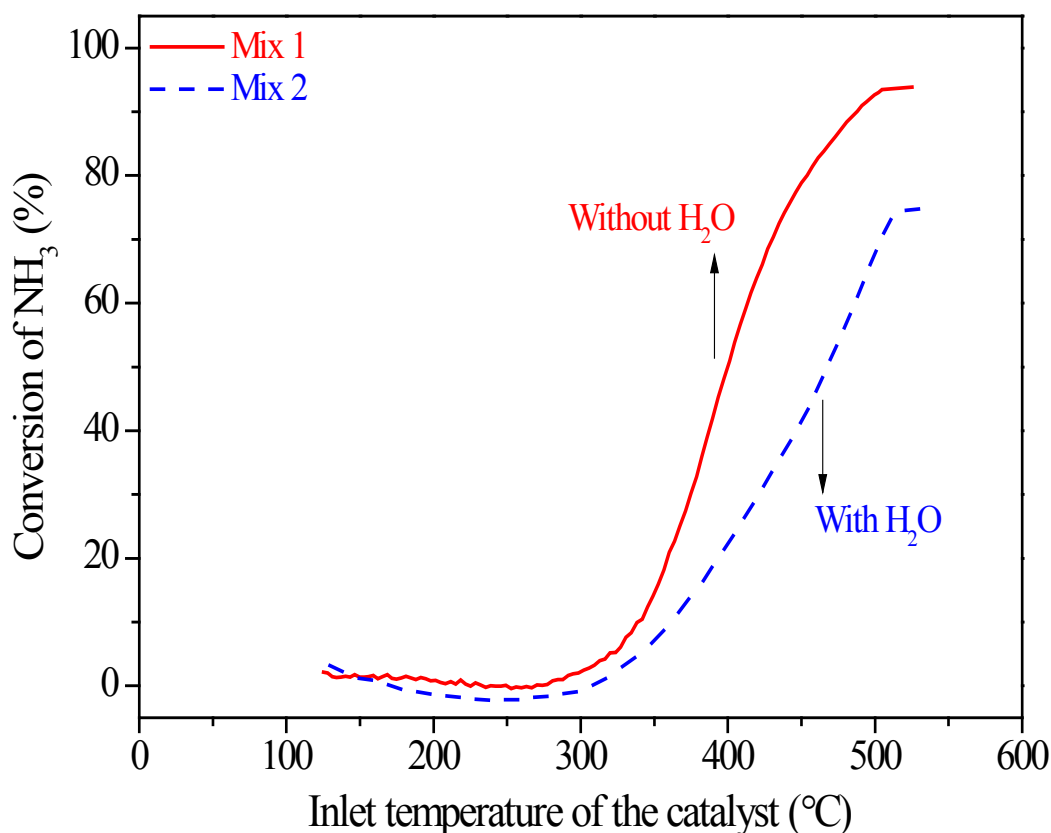


Fig. 5.1 Conversion profiles of NH_3 oxidation over Fresh SCR monolith catalyst without/with H_2O

5.1.2.2 NO oxidation capability of the Fresh commercial V₂O₅-based SCR catalyst in monolith form

Similarly, in order to acquire the NO oxidation capability of the Fresh V₂O₅ -based SCR catalyst in the monolith form, activity tests were carried out over the used catalyst under NO/O₂ atmosphere. Furthermore, the influence of steam on the NO oxidation was studied. The pertinent results were shown in Fig. 5.2. As can be seen, the Fresh V₂O₅ -based SCR catalyst can be considered as ineffective with respect to NO oxidation in the whole temperature range. Raising temperature does not significantly bring higher NO oxidation. Another point of interest is that the presence of steam actually improves the NO oxidation performance over the used catalyst, in contrast to the NH₃ oxidation shown previously.

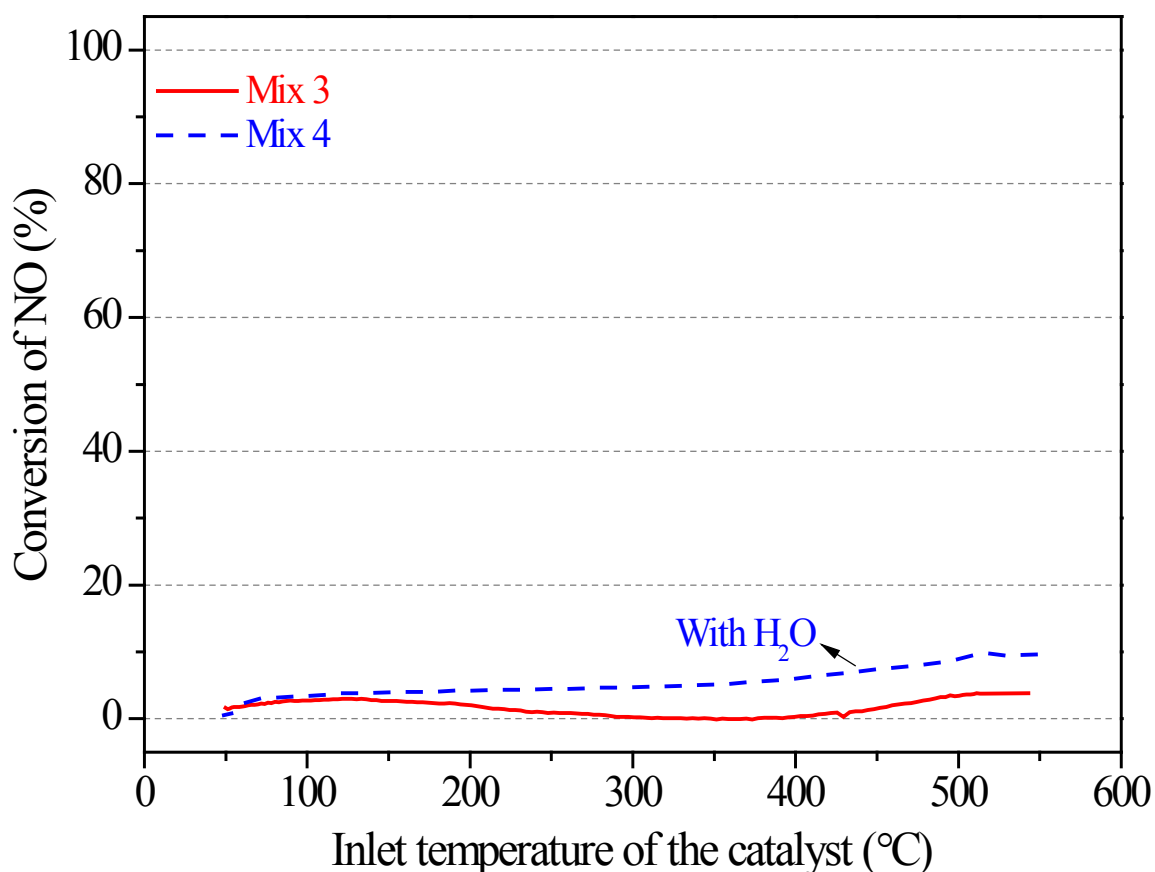


Fig. 5.2 Conversion profiles of NO oxidation over Fresh SCR monolith catalyst without/with H₂O

5.1.2.3 Performance of the Fresh commercial V₂O₅-based SCR catalyst in monolith form under NH₃+NO atmosphere

Fig. 5.3 shows the conversion profiles of reactants of interest (NH_3 and NO) over the used catalyst under $\text{NH}_3/\text{NO}/\text{O}_2$ atmosphere without/with H_2O . From Fig. 5.3, it can be noted that under dry conditions, both the NO and NH_3 start to react at 150°C , and can be considered as simultaneously thereafter, until reaching the maxima. Actually, it follows the Standard SCR reaction. At temperature up to 400°C , high NO conversion is achieved, indicating high NO removal efficiency for the used catalyst. It should be meaningful to divide the conversions of reactants into two stages in the temperature window of the SCR reaction, with 300°C serving as the watershed. The light-off occurs close to 250°C . When the temperature is above 300°C , however, the reaction loses its momentum, flattening out soon after. Meanwhile, from Fig. 5.1, it is found that NH_3 oxidation is ready to shoot up upon its occurrence. According to Lietti et al., the occurrence of the ammonia oxidation reaction can be one of the major factors governing the catalyst reactivity in the high-temperature region ^[247].

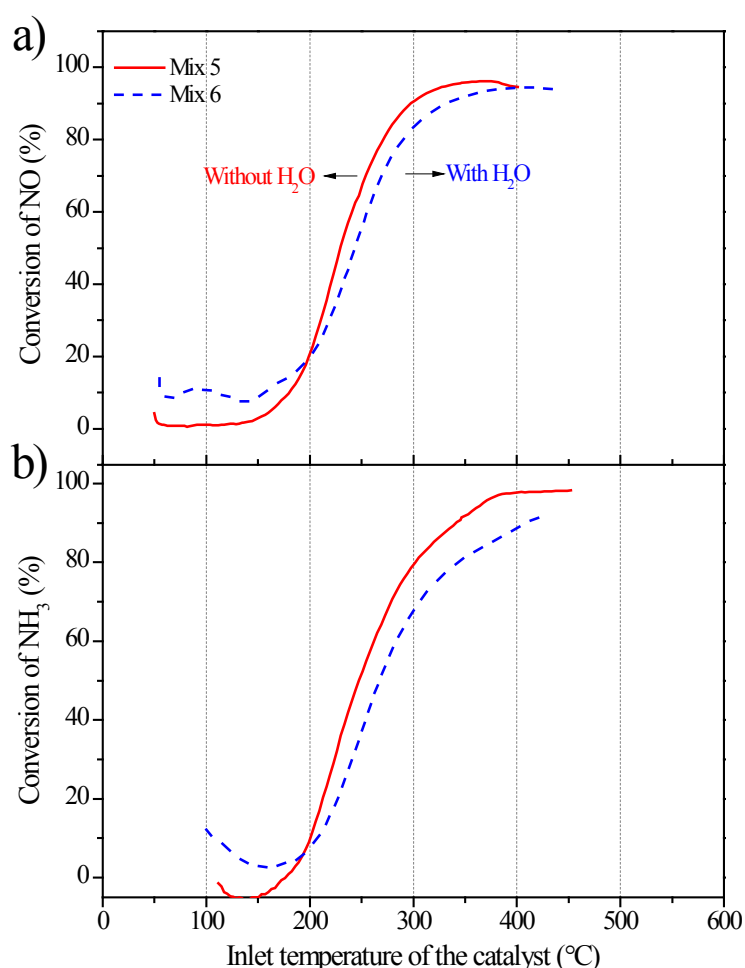


Fig. 5.3 Conversion profiles of reactants of interest over Fresh catalyst without/with H_2O :

a), Conversions of NO , and b), Conversions of NH_3 .

It is also noticeable that the feeding of steam in the first place, imposes negative influence on the reaction involving NH_3 and NO . In their review, Busca et al. stated that it's generally agreed that water hinders the SCR reaction ^[33]. The inhibiting effect of water has been explained in terms of competition against NH_3 for the adsorption onto the active sites or as modification of the structure of the active sites, e.g., transformation of Lewis acid sites into Brønsted acid sites ^[33,247].

Another point of interest is that the presence of steam brings different effects on the conversions of NO and NH_3 , particularly at relatively high temperatures ($> 300^\circ\text{C}$). It is evidenced by the diversion of NH_3 conversions (Fig. 5.3b). It can be rationalized by the inhibition of water on NH_3 oxidation (Fig. 5.1) while part of loss in the SCR reactivity for NO is compensated by the promotion of water on NO oxidation (Fig. 5.2). This is also in line with reported literature ^[247].

5.1.3 Effects of the presence of alkali compounds on the performance of a commercial V_2O_5 -based SCR catalyst in monolith form

Fig. 5.4 displays the conversion profiles of NO over different SCR catalysts, Fresh and doped ones, under model gas condition Mix 3. In general, it seems that all studied SCR catalyst can be considered as ineffective concerning NO transformation in the whole temperature range if the intrinsic error of the system is taken into account. Still, it's worth pointing out that the NO conversion over the Na-doped SCR catalyst is enhanced. It can be rationalized by the strengthening of metal- NO bond due to the addition of Na over the catalyst surface.

Fig. 5.5 presents the conversion profiles of NO over different SCR catalysts under simulating gas condition Mix 4. As a whole, there exists no major difference with increasing temperature or among varied catalysts since the NO conversions can be generally regarded as negligible.

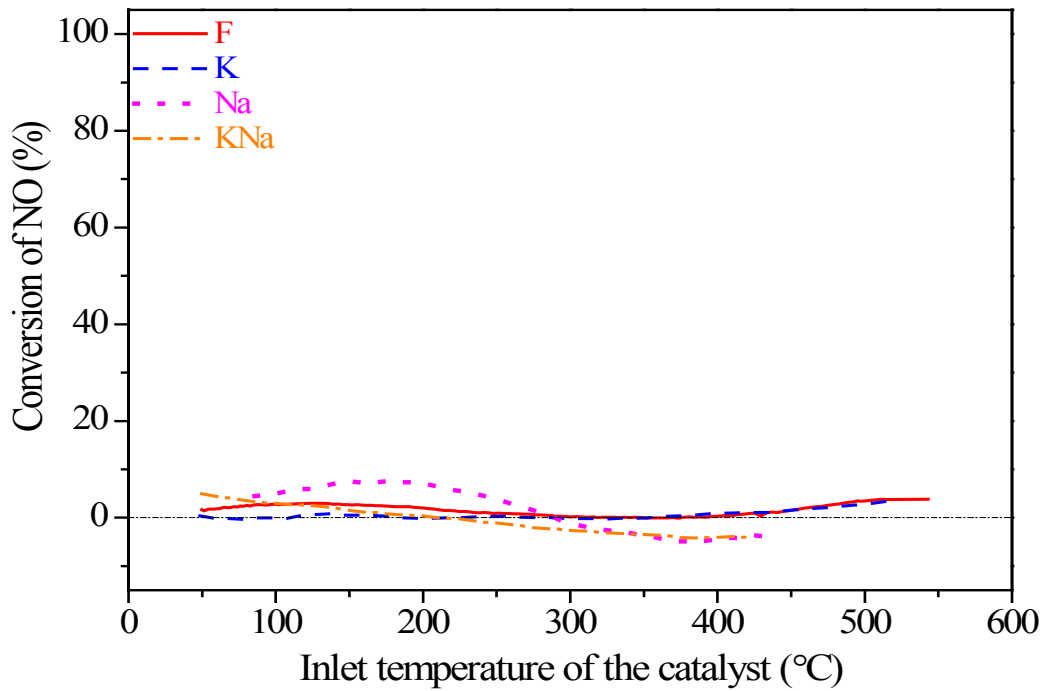


Fig. 5.4 Conversion profiles of NO over different SCR catalysts under Mix 3

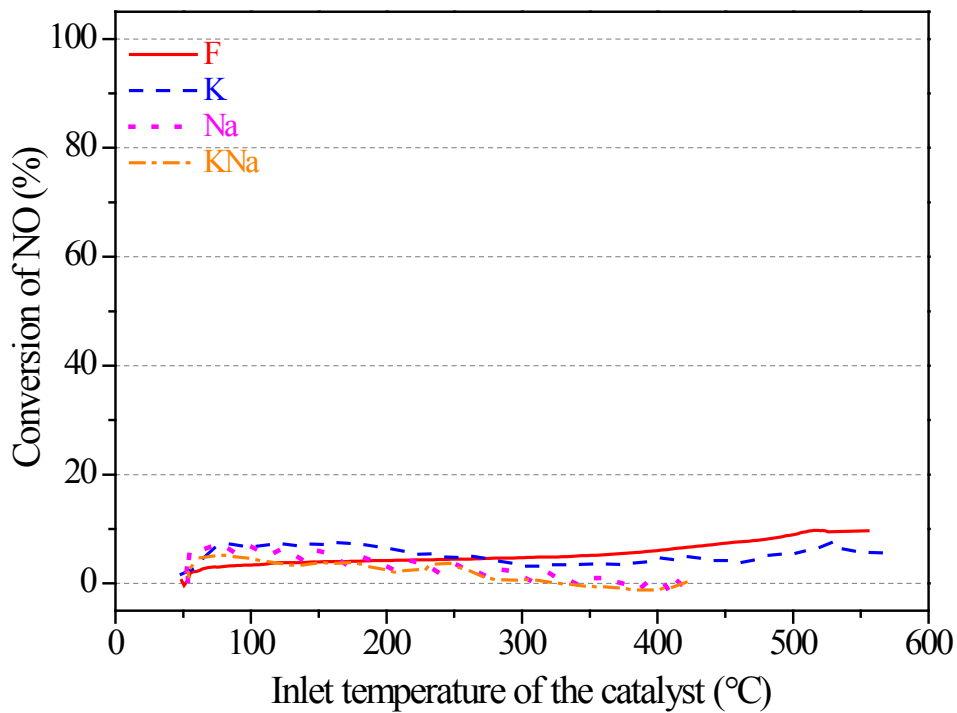


Fig. 5.5 Conversion profiles of NO over different SCR catalysts under Mix 4

Fig. 5.6 depicts the conversion profiles of NO and NH₃ over different SCR catalysts under simulating gas condition Mix 5, corresponding to Standard SCR without feeding steam in the first place. As can be seen, the activities of the catalysts drastically decrease when alkali

metals are doped onto the catalysts surface. According to reported literature, the deposition of alkali metals can decrease both the number and the strength of Brønsted acid sites, resulting in a reduced ammonia storage capacity and thus lower SCR activity [214, 241 - 243]. The resulted reducibility of dispersed vanadia species due to the interaction between vanadia and doped alkali metal was also thought to play some role, not a major part though [241]. In contrast to most studies reporting that in terms of poisoning effect, it decreases in the order $K > Na$ on the base of the same molar concentration, the present study seems to show that Na exhibits stronger poisoning effect than K on the same mass basis [214, 243]. It may be explained by higher molar concentration of Na than K when their mass is the same.

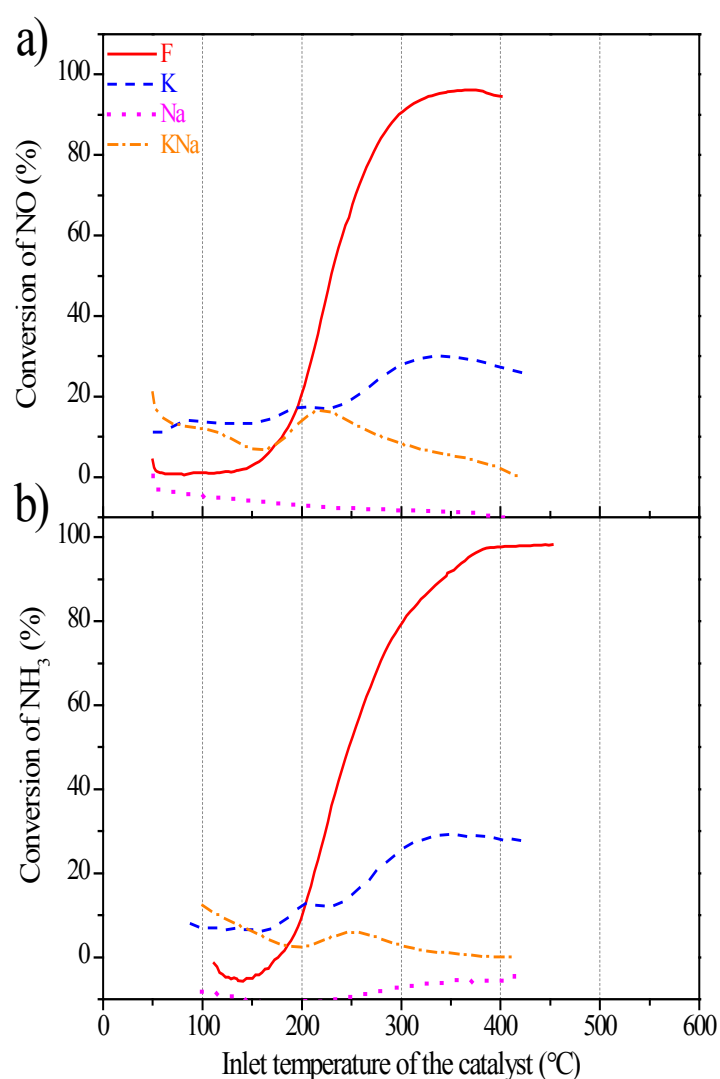


Fig. 5.6 Conversion profiles of reactants of interest over different SCR catalysts under Mix 5: a), Conversions of NO; and b), Conversions of NH_3 .

Fig. 5.7 depicts the conversion profiles of NO and NH₃ over different SCR catalysts under simulating gas condition Mix 6, corresponding to Standard SCR with feeding steam in the first place. Obviously, the activities of the catalysts drastically decrease when alkali metals are doped onto the catalysts surface. A point of interest is that in presence of steam, the activity of the used catalysts is completely lost due to the introduction of Na either in single form or in conjunction with K.

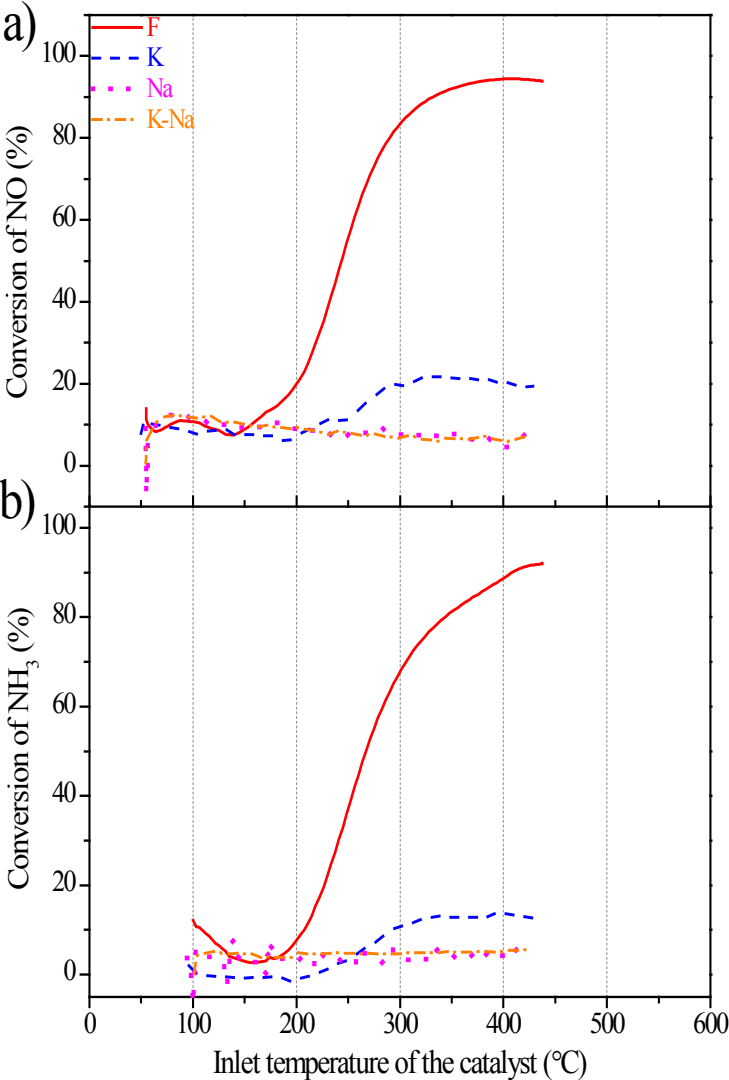


Fig. 5.7 Conversion profiles of reactants of interest over different SCR catalysts under Mix 6: a), Conversions of NO; and b), Conversions of NH₃.

Fig. 5.8 depicts the conversion profiles of NO, NO₂ and NH₃ over different SCR catalysts under simulating gas condition Mix 8, corresponding to Fast SCR under wet conditions. Similar to the case of Standard SCR, the activities of the catalysts pronouncedly decrease with doping of alkali metals. In terms of performance, it generally follows the order Fresh > K >

Na > K-Na. Again, as long as Na is present (alone or in combination with K), the activities of the catalysts are significantly suppressed.

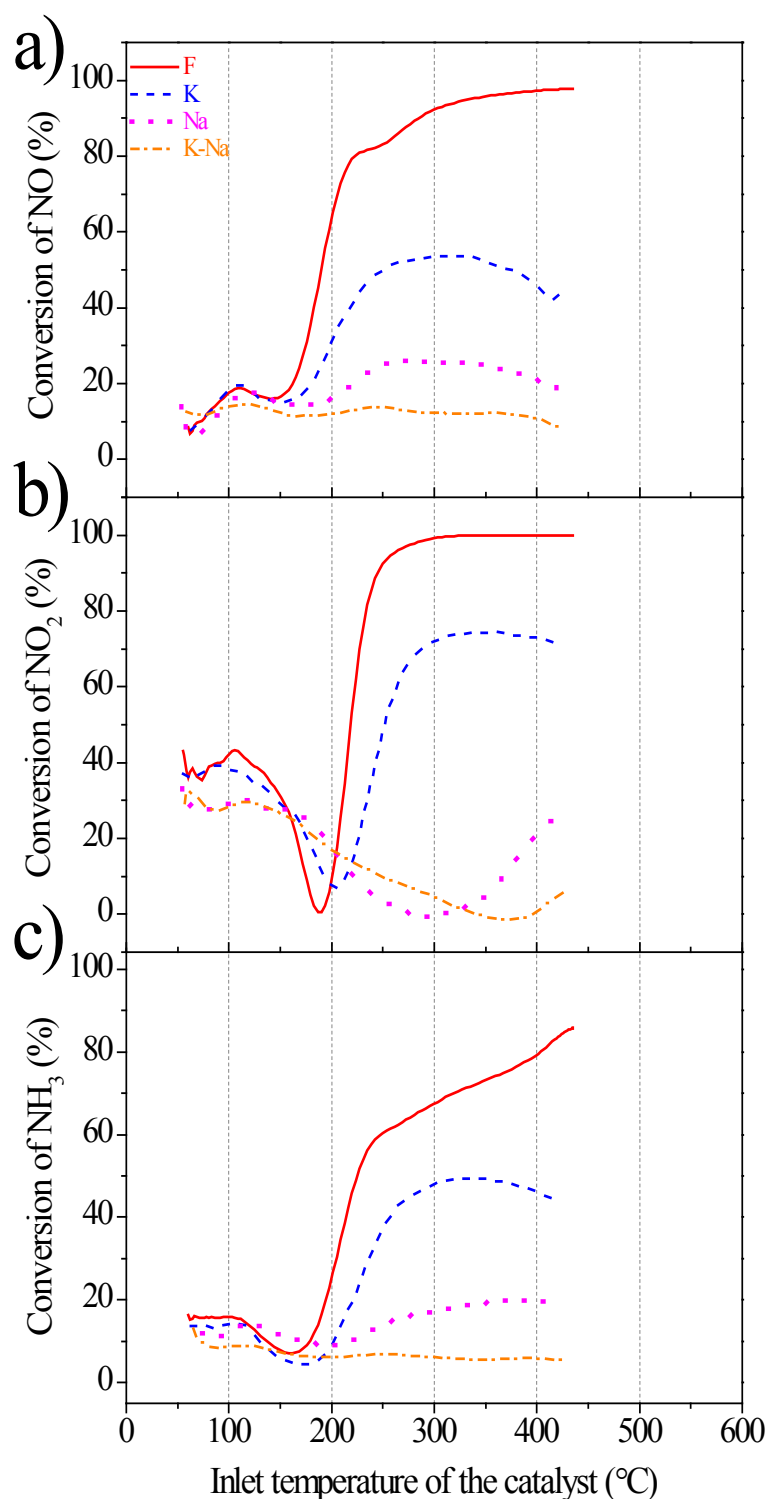


Fig. 5.8 Conversion profiles of reactants of interest over different SCR catalysts under Mix 8: a), Conversions of NO; b), Conversions of NO₂; and c), Conversions of NH₃.

5.1.4 Concluding remarks

On a commercial SCR catalyst, studied in the monolithic form, under model exhaust gases mixtures, it was clearly showed that the introduction of dopants leads to either negative impacts on the catalytic performance of the used catalysts. In terms of poisoning effect, it seems that Na exhibits stronger inhibition than K on the same mass basis which is possibly due to higher molar concentration of Na than K resulting in drastic reduction of active sites. Additionally, it is found that their combination usually leads to the complete loss of activities whether it's with respects to Standard SCR or Fast SCR.

CHAPTER 6: CONCLUSIONS AND PERSPECTIVES

6. Conclusions and perspectives

To explore what it means for the diesel exhaust after-treatment systems when bio-diesel is utilized as the alternative fuel, experimental investigations were conducted over two systems, Diesel Oxidation Catalysts and SCR catalysts.

The aging study on DOC shows that thermal aging significantly affects the overall oxidation activities of the catalysts. It turns out that mild thermal aging actually activates the catalyst. Mild thermal aging on the catalyst improves the oxidation performance of C_3H_6 as well as CO to a large extent while severe aging improves a little bit. NO oxidation over severely aged catalyst gets better. Over these DOC samples, fresh and aged ones, the CO oxidation takes place at lower temperature than C_3H_6 oxidation. Meanwhile, the NO_2 is a strong oxidant which reacts with CO if present to give out NO, enhancing the CO oxidation and formation of NO at low temperature. Moreover, the NO competes for the oxidations sites against C_3H_6 .

The results of doping of alkali metals on the same type of commercial DOC in the monolithic form illustrate that the introduction of dopants leads to either negative or positive impacts on the catalytic oxidation. The K addition leads to a promotion of oxidation reactions while the Na addition inhibits the same reactions. There is no impact of exhaust gas composition on the ranking of catalysts. However, it was shown that the presence of NO_2 promotes the oxidation reaction whereas in the presence of NO, the competition in terms of oxidation in the same catalytic sites leads to a shift of light off temperature for CO and C_3H_6 to higher temperatures.

Also studied on a commercial Diesel Oxidation Catalyst, in the monolithic form, under representative exhaust gases mixtures, it is clearly showed that the mild thermal aging leads to positive impacts on the catalytic oxidation, so does the introduction of K. Their combination, however, results in the drastic reduction of the oxidation performance.

The results of doping of alkali metals on a home-made model DOC in the powder form demonstrate that the addition of alkali compound (K or/and Na) leads to a promotion of the C_3H_6 oxidation reactions while incurs an inhibition on the NO conversion. From the analysis of changing the pollutants in the feed, it's concluded that C_3H_6 and NO are mutually inhibitor to each other when it comes to their oxidation. Moreover, the influence of CO on NO conversion is negligible though the presence of CO brings negative impact to the C_3H_6

oxidation. There is no impact of exhaust gas composition on the ranking of catalysts in terms of activity.

The performed comparison of lab-based research work on monolith DOC to powder DOC in the presence of alkali compounds under a typical mixture representative of diesel exhaust justifies that the catalyst form is of great importance. It is concluded that the introduction of K strongly promotes the C_3H_6 oxidation reaction over the catalyst in the monolith form while the introduction of double dopants (K and Na) strongly affects the CO oxidation reaction over the catalyst in the monolith form in a negative way. The introduction of Na strongly promotes the NO conversion over the catalyst in the monolith form while it acts as an inhibitor when it affects the powder catalyst.

Finally, the results of doping of alkali metals on a commercial SCR catalyst in the monolithic form under varied model exhaust gases mixtures indicate that the introduction of dopants leads to either negative impacts on the catalytic performance of the used catalysts. In terms of poisoning effect, it seems that Na exhibits stronger inhibition than K on the same mass basis which is possibly due to higher molar concentration of Na than K resulting in drastic reduction of active sites. What's more, it is found that their combination usually leads to the complete loss of activities whether it's with respects to Standard SCR or Fast SCR.

As for further study based on this thesis, varied operating parameters as well as advanced characterization techniques can be employed to get insights into the reaction mechanism. In particular, operando spectroscopy techniques should offer huge amount of information regarding the evolutions of active components of the catalyst, evolutions of reactions, and evolutions of varied interactions in heterogeneous catalysis.

References

- [1] BP Global. BP Energy Outlook 2017. Available online: <https://www.bp.com/content/dam/bp/pdf/energy-economics/energy-outlook-2017/bp-energy-outlook-2017.pdf>
- [2] EIA. The International Energy Outlook 2016. Washington, DC: U.S. Energy Information Administration; 2016. Available online: https://www.eia.gov/pressroom/presentations/sieminski_05112016.pdf
- [3] Štrach P, Everett AM. Brand corrosion: mass-marketing's threat to luxury automobile brands after merger and acquisition. *Journal of Product & Brand Management*. 2006;15(2):106-20.
- [4] International Organization of Motor Vehicle Manufacturers (OICA). World motor vehicle production by country and type. Available online: <http://www.oica.net/wp-content/uploads//Total-2015-Q4-March-16.pdf>
- [5] International Organization of Motor Vehicle Manufacturers (OICA). Registrations or sales of new vehicles - all types. Available online: <http://www.oica.net/wp-content/uploads//total-sales-20151.pdf>
- [6] Shepard S, Jerram L. Transportation Forecast: Light Duty Vehicles. Boulder, CO: Navigant Consulting, Inc. 2015.
- [7] Webster D. 25 years of catalytic automotive pollution control: a collaborative effort. *Topics in Catalysis*. 2001;16(1-4):33-8.
- [8] Sanchez FP, Bandivadekar A, German J. Estimated cost of emission reduction technologies for light-duty vehicles. International Council on Clean Transportation. 2012.
- [9] Holloway H. UK under pressure from European air quality ruling. Available online: <https://www.autocar.co.uk/car-news/industry/uk-under-pressure-european-air-quality-ruling>
- [10] Cames M, Helmers E. Critical evaluation of the European diesel car boom-global comparison, environmental effects and various national strategies. *Environmental Sciences Europe*. 2013;25(1):15.
- [11] European Automobile Manufacturers' Association (ACEA). Share of diesel in new passenger cars in Western Europe. Available online: <http://www.acea.be/statistics/tag/category/share-of-diesel-in-new-passenger-cars>
- [12] European Automobile Manufacturers' Association (ACEA). Trends in fuel type of new cars between 2015 and 2016, by country. Available online: <http://www.acea.be/statistics/article/trends-in-fuel-type-of-new-cars-between-2015-and-2016-by-country>
- [13] Majewski WA, Khair MK. Diesel emissions and their control: Society of Automotive Engineers; 2006.
- [14] Russell A, Epling WS. Diesel Oxidation Catalysts. *Catalysis Reviews*. 2011;53(4):337-423.
- [15] NGK. EURO standards. Available online: <https://www.ngk.de/en/technology-in-detail/lambda-sensors/basic-exhaust-principles/euro-standards/>
- [16] European Union. Regulation (EC) No 715/2007 of the European Parliament and of the Council of 20 June 2007 on type approval of motor vehicles with respect to emissions from light passenger and commercial vehicles (Euro 5 and Euro 6) and on access to vehicle repair and maintenance information (Text with EEA relevance). *Official Journal of the European Union*, L 171, 29 June 2007.
- [17] Farrauto RJ, Hoke J. Automotive Emission Control: Past, Present and Future. *Handbook of Green Chemistry*: Wiley-VCH Verlag GmbH & Co. KGaA; 2010.

- [18] Khajepour A, Fallah MS, Goodarzi A. Electric and Hybrid Vehicles: Technologies, Modeling and Control-A Mechatronic Approach: John Wiley & Sons; 2014.
- [19] Eastwood P. Critical Topics in Exhaust Gas Aftertreatment: Research Studies Press; 2000.
- [20] Twigg MV. Progress and future challenges in controlling automotive exhaust gas emissions. *Applied Catalysis B: Environmental*. 2007;70(1-4):2-15.
- [21] Katare SR, Patterson JE, Laing PM. Diesel Aftertreatment Modeling: A Systems Approach to NO_x Control. *Industrial & Engineering Chemistry Research*. 2007;46(8):2445-54.
- [22] Corro G. Sulfur impact on diesel emission control-A review. *Reaction Kinetics and Catalysis Letters*. 2002;75(1):89-106.
- [23] Haaß F, Fuess H. Structural characterization of automotive catalysts. *Advanced Engineering Materials*. 2005;7(10):899-913.
- [24] Bhatia D, McCabe RW, Harold MP, Balakotaiah V. Experimental and kinetic study of NO oxidation on model Pt catalysts. *Journal of Catalysis*. 2009;266(1):106-19.
- [25] Auvray X. Fundamental studies of catalytic systems for diesel emission control: Chalmers University of Technology; 2013.
- [26] Posada F, Bandivadekar A, German J. Estimated Cost of Emission Control Technologies for Light-Duty Vehicles Part 2 - Diesel. SAE International; 2013.
- [27] Tourlonias P, Koltsakis G. Model-based comparative study of Euro 6 diesel aftertreatment concepts, focusing on fuel consumption. *International Journal of Engine Research*. 2011;12(3):238-51.
- [28] European Commission. Euro 5 and 6 will reduce emissions from cars. MEMO/06/409. Brussels, 7th November 2006. Available online: http://europa.eu/rapid/press-release_MEMO-06-409_en.htm?locale=EN
- [29] Takahashi N, Shinjoh H, Iijima T, Suzuki T, Yamazaki K, Yokota K, et al. The new concept 3-way catalyst for automotive lean-burn engine: NO_x storage and reduction catalyst. *Catalysis Today*. 1996;27(1):63-9.
- [30] Erkfeldt S, Jobson E, Larsson M. The effect of carbon monoxide and hydrocarbons on NO_x storage at low temperature. *Topics in Catalysis*. 2001;16(1-4):127-31.
- [31] Hodjati S, Bernhardt P, Petit C, Pitchon V, Kiennemann A. Removal of NO_x: Part I. Sorption/desorption processes on barium aluminate. *Applied Catalysis B: Environmental*. 1998;19(3):209-19.
- [32] Olsson L, Persson H, Fridell E, Skoglundh M, Andersson B. A Kinetic Study of NO Oxidation and NO_x Storage on Pt/Al₂O₃ and Pt/BaO/Al₂O₃. *The Journal of Physical Chemistry B*. 2001;105(29):6895-906.
- [33] Busca G, Lietti L, Ramis G, Berti F. Chemical and mechanistic aspects of the selective catalytic reduction of NO_x by ammonia over oxide catalysts: A review. *Applied Catalysis B: Environmental*. 1998;18(1):1-36.
- [34] Bertelsen BI. Future US motor vehicle emission standards and the role of advanced emission control technology in meeting those standards. *Topics in Catalysis*. 2001;16(1-4):15-22.
- [35] Knecht W. Diesel engine development in view of reduced emission standards. *Energy*. 2008;33(2):264-71.
- [36] Demirbas A. Progress and recent trends in biofuels. *Progress in Energy and Combustion Science*. 2007;33(1):1-18.
- [37] EU-Commission. Directive 2003/30/EC of the European Parliament and of the Council of 8 May 2003 on the promotion of the use of biofuels or other renewable fuels for transport. *Official Journal of the European Union*. 2003;5.

- [38] Xue J, Grift TE, Hansen AC. Effect of biodiesel on engine performances and emissions. *Renewable and Sustainable Energy Reviews*. 2011;15(2):1098-116.
- [39] Zheng M, Mulenga MC, Reader GT, Wang M, Ting DS, Tjong J. Biodiesel engine performance and emissions in low temperature combustion. *Fuel*. 2008;87(6):714-22.
- [40] Nemery B, Hoet PHM, Nemmar A. The Meuse Valley fog of 1930: an air pollution disaster. *The Lancet*. 2001;357(9257):704-8.
- [41] Pope CA. Air pollution and health-good news and bad. *New England Journal of Medicine*. 2004;351:1132-3.
- [42] Fletcher RD. The Donora Smog Disaster - A Problem in Atmospheric Pollution. *Weatherwise*. 1949;2(3):56-60.
- [43] Bell ML, Davis DL, Fletcher T. A retrospective assessment of mortality from the London smog episode of 1952: the role of influenza and pollution. *Environmental Health Perspectives*. 2004;112(1):6-8.
- [44] Butcher G. In the Fog about Smog: Solving the Smog Puzzle on Earth and from Space. *ChemMatters*. 2013; 31(2): 9-11.
- [45] Bachmann J. Will the circle be unbroken: a history of the US National Ambient Air Quality Standards. *Journal of the Air & Waste Management Association*. 2007;57(6):652-97.
- [46] Haagen-Smit AJ. Chemistry and Physiology of Los Angeles Smog. *Industrial & Engineering Chemistry*. 1952;44(6):1342-6.
- [47] Twigg MV. Controlling automotive exhaust emissions: successes and underlying science. *Philosophical Transactions of the Royal Society A: Mathematical, Physical and Engineering Sciences*. 2005;363(1829):1013-33.
- [48] Bera P, Hegde M. Recent advances in auto exhaust catalysis. *Journal of the Indian Institute of Science*. 2010;90(2):299-325.
- [49] Hall CW. *A Biographical Dictionary of People in Engineering: From the Earliest Records Until 2000*: Purdue University Press; 2008.
- [50] Pardiwala JM, Patel F, Patel S. Review paper on Catalytic Converter for Automotive Exhaust Emission. *gas*. 2011;18:19.
- [51] Houdry EJ, inventor; Oxy Catalyst Inc, assignee. Catalytic structure and composition. United States patent US 2,742,437. 1956 Apr 17.
- [52] Vessel SP. Corning Researchers Honored for Pollution-Control Invention. *Journal of Failure Analysis and Prevention*. 2005;5:4.
- [53] Nriagu JO. The rise and fall of leaded gasoline. *Science of the total environment*. 1990;92:13-28.
- [54] Twigg MV. Rôles of catalytic oxidation in control of vehicle exhaust emissions. *Catalysis Today*. 2006;117(4):407-18
- [55] Klepetar D. Technology-Forcing and Law-Forcing: The California Effect in Environmental Regulatory Policy. 2012.
- [56] Zelenka P, Cartellieri W, Herzog P. Worldwide diesel emission standards, current experiences and future needs. *Applied Catalysis B: Environmental*. 1996;10(1):3-28.
- [57] Platinum Matthey. Palladium use in diesel oxidation catalysts. Available online: <http://www.platinum.matthey.com/documents/market-review/2009/special-feature-downloads/palladium-use-in-diesel-oxidation-catalysts-.pdf>
- [58] Zelenka P, Ostgathe K, Lox E. Reduction of Diesel Exhaust Emissions by Using Oxidation Catalysts. SAE International; 1990.
- [59] Majewski W, Khair M. Commercial DOC Technologies. Revision; 2011.
- [60] Nova I, Tronconi E. Urea-SCR technology for deNOx after treatment of diesel exhausts: Springer; 2014.

- [61] Skalska K, Miller JS, Ledakowicz S. Trends in NO_x abatement: A review. *Science of the total environment*. 2010;408(19):3976-89.
- [62] Roy S, Hegde MS, Madras G. Catalysis for NO_x abatement. *Applied Energy*. 2009;86(11):2283-97.
- [63] Iwamoto M, Hamada H. Removal of nitrogen monoxide from exhaust gases through novel catalytic processes. *Catalysis Today*. 1991;10(1):57-71.
- [64] Yokota K, Fukui M, Tanaka T. Catalytic removal of nitric oxide with hydrogen and carbon monoxide in the presence of excess oxygen. *Applied Surface Science*. 1997;121:273-7.
- [65] Savva PG, Costa CN. Hydrogen Lean-DeNO_x as an Alternative to the Ammonia and Hydrocarbon Selective Catalytic Reduction (SCR). *Catalysis Reviews*. 2011;53(2):91-151.
- [66] Costa CN, Efstathiou AM. Mechanistic Aspects of the H₂-SCR of NO on a Novel Pt/MgO-CeO₂ Catalyst. *The Journal of Physical Chemistry C*. 2007;111(7):3010-20.
- [67] Liu Z, Ihl Woo S. Recent Advances in Catalytic DeNO_x Science and Technology. *Catalysis Reviews*. 2006;48(1):43-89.
- [68] Held W, König A, Richter T, Puppe L. Catalytic NO_x Reduction in Net Oxidizing Exhaust Gas. *SAE International*; 1990.
- [69] Held W, König A, Puppe L. Verfahren zur Reduktion von in Abgasen enthaltenen Stickoxiden mittels eines zeolithhaltigen Katalysators. DE3830045. 1988;3.
- [70] Bowers WE. Reduction of nitrogen-based pollutants through the use of urea solutions containing oxygenated hydrocarbon solvents. *Google Patents*; 1988.
- [71] Gabrielsson PLT. Urea-SCR in Automotive Applications. *Topics in Catalysis*. 2004;28(1):177-84.
- [72] Granger P, Parvulescu VI. Catalytic NO_x Abatement Systems for Mobile Sources: From Three-Way to Lean Burn after-Treatment Technologies. *Chemical Reviews*. 2011;111(5):3155-207.
- [73] Koebel M, Elsener M, Kleemann M. Urea-SCR: a promising technique to reduce NO_x emissions from automotive diesel engines. *Catalysis Today*. 2000;59(3-4):335-45.
- [74] Lundström A, Snelling T, Morsing P, Gabrielsson P, Senar E, Olsson L. Urea decomposition and HNCO hydrolysis studied over titanium dioxide, Fe-Beta and γ -Alumina. *Applied Catalysis B: Environmental*. 2011;106(3-4):273-9.
- [75] Mendes N, Miguel A. Development of an innovative system for pollution abatement in the new natural gas vehicles: Paris 6; 2015.
- [76] Yao YY, Kummer J. A study of high temperature treated supported metal oxide catalysts. *Journal of Catalysis*. 1977;46(3):388-401.
- [77] Neyestanaki AK, Klingstedt F, Salmi T, Murzin DY. Deactivation of postcombustion catalysts, a review. *Fuel*. 2004;83(4-5):395-408.
- [78] Gandhi H, Graham G, McCabe RW. Automotive exhaust catalysis. *Journal of Catalysis*. 2003;216(1):433-42.
- [79] Gandhi HS, Stepien H, Shelef M. Optimization of ruthenium-containing, stabilized, nitric oxide reduction catalysts. *Materials Research Bulletin*. 1975;10(8):837-45.
- [80] Heck RM, Farrauto RJ. Automobile exhaust catalysts. *Applied Catalysis A: General*. 2001;221(1):443-57.
- [81] Kummer J. Use of noble metals in automobile exhaust catalysts. *The Journal of Physical Chemistry*. 1986;90(20):4747-52.
- [82] Wang H-F, Guo Y-L, Lu G, Hu P. NO Oxidation on Platinum Group Metals Oxides: First Principles Calculations Combined with Microkinetic Analysis. *The Journal of Physical Chemistry C*. 2009;113(43):18746-52.

- [83] Kim CH, Schmid M, Schmiege SJ, Tan J, Li W. The effect of Pt-Pd ratio on oxidation catalysts under simulated diesel exhaust. SAE Technical Paper, 2011 0148-7191.
- [84] Kaneeda M, Iizuka H, Hiratsuka T, Shinotsuka N, Arai M. Improvement of thermal stability of NO oxidation Pt/Al₂O₃ catalyst by addition of Pd. Applied Catalysis B: Environmental. 2009;90(3–4):564-9.
- [85] Shakya BM, Sukumar B, López-De Jesús YM, Markatou P. The Effect of Pt:Pd Ratio on Heavy-Duty Diesel Oxidation Catalyst Performance: An Experimental and Modeling Study. SAE Int J Engines. 2015;8(3):1271-82.
- [86] Skoglundh M, Löwendahl LO, Otterstedt JE. Combinations of platinum and palladium on alumina supports as oxidation catalysts. Applied Catalysis. 1991;77(1):9-20.
- [87] Stein HJ. Diesel oxidation catalysts for commercial vehicle engines: strategies on their application for controlling particulate emissions. Applied Catalysis B: Environmental. 1996;10(1):69-82.
- [88] Henk M, Williamson W, Silver R. Diesel catalysts for low particulate and low sulfate emissions. SAE Technical Paper, 1992 0148-7191.
- [89] Gland JL, Sexton BA, Fisher GB. Oxygen interactions with the Pt(111) surface. Surface Science. 1980;95(2):587-602.
- [90] Imbihl R, Demuth JE. Adsorption of oxygen on a Pd(111) surface studied by high resolution electron energy loss spectroscopy (EELS). Surface Science. 1986;173(2):395-410.
- [91] Nolan PD, Lutz BR, Tanaka PL, Davis JE, Mullins CB. Molecularly chemisorbed intermediates to oxygen adsorption on Pt(111): A molecular beam and electron energy-loss spectroscopy study. The Journal of Chemical Physics. 1999;111(8):3696-704.
- [92] Artsyukhovich AN, Ukraintsev VA, Harrison I. Low temperature sticking and desorption dynamics of oxygen on Pt(111). Surface Science. 1996;347(3):303-18.
- [93] Salomons S, Hayes RE, Votsmeier M, Drochner A, Vogel H, Malmberg S, et al. On the use of mechanistic CO oxidation models with a platinum monolith catalyst. Applied Catalysis B: Environmental. 2007;70(1–4):305-13.
- [94] Keren I, Sheintuch M. Modeling and analysis of spatiotemporal oscillatory patterns during CO oxidation in the catalytic converter. Chemical Engineering Science. 2000;55(8):1461-75.
- [95] Langmuir I. The mechanism of the catalytic action of platinum in the reactions $2\text{CO} + \text{O}_2 = 2\text{CO}_2$ and $2\text{H}_2 + \text{O}_2 = 2\text{H}_2\text{O}$. Trans Faraday Soc. 1922;17:621-54.
- [96] McClure SM, Goodman DW. New insights into catalytic CO oxidation on Pt-group metals at elevated pressures. Chemical Physics Letters. 2009;469(1–3):1-13.
- [97] Campbell CT, Ertl G, Kuipers H, Segner J. A molecular beam study of the catalytic oxidation of CO on a Pt(111) surface. The Journal of Chemical Physics. 1980;73(11):5862-73.
- [98] Engel T, Ertl G. A molecular beam investigation of the catalytic oxidation of CO on Pd (111). The Journal of Chemical Physics. 1978;69(3):1267-81.
- [99] Barteau MA, Ko EI, Madix RJ. The oxidation of CO on the Pt(100)-(5 × 20) surface. Surface Science. 1981;104(1):161-80.
- [100] Krischer K, Eiswirth M, Ertl G. Oscillatory CO oxidation on Pt (110): Modeling of temporal self-organization. The Journal of Chemical Physics. 1992;96(12):9161-72.
- [101] Bonzel HP, Ku R. Mechanisms of the catalytic carbon monoxide oxidation on Pt (110). Surface Science. 1972;33(1):91-106.
- [102] Barteau MA, Ko EI, Madix RJ. The adsorption of CO, O₂, and H₂ on Pt(100)-(5×20). Surface Science. 1981;102(1):99-117.

- [103] Gao F, McClure SM, Cai Y, Gath KK, Wang Y, Chen MS, et al. CO oxidation trends on Pt-group metals from ultrahigh vacuum to near atmospheric pressures: A combined in situ PM-IRAS and reaction kinetics study. *Surface Science*. 2009;603(1):65-70.
- [104] Carlsson P-A, Österlund L, Thormählen P, Palmqvist A, Fridell E, Jansson J, et al. A transient in situ FTIR and XANES study of CO oxidation over Pt/Al₂O₃ catalysts. *Journal of Catalysis*. 2004;226(2):422-34.
- [105] Sales BC, Turner JE, Maple MB. Oscillatory oxidation of CO over Pt, Pd and Ir catalysts: Theory. *Surface Science*. 1982;114(2):381-94.
- [106] Briot P, Auroux A, Jones D, Primet M. Effect of particle size on the reactivity of oxygen-adsorbed platinum supported on alumina. *Applied Catalysis*. 1990;59(1):141-52.
- [107] Putna ES, Vohs JM, Gorte RJ. Oxygen desorption from α -Al₂O₃ (0001) supported Rh, Pt and Pd particles. *Surface Science*. 1997;391(1-3):L1178-L82.
- [108] Lee J-H, Kung HH. Effect of Pt dispersion on the reduction of NO by propene over alumina-supported Pt catalysts under lean-burn conditions. *Catalysis Letters*. 1998;51(1):1-4.
- [109] Yao Y-FY. Oxidation of Alkanes over Noble Metal Catalysts. *Industrial & Engineering Chemistry Product Research and Development*. 1980;19(3):293-8.
- [110] Patterson MJ, Angove DE, Cant NW. The effect of carbon monoxide on the oxidation of four C₆ to C₈ hydrocarbons over platinum, palladium and rhodium. *Applied Catalysis B: Environmental*. 2000;26(1):47-57.
- [111] Yao HC, Stepien HK, Gandhi HS. The effects of SO₂ on the oxidation of hydrocarbons and carbon monoxide over Pt γ -Al₂O₃ catalysts. *Journal of Catalysis*. 1981;67(1):231-6.
- [112] Barresi AA, Baldi G. Deep Catalytic Oxidation of Aromatic Hydrocarbon Mixtures: Reciprocal Inhibition Effects and Kinetics. *Industrial & Engineering Chemistry Research*. 1994;33(12):2964-74.
- [113] Benard S, Baylet A, Vernoux P, Valverde JL, Giroir-Fendler A. Kinetics of the propene oxidation over a Pt/alumina catalyst. *Catalysis Communications*. 2013;36:63-6.
- [114] Cant NW, Hall WK. Catalytic oxidation: II. Silica supported noble metals for the oxidation of ethylene and propylene. *Journal of Catalysis*. 1970;16(2):220-31.
- [115] Baylet A, Capdeillayre C, Retailleau L, Valverde JL, Vernoux P, Giroir-Fendler A. Parametric study of propene oxidation over Pt and Au catalysts supported on sulphated and unsulphated titania. *Applied Catalysis B: Environmental*. 2011;102(1-2):180-9.
- [116] Carballo LM, Wolf EE. Crystallite size effects during the catalytic oxidation of propylene on Pt γ -Al₂O₃. *Journal of Catalysis*. 1978;53(3):366-73.
- [117] Denton P, Giroir-Fendler A, Praliaud H, Primet M. Role of the Nature of the Support (Alumina or Silica), of the Support Porosity, and of the Pt Dispersion in the Selective Reduction of NO by C₃H₆ under Lean-Burn Conditions. *Journal of Catalysis*. 2000;189(2):410-20.
- [118] Haneda M, Watanabe T, Kamiuchi N, Ozawa M. Effect of platinum dispersion on the catalytic activity of Pt/Al₂O₃ for the oxidation of carbon monoxide and propene. *Applied Catalysis B: Environmental*. 2013;142-143:8-14.
- [119] Oh H, Luo J, Epling WS. NO Oxidation Inhibition by Hydrocarbons over a Diesel Oxidation Catalyst: Reaction Between Surface Nitrates and Hydrocarbons. *Catalysis Letters*. 2011;141(12):1746-51.

- [120] Weiss BM, Iglesia E. NO Oxidation Catalysis on Pt Clusters: Elementary Steps, Structural Requirements, and Synergistic Effects of NO₂ Adsorption Sites. *The Journal of Physical Chemistry C*. 2009;113(30):13331-40.
- [121] Mulla SS, Chen N, Cumarantunge L, Blau GE, Zemlyanov DY, Delgass WN, et al. Reaction of NO and O₂ to NO₂ on Pt: Kinetics and catalyst deactivation. *Journal of Catalysis*. 2006;241(2):389-99.
- [122] Mulla SS, Chen N, Delgass WN, Epling WS, Ribeiro FH. NO₂ inhibits the catalytic reaction of NO and O₂ over Pt. *Catalysis Letters*. 2005;100(3):267-70.
- [123] Smeltz AD, Getman RB, Schneider WF, Ribeiro FH. Coupled theoretical and experimental analysis of surface coverage effects in Pt-catalyzed NO and O₂ reaction to NO₂ on Pt(1 1 1). *Catalysis Today*. 2008;136(1–2):84-92.
- [124] Després J, Elsener M, Koebel M, Kröcher O, Schnyder B, Wokaun A. Catalytic oxidation of nitrogen monoxide over Pt/SiO₂. *Applied Catalysis B: Environmental*. 2004;50(2):73-82.
- [125] Boudart M, Djéga-Mariadassou G. *Kinetics of heterogeneous catalytic reactions*: Princeton University Press; 2014.
- [126] Olsson L, Westerberg B, Persson H, Fridell E, Skoglundh M, Andersson B. A Kinetic Study of Oxygen Adsorption/Desorption and NO Oxidation over Pt/Al₂O₃ Catalysts. *The Journal of Physical Chemistry B*. 1999;103(47):10433-9.
- [127] Olsson L, Persson H, Fridell E, Skoglundh M, Andersson B. A Kinetic Study of NO Oxidation and NO_x Storage on Pt/Al₂O₃ and Pt/BaO/Al₂O₃. *The Journal of Physical Chemistry B*. 2001;105(29):6895-906.
- [128] Crocoll M, Kureti S, Weisweiler W. Mean field modeling of NO oxidation over Pt/Al₂O₃ catalyst under oxygen-rich conditions. *Journal of Catalysis*. 2005;229(2):480-9.
- [129] Clayton RD, Harold MP, Balakotaiah V, Wan CZ. Pt dispersion effects during NO_x storage and reduction on Pt/BaO/Al₂O₃ catalysts. *Applied Catalysis B: Environmental*. 2009;90(3–4):662-76.
- [130] Matam SK, Kondratenko EV, Aguirre MH, Hug P, Rentsch D, Winkler A, et al. The impact of aging environment on the evolution of Al₂O₃ supported Pt nanoparticles and their NO oxidation activity. *Applied Catalysis B: Environmental*. 2013;129:214-24.
- [131] Xue E, Seshan K, Ross JRH. Roles of supports, Pt loading and Pt dispersion in the oxidation of NO to NO₂ and of SO₂ to SO₃. *Applied Catalysis B: Environmental*. 1996;11(1):65-79.
- [132] Hauptmann W, Votsmeier M, Gieshoff J, Drochner A, Vogel H. Inverse hysteresis during the NO oxidation on Pt under lean conditions. *Applied Catalysis B: Environmental*. 2009;93(1–2):22-9.
- [133] Hauff K, Tuttlies U, Eigenberger G, Nieken U. Platinum oxide formation and reduction during NO oxidation on a diesel oxidation catalyst – Experimental results. *Applied Catalysis B: Environmental*. 2012;123–124:107-16.
- [134] Kröcher O, Widmer M, Elsener M, Rothe D. Adsorption and Desorption of SO_x on Diesel Oxidation Catalysts. *Industrial & Engineering Chemistry Research*. 2009;48(22):9847-57.
- [135] Cichanowicz J, Muzio L, editors. *Twenty-five years of SCR evolution: implications for US application and operation*. Proceedings of the EPRI/EPA/DOE MEGA Symposium Chicago, IL; 2001.
- [136] Muzio LJ, Quartucy GC. Implementing NO_x control: Research to application. *Progress in Energy and Combustion Science*. 1997;23(3):233-66.

- [137] Pârvulescu VI, Grange P, Delmon B. Catalytic removal of NO. *Catalysis Today*. 1998;46(4):233-316.
- [138] Schnelle KB, Brown CA. *Air pollution control technology handbook*: CRC press Boca Raton, FL; 2002.
- [139] Madia G, Koebel M, Elsener M, Wokaun A. The Effect of an Oxidation Precatalyst on the NO_x Reduction by Ammonia SCR. *Industrial & Engineering Chemistry Research*. 2002;41(15):3512-7.
- [140] Gómez-García MA, Pitchon V, Kiennemann A. Pollution by nitrogen oxides: an approach to NO_x abatement by using sorbing catalytic materials. *Environment International*. 2005;31(3):445-67.
- [141] Kato A, Matsuda S, Kamo T, Nakajima F, Kuroda H, Narita T. Reaction between nitrogen oxide (NO_x) and ammonia on iron oxide-titanium oxide catalyst. *The Journal of Physical Chemistry*. 1981;85(26):4099-102.
- [142] Devadas M, Kröcher O, Elsener M, Wokaun A, Söger N, Pfeifer M, et al. Influence of NO₂ on the selective catalytic reduction of NO with ammonia over Fe-ZSM5. *Applied Catalysis B: Environmental*. 2006;67(3-4):187-96.
- [143] Koebel M, Elsener M, Madia G. Reaction Pathways in the Selective Catalytic Reduction Process with NO and NO₂ at Low Temperatures. *Industrial & Engineering Chemistry Research*. 2001;40(1):52-9.
- [144] Nova I, Ciardelli C, Tronconi E, Chatterjee D, Bandl-Konrad B. NH₃-NO/NO₂ chemistry over V-based catalysts and its role in the mechanism of the Fast SCR reaction. *Catalysis Today*. 2006;114(1):3-12.
- [145] Luo J-Y, Hou X, Wijayakoon P, Schmiege SJ, Li W, Epling WS. Spatially resolving SCR reactions over a Fe/zeolite catalyst. *Applied Catalysis B: Environmental*. 2011;102(1-2):110-9.
- [146] Koebel M, Madia G, Elsener M. Selective catalytic reduction of NO and NO₂ at low temperatures. *Catalysis Today*. 2002;73(3-4):239-47.
- [147] Burch R, Millington PJ. Selective reduction of nitrogen oxides by hydrocarbons under lean-burn conditions using supported platinum group metal catalysts. *Catalysis Today*. 1995;26(2):185-206.
- [148] García-Cortés JM, Pérez-Ramírez J, Illán-Gómez MJ, Kapteijn F, Moulijn JA, Salinas-Martínez de Lecea C. Comparative study of Pt-based catalysts on different supports in the low-temperature de-NO_x-SCR with propene. *Applied Catalysis B: Environmental*. 2001;30(3-4):399-408.
- [149] Colombo M, Nova I, Tronconi E. A comparative study of the NH₃-SCR reactions over a Cu-zeolite and a Fe-zeolite catalyst. *Catalysis Today*. 2010;151(3-4):223-30.
- [150] Qi G, Yang RT. Ultra-active Fe/ZSM-5 catalyst for selective catalytic reduction of nitric oxide with ammonia. *Applied Catalysis B: Environmental*. 2005;60(1-2):13-22.
- [151] Fedeyko JM, Chen B, Chen H-Y. Mechanistic study of the low temperature activity of transition metal exchanged zeolite SCR catalysts. *Catalysis Today*. 2010;151(3-4):231-6.
- [152] Rahkamaa-Tolonen K, Maunula T, Lomma M, Huuhtanen M, Keiski RL. The effect of NO₂ on the activity of fresh and aged zeolite catalysts in the NH₃-SCR reaction. *Catalysis Today*. 2005;100(3-4):217-22.
- [153] Kwak JH, Tonkyn RG, Kim DH, Szanyi J, Peden CHF. Excellent activity and selectivity of Cu-SSZ-13 in the selective catalytic reduction of NO_x with NH₃. *Journal of Catalysis*. 2010;275(2):187-90.
- [154] Moliner M, Franch C, Palomares E, Grill M, Corma A. Cu-SSZ-39, an active and hydrothermally stable catalyst for the selective catalytic reduction of NO_x. *Chemical Communications*. 2012;48(66):8264-6.

- [155] Yun BK, Kim MY. Modeling the selective catalytic reduction of NO_x by ammonia over a Vanadia-based catalyst from heavy duty diesel exhaust gases. *Applied Thermal Engineering*. 2013;50(1):152-8.
- [156] Long RQ, Yang RT. Catalytic Performance of Fe-ZSM-5 Catalysts for Selective Catalytic Reduction of Nitric Oxide by Ammonia. *Journal of Catalysis*. 1999;188(2):332-9.
- [157] Busca G, Larrubia MA, Arrighi L, Ramis G. Catalytic abatement of NO_x: Chemical and mechanistic aspects. *Catalysis Today*. 2005;107-108:139-48.
- [158] Arnarson L, Falsig H, Rasmussen SB, Lauritsen JV, Moses PG. The reaction mechanism for the SCR process on monomer V⁵⁺ sites and the effect of modified Bronsted acidity. *Physical Chemistry Chemical Physics*. 2016;18(25):17071-80.
- [159] Komatsu T, Nunokawa M, Moon IS, Takahara T, Namba S, Yashima T. Kinetic Studies of Reduction of Nitric Oxide with Ammonia on Cu²⁺-Exchanged Zeolites. *Journal of Catalysis*. 1994;148(2):427-37.
- [160] Iwasaki M, Yamazaki K, Banno K, Shinjoh H. Characterization of Fe/ZSM-5 DeNO_x catalysts prepared by different methods: Relationships between active Fe sites and NH₃-SCR performance. *Journal of Catalysis*. 2008;260(2):205-16.
- [161] Takagi M, Kawai T, Soma M, Onishi T, Tamaru K. The mechanism of the reaction between NO_x and NH₃ on V₂O₅ in the presence of oxygen. *Journal of Catalysis*. 1977;50(3):441-6.
- [162] Inomata M, Miyamoto A, Murakami Y. Mechanism of the reaction of NO and NH₃ on vanadium oxide catalyst in the presence of oxygen under the dilute gas condition. *Journal of Catalysis*. 1980;62(1):140-8.
- [163] Janssen FJJG, Van den Kerkhof FMG, Bosch H, Ross JRH. Mechanism of the reaction of nitric oxide, ammonia, and oxygen over vanadia catalysts. 2. Isotopic transient studies with oxygen-18 and nitrogen-15. *The Journal of Physical Chemistry*. 1987;91(27):6633-8.
- [164] Ramis G, Busca G, Bregani F, Forzatti P. Fourier transform-infrared study of the adsorption and coadsorption of nitric oxide, nitrogen dioxide and ammonia on vanadia-titania and mechanism of selective catalytic reduction. *Applied Catalysis*. 1990;64:259-78.
- [165] Topsøe N, Dumesic J, Topsøe H. Vanadia-titania catalysts for selective catalytic reduction of nitric-oxide by ammonia: II Studies of active sites and formulation of catalytic cycles. *Journal of Catalysis*. 1995;151(1):241-52.
- [166] Tronconi E, Nova I, Ciardelli C, Chatterjee D, Weibel M. Redox features in the catalytic mechanism of the “standard” and “fast” NH₃-SCR of NO_x over a V-based catalyst investigated by dynamic methods. *Journal of Catalysis*. 2007;245(1):1-10.
- [167] Arnarson L, Falsig H, Rasmussen SB, Lauritsen JV, Moses PG. A complete reaction mechanism for standard and fast selective catalytic reduction of nitrogen oxides on low coverage VO_x/TiO₂(0 0 1) catalysts. *Journal of Catalysis*. 2017;346:188-97.
- [168] Lietti L, Ramis G, Berti F, Toledo G, Robba D, Busca G, et al. Chemical, structural and mechanistic aspects on NO_x SCR over commercial and model oxide catalysts. *Catalysis Today*. 1998;42(1-2):101-16.
- [169] Forzatti P. Present status and perspectives in de-NO_x SCR catalysis. *Applied Catalysis A: General*. 2001;222(1-2):221-36.
- [170] Ramis G, Yi L, Busca G. Ammonia activation over catalysts for the selective catalytic reduction of NO_x and the selective catalytic oxidation of NH₃. An FT-IR study. *Catalysis Today*. 1996;28(4):373-80.

- [171] Jug K, Homann T, Bredow T. Reaction Mechanism of the Selective Catalytic Reduction of NO with NH₃ and O₂ to N₂ and H₂O. *The Journal of Physical Chemistry A*. 2004;108(15):2966-71.
- [172] Topsoe N, Topsoe H, Dumesic J. Vanadia/titania catalysts for selective catalytic reduction (SCR) of nitric-oxide by ammonia: I. Combined temperature-programmed in-situ FTIR and on-line mass-spectroscopy studies. *Journal of Catalysis*. 1995;151(1):226-40.
- [173] Lietti L, Nova I, Camurri S, Tronconi E, Forzatti P. Dynamics of the SCR-DeNO_x reaction by the transient-response method. *AIChE Journal*. 1997;43(10):2559-70.
- [174] Koebel M, Madia G, Raimondi F, Wokaun A. Enhanced Reoxidation of Vanadia by NO₂ in the Fast SCR Reaction. *Journal of Catalysis*. 2002;209(1):159-65.
- [175] Janssens TVW, Falsig H, Lundegaard LF, Vennestrøm PNR, Rasmussen SB, Moses PG, et al. A Consistent Reaction Scheme for the Selective Catalytic Reduction of Nitrogen Oxides with Ammonia. *ACS Catalysis*. 2015;5(5):2832-45.
- [176] Bartholomew CH. Mechanisms of catalyst deactivation. *Applied Catalysis A: General*. 2001;212(1–2):17-60.
- [177] Forzatti P, Lietti L. Catalyst deactivation. *Catalysis Today*. 1999;52(2–3):165-81.
- [178] Argyle M, Bartholomew C. Heterogeneous Catalyst Deactivation and Regeneration: A Review. *Catalysts*. 2015;5(1):145.
- [179] Jennings JR. *Catalytic ammonia synthesis: fundamentals and practice*: Springer Science & Business Media; 2013.
- [180] Walke S, Kambale S. Catalyst Deactivation and Regeneration. *International Journal of Scientific Engineering and Technology*. 2015;4(5).
- [181] Trimm DL. Thermal Stability of Catalyst Supports. In: Calvin HB, John BB, editors. *Studies in Surface Science and Catalysis*: Elsevier; 1991. p. 29-51.
- [182] Arai H, Machida M. Thermal stabilization of catalyst supports and their application to high-temperature catalytic combustion. *Applied Catalysis A: General*. 1996;138(2):161-76.
- [183] Flynn PC, Wanke SE. Experimental studies of sintering of supported platinum catalysts. *Journal of Catalysis*. 1975;37(3):432-48.
- [184] Wanke SE, Flynn PC. The Sintering of Supported Metal Catalysts. *Catalysis Reviews*. 1975;12(1):93-135.
- [185] Lassi U. Deactivation correlations of Pd/Rh three-way catalysts designed for Euro IV Emission Limits: effect of ageing atmosphere, temperature and time: Oulun yliopisto; 2003.
- [186] Fiedorow RMJ, Wanke SE. The sintering of supported metal catalysts. *Journal of Catalysis*. 1976;43(1):34-42.
- [187] Chen M, Schmidt LD. Morphology and composition of Pt□Pd alloy crystallites on SiO₂ in reactive atmospheres. *Journal of Catalysis*. 1979;56(2):198-218.
- [188] Harris PJF. Growth and structure of supported metal catalyst particles. *International Materials Reviews*. 1995;40(3):97-115.
- [189] Knothe G, Sharp CA, Ryan TW. Exhaust Emissions of Biodiesel, Petrodiesel, Neat Methyl Esters, and Alkanes in a New Technology Engine. *Energy & Fuels*. 2006;20(1):403-8.
- [190] Hoekman SK, Robbins C. Review of the effects of biodiesel on NO_x emissions. *Fuel Processing Technology*. 2012;96:237-49.
- [191] Graboski M, McCormick R, Alleman T, Herring A. The effect of biodiesel composition on engine emissions from a DDC series 60 diesel engine. National Renewable Energy Laboratory (Report No: NREL/SR-510-31461). 2003.

- [192] Knothe G. “Designer” biodiesel: optimizing fatty ester composition to improve fuel properties. *Energy & Fuels*. 2008;22(2):1358-64.
- [193] McCormick RL, Williams A, Ireland J, Hayes R. Effects of biodiesel blends on vehicle emissions: fiscal year 2006 annual operating plan milestone 10.4. National Renewable Energy Laboratory (NREL), Golden, CO., 2006.
- [194] Lapuerta M, Armas O, Rodríguez-Fernández J. Effect of biodiesel fuels on diesel engine emissions. *Progress in Energy and Combustion Science*. 2008;34(2):198-223.
- [195] Meher LC, Vidya Sagar D, Naik SN. Technical aspects of biodiesel production by transesterification—a review. *Renewable and Sustainable Energy Reviews*. 2006;10(3):248-68.
- [196] Demirbas A. Importance of biodiesel as transportation fuel. *Energy Policy*. 2007;35(9):4661-70.
- [197] Williams A, McCormick R, Luecke J, Brezny R, Geisselmann A, Voss K, et al. Impact of Biodiesel Impurities on the Performance and Durability of DOC, DPF and SCR Technologies: Preprint: ; National Renewable Energy Laboratory (NREL), Golden, CO.; 2011. Medium: ED; Size: 23 pp. p.
- [198] Sharp CA. Transient emissions testing of biodiesel and other additives in a DDC Series 60 engine. Southwest Research Institute, Final Report to the National Biodiesel Board. 1994.
- [199] Sharp CA. Emissions and Lubricity Evaluation of Rapeseed Derived Biodiesel Fuels: Final Report: Southwest Research Institute; 1996.
- [200] Graboski MS, Ross JD, McCormick RL. Transient Emissions from No. 2 Diesel and Biodiesel Blends in a DDC Series 60 Engine. SAE International; 1996.
- [201] Starr ME. Influence on Transient Emissions at Various Injection Timings, Using Cetane Improvers, Bio-Diesel, and Low Aromatic Fuels. SAE International; 1997.
- [202] Sharp CA, Howell SA, Jobe J. The Effect of Biodiesel Fuels on Transient Emissions from Modern Diesel Engines, Part I Regulated Emissions and Performance. SAE International; 2000.
- [203] McCormick RL, Graboski MS, Alleman TL, Herring AM, Tyson KS. Impact of Biodiesel Source Material and Chemical Structure on Emissions of Criteria Pollutants from a Heavy-Duty Engine. *Environmental Science & Technology*. 2001;35(9):1742-7.
- [204] McCormick RL, Alvarez JR, Graboski MS, Tyson KS, Vertin K. Fuel Additive and Blending Approaches to Reducing NO_x Emissions from Biodiesel. SAE International; 2002.
- [205] Korotney D. A comprehensive analysis of biodiesel impacts on exhaust emissions. Draft report of the US Environmental Protection Agency, Washington, DC. 2002.
- [206] Dou D, Balland J. Impact of Alkali Metals on the Performance and Mechanical Properties of NO_x Adsorber Catalysts. SAE International; 2002.
- [207] Cavataio G, Jen H-W, Dobson DA, Warner JR. Laboratory Study to Determine Impact of Na and K Exposure on the Durability of DOC and SCR Catalyst Formulations. SAE International; 2009.
- [208] Williams A, Burton J, McCormick RL, Toops T, Wereszczak AA, Fox EE, et al. Impact of Fuel Metal Impurities on the Durability of a Light-Duty Diesel Aftertreatment System. SAE International; 2013.
- [209] Lance M, Wereszczak A, Toops TJ, Ancimer R, An H, Li J, et al. Evaluation of Fuel-Borne Sodium Effects on a DOC-DPF-SCR Heavy-Duty Engine Emission Control System: Simulation of Full-Useful Life. *SAE Int J Fuels Lubr*. 2016;9(3):683-94.

- [210] Kristensen SB, Kunov-Kruse AJ, Riisager A, Rasmussen SB, Fehrmann R. High performance vanadia–anatase nanoparticle catalysts for the Selective Catalytic Reduction of NO by ammonia. *Journal of Catalysis*. 2011;284(1):60-7.
- [211] Wang P, Wang H, Chen X, Liu Y, Weng X, Wu Z. Novel SCR catalyst with superior alkaline resistance performance: enhanced self-protection originated from modifying protonated titanate nanotubes. *Journal of Materials Chemistry A*. 2015;3(2):680-90.
- [212] Zheng Y, Jensen AD, Johnsson JE. Deactivation of V₂O₅-WO₃-TiO₂ SCR catalyst at a biomass-fired combined heat and power plant. *Applied Catalysis B: Environmental*. 2005;60(3–4):253-64.
- [213] Kling Å, Andersson C, Myringer Å, Eskilsson D, Järås SG. Alkali deactivation of high-dust SCR catalysts used for NO_x reduction exposed to flue gas from 100 MW-scale biofuel and peat fired boilers: Influence of flue gas composition. *Applied Catalysis B: Environmental*. 2007;69(3–4):240-51.
- [214] Lisi L, Lasorella G, Malloggi S, Russo G. Single and combined deactivating effect of alkali metals and HCl on commercial SCR catalysts. *Applied Catalysis B: Environmental*. 2004;50(4):251-8.
- [215] Williams A, McCormick R, Luecke J, Brezny R, Geisselmann A, Voss K, et al. Impact of Biodiesel Impurities on the Performance and Durability of DOC, DPF and SCR Technologies. *SAE Int J Fuels Lubr*. 2011;4(1):110-24.
- [216] Bartolomeu R. Nox selective catalytic reduction in biofuel powered vehicles: Paris 6; 2013.
- [217] Diaz I, Mayoral A. TEM studies of zeolites and ordered mesoporous materials. *Micron*. 2011;42(5):512-27.
- [218] Niemantsverdriet JW. *Spectroscopy in catalysis*: John Wiley & Sons; 2007.
- [219] Manigrasso A, Fouchal N, Darcy P, Da Costa P. Hysteresis effect study on diesel oxidation catalyst for a better efficiency of SCR systems. *Catalysis Today*. 2012;191(1):52-8.
- [220] Wiebenga MH, Kim CH, Schmiege SJ, Oh SH, Brown DB, Kim DH, et al. Deactivation mechanisms of Pt/Pd-based diesel oxidation catalysts. *Catalysis Today*. 2012;184(1):197-204.
- [221] Xie Y, Rodrigues E, Furtado N, Matynia A, Arlt T, Rodatz P, et al. Aging of Commercial Diesel Oxidation Catalysts: A preliminary Structure/Reactivity Study. *Topics in Catalysis*. 2016;59(10):1039-43.
- [222] Bamwenda GR, Obuchi A, Ogata A, Oi J, Kushiyama S, Mizuno K. The role of the metal during NO₂ reduction by C₃H₆ over alumina and silica-supported catalysts. *Journal of Molecular Catalysis A: Chemical*. 1997;126(2):151-9.
- [223] Benard S, Retailleau L, Gaillard F, Vernoux P, Giroir-Fendler A. Supported platinum catalysts for nitrogen oxide sensors. *Applied Catalysis B: Environmental*. 2005;55(1):11-21.
- [224] Schmeißer V, de Riva Pérez J, Tuttlies U, Eigenberger G. Experimental results concerning the role of Pt, Rh, Ba, Ce and Al₂O₃ on NO_x-storage catalyst behaviour. *Topics in Catalysis*. 2007;42(1):15-9.
- [225] Millet C-N, Chédotal R, Da Costa P. Synthetic gas bench study of a 4-way catalytic converter: Catalytic oxidation, NO_x storage/reduction and impact of soot loading and regeneration. *Applied Catalysis B: Environmental*. 2009;90(3–4):339-46.
- [226] Khosravi M, Abedi A, Hayes RE, Epling WS, Votsmeier M. Kinetic modelling of Pt and Pt:Pd diesel oxidation catalysts. *Applied Catalysis B: Environmental*. 2014;154–155:16-26.

- [227] Irani K, Epling WS, Blint R. Effect of hydrocarbon species on NO oxidation over diesel oxidation catalysts. *Applied Catalysis B: Environmental*. 2009;92(3–4):422-8.
- [228] Auvray X, Olsson L. Stability and activity of Pd-, Pt- and Pd–Pt catalysts supported on alumina for NO oxidation. *Applied Catalysis B: Environmental*. 2015;168–169:342-52.
- [229] Milt VG, Peralta MA, Ulla MA, Miró EE. Soot oxidation on a catalytic NO_x trap: Beneficial effect of the Ba–K interaction on the sulfated Ba,K/CeO₂ catalyst. *Catalysis Communications*. 2007;8(5):765-9.
- [230] Gálvez ME, Ascaso S, Moliner R, Lázaro MJ. Me (Cu, Co, V)-K/Al₂O₃ supported catalysts for the simultaneous removal of soot and nitrogen oxides from diesel exhausts. *Chemical Engineering Science*. 2013;87:75-90.
- [231] Chen Y, He J, Tian H, Wang D, Yang Q. Enhanced formaldehyde oxidation on Pt/MnO₂ catalysts modified with alkali metal salts. *Journal of Colloid and Interface Science*. 2014;428:1-7.
- [232] Lang W, Laing P, Cheng Y, Hubbard C, Harold MP. Co-oxidation of CO and propylene on Pd/CeO₂-ZrO₂ and Pd/Al₂O₃ monolith catalysts: A light-off, kinetics, and mechanistic study. *Applied Catalysis B: Environmental*. 2017;218:430-42.
- [233] Yentekakis IV, Tellou V, Botzolaki G, Rapakousios IA. A comparative study of the C₃H₆ + NO + O₂, C₃H₆ + O₂ and NO + O₂ reactions in excess oxygen over Na-modified Pt/γ-Al₂O₃ catalysts. *Applied Catalysis B: Environmental*. 2005;56(3):229-39.
- [234] Gálvez ME, Ascaso S, Stelmachowski P, Legutko P, Kotarba A, Moliner R, et al. Influence of the surface potassium species in Fe–K/Al₂O₃ catalysts on the soot oxidation activity in the presence of NO_x. *Applied Catalysis B: Environmental*. 2014;152–153:88-98.
- [235] Filkin NC, Tikhov MS, Palermo A, Lambert RM. A Kinetic and Spectroscopic Study of the in Situ Electrochemical Promotion by Sodium of the Platinum-Catalyzed Combustion of Propene. *The Journal of Physical Chemistry A*. 1999;103(15):2680-7.
- [236] Yentekakis IV, Konsolakis M, Lambert RM, Macleod N, Nalbantian L. Extraordinarily effective promotion by sodium in emission control catalysis: NO reduction by propene over Na-promoted Pt/γ-Al₂O₃. *Applied Catalysis B: Environmental*. 1999;22(2):123-33.
- [237] Koukiou S, Konsolakis M, Lambert RM, Yentekakis IV. Spectroscopic evidence for the mode of action of alkali promoters in Pt-catalyzed de-NO_x chemistry. *Applied Catalysis B: Environmental*. 2007;76(1):101-6.
- [238] Konsolakis M, Yentekakis IV. NO reduction by propene or CO over alkali-promoted Pd/YSZ catalysts. *Journal of Hazardous Materials*. 2007;149(3):619-24.
- [239] Vernoux P, Leinekugel-Le-Cocq AY, Gaillard F. Effect of the addition of Na to Pt/Al₂O₃ catalysts for the reduction of NO by C₃H₈ and C₃H₆ under lean-burn conditions. *Journal of Catalysis*. 2003;219(1):247-57.
- [240] Jeong G, Oh Y. Emission profile of rapeseed methyl ester and its blend in a diesel engine. *Applied Biochemistry and Biotechnology*. 2006;129:165-78.
- [241] Chen JP, Buzanowski MA, Yang RT, Cichanowicz JE. Deactivation of the Vanadia Catalyst in the Selective Catalytic Reduction Process. *Journal of the Air & Waste Management Association*. 1990;40(10):1403-9.
- [242] Chen JP, Yang RT. Mechanism of poisoning of the V₂O₅/TiO₂ catalyst for the reduction of NO by NH₃. *Journal of Catalysis*. 1990;125(2):411-20.
- [243] Klimczak M, Kern P, Heinzelmann T, Lucas M, Claus P. High-throughput study of the effects of inorganic additives and poisons on NH₃-SCR catalysts—Part I: V₂O₅–WO₃/TiO₂ catalysts. *Applied Catalysis B: Environmental*. 2010;95(1–2):39-47.

- [244] Tang F, Xu B, Shi H, Qiu J, Fan Y. The poisoning effect of Na⁺ and Ca²⁺ ions doped on the V₂O₅/TiO₂ catalysts for selective catalytic reduction of NO by NH₃. *Applied Catalysis B: Environmental*. 2010;94(1–2):71-6.
- [245] Peng Y, Li J, Shi W, Xu J, Hao J. Design strategies for development of SCR catalyst: improvement of alkali poisoning resistance and novel regeneration method. *Environmental Science & Technology*. 2012;46(22):12623-9.
- [246] Li Y, Armor JN. Selective NH₃ oxidation to N₂ in a wet stream. *Applied Catalysis B: Environmental*. 1997;13(2):131-9.
- [247] Lietti L, Nova I, Forzatti P. Selective catalytic reduction (SCR) of NO by NH₃ over TiO₂-supported V₂O₅–WO₃ and V₂O₅–MoO₃ catalysts. *Topics in Catalysis*. 2000;11(1):111-22.

List of Figures

Fig. 1.1 World delivered energy consumption by end-use sector (quadrillion Btu), 2012-2040.	1
Fig. 1.2 Powertrain map of major markets.....	2
Fig. 1.3 Share of diesel in new passenger car registrations in Western Europe, 1990-2016.	3
Fig. 1.4 Technologies required for compliance: Diesel.	6
Fig. 1.5 Combination of catalysts to control diesel exhaust emissions.....	6
Fig. 2.1 Schematic diagram of a three-way catalyst converter (Image courtesy of ClearMechanic.com)	12
Fig. 2.2 Schematic diagram of a urea-SCR system.....	15
Fig. 2.3 NO oxidation thermodynamic equilibrium curve for a stream initially of 300 ppm NO and 10% O ₂	25
Fig. 2.4 Mechanism of the NO–NH ₃ reaction over vanadia-based catalysts proposed by Ramis et al. in the presence of oxygen.	31
Fig. 2.5 Scheme illustrating the catalytic cycle of the SCR reaction over vanadia/titania catalyst in the presence of oxygen proposed by Topsoe et al.	32
Fig. 2.6 A reaction mechanism for the SCR process proposed by Arnarson et al.	33
Fig. 2.7 Schematic of deactivation by coke forming.....	35
Fig. 2.8 Phase transformation and specific surface area of alumina.....	37
Fig. 2.9 Schematic of surface dehydroxylation from contact area of two adjacent particles....	38
Fig. 2.10 Two principal mechanisms of metal crystallite growth due to sintering: (A), atomic migration, and (B), crystallite migration.	39
Fig. 2.11 Biodiesel processing flow diagram.....	41
Fig. 2.12 Average emission impacts of biodiesel content as estimated from published engine dynamometer data in the EPA study.	42
Fig. 3.1 Schematic overview of synthetic gas bench (SGB) plant for monolithic DOCs study.	47
Fig. 3.2 Pictures of synthetic gas bench (SGB) plant for monolithic DOCs study.....	49
Fig. 3.3 Schematic overview of synthetic gas bench plant for monolithic SCR catalysts study.	50
Fig. 3.4 Schematic overview of synthetic gas bench (SGB) plant for powdered DOCs study.	51
Fig. 3.5 Picture of synthetic gas bench (SGB) plant for powdered DOCs study.	53
Fig. 3.6 XRD patterns obtained from the <i>PDF-2 Release 2005</i> database for PdO and Pt ⁰	54
Fig. 3.7 The temperature program for TPR test.	57
Fig. 4.1 Evolution profiles of C ₃ H ₆ , CO and NO _x for Mix 1 versus temperature for reference and aged catalysts: (a). Conversions of C ₃ H ₆ , (b). Conversions of CO and (c). Transformations of NO _x	63
Fig. 4.2 TEM analysis of aged catalysts.....	64

Fig. 4.3 Evolution profiles of C ₃ H ₆ , CO and NO for Mix 2 versus temperature for reference and aged catalysts: (a). Conversions of C ₃ H ₆ , (b). Conversions of CO and (c). Conversions of NO	65
Fig. 4.4 Effect of gas compositions on the evolution profiles of fresh catalyst: (a). C ₃ H ₆ , (b). CO, and (c). NO _x	67
Fig. 4.5 Effect of gas compositions on the evolution profiles of A750 catalyst: (a). C ₃ H ₆ , (b). CO, and (c). NO _x	69
Fig. 4.6 Effect of gas compositions on the evolution profiles of A950 catalyst: (a). C ₃ H ₆ , (b). CO, and (c). NO _x	71
Fig. 4.7 Effect of gas compositions on the evolution profiles of C ₃ H ₆ : (a). Fresh catalyst, (b). K-doped catalyst, (c). Na-doped catalyst and (d). K/Na-doped catalyst.....	76
Fig. 4.8 Effect of gas compositions on the evolution profiles of CO: (a). Fresh catalyst, (b). K-doped catalyst, (c). Na-doped catalyst and (d). K/Na-doped catalyst	77
Fig. 4.9 Effect of gas compositions on the evolution profiles of NO _x : (a). Fresh catalyst, (b). K-doped catalyst, (c). Na-doped catalyst and (d). K/Na-doped catalyst.....	78
Fig. 4.10 Effect of gas compositions on the evolution profiles of Fresh catalyst: (a). C ₃ H ₆ , (b). CO, and.....	80
Fig. 4.11 Evolution profiles of C ₃ H ₆ , CO and NO _x for Mix 1 versus temperature for reference and conditioned catalysts: (a). Conversions of C ₃ H ₆ , (b). Conversions of CO and (c). Transformations of NO _x	84
Fig. 4.12 Evolution profiles of C ₃ H ₆ , CO and NO for Mix 2 versus temperature for reference and conditioned catalysts: (a). Conversions of C ₃ H ₆ , (b). Conversions of CO and (c). Conversions of NO	85
Fig. 4.13 Evolution profiles of C ₃ H ₆ , CO and NO ₂ for Mix 3 versus temperature for reference and conditioned catalysts: (a). Conversions of C ₃ H ₆ , (b). Conversions of CO and (c). Conversions of NO ₂	86
Fig. 4.14 Evolution profiles of C ₃ H ₆ and NO _x for Mix 4 versus temperature for reference and conditioned catalysts: (a). Conversions of C ₃ H ₆ , and (b). Transformations of NO _x	87
Fig. 4.15 Evolution profiles of C ₃ H ₆ and CO for Mix 5 versus temperature for reference and conditioned catalysts: (a). Conversions of C ₃ H ₆ , and (b). Conversions of CO.....	88
Fig. 4.16 Effect of gas compositions on the evolution profiles of Fresh catalyst: (a). C ₃ H ₆ , (b). CO, and.....	89
Fig. 4.17 Evolution profiles of C ₃ H ₆ , CO and NO _x for Mix 1 versus temperature for reference and conditioned catalysts: (a). Conversions of C ₃ H ₆ , (b). Conversions of CO and (c). Transformations of NO _x	93
Fig. 4.18 Evolution profiles of C ₃ H ₆ , CO and NO for Mix 2 versus temperature for reference and conditioned catalysts: (a). Conversions of C ₃ H ₆ , (b). Conversions of CO and (c). Transformations of NO	95

Fig. 4.19 Evolution profiles of C ₃ H ₆ , CO and NO ₂ for Mix 3 versus temperature for reference and conditioned catalysts: (a). Conversions of C ₃ H ₆ , (b). Conversions of CO and (c). Conversions of NO ₂	96
Fig. 4.20 Evolution profiles of C ₃ H ₆ and NO _x for Mix 4 versus temperature for reference and conditioned catalysts: (a). Conversions of C ₃ H ₆ and (b). Transformations of NO _x	97
Fig. 4.21 Evolution profiles of C ₃ H ₆ and CO for Mix 5 versus temperature for reference and conditioned catalysts: (a). Conversions of C ₃ H ₆ , and (b). Conversions of CO.....	98
Fig. 4.22 Effect of gas compositions on the evolution profiles of C ₃ H ₆ : (a). Fresh catalyst, (b). A750 catalyst,.....	99
Fig. 4.23 Effect of gas compositions on the evolution profiles of CO: (a). Fresh catalyst, (b). A750 catalyst, (c). K catalyst and (d). K-A750 catalyst	100
Fig. 4.24 Effect of gas compositions on the evolution profiles of NO _x : (a). Fresh catalyst, (b). A750 catalyst, (c). K catalyst and (d). K-A750 catalyst	101
Fig. 4.25 Evolution profiles of C ₃ H ₆ , CO and NO for Mix 1 versus temperature for reference and conditioned catalysts: (a). Conversions of C ₃ H ₆ , (b). Conversions of CO and (c). Conversions of NO.....	104
Fig. 4.26 Evolution profiles of CO and NO for Mix 2 versus temperature for reference and conditioned catalysts: (a). Conversions of CO and (b). Conversions of NO	106
Fig. 4.27 Evolution profiles of C ₃ H ₆ and CO for Mix 3 versus temperature for reference and conditioned catalysts: (a). Conversions of C ₃ H ₆ and (b). Conversions of CO	107
Fig. 4.28 Evolution profiles of C ₃ H ₆ and NO for Mix 4 versus temperature for reference and conditioned catalysts: (a). Conversions of C ₃ H ₆ and (b). Conversions of NO.....	108
Fig. 4.29 Effect of gas compositions on the evolution profiles of C ₃ H ₆ : (a). Fresh, (b). K and (c). Na.....	109
Fig. 4.30 Effect of gas compositions on the evolution profiles of CO: (a). Fresh, (b). K and (c). Na.....	110
Fig. 4.31 Effect of gas compositions on the evolution profiles of NO: (a). Fresh, (b). K and (c). Na.....	110
Fig. 4.32 The activity profiles of C ₃ H ₆ , CO and NO as a function of temperature under Mix 1 over Fresh monolith and powder catalysts: (a). Conversions of C ₃ H ₆ , (b). Conversions of CO and (c). Conversions of NO.....	113
Fig. 4.33 The activity profiles of C ₃ H ₆ , CO and NO as a function of temperature under Mix 1 over K-doped monolith and powder catalysts: (a). Conversions of C ₃ H ₆ , (b). Conversions of CO and (c). Conversions of NO	114
Fig. 4.34 The activity profiles of C ₃ H ₆ , CO and NO as a function of temperature under Mix 1 over Na-doped monolith and powder catalysts: (a). Conversions of C ₃ H ₆ , (b). Conversions of CO and.....	115
Fig. 4.35 The activity profiles of C ₃ H ₆ , CO and NO as a function of temperature under Mix 1 over K-Na monolith and powder catalysts: (a). Conversions of C ₃ H ₆ , (b). Conversions of CO and (c). Conversions of NO.....	116

Fig. 4.36 The activity profiles of C ₃ H ₆ , CO and NO as a function of temperature under Mix 1 over K-A750 monolith and powder catalysts: (a). Conversions of C ₃ H ₆ , (b). Conversions of CO and (c). Conversions of NO	117
Fig. 4.37 Conversion profiles of C ₃ H ₆ as a function of temperature under Mix 1 over Fresh and doped monolith and powder catalysts: (a). Fresh, (b). K, (c). Na, and (d) K-Na	118
Fig. 4.38 Conversion profiles of CO as a function of temperature under Mix 1 over Fresh and doped monolith and powder catalysts: (a). Fresh, (b). K, (c). Na, and (d) K-Na.....	119
Fig. 4.39 Conversion profiles of NO as a function of temperature under Mix 1 over Fresh and doped monolith and powder catalysts: (a). Fresh, (b). K, (c). Na, and (d) K-Na.....	120
Fig. 5.1 Conversion profiles of NH ₃ oxidation over Fresh SCR monolith catalyst without/with H ₂ O.....	125
Fig. 5.2 Conversion profiles of NO oxidation over Fresh SCR monolith catalyst without/with H ₂ O.....	126
Fig. 5.3 Conversion profiles of reactants of interest over Fresh catalyst without/with H ₂ O:	127
Fig. 5.4 Conversion profiles of NO over different SCR catalysts under Mix 3.....	129
Fig. 5.5 Conversion profiles of NO over different SCR catalysts under Mix 4.....	129
Fig. 5.6 Conversion profiles of reactants of interest over different SCR catalysts under Mix 5: a), Conversions of NO; and b), Conversions of NH ₃	130
Fig. 5.7 Conversion profiles of reactants of interest over different SCR catalysts under Mix 6: a), Conversions of NO; and b), Conversions of NH ₃	131
Fig. 5.8 Conversion profiles of reactants of interest over different SCR catalysts under Mix 8: a), Conversions of NO; b), Conversions of NO ₂ ; and c), Conversions of NH ₃	132
Fig. A.1 Results of Mix 6_TPD tests for home-made DOC: a), Concentrations of NO; b), Concentrations of NO ₂ ; and c), Concentrations of NO _x	158

List of Tables

Table 1.1 EU emissions standards for diesel passenger cars, g/km	4
Table 2.1 Mechanisms of catalyst deactivation.	34
Table 2.2 Average emissions change for B20 from published engine dynamometer data in the EPA review.	42
Table 3.1 Description of the gases used for monolithic DOCs study.....	48
Table 3.2 Detectors of synthetic gas bench (SGB) plant for monolithic DOCs study.....	48
Table 3.3 Description of the gases used for monolithic SCR catalysts study.	50
Table 3.4 Detectors of synthetic gas bench (SGB) plant for monolithic SCR catalysts study	51
Table 3.5 Description of the gases used for powdered DOCs study	52
Table 3.6 Detectors of synthetic gas bench (SGB) plant for powdered DOCs study	52
Table 4.1 Different aging methods dealing with commercial monolithic DOC.....	60
Table 4.2 Synthetic gas bench experimental conditions	62
Table 4.3 Different doping methods dealing with DOC	73
Table 4.4 Synthetic gas bench experimental conditions for alkali-as-dopant DOC study.....	75
Table 4.5 Different methods dealing with DOC for dual deactivation study	91
Table 4.6 Synthetic gas bench experimental conditions for DOC dual deactivation study	92
Table 4.7 Different methods dealing with powder DOC.	102
Table 4.8 Synthetic gas bench experimental conditions for powder DOCs.....	103
Table 4.9 Experimental setup of monolith catalysts for the comparison study	112
Table 4.10 Experimental setup of powder catalysts for the comparison study.....	112
Table 5.1 Different methods dealing with monolithic SCR catalysts.....	123
Table 5.2 Synthetic gas bench experimental conditions for monolithic SCR catalysts.....	124
Table A.1 List of abbreviations used in this thesis.	156

Annexes

Annex A. Abbreviations and symbols

Table A.1 List of abbreviations used in this thesis

UPMC	Université Pierre et Marie Curie
FRT	Fluides Réactifs et Turbulence
CSC	China Scholarship Council
DOC	Diesel Oxidation Catalysts
SCR	Selective Catalytic Reduction
DPF	Diesel Particulate Filter
GDP	Gross Domestic Product
VOC	Volatile Organic Compound
TWC	Three-way Catalyst
HC	Hydrocarbon
A/F	Air-to-Fuel
PM	Particulate Matter
LNT	Lean NO _x Trap
SOF	Soluble Organic Fraction
EPA	Environmental Protection Agency
UWS	Urea-Water-Solutions
DEF	Diesel Exhaust Fluid
AUS	Aqueous Urea Solution
UHV	Ultra-High Vacuum
AES	Auger Electron Spectroscopy
LEED	Low-Energy Electron Diffraction
L.H.	Langmuir-Hinshelwood
E.R.	Eley-Rideal
PM-IRAS	Polarization-Modulated Infrared Absorbance Spectroscopy
PGM	Platinum Group Metal

Table A.1 Continued

TPD	Temperature Programmed Desorption
RDS	Rate-Determining Step
FT-IR	Fourier Transform Infrared
DFT	Density Functional Theory
ASTM	American Society for Testing and Materials
EPMA	Electron Probe Microanalysis
ULSD	Ultra-Low Sulfur Diesel
SGB	Synthetic Gas Bench
ID	Inner Diameter
FID	Flame Ionization Detector
XRD	X-Ray Diffraction
TEM	Transmission Electron Microscopy
BET	Brunauer-Emmett-Teller
ICDD	International Center for Diffraction Data
HRTEM	High Resolution TEM
EDS	Energy-dispersive X-ray Spectroscopy
BJH	Barrett-Joyner-Halenda
TCD	Thermal Conductivity Detector
TPR	Temperature Programmed Reduction
pg	Page
CPSI	Channels Per Square Inches
PXRD	Powder XRD
GHSV	Gas Hourly Space Velocity
DPNR	Diesel Particulate NO _x Reduction
wt.	Weight
SEM	Scanning Electron Microscopy
EHMO	Extended Hückel Molecular Orbital
MSW	Municipal Solid Waste
DOE	Design of Experiments

Annex B. Results of Mix 6_TPD tests for home-made DOC

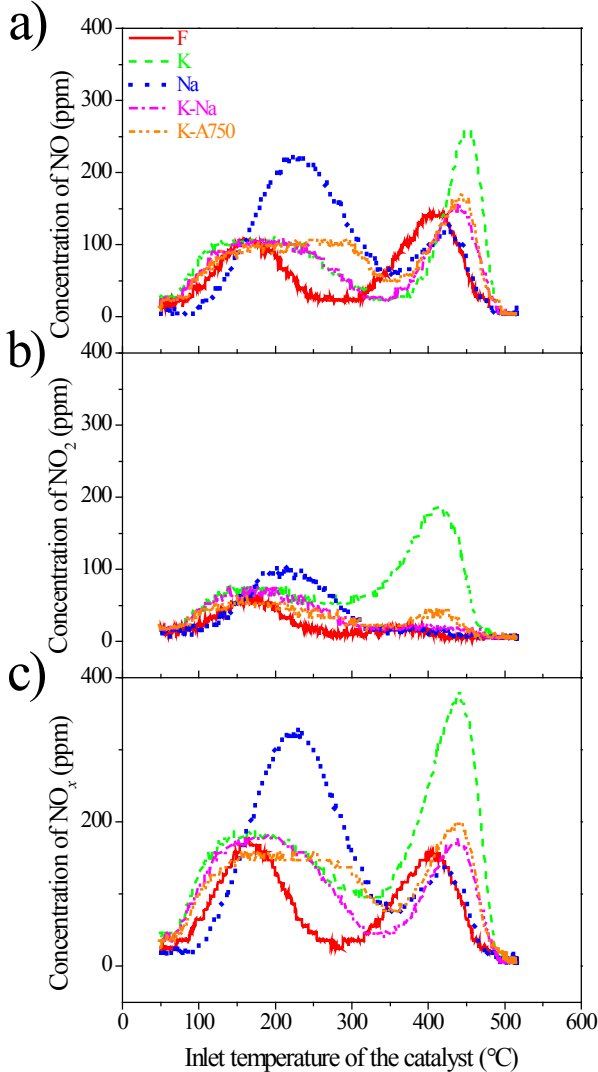


Fig. A.1 Results of Mix 6_TPD tests for home-made DOC: a), Concentrations of NO; b), Concentrations of NO₂; and c), Concentrations of NO_x.